

**Insights into Membrane Type-1 Matrix
Metalloproteinase cleavage of the Low-density
Lipoprotein Receptor**

by

Adekunle Alabi

A thesis submitted in partial fulfillment of the requirements for the degree of

Doctor of Philosophy

Department of Biochemistry

University of Alberta

© Adekunle Alabi, 2020

Abstract

The Low-density lipoprotein receptor (LDLR) mediated cellular uptake of LDL is the main pathway for plasma LDL cholesterol (LDL-C) clearance. However, the LDLR can be proteolytically cleaved to release its soluble ectodomain (sLDLR) into the extracellular milieu and as such reducing its LDL-C clearance efficiency. Plasma sLDLR levels are positively correlated with plasma LDL-C levels. Membrane type 1-matrix metalloproteinase (MT1-MMP) is a Zn^{2+} -dependent endopeptidase that can cleave extracellular matrix and non-matrix substrates.

The work presented in this thesis investigates, the proteinase responsible for LDLR cleavage and as such identifies MT1-MMP as a key metalloproteinase responsible for LDLR shedding. We found that knockdown of *MT1-MMP* increased cellular LDLR abundance and reduced the levels of sLDLR in cultured hepatocytes. Interaction between both proteins was ascertained by their co-immunoprecipitation and co-localization in hepatoma cell lines. Consistently, mice lacking hepatic *MT1-MMP* displayed an increase in cellular LDLR levels and a corresponding reduction in plasma levels of sLDLR, HDL-cholesterol, and non-HDL cholesterol. Opposite effects were observed when *MT1-MMP* was overexpressed. We also demonstrated that hepatocyte-specific overexpression of *MT1-MMP* significantly increased atherosclerotic lesion area in *ApoE* knockout mice.

In addition, we found that the majority of circulating sLDLR were associated with apoB and apoE-containing lipoproteins in both mouse and human plasma. The sLDLR retains its ability to bind to LDLR ligands and as such reduces ligands available to be cleared by the LDLR. Combined treatment of *MT1-MMP* knockdown and inhibition of other LDLR regulating pathways such as

statin inhibition of HMG-CoA reductase, inhibition of PCSK9 and γ -secretase, had a combined beneficial increase on LDLR levels invitro accompanied with an improved clearance of circulating cholesterol in vivo with statin treatment.

It was determined that MT1-MMP cleaves the LDLR possibly at multiple sites within the protein. Deletion of various regions on the protein did not abrogate its MT1-MMP cleavage nor did mutation of cleavage sites as determined by CleavePredict affect LDLR cleavage by MT1-MMP. MT1-MMP cleaved LDLR structurally related proteins such as ApoER2 and VLDLR. Similarly, MT1-MMP structurally related metalloproteinase MT2-MMP cleaves the LDLR but with a lesser efficiency as compared to MT1-MMP.

We identified a variant of MT1-MMP (rs139288377) in the Dallas Heart Study with the mutation A37P; this variant was significantly associated with plasma LDL-C levels. The average LDL-C levels of 36 people with the variant were 87 mg/dl, compared with 110 mg/dl in the control group. Our experiments showed that this mutation reduces the ability of MT1-MMP to efficiently cleave the LDLR.

Thus, this thesis demonstrates that MT1-MMP promotes ectodomain shedding of hepatic LDLR, thereby regulating plasma cholesterol levels and the development of atherosclerosis.

Preface

This thesis is original work by Adekunle Alabi. All animal procedures were approved by the University of Alberta's Animal Care and Use Committee with study ID AUP00000456; experiments were conducted in accordance with the guidelines of the Canadian Council on Animal Care. The contributions made by the candidate, Adekunle Alabi and the co-authors of these studies are as described below.

Chapter 3 is under peer review to be published as **Alabi, A.**, Gu, H.M., Xia, X.D., Wang, F., Adijiang, A., Shijun D., Yang ,N., Douglas, D., Kneteman, N., Xue,Y., Chen, L., Qin, S., and Zhang D, W (2020). “Membrane type 1 matrix metalloproteinase promotes ectodomain shedding of low-density lipoprotein receptor and accelerates the development of atherosclerosis”. Nature Communications. A.A., and D.W.Z., designed and performed the experiments, collected, and analyzed data. H.M.G., X.X., F.W., S.D., and A.A., performed the experiments, collected, and analyzed data. N.Y., Y.X., L.C., and S.Q., collected, processed, and analyzed human plasma samples. D.N.D., and N.M.K., provided technical support and guidance in the study of primary human hepatocytes, A.A. and D.W.Z. wrote the manuscript. Contributions of all individuals is as stated on the introductory page to chapter 3 of this thesis.

Chapter 4 is in preparation for publication as **Alabi, A.**, Wang, F., and Zhang D, W. “Tandem inhibition of MT1-MMP and other LDLR regulating pathways increase availability of LDLR and cholesterol clearance”. A.A., and D.W.Z., designed and performed the experiments, collected, and analyzed data. A.A and D.W.Z. wrote the manuscript. Contributions of all individuals is as stated on the introductory page to chapter 4 of this thesis.

Dedication

In loving memory of my grandparents Pa Joshua Adekunle Alabi and Mama Abigail Bolaji Alabi. Thank you for believing in me and investing in my education.

Acknowledgements

My utmost gratitude goes to my supervisor Dr. Dawei Zhang for his tutelage and mentorship. Thank you for the opportunity to work on this novel and exciting project that has helped broaden my scientific acumen. I am forever grateful; my story will never be written without a mention of your immense scientific contribution to my career. I would also like to extend my appreciation to the members of my supervisory committee Dr. Richard Lehner, Dr. Maria Febbraio, and Dr. Carlos Fernandez-Patron, thank you for your insightful comments and suggestions towards the completion of this thesis.

My appreciation also goes to the supportive members of the Zhang lab especially Hongmei Gu, she helped in effectively coordinating the lab for the successful completion of my work, Dr. Faqi Wang for her mentorship on my arrival in the lab. My colleagues and friends in the lab also deserve worthy mentions for motivating me and creating a conducive environment for me in the laboratory, Dr. Shijun Deng, Dr. Xiaodan Xie, Dr. Shoudong Guo, Dr. Jiang Miao, Yishi Shen, and Roxan Priela.

I would also like to express gratitude to the members of the Molecular and Cell Biology of Lipid group (MCBL) for their scientific critic and suggestions during my research presentation. The discussion from our meetings led to great ideas that were key to the effective completion of this thesis.

Finally, I would like to thank my family and friends for their emotional and moral support, I did hit rock bottom many times but thanks to the following people for always been there for me: my family, Mrs. Bolajoko Alabi, Taiye and Kehinde Alabi, Jesuseun Alabi, Mr. and Mrs. Adejumobi, Champion Adejumobi, Samuel Adejumobi, Wisdom Adejumobi and Mr. Adebayo Alabi. My

friends; Ravion Mackins, Umjuma Lori, Pearl Onukogwu, Danielle Thornton, Seun Odofofin, Tutu Odofofin, Brittney Hislop, Sereana Wan, Jacqueline krysa, Olaide Odunuga, Seyi Falekun, Taiwo Fasoranti, and Amb Monday Okooza.

Table of Contents

Chapter 1	1
Introduction	1
1.1 Cardiovascular Diseases	2
1.2 Cholesterol and its functions	3
1.2.1 Cholesterol Biosynthesis	4
1.2.2 Dietary Cholesterol.....	4
1.3 Lipoproteins and cholesterol transport	5
1.3.1 Exogenous pathway	9
1.3.2 Endogenous pathway	10
1.3.3 Reverse cholesterol transport.....	11
1.4 The Low-Density lipoprotein receptor	12
1.4.1 Structure and function of the low-density lipoprotein receptor.....	13
1.4.1.1 Structural Domains of the LDLR and their function	14
1.4.1.2 LDLR ligand binding, endocytosis, and Recycling	18
1.4.2 LDL Receptor-Related Proteins	20
1.5 The Role of LDL- cholesterol in Cardiovascular Diseases	21
1.5.1 Atherosclerosis	23
1.5.2 Statin Treatment of Hypercholesterolemia.....	25
1.6 Regulation of the low-density lipoprotein Receptor	26
1.6.1 Transcriptional Regulation	26
1.6.2 Post-translational regulation of LDLR	27
1.6.2.1 Proprotein Convertase Subtilisin/ Kexin type 9 (PCSK9)	27
1.6.2.2 Inducible Degradation of LDLR (IDOL).....	28
1.6.2.3 LDLR shedding	28

1.7 Matrix Metalloproteinases	30
1.7.1 Membrane Type-1 Matrix Metalloproteinase (MT1-MMP)	34
1.7.2 Structure and function of MT1-MMP	35
1.7.3 Regulation of MT1-MMP.....	38
1.7.3.1 Transcriptional Regulation of MT1-MMP Gene Expression	38
1.7.3.2 Post-transcriptional Regulation of MT1-MMP.....	39
1.7.4 MT1-MMP and Atherosclerosis.....	40
1.8 Rationale, Hypothesis and Aim of thesis.....	42
Chapter 2	44
Materials and Methods.....	44
2.1 Materials	45
2.2 Animal	46
2.3 Culture and treatment of cell lines	47
2.3.1 Cell Culture.....	47
2.3.2 Thawing of frozen cells	47
2.3.3 Cryopreservation of immortalized Cells.....	48
2.3.4 Immortalized cells	48
2.3.5 Primary Hepatocytes.....	48
2.3.5.1 Primary Human Hepatocyte	48
2.3.5.2 Primary Mice Hepatocyte	49
2.3.6 Transfection	49
2.3.6.1 X-tremeGENE HP Transfection	50
2.3.6.2 Lipofectamine 3000 Transfection	50
2.3.6.3 RNAiMAX Transfection	50
2.3.7 Drug and inhibitor treatment of cells.....	51

2.3.7.1 Statin Treatment.....	51
2.3.7.1 Iloprost GM6001	51
2.3.7.3 DAPT (tert-butyl (2S)-2-[[[(2S)-2-[[2-(3,5-difluorophenyl) acetyl] amino] propanoyl] amino]-2-phenylacetate).....	51
2.3.8 Binding of PCSK9 to recombinant extracellular LDLR	51
2.3.8.1 Incubation of PCSK9 and LDLR	51
2.3.8.2 Addition of LDLR and PCSK9 mixture to Huh7 cells	52
2.3.9 PCSK9-promoted LDLR degradation	52
2.3.10 Measurement of Dil-LDL uptake in Huh7 cells.....	52
2.3.10.1 Dil-LDL incubation in cells with MT1-MMP Knockdown prior to LDL uptake assay.....	52
2.3.10.2 Recombinant LDLR incubation with Dil-LDL prior to LDL uptake assay.....	53
2.3.10.3 Fluorescent detection of LDL uptake	53
2.3.11 Biotinylation of cell surface proteins.....	53
2.4 Quantification of mRNA Expression.....	54
2.4.1 RNA Isolation.....	54
2.4.2 cDNA synthesis	55
2.4.3 Quantitative Real-Time PCR (qRT-PCR).....	56
2.5 Site-directed mutagenesis	57
2.6 Western Blot and Protein Expression Analysis.....	60
2.6.1 Protein extraction from cultured cells	60
2.6.2 Protein extraction from animal tissues	61
2.6.3 Protein Assay and quantification	61
2.6.4 Immunoprecipitation	62
2.6.4.1 Immunoprecipitation of LDLR and MT1 from cell lysate.....	62
2.6.4.2 Immunoprecipitation of sLDLR From Plasma	62

2.6.4.3	Elution of immunoprecipitated Protein	62
2.6.5	Immunoblotting	63
2.6.6	TCA Precipitation.....	64
2.6.7	Gelatin Zymography.....	65
2.6.8	Immunofluorescence	65
2.6.9	Immunohistochemistry	66
2.7	Agarose Gel Electrophoresis and MT1-MMP FLOX genotyping.....	66
2.7.1	DNA Extraction from tissue.....	66
2.7.2	Agarose gel.....	68
2.7.3	Gel Electrophoresis.....	68
2.8	Extraction of lipids.....	68
2.9	Plasma lipid and Alanine aminotransferase (ALT)	69
2.9.1	ALT determination	69
2.9.2	Cholesterol determination.....	70
2.9.3	Triglycerides determination.....	70
2.10	ELISA Measurement of sLDLR and PCSK9	71
2.10.1	Plate Preparation.....	71
2.10.2	Assay Procedure	71
2.11	Expression of MT1-MMP in mice using Adenovirus or Adeno-associated virus (AAV).....	73
2.12	Atherosclerosis Study.....	74
2.12.1	Histological Quantification of Plaques.....	74
2.12.2	Lipid Extraction and Cholesterol Ester Determination from the Aorta.....	75
2.13	Statistical analysis	75
2.14	Primers	76

Chapter 3	80
Membrane type 1 matrix metalloproteinase promotes ectodomain shedding of low-density lipoprotein receptor and accelerates the development of atherosclerosis	80
3.1 Introduction	81
3.2 Results	84
3.2.1 MT1-MMP regulates LDLR expression.....	84
3.2.2 MT1-MMP promotes ectodomain cleavage of LDLR	89
3.2.3 MT1-MMP promotes LDLR cleavage in vivo	96
3.2.4 sLDLR and plasma lipoproteins	106
3.3 Discussion.....	115
Chapter 4	120
Tandem inhibition of MT1-MMP and other LDLR regulating pathways increase availability of LDLR and cholesterol clearance	120
4.1 Introduction	121
4.2 Results	123
4.2.1 Combined treatment of MT1-MMP knockdown and other LDLR regulating mechanisms	123
4.2.1.1 Gamma-secretase inhibition.....	123
4.2.1.2 PCSK9 inhibition.....	124
4.2.1.3 Statin treatment	127
4.2.2 LDLR Extracellular Domain binds LDL and prevents its Endocytosis	132
4.2.3 LDLR Extracellular Domain binds PCSK9 and inhibits its ability to mediate LDLR Degradation	133
4.2.4 Soluble LDLR is not a mediator of PCSK9 binding to LDL in Circulation.	134
4.3 Discussion.....	137
Chapter 5	140

Mechanistic Study of MT1-MMP cleavage of the Low-Density Lipoprotein Receptor and its related Proteins	140
5.1 Introduction	141
5.2 Results	143
5.2.1 MT1-MMP-Mediated LDLR Cleavage occurs at Multiple Sites on the LDLR.....	143
5.2.2 The Catalytic Domain of MT1-MMP is critical for LDLR Shedding.....	147
5.2.3 MT1-MMP Cleaves Members of the LDLR related Protein Family	148
5.2.4 Effect of MT1-MMP related Metalloproteinase on LDLR Cleavage	149
5.2.5 A37P mutation in the Pro-domain of MT1-MMP Reduces its ability to cleave LDLR	152
5.3 Discussion.....	155
Chapter 6	158
Conclusion and Future Directions.....	158
6.1 Conclusion.....	159
6.2 Future work	164
Bibliography	166

List of Tables

Table 1. 1- Types of Apolipoproteins, their sources, associations, and function.....	7
Table 1. 2- Classes of Lipoproteins, their sizes, density, apolipoproteins and major lipid content.....	8
Table 1. 3-Interpretation of levels of cholesterol in humans.....	22
Table 1. 4- Classifications of MMPs, substrates and phenotypes from knock out animals.	34
Table 2. 1-Reverse transcription Reaction mixture.....	56
Table 2. 2-qRT-PCR reaction mixture.....	56
Table 2. 3-qRT-PCR running parameters.....	57
Table 2. 4-Mutagenesis PCR Reaction Mixture.....	59
Table 2. 5-Mutagenesis PCR parameters	60
Table 2. 6-Antibody dilution	64
Table 2. 7-Reaction Mixture for Genotyping	67
Table 2. 8-PCR parameters for Genotyping.....	67
Table 2. 9-Working Concentration of Reagents and Samples for ELISA measurement of sLDLR and PCSK9.....	72
Table 5. 1-LDLR Cleavage site prediction by CleavePredict.	146

List of Figures

Fig 1. 1. Chemical structure of cholesterol	3
Fig 1. 2. Lipoprotein metabolism	12
Fig 1. 3. Diagrammatic representation of the LDLR gene	13
Fig 1. 4. Structural representation of the low-density lipoprotein receptor	17
Fig 1. 5. LDLR uptake of LDL	19
Fig 1. 6. Pictorial description of LDLR-related proteins, with structural comparison to the LDLR.	21
Fig 1. 7. Diagrammatic representation of the sequence of events leading to the development of atherosclerotic plaque.	24
Fig 1. 8. Cleavage of ApoE receptor proteins and the release of their soluble forms into extracellular space	30
Fig 1. 9. Structure of matrix metalloproteinases and their various classes based on their structure and function	32
Fig 1. 10. <i>MT1-MMP</i> gene located on chromosome 14	35
Fig 1. 11. Activation of MT1-MMP and interaction of water molecule with glutamate residue to attain nucleophilicity	37
Fig 3. 1. MT1-MMP-mediated LDLR degradation..	86
Fig 3. 2. MT1-MMP-mediated LDLR cleavage	91
Fig 3. 3. Effects of MT1-MMP on LDLR	94
Fig 3. 4. Metabolic effects of <i>MT1^{LKO}</i> mice	97
Fig 3. 5. Phenotype associated with MT1-MMP loss in <i>MT1^{LKO}</i> mice I.	99

Fig 3. 6. Phenotype associated with MT1-MMP loss in <i>MT1^{LKO}</i> mice II.....	101
Fig 3. 7. MT1-MMP overexpression in C57BL/6J mice and effect of western-type diet feeding in <i>MT1^{LKO}</i> mice.....	103
Fig 3. 8. Phenotypes associated with 8-weeks western-type diet feeding in <i>MT1^{LKO}</i> mice.	105
Fig 3. 9. Analysis of plasma sLDLR.	107
Fig 3. 10. Association between plasma sLDLR and LDL-C, Total cholesterol, PCSK9 in humans.....	110
Fig 3. 11. Atherosclerosis study	113
Fig 4. 1. Combined knockdown of MT1-MMP and inhibition of other LDLR regulating pathways invitro.....	124
Fig 4. 2. Combined gene knockdown of <i>MT1-MMP</i> and <i>PCSK9</i>.....	126
Fig 4. 3. <i>MT1-MMP</i> knockdown and statin treatment in Huh7 cells.	128
Fig 4. 4. MT1-MMP knockdown and statin treatment.....	129
Fig 4. 5. Effect of MT1-MMP knockdown and statin treatment on apolipoproteins and lipoprotein cholesterol levels	131
Fig 4. 6. Recombinant LDLR binds LDL and prevents its endocytosis.....	133
Fig 4. 7. Recombinant LDLR binds PCSK9 and inhibits LDLR degradation.....	134
Fig 4. 8. Soluble LDLR does not mediate PCSK9 binding to LDL (a) Plasma soluble LDLR quantification.....	136
Fig 5. 1. MT1-MMP Cleavage of the LDLR is not restricted to a single region within the protein.....	145
Fig 5. 2. MT1-MMP catalytic region plays a critical role in the cleavage of the LDLR	148

Fig 5. 3. MT1-MMP sheds closely related family members within the LDLR family.....	149
Fig 5. 4. MT2-MMP cleaves the LDLR in a similar fashion as MT1-MMP but to a lower extent	151
Fig 5. 5. Sequence alignment, showing residues 1-58 of MT1-MMP and conservation of alanine (a) at position 37 across a variety of species.....	152
Fig 5. 6. Effect of A37P mutation on MT1-MMP's ability to cleave the LDLR.....	154
Fig 6. 1. Final Model of proposed MT1-MMP cleavage of the LDLR and fate of sLDLR.	163
Fig 6. 2. Chromatogram of rLDLR ionization by MALDI-MS.....	164

List of Abbreviation

AAV	Adeno-associated viruses
ABCA1	ATP- binding cassette A1
ABCG1	ATP- binding cassette G1
ACAT	Acyl-CoA:cholesterol acyltransferase
ALT	Alanine aminotransaminase
AP-4	Adaptor protein 4
ApoAI	Apolipoprotein AI
ApoB-48	Apolipoprotein B-48
ApoB-100	Apolipoprotein B-100
ApoE	Apolipoprotein E
CETP	Cholesterol ester transfer protein
CMV	Cytomegalovirus
CON	Control
CVD's	Cardiovascular Diseases
ECM	Extracellular matrix
EGF	Epidermal growth factor
ER	Endoplasmic reticulum

FBS	Fetal bovine serum
FH	Familial hypercholesterolaemia
HDL	High-density lipoprotein
HMGCR	HMG-CoA reductase
IDL	Intermediate density lipoprotein
IDOL	Inducible degrader of the LDL receptor
Insig	Insulin induced gene
LCAT	Lecithin-cholesterol acyl transferase
LDL	Low density lipoprotein
LDLR	Low density lipoprotein receptor
LPL	Lipoprotein lipase
LXR	Liver X receptor
MMP	Matrix Metalloproteinase
MT-MMP's	Membrane type matrix metalloproteinases
MT1-MMP	Membrane type matrix metalloproteinase 1
MT2-MMP	Membrane type matrix metalloproteinase 2
NCLPPS	Newborn calf lipoprotein poor serum
NPC1L1	Niemann–pick C1-like 1

OxLDL	Oxidized LDL
PCSK9	Proprotein convertase subtilisin/ kexin type 9
PMSF	Phenylmethanesulfonyl fluoride
rLDLR	Recombinant LDLR
SCAP	SREBP cleavage-activating protein
SD	Standard deviation
SEM	Standard error of the mean
sLDLR	Soluble LDLR
SRE	Sterol response elements
SREBP	Sterol response element binding protein
TG	Triglyceride
TGF- β 1	Transforming growth factor-beta 1
TIMP's	Tissue inhibitor of metalloproteinase
TNF- α	Tumour necrosis factor
TBG	Thyroxine binding globulin
VLDL	Very low-density lipoprotein

Chapter 1

Introduction

1.1 Cardiovascular Diseases

Cardiovascular diseases (CVD's) are the prime cause of death worldwide. 17.9 million people were estimated to have died from CVD's in 2016 alone, representing 31% of total death globally (WHO, 2017). The world health organization predicts that almost 23.6 million people will die from CVD's by the year 2030 and as such CVD's are projected to remain the leading cause of death globally. Cardiovascular diseases are a group of ailment that affects the heart and blood vessels (Biglu, Ghavami, & Biglu, 2016), they include coronary heart disease (associated with blood vessels that supply the heart), peripheral arterial disease (associated with blood vessels that supply arms and legs), cerebrovascular disease (associated with blood vessels that supply the brain), congenital heart disease (structural compromise of the heart at birth), deep vein thrombosis and pulmonary embolism (blood clots originating from the leg which may block blood vessels in the lungs and heart). Heart attacks and strokes are major acute events resulting from these diseases, they also contribute largely to CVD death toll (Benjamin et al., 2017). Cardiovascular heart disease is one of the most prevalent and it results from the blockade of the coronary artery perpetrated by ruptured plaques (Ross, 1999). The critical step in the development of plaques is the deposition of cholesterol in the arterial wall (Kerr, 2016).

1.2 Cholesterol and its functions

Cholesterol is a steroidal lipid containing a core phenanthrene ring, its name originates from the Greek words ‘chole’ meaning bile, ‘stereos’ meaning solid and the suffix ‘ol’ depicting an alcohol signature (Merriam-Webster, n.d.) (**fig1.1**).

Cholesterol is an essential component of the eukaryotic cell, where it plays very critical roles in maintaining membrane fluidity, permeability, bile acid formation, steroidogenesis and signal transduction.

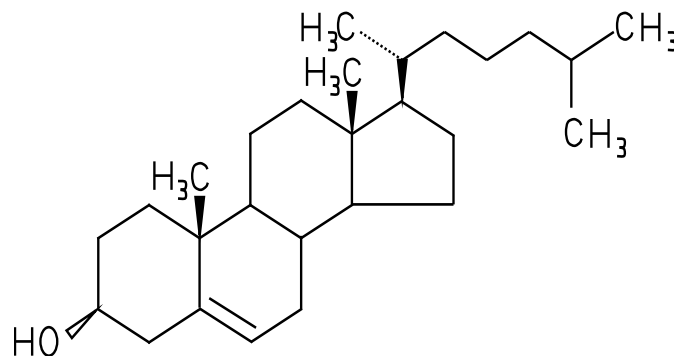


Fig 1. 1. Chemical structure of cholesterol

Cholesterol makes up 30 to 40% of cellular lipids, it is transported dynamically in the cell to various compartments where it elicits its functions. Cholesterol concentration is highest in the plasma membrane at 60 to 80%, where it helps maintain structural integrity (Maxfield & Wüstner, 2002), cholesterol is also found at 0.5-1% of cellular lipid in the endoplasmic reticulum where it is esterified for storage in lipid droplets or for lipoprotein secretion (Vance & Vance, 1990). In the mitochondria as well as peroxisome, cholesterol is oxidized and converted to bile acids or steroids (Ishibashi, Schwarz, Philip, Joachim, & David, 1996). Insufficient availability of cholesterol is detrimental to cellular function, body physiology, and tissue development. Similarly, excess cholesterol also poses deleterious effects, and as such cholesterol metabolism is adequately regulated by various mechanisms in the body (Yu, Zhang, Zheng, & Tang, 2019). Cholesterol is acquired either from dietary sources or by de novo synthesis from acetyl-CoA.

1.2.1 Cholesterol Biosynthesis

Cholesterol synthesis accounts for 75% of total cholesterol in the body, this synthesis occurs in cells of the liver, intestine, adrenal glands, and steroidogenic reproductive organs (Feingold & Grunfeld, 2000). Cholesterol is synthesized in the cell through an energy-consuming pathway that utilizes 18 moles of acetyl-CoA, 16 moles of NADPH and 36 moles of ATP. The de-novo synthesis of cholesterol starts in the cytoplasm, followed by a series of reactions catalyzed by enzymes resident in the endoplasmic reticulum and peroxisome (Voet & Voet, 2011). The rate-limiting step of the pathway is catalyzed by the enzyme Hydroxyl methyl glutaryl-CoA reductase (HMGCR), the reaction converts HMG-CoA to mevalonate. The cholesterol biosynthetic pathway also provides other sterol derived products such as Vitamin D, steroid hormones and non-sterol substances for the cell such as ubiquinone and heme A for electron transport, dolichol required for glycoprotein synthesis, farnesyl and geranylgeranyl pyrophosphate required for post-translational modification of proteins (Bradfute & Simoni, 1994). Cholesterol biosynthesis is the major source of cholesterol in the body and as such, it is tightly regulated to maintain adequate homeostasis.

1.2.2 Dietary Cholesterol

Cholesterol consumed in diet constitute about 25% of total cholesterol in the body, the human body is well equipped to absorb a large proportion of the cholesterol ingested. In order to attenuate the cumbersome and energy-consuming process of cholesterol biosynthesis, readily available cholesterol molecules are absorbed in the intestinal lumen (Jia, Betters, & Yu, 2011). Intestinal cholesterol absorption occurs in three stages which involve, (1) Emulsification and solubilization of cholesterol in mixed micelles containing bile acids and phospholipids, this is critical for the diffusion of free cholesterol across a layer of water in order to reach intestinal brush border membrane where cholesterol is taken up by enterocytes, (2) Transportation across the apical

membrane of enterocytes by the protein NPC1L1, (3) Mobilization and packaging to form chylomicrons to be secreted into the blood and lymph (Better & Yu, 2010). The intestinal uptake of cholesterol constitutes a major pathway for the body to obtain cholesterol and as such, it is an attractive drug target for the control of cholesterol in the body.

1.3 Lipoproteins and cholesterol transport

Cholesterol and triglycerides are hydrophobic, hence the effective transport of these lipids across the body requires associations with hydrophilic proteins in circulation to form lipoproteins. The proteins that help in the transport of these lipids are referred to as apolipoproteins. Apolipoproteins play multiple functions in their association with lipids aside from the formation of lipoproteins. 1) They act as ligands for lipoprotein receptors, 2) structural support for lipoproteins, 3) apolipoproteins serve as inhibitors or activators of enzymes critical for lipoprotein metabolism (Feingold & Grunfeld, 2000). **Table 1.1**

Lipoproteins are a complex biochemical assembly of proteins in association with lipids, consisting of a central hydrophobic inner core of lipophilic lipids such as cholesterol esters and triglycerides. The core of hydrophobic molecules is surrounded by an outer hydrophilic membrane consisting of a phospholipid layer in association with apolipoproteins, which shields the hydrophobic core of lipophilic lipids from surrounding environmental fluids and as such aid their transport (Ramasamy, 2014). Seven classes of plasma lipoproteins have been identified so far, with their classification based on size, the composition of lipid content and resident apolipoproteins: Chylomicrons, Chylomicron remnants, Very low-density lipoprotein (VLDL), Intermediate density lipoprotein

(IDL), Low-density lipoprotein (LDL), High-density lipoprotein (HDL) and Lipoprotein (a) (LPA)

Table 1.2.

Apolipoprotein	Molecular Weight (Da)	Main Source	Lipoprotein Association	Function
Apo A-I	28,000	Liver, Intestine	HDL, chylomicrons	Structural protein for HDL, Activates LCAT
Apo A-II	17,000	Liver	HDL, chylomicrons	Structural protein for HDL, and also Activates hepatic lipase
Apo A-IV	45,000	Intestine	HDL, chylomicrons	Participate in chylomicron assembly and secretion
Apo A-V	39,000	Liver	VLDL, chylomicrons, HDL	Promotes LPL mediated triglyceride lipolysis
Apo B-48	241,000	Intestine	Chylomicrons	Structural protein for chylomicrons

Apo B-100	512,000	Liver	VLDL, IDL, LDL, Lp (a)	A structural protein, Ligand for LDL receptor
Apo C-I	6,600	Liver	Chylomicrons, VLDL, HDL	Activates LCAT
Apo C-II	8,800	Liver	Chylomicrons, VLDL, HDL	Co-factor for Lipoprotein lipase
Apo C-III	8,800	Liver	Chylomicrons, VLDL, HDL	Inhibits Lipoprotein lipase and uptake of lipoproteins
Apo E	34,000	Liver	Chylomicron remnants, IDL, HDL	Ligand for low-density lipoprotein receptor
Apo (a)	250,000- 800,00	Liver	Lp (a)	Inhibits plasminogen activation

Table 1. 1- Types of Apolipoproteins, their sources, associations, and function as adapted and modified from (Feingold & Grunfeld, 2000).

Lipoprotein	Density (g/ml)	Size (nm)	Major Lipid content	Major Apolipoproteins
Chylomicrons	<0.930	75-1200	Triglycerides	Apo B-48, Apo C's, Apo E, Apo A-I, A-II, A-IV
Chylomicron Remnants	0.930- 1.006	30-80	Triglycerides Cholesterol	Apo B-48, Apo E
VLDL	0.930- 1.006	30-80	Triglycerides	Apo B-100, Apo E, Apo C's
IDL	1.006- 1.019	25-35	Triglycerides Cholesterol	Apo B-100, Apo E, Apo C's
LDL	1.019- 1.063	18- 25	Cholesterol	Apo B-100
HDL	1.063- 1.210	5- 12	Cholesterol Phospholipids	Apo A-I, Apo A-II, Apo C's, Apo E
Lp (a)	1.055- 1.085	~30	Cholesterol	Apo B-100, Apo (a)

Table 1. 2- Classes of Lipoproteins, their sizes, density, apolipoproteins and major lipid content as adapted and modified from (Feingold & Grunfeld, 2000)

The metabolism of lipoprotein particles is divided into three pathways depending largely on the source of the lipid content: dietary lipids (exogenous), from the liver through de novo synthesis (endogenous) and majorly originating from peripheral tissues back to the liver (reverse cholesterol transport).

1.3.1 Exogenous pathway

The exogenous pathway is also known as the chylomicron pathway, given that chylomicrons are the major lipoproteins involved in the transport of dietary lipids. Bile emulsified dietary fat and triglycerides (TG) are hydrolyzed by pancreatic lipases to form fatty acids and monoacylglycerol. Fatty acids and monoacylglycerol are readily absorbed, while cholesterol uptake from the intestinal lumen into intestinal cells of enterocytes is facilitated by NPC1L1. In the enterocytes, fatty acids and monoacylglycerols are re-esterified to form TG while free cholesterol is esterified to form cholesteryl esters, these lipids are then assembled with apolipoprotein B-48 (ApoB48) and phospholipids to form nascent chylomicrons. These particles are then secreted into the intestinal lymph where they are further delivered via the thoracic duct into the systemic circulation. The chylomicrons then interact with HDL particles and acquire apolipoprotein C and E (ApoC-I, ApoC-II, ApoC-III and ApoE), at this stage the nascent chylomicron is said to be matured. ApoC-II plays a critical role in chylomicron metabolism, it serves as a cofactor for lipoprotein lipase (LPL), which hydrolyzes TG on chylomicrons to free fatty acids and glycerol (Cooper, 1997). The fatty acids are taken up by peripheral tissues such as muscles for energy or adipose tissue for storage in lipid droplets. Lipolysis of chylomicrons leads to continuous shrinkage in size due to the loss of TG content, which eventually forms chylomicron remnants enriched in cholesterol esters and ApoE. These remnant chylomicrons continue in circulation until they are cleared by the

Low-density lipoprotein receptor (LDLR) and LDLR-related protein 1 (LRP1) in the liver (Brown & Goldstein, 1983).

1.3.2 Endogenous pathway

A central organ for lipid handling in the body is the liver, the endogenous pathway involves hepatic metabolism and secretion of apolipoprotein B containing particles, such as VLDL. (Rader & Hobbs, 2014). TG and cholesteryl esters are assembled in the hepatocytes with apolipoprotein B-100 and phospholipids to form nascent VLDL particles. The nascent VLDL particles enter the bloodstream where they further interact with HDL particles; consequently, there is a transfer of Apo-E and Apo-C's to the nascent VLDL from HDL, which makes it attains maturity. Matured VLDL particles are hydrolyzed by LPL in a similar fashion as described with chylomicrons, generating glycerol and free fatty acids taken up by peripheral tissues. The diminished and hydrolyzed VLDL is also enriched in cholesteryl ester by cholesteryl ester exchange transfer from HDL in a reaction catalyzed by the enzyme cholesteryl ester transfer protein (CETP) to form intermediate-density lipoprotein (IDL) in humans (Mabuchi, Nohara, & Inazu, 2014). The liver can clear IDL's from circulation by LDLR and LRP, further lipolysis of IDL by hepatic lipases leads to the loss of TG and all other apolipoproteins except ApoB-100, the IDL remnants left now forms LDL, with a relatively high cholesterol content. LDL continues in circulation until it is cleared by the liver and other tissues that possess the LDLR.

1.3.3 Reverse cholesterol transport

Accumulation of cholesterol in peripheral cells occurs via uptake of lipoproteins in circulation and de novo synthesis of cholesterol, however, cholesterol cannot be broken down in catabolism. It needs to be converted to form other biologically relevant biomolecules. Cells involved in steroid hormone production convert cholesterol into sterols such as testosterone, estrogen and glucocorticoids, while the liver converts cholesterol to form bile acids that are secreted into the bile. It is important for cells to reduce their cholesterol content as excessive cholesterol is toxic to the cells, this is achieved by efflux and transport of cholesterol back to the liver in the process referred to as the classic reverse cholesterol transport which is facilitated by HDL. The ATP binding cassette proteins A1 and G1 (ABCA1 & ABCG1) are critical for the efflux of cholesterol from cells to lipid poor pre-beta Apo A-I particles and HDL, respectively. It has been shown that Scavenger Receptor class B1 (SR-B1) may also play a role in the efflux of cholesterol to HDL particles, in addition, passive cholesterol diffusion from the plasma membrane to HDL may also contribute to cholesterol efflux (Rosenson et al., 2012). Free cholesterol acquired from efflux on HDL is then esterified by lecithin-cholesterol acyltransferase (LCAT); this enzyme binds to HDLs and catalyzes a two-step reaction of fatty acid cleavage from phospholipids and transesterification of cholesterol, which is later sequestered to the lipoprotein core, thereby transforming newly synthesized small HDLs into larger and spherical lipoproteins (Fielding, Shore, & Fielding, 1972; Jonas, 1991). After cholesterol transfer from cells and maturity of HDL, the pathway for clearance of cholesterol by the liver is destined for either of two paths, 1) HDL can be selectively taken up by SR-B1 on the liver, alternatively 2) CETP can transfer cholesterol esters from HDL to other ApoB containing lipoproteins such as VLDL, Chylomicron remnants and LDL, which can then be taken up by the liver. Once cholesterol has been delivered to the liver, it can be eliminated by direct

secretion into the bile or converted into bile acids and then secreted into the bile. ABCG5 and ABCG8) activate cholesterol transport into the bile while the expression of these genes is upregulated by the Liver X receptor (LXR) (Fielding & Fielding, 1995).

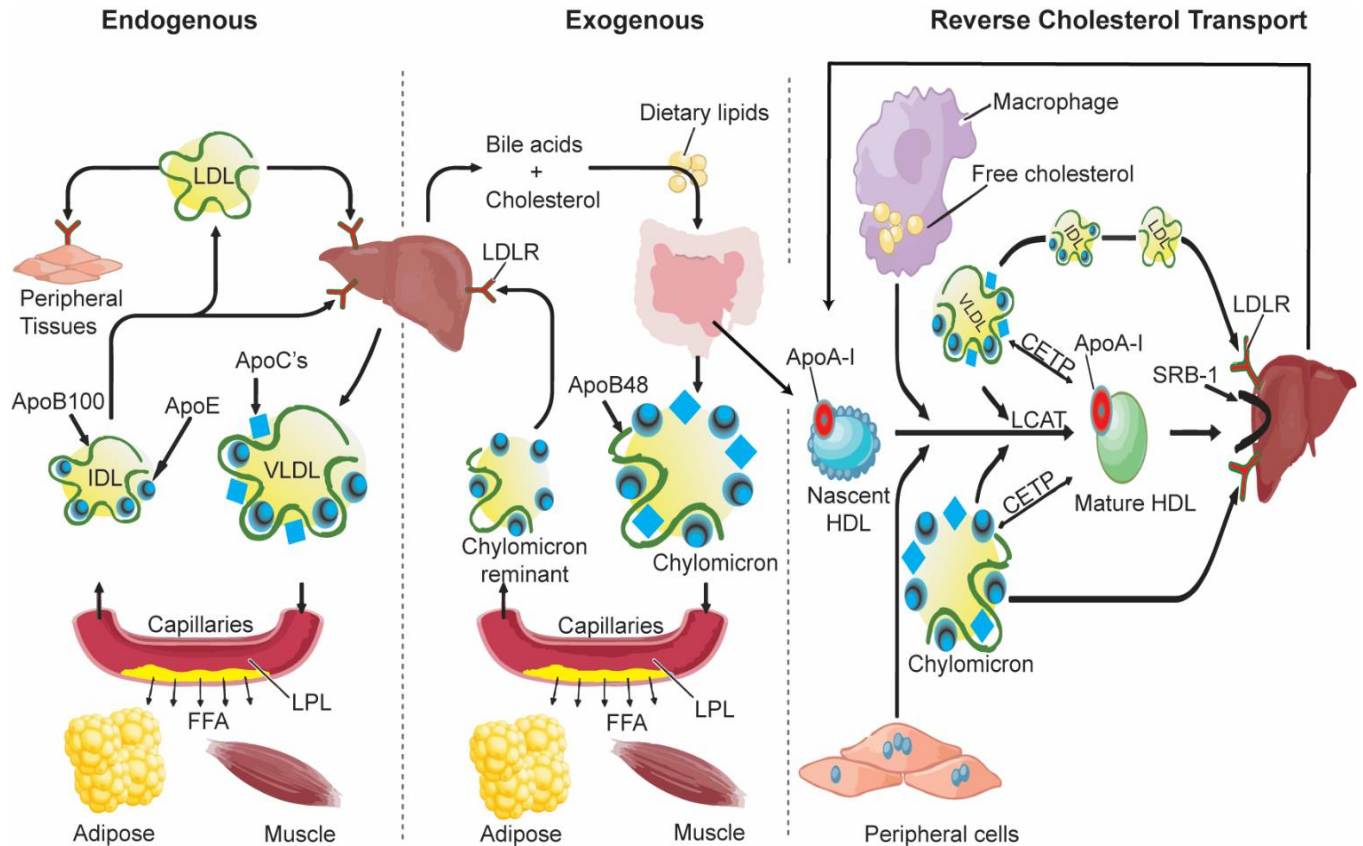


Fig 1. 2. Lipoprotein metabolism. The fate of lipids derived from endogenous synthesis, exogenous dietary consumption, and reverse cholesterol transport. Figure made by Adekunle Alabi, idea adapted from (Rader & Hobbs, 2014)

1.4 The Low-Density lipoprotein receptor

The identification and characterization of LDLR is credited to the work of Brown and Goldstein in 1973, during their search to unravel the molecular basis for familial hypercholesterolemia (FH) (Goldstein & Brown, 2009a). Brown and Goldstein observed that healthy fibroblasts suppressed

endogenous synthesis of cholesterol after cells were supplied with cholesterol via serum LDL. On the other hand, fibroblasts from FH patients did not suppress endogenous cholesterol synthesis after treatment with serum LDL except when cholesterol was provided directly in soluble forms other than the LDL (Goldstein & Brown, 1974). Their studies led to the discovery of a cell surface receptor for LDL which was called the LDL-receptor and the mechanism involved in the way LDLR carries out its function. Brown and Goldstein consequently discovered that FH was caused by a genetic defect in the LDL-receptor.

1.4.1 Structure and function of the low-density lipoprotein receptor

The *LDLR* gene contains 18 exons and 17 introns with a 45kb sequence, mapped on chromosome 19 in bands p13.1-13.3 in humans (**fig 1.3**) and on chromosome 9 in mice (Lindgren, Luskey, Russell, & Francke, 1985). The length of its mRNA transcript is 5.3kb, a large proportion of this transcript is occupied by a 2.7kb 3' untranslated protein region, leaving 2.6kb of the mRNA transcript which encodes an 860-amino acid protein.

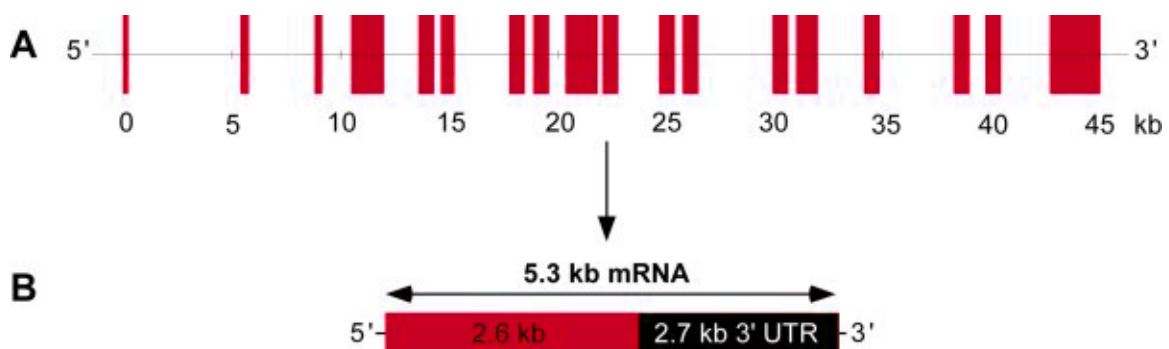


Fig 1. 3. Diagrammatic representation of the LDLR gene. A) 45kb LDLR gene encodes 18 exons and 17 introns, B) Transcript of LDLR mRNA with 2.7 kb of 3' untranslated region (3'UTR) and 2.6kb protein-coding region. Adapted and modified from (Al-Allaf et al., 2010).

The *LDLR* mRNA is translated by the established cellular apparatus involved in protein synthesis in the endoplasmic reticulum (ER) (Al-Allaf et al., 2010). The immature LDLR protein in the ER is further transported across the secretory pathway where it acquires post-translational modification with the incorporation of O-linked carbohydrate sugar chains in the Golgi apparatus, after which a 160kda matured protein is translocated to the cell surface (Hobbs, Russell, Brown, & Goldstein, 1990).

1.4.1.1 Structural Domains of the LDLR and their function

The LDLR is an 860 amino acid protein. However, it matures into an 839 amino acid glycoprotein on the plasma membrane after the removal of its signal peptide (Beglova & Blacklow, 2005). Exon 1 of the *LDLR* encodes the signal peptide and the 5' untranslated region (5'UTR).

Exon 2 to 6 encodes the ligand-binding repeats. This region contains seven repetitive groups of approximately 40 amino acids, which serves as ligand binding repeat 1 to 7. Each of these repeats is encoded mainly by a single exon except in the case of repeat 3,4 and 5 which are joined by a single exon (Hobbs et al., 1990). Each ligand binding repeat contains a total of 6 cysteine residues capable of forming three intra-repeat disulfide bonds coordinated to a calcium ion forming an octahedral lattice, which gives the protein stability and flexibility required for its effective function in the harsh internal environment of the cell (Brown, Herz, & Goldstein, 1997). The C-terminal region of each repeat contains a negatively charged triplet of Ser-Asp-Glu, which is critical for ligand binding. The LDLR binds two major apolipoproteins, ApoB-100 on LDL and ApoE on ApoE containing lipoproteins such as VLDL, chylomicron remnants and HDL; both apolipoproteins are enriched with basic and positively charged amino acids which may mediate the ionic interaction between negatively charged ligand-binding repeats and positively charged

apolipoproteins (Brown et al., 1997). Deletion mutants generated within the ligand-binding repeats (LRs) reveal that LR3 to LR7 is important for LDL binding, as deletion of any repeat within this region abrogates LDL uptake on the cell surface (Beglova & Blacklow, 2005). LR4 to LR5 of the LDLR is sufficient enough to bind to ApoE lipoproteins of β -VLDL particles (Fisher, Abdul-Aziz, & Blacklow, 2004), indicating these regions as important for VLDL binding to LDLR. The ligand-binding repeats are not in direct contact with each other but rather contain linkers of four to five residues except for the linker between LR4-5 which contains 12 residues. These linkers impact the flexibility of the LRs by reducing contact constraints, such that the LDLR is able to adjust its shape to bind its various lipoprotein ligands of different shapes and sizes (Beglova & Blacklow, 2005; Rudenko et al., 2002).

The ligand-binding repeats are immediately followed by the epidermal growth factor (EGF) precursor, which is composed of 400 amino acids sequence encoded by exons 7-14. It shares a 33% sequence homology to the human epidermal growth factor gene (Sudhof, Goldstein, Brown, & Russell, 1985). The EGF consists of three repeats A, B and C with 40 amino acid sequence rich in cysteine, EGF B and C are separated by a 280-amino acid sequence called the YWTD β -propeller domain. The EGF is critical for acid-dependent dissociation of ligands in the endosome during the process of recycling. Deletion of the whole EGF region does not affect ligand binding but rather causes the receptor to lose its ability to release its ligands at low pH, hence the mutant receptor fails to be recycled and is more prone to degradation (Davis et al., 1987). The β -propeller serves as the critical region within the EGF that mediates ligand release, it displaces lipoprotein ligands and serves as an alternative substrate for LR4-5. The LDLR has an open conformation on the cell surface at neutral pH; however, it takes a closed conformation in the acidic pH of the endosome. This is as a result of histidine residues within the β -propeller acquiring a net positive

charge that can form ionic interaction with the ligand binding repeats (Innerarity, 2002). The interaction between the positively charged histidine in the β -propeller and negatively charge in the ligand binding repeats ultimately leads to the release of ligands.

The O-linked sugar region follows the EGF region, it is a 58 amino acid sequence encoded by exon 15. This domain serves as the region for post-translational modification with the attachment of O-linked carbohydrates, the region is enriched with threonine and serine which aids its participation in the formation of O-glycosidic bonds with sugars. Aside from giving the protein stability in the presence of cellular proteases, the function of the O-linked sugar domain is not well understood. The complete deletion of this domain does not affect LDLR functionality in fibroblasts (Davis et al., 1986). It has been postulated (Gent & Braakman, 2004) that the O-linked sugar region may; 1) act as a spacer that helps push the LDLR beyond the extracellular matrix and modulate the presentation of the LDLR extracellular domain, 2) stabilize the LDLR in the acidic pH of the endosome and/or 3) help prevent proteolytic cleavage of the LDLR extracellular domain by metalloproteinase on the cell surface (Kozarsky, Kingsley, & Krieger, 1988).

Exon 16 and the 5' section of exon 17 encode 22 hydrophobic amino acid sequence which makes up the membrane-spanning domain of the protein. This region helps maintain the protein integration into the plasma membrane, mutations or deletion of this region lead to mislocalization of the protein with respect to the plasma membrane, and as such the 160kDa protein is secreted out of the cell, thus losing its functionality (Strøm, Laerdahl, & Leren, 2015). Similarly, mutations in this region have been reported to predispose LDLR to metalloproteinase shedding of its ectodomain, causing the release of a soluble form of LDLR (sLDLR) into cell culture media (Strom, Tveten, Laerdahl, & Leren, 2014).

The rest of Exon 17 and the 5' end of exon 18 encode a 50-amino acid cytoplasmic domain. The cytoplasmic tail of the LDLR contains sequences critical for receptor clustering in clathrin-coated pits and internalization of the receptor (Keyel et al., 2006). One of the most prominent motifs within this region is the NPVY that is required for internalization of the LDLR; mutation of tyrosine at position 807 in this motif to cysteine causes familial hypercholesterolemia as a result of the inability of the LDLR to internalize its ligands. This mutation is known as the J.D mutation coined from the patient which the mutation was first identified (Davis et al., 1986).

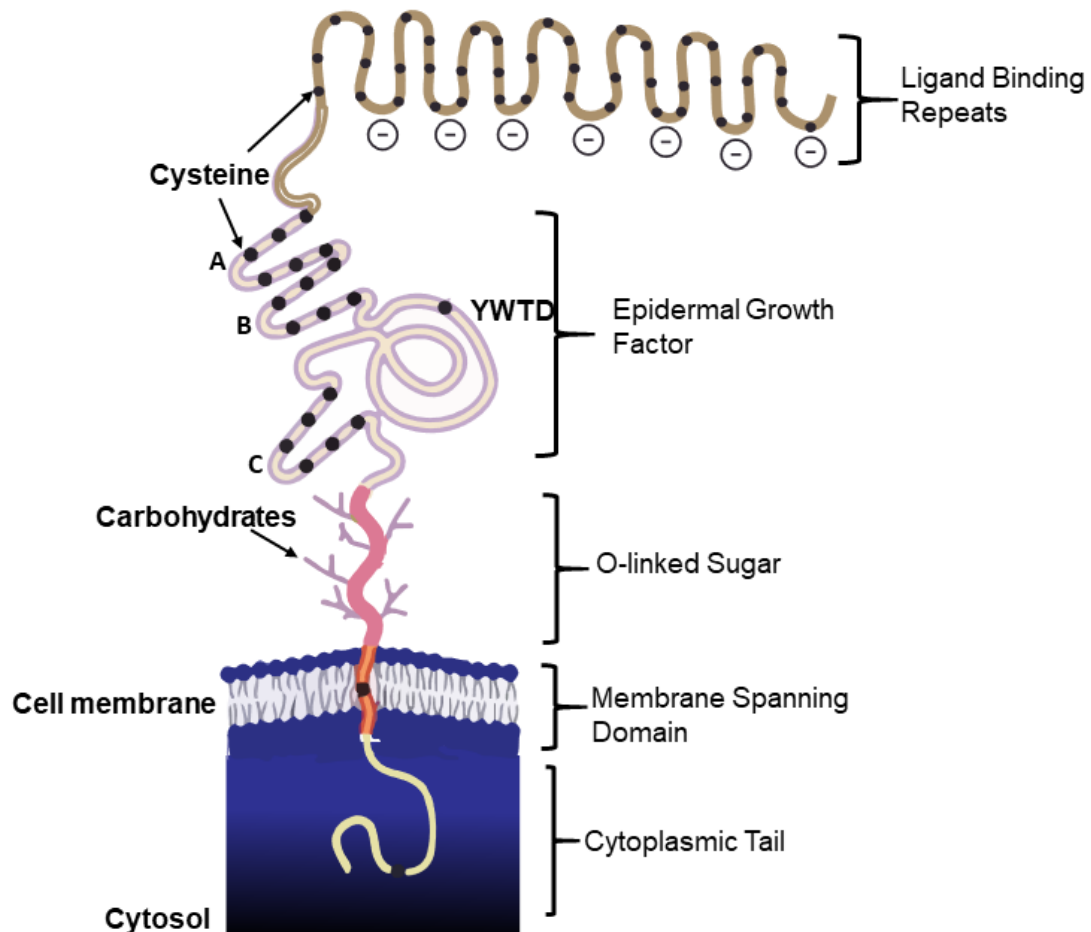


Fig 1. 4. Structural representation of the low-density lipoprotein receptor. Indicating its domains. Figure made by Adekunle Alabi, idea adapted from (Al-Allaf et al., 2010)

1.4.1.2 LDLR ligand binding, endocytosis, and Recycling

The matured LDLR is an integral membrane glycoprotein, which binds to and mediates the internalization of its ligands on the cell surface, majorly lipoprotein particles containing apoB100 or E. Lipoproteins internalized by the LDLR include LDL, VLDL, IDL and chylomicron remnants (Goldstein, Brown, Anderson, Russell, & Schneider, 1985). The interaction of apoE with LDLR is driven by lipidation of the particle, lipid depleted apoE particles have 500 times less affinity for LDLR binding (Wilson, Wardell, Weisgraber, Mahley, & Agard, 1991). It is possible that apoE lipidation causes conformational changes that lead to rearrangement and exposure of basic residues on the surface (Sehayek, Lewin-Velvert, Chajek-Shaul, & Eisenberg, 1991). The ability of apoB100 to bind LDLR is dependent on the conformation of its C-terminal domain which bears the LDLR binding site, this region is essential because it contains motifs enriched in arginine and lysine residues which can form ionic interaction with negatively charged acidic residues in the ligand-binding repeats of the LDLR (Boren et al., 1998).

After binding to its ligands on the cell surface, the LDLR undergoes receptor-mediated endocytosis by associating with clathrin-coated pits. The LDLR is then internalized into the acidic environment of the endosome where it separates from the ligand, the ligand is delivered to the lysosome where cholesterol esters are hydrolyzed into its constituents, free cholesterol and fatty acids, while the apolipoproteins are degraded into free amino acids (Goldstein et al., 1985). The LDLR, on the other hand, is quickly recycled back to the cell surface, where it can initiate another ligand binding (**fig1.5**). Every 10 to 20 minutes, the LDLR undergoes a complete cycle of ligand binding, endocytosis, endosomal discharge of ligand and recycling (Brown et al., 1997).

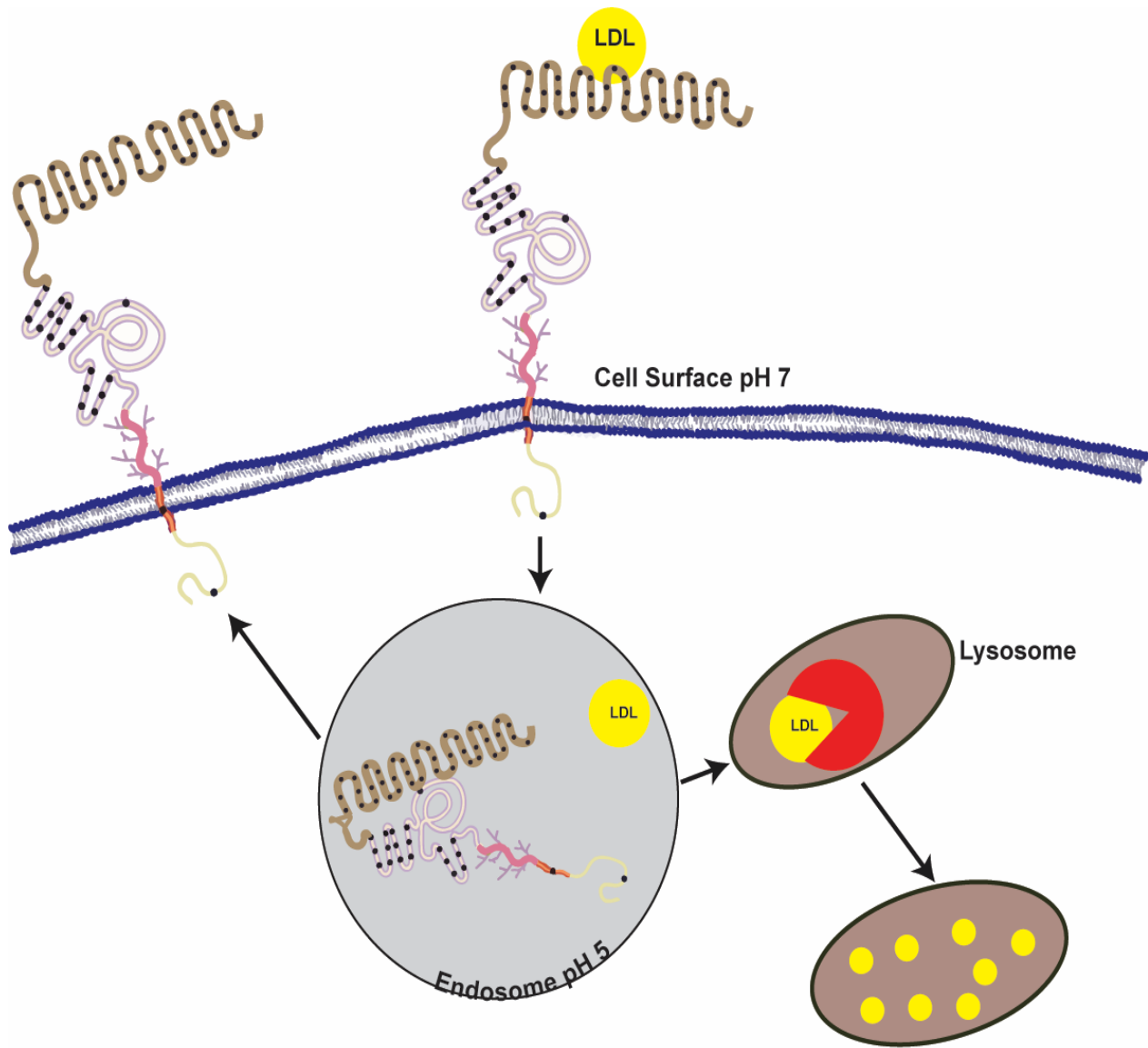


Fig 1. 5. LDLR uptake of LDL. The LDLR binds to LDL on the cell surface and mediates LDL uptake into the cell via endocytosis. Endosomal low pH leads to the release of LDL and LDLR is recycled to the cell. Consequently, the LDL is degraded in the lysosome. Figure made by Adekunle Alabi.

1.4.2 LDL Receptor-Related Proteins

The LDLR is a member of a family of receptors, which bind and internalize multiple ligands including exotoxins, lipid carrier complexes as well as lipoproteins (Willnow, Nykjaer, & Herz, 1999). Family members are functionally and structurally related to LDLR; containing ligand-binding repeats, Epidermal growth factor-like domain, β propeller, O-linker sugar region except in LRP1 and the NPXY motif required for receptor-mediated endocytosis. The differences in the number of occurrences and positioning of each of the domains create diversity in the LDLR family proteins (Go & Mani, 2012). LDLR, LRP1, VLDLR, and ApoER2 (LRP8) are ApoE receptor members of this family that play a pivotal role in lipid metabolism. They have also been reported to exist as soluble circulating forms, resulting from shedding by proteases (Rebeck, LaDu, Estus, Bu, & Weeber, 2006).

VLDLR and ApoER2 are the most structurally related to LDLR, while VLDLR is mainly expressed in adipose tissues, endothelial cells of capillaries, heart, and skeletal muscles but not in the liver; ApoER2 is mainly expressed in the brain, testis, and placenta. VLDLR regulates the extrahepatic metabolism of lipoproteins enriched in TG, by uptake of TG-rich VLDL but not LDL, providing sufficient energy substrates for peripheral tissues (Go & Mani, 2012). ApoE containing VLDL is not only restricted to binding VLDLR but also other family proteins such as LDLR, ApoER2, and LRP1. LRP1 is ubiquitously expressed in most tissues and functions as a scavenger receptor mediating the uptake of numerous ligands such as anionic liposomes, lipoprotein lipase, thrombospondins 1 and 2, 2-macroglobulin-protease complexes, and matrix metalloproteinases MMP-13, MMP-2 (gelatinase A), and MMP-9 (gelatinase B) (Rozaanov, Hahn-Dantona, Strickland, & Strongin, 2004).

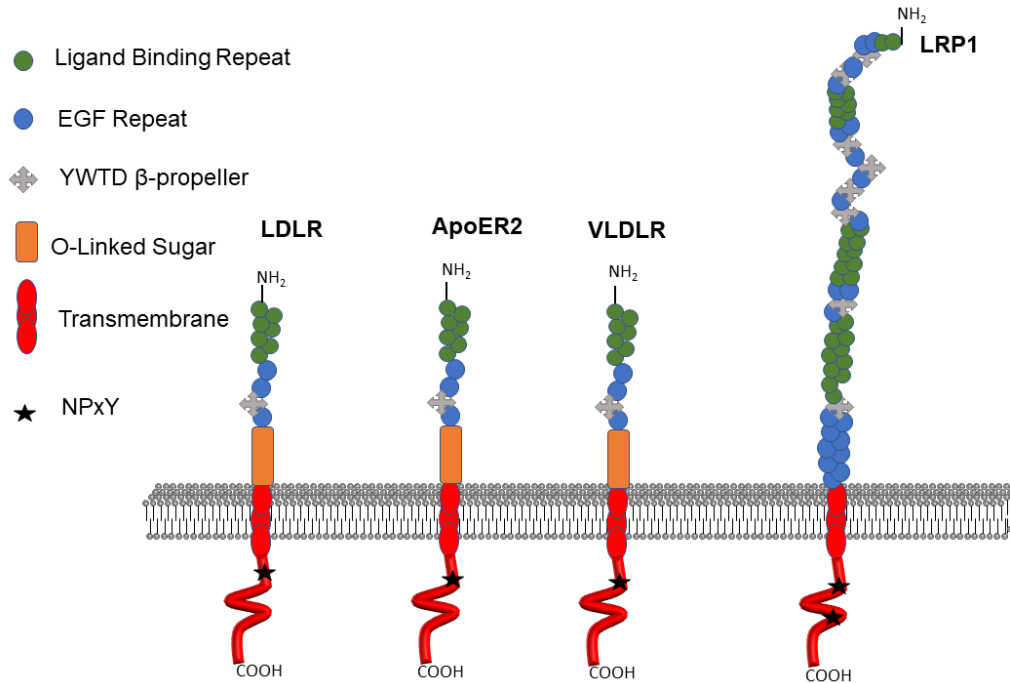


Fig 1. 6. Pictorial description of LDLR-related proteins, with structural comparison to the LDLR. Each receptor consists of ligand repeats, epidermal growth factor, YWTD, transmembrane, NPxY motif, and an O-linked sugar domain except for LRP1. Figure made by Adekunle Alabi, idea adapted from (Rebeck et al., 2006)

1.5 The Role of LDL- cholesterol in Cardiovascular Diseases

Hypercholesterolemia is simply described as a state of elevated cholesterol levels in circulation. The condition is characterized by a high circulating amount of non-HDL lipoproteins, majorly in the form of LDL-C. Hypercholesterolemia is usually caused by a disturbance in the normal homeostasis of cholesterol, which may be as a result of increased secretion of cholesterol-containing lipoproteins into circulation or reduced clearance of cholesterol as a result of factors that compromise the function of LDLR. Hypercholesterolemia can be polygenic, developing from

inappropriate lifestyle (diet, smoking, lack of physical activity, obesity, and excessive alcohol consumption) and activities of multiple genes. The other type is a Mendelian disorder called familial hypercholesterolemia (FH) which results from defects in a single gene (Fairwozy, 2018).

Cholesterol type	mg/dL	mmol/L	Interpretation
Total cholesterol	<200	<5.2	Normal
	200–239	5.2–6.2	Borderline
	>240	>6.2	High
LDL cholesterol	<100	<2.6	Desirable
	100–129	2.6–3.3	Normal
	130–159	3.4–4.1	Borderline
	160–189	4.1–4.9	High and undesirable
	>190	>4.9	Very high
HDL cholesterol	<40	<1.0	Undesirable; increased risk of CVD
	41–59	1.0–1.5	Normal, but not optimal
	>60	>1.55	Good; lowered risk of CVD

Table 1. 3-Interpretation of levels of cholesterol in humans. Adapted from (“Understanding Your Cholesterol Numbers | Cleveland Clinic,” n.d.)

Evidence of a relationship between cholesterol and cardiovascular disease (CVD) dates back to 1913 when Nikolaj Nikolajewitsch Anitschkow established a correlation between high levels of cholesterol and the development of atherosclerosis (Anitschkow N, 1913) since then LDL-

cholesterol has been shown to be one of the leading causes of CVD's. Similarly, the reduction of LDL-cholesterol has been shown to reduce the incidence of CVD's (Storey et al., 2018).

1.5.1 Atherosclerosis

Atherosclerosis is a leading cause of cardiovascular diseases, and it is characterized by chronic lipid accumulation and inflammatory conditions in blood vessels. This results from an imbalance of lipid metabolism and a compromised immune response driven by the accumulation of cholesterol-laden macrophages in the walls of the arteries (Kerr, 2016; Libby, Ridker, & Hansson, 2011). It is a progressive disorder with multiple stages, causing various extent of lesion at each stage of development. The process is mostly initiated by the retention and deposition of apoB containing lipoproteins, especially LDL-cholesterol, in the sub-endothelium. Retention is facilitated by the interaction of positively charged residues on apoB and negatively charged sulfate groups of proteoglycans on the arterial wall (Khalil, Wagner, & Goldberg, 2004). After retention in the intima, the LDL-cholesterol is susceptible to oxidation by reactive oxygen species and other enzymes such as lipoxygenases, generating oxidized LDL (oxLDL). The accumulation of oxLDL leads to the recruitment of lymphocytes and monocytes with an increase in the presence of growth factors and cytokines. Eventually, monocytes are converted to macrophages which then uptake oxLDL (Libby et al., 2011). Macrophages take up oxLDL through scavenger receptors in an unregulated fashion, becoming lipid loaded and eventually turning into foam cells (Steinberg & Witztum, 2010), which form fatty streak lesions that eventually activate inflammatory responses. During atherogenesis, smooth muscle cells migrate from the media of arterial wall to the intima, where they proliferate and produce extracellular matrix materials such as elastin and collagen, forming a fibrous cap to cover plaques. Smooth muscles also take up oxLDL and become foam cells. In humans and *ApoE* knockout mice, most foam cells are derived from smooth muscle cells

(Wang et al., 2019). Continuous accumulation of cholesterol crystals, extracellular lipids from apoptotic cells and debris of dead plaque macrophages and smooth muscle cells, leads to the formation of a necrotic core within the plaque. Plaque rupture may occur from the degradation of the extracellular matrix by metalloproteinases such as collagenases and gelatinases. The destabilization of plaques may cause thrombosis and ultimately a blockage of the artery, leading to cardiovascular dysfunctional diseases (Libby et al., 2011).

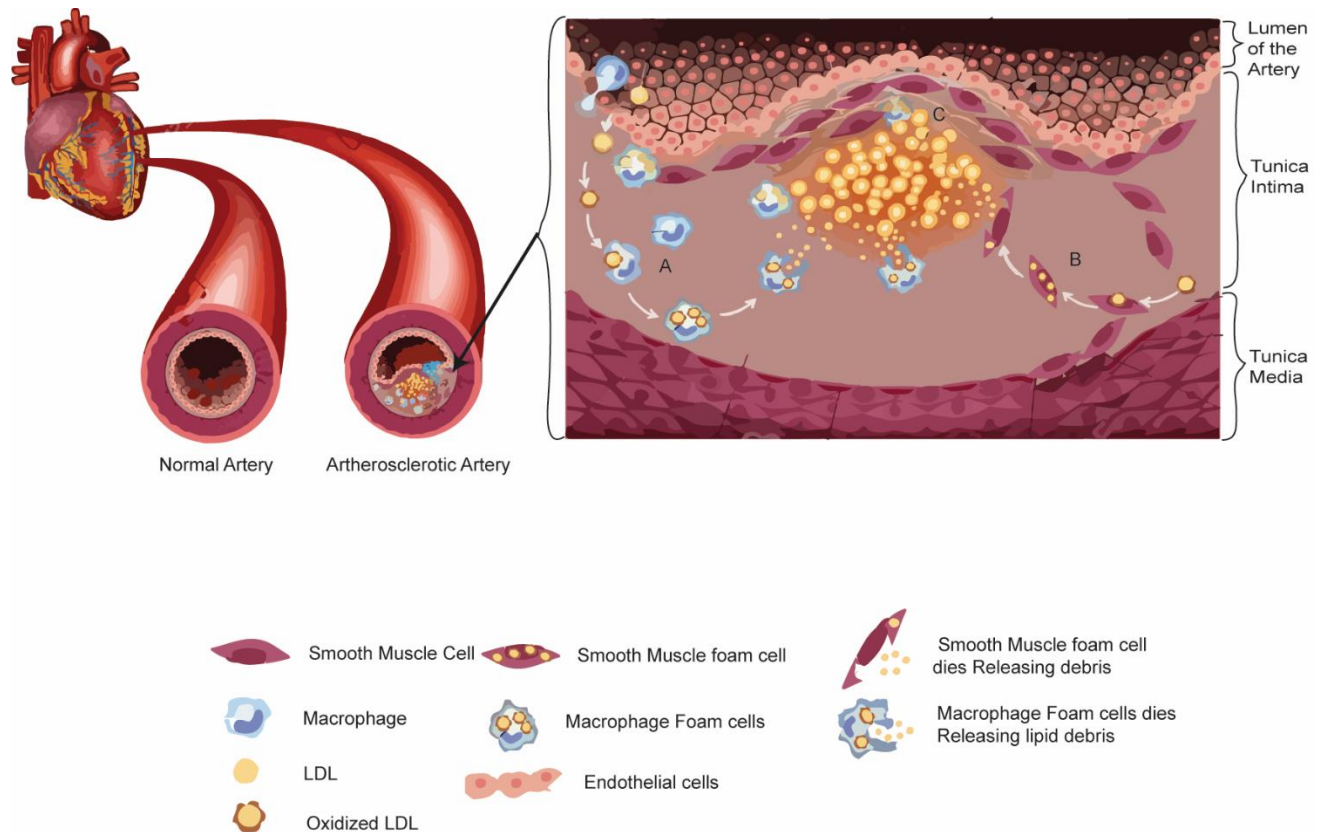


Fig 1. 7. Diagrammatic representation of the sequence of events leading to the development of atherosclerotic plaque. A – Macrophages uptake oxLDL in the intima and transforms into foam cells, which eventually leads to their death and release of lipid debris. B- Smooth muscle cells uptake oxLDL and become foam cells. They migrate from the media of arterial wall to the intima, where they proliferate and produce extracellular matrix materials, forming a fibrous cap to cover plaques. C - Continuous accumulation of cholesterol crystals, extracellular lipids from apoptotic cells, the debris of dead plaque macrophages and smooth muscle, leads to the formation

of a necrotic core within the plaque. Figure made by Adekunle Alabi, idea adapted and modified from (“Atherosclerosis. Fibrous Plaque Formation In The Artery. Artery.. Royalty Free Cliparts, Vectors, And Stock Illustration. Image 38814972.,” n.d.)

1.5.2 Statin Treatment of Hypercholesterolemia

Statins are currently the primary therapy for the treatment of hypercholesterolemia, it has been reported to reduce the incidence of cardiovascular events by 31% as a result of a 26% reduction in LDL-cholesterol from the West of Scotland Coronary Prevention Study (Shepherd et al., 1995). Statins elicit their action by inhibiting the rate-limiting enzyme of the cholesterol biosynthetic pathway HMG-CoA reductase. Inhibition of the enzyme sends a low sterol signal in the cells, which causes cellular processing of the transcriptional factor SREBP2. The transcriptional active form of SREBP2 binds to the sterol response element (SRE) in the promoter of the *LDLR* gene and upregulates its transcription, ultimately increasing the levels of LDLR on the cell surface and consequently enhancing the clearance of LDL-cholesterol from circulation (Stancu & Sima, 2001). Despite efficiency credited to the use of statins, often the target LDL-C concentrations cannot be attainable with statin monotherapy in many patients with familial or polygenic hypercholesterolemia. Hence, the aim of treatment would be to maximize LDL-C reduction attainable with an appropriate combination of treatments at tolerable doses. An example is the use of statins in combination with cholesterol absorption inhibitor ezetimibe (Fairwozy, 2018). Side effects associated with the use of statins have also been noticed in patients on the medication. This includes muscle pains, sleep disorders, nausea, rash, erectile dysfunction, and arthritis (Banach et al., 2015). Current research in the field focuses on the development of alternative therapy to statins or therapies that could be used in combination with statins.

1.6 Regulation of the low-density lipoprotein Receptor

1.6.1 Transcriptional Regulation

The promoter of *LDLR* contains sterol sensing sequences called the SRE, which is responsible for the transcriptional regulation of *LDLR* (Südhof, Russell, Brown, & Goldstein, 1987). The transcription factor SREBP2 binds to the SRE and initiates the transcription of *LDLR* and other genes involved in cholesterol biosynthesis (Horton et al., 2003).

SREBP-2 is located on the ER and its processing is strictly regulated by sterols and the levels of intracellular cholesterol. SREBP-2 in the ER exists in a complex with a sterol sensing protein SREBP-Cleavage Activating Protein (SCAP) that interacts with an ER protein, Insulin Induced gene (INSIG) when the levels of cholesterol in the ER are more than 5% of total ER lipids. The association between INSIG and SCAP keeps the SREBP and SCAP complex in the ER (Eberlé, Hegarty, Bossard, Ferré, & Foufelle, 2004). When the concentration of cholesterol in the ER is below 5% of total ER lipids, the association between INSIG and SCAP is severed, such that the SREBP-2/SCAP complex can be transported to the Golgi apparatus (Radhakrishnan, Goldstein, McDonald, & Brown, 2008). On arrival in the Golgi, the SREBP-2 is cleaved by site 1 & 2 proteases (S1P & S2P) sequentially, thereby releasing the mature and active N-terminal domain of SREBP. This is then able to enter the nucleus where it binds to the SRE and activates the transcription of *LDLR* (Brown & Goldstein, 2009).

1.6.2 Post-translational regulation of LDLR

1.6.2.1 Proprotein Convertase Subtilisin/ Kexin type 9 (PCSK9)

PCSK9 is a serine protease predominantly synthesized in the liver as a 75kDa proprotein (Shapiro, Tavori, & Fazio, 2018). It consists of a pro-domain which stays loosely attached to the protein after autocatalytic cleavage; a catalytic domain that has no other known proteolytic target than its own autocatalysis and a C-terminal domain (Tibolla, Norata, Artali, Meneghetti, & Catapano, 2011). Hepatic expression of *PCSK9* is mainly dependent on the levels of intracellular sterols. *PCSK9* is regulated alongside other genes involved in cholesterol metabolism such as HMG-CoA reductase, HMG-CoA synthase and *LDLR* (Horton et al., 2003). *PCSK9* promoter contains SRE, which is a binding site for SREBP2, and as such SREBP2 initiates the transcription of *PCSK9* (Tibolla et al., 2011).

PCSK9 is known to interact and bind with the *LDLR* intracellularly within the trans-Golgi or extracellularly at the cell surface. In both cases. Binding of *PCSK9* to the *LDLR* targets the receptor for lysosomal degradation, ultimately abrogating the recycling of the receptor (Lagace, 2014). At neutral pH, the *PCSK9* catalytic domain interacts with the EGF-A domain of *LDLR* at a 1:1 stoichiometry (Zhang et al., 2007). The *PCSK9*-*LDLR* interaction is further strengthened on arrival in the low pH environment of the endosome probably via the binding of *PCSK9* c-terminal domain to the ligand-binding repeats of the *LDLR* (Yamamoto, Lu, & Ryan, 2011). This blocks the recycling of the *LDLR* and redirects the *LDLR/PCSK9* complex for lysosomal degradation.

1.6.2.2 Inducible Degradation of LDLR (IDOL)

IDOL is an E3 ubiquitin ligase, widely expressed in tissues such as the lung, liver, kidney, placenta, brain, muscle, heart, and pancreas. The protein is regulated by the sterol sensing transcriptional factor Liver X Receptor (LXR), high levels of cellular cholesterol lead to the production of oxysterols which serves as ligands for the LXR activation (Janowski et al., 1999). LXR activation causes the induction of genes that encode proteins critical for cholesterol efflux and reduction of cholesterol influx into the cell (Zhang, Reue, Fong, Young, & Tontonoz, 2012).

IDOL ubiquitinates the LDLR cytoplasmic domain and targets the protein for lysosomal degradation (Sorrentino & Zelcer, 2012). Overexpression of IDOL in mice liver via adenovirus showed a significant reduction in the LDLR accompanied by elevated levels of plasma LDL cholesterol (Zelcer, Hong, Boyadjian, & Tontonoz, 2009).

1.6.2.3 LDLR shedding

The term shedding describes the proteolytic cleavage and removal of a portion or entire ectodomain of a protein from the membrane into extracellular space, leading to alteration of the protein function (Lichtenthaler, Lemberg, & Fluhrer, 2018). Shedding is not limited to proteins in the plasma membrane; it occurs in all cellular organelles of the endocytic and secretory pathway and in regions within or outside the transmembrane domain of such proteins. Proteases involved in the process include membrane-bound, soluble and intramembrane proteases (Lichtenthaler et al., 2018). The proteases involved in the process of shedding are referred to as sheddases. The process has emerged as a critical mechanism to control protein abundance, release of growth

factors and cytokines from the membrane, and degrade receptors and adhesion proteins (Black et al., 1997; Peschon et al., 1998).

Soluble forms of ApoE receptor subfamily members such as LRP1, ApoER2, VLDLR, and LDLR have been observed *in vitro* and *in vivo*. They are generated from the shedding of the transmembrane receptors (Garcia-Touchard et al., 2005) or as a result of alternatively spliced mRNAs lacking the transmembrane domain (Xing, Xu, & Lee, 2003). Both processes are critical for the regulation of ApoE receptors and their functions. γ -secretase, furin and sheddases have all been implicated in the cleavage of ApoE receptors (**Fig 1.8**) (LRP1, ApoER2, VLDLR and LDLR) (Rebeck et al., 2006).

The ectodomain of the LDLR can be cleaved by sheddases releasing a soluble extracellular LDLR (sLDLR) into cell culture media and human plasma (Begg, Sturrock, & van der Westhuyzen, 2004; Fischer, Tal, Novick, Barak, & Rubinstein, 1993). Serum levels of sLDLR are positively correlated with plasma LDL-cholesterol (LDL-C) levels (Shimohiro, Taniguchi, Koda, Sakai, & Yamada, 2015). The sheddase responsible for LDLR cleavage has not been identified. However, broad-spectrum inhibitors of metalloproteinases reduce LDLR cleavage and sLDLR production (Begg et al., 2004), suggesting that the sheddase may be a metalloproteinase. Alabi et' al (2020) recently identified Membrane type 1- matrix metalloproteinase (MT1-MMP) as a sheddase that cleaves the LDLR.

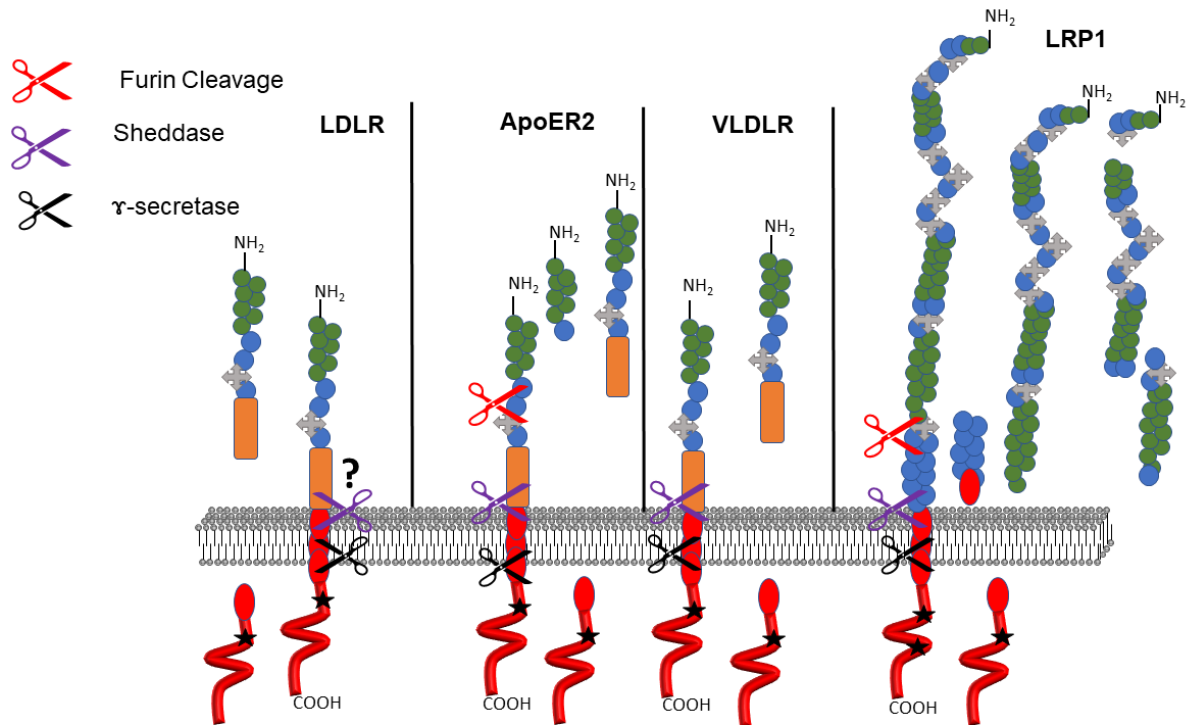


Fig 1. 8. Cleavage of ApoE receptor proteins and the release of their soluble forms into extracellular space. Figure made by Adekunle Alabi, idea adapted and modified from (Rebeck et al., 2006)

1.7 Matrix Metalloproteinases

Matrix metalloproteinases (MMPs) were first discovered in 1962 by Jerome Gross and Charles Lapiere. They found that anuran tadpole explant degraded collagen triple helix structure when placed on a collagen gel (Gross & Lapiere, 1962; Gross & Nagai, 1965). MMPs belong to the metzincin group of protease superfamily, synthesized as inactive precursors and degrade the extracellular matrix (ECM) in a concerted manner (Page-McCaw, Ewald, & Werb, 2007). Their unique capabilities to degrade most proteins of the ECM such as collagen, laminin, elastin and integrins make them very critical in tissue remodeling, pericellular proteolysis and cell migration

(Rozario & DeSimone, 2010). MMPs also play a key role in other biological activities such as embryonic development, morphogenesis, angiogenesis, cell receptor cleavage, chemokine/cytokine inactivation and release of apoptotic ligands (Peng et al., 2012; Van Lint & Libert, 2007). Additionally, they have been implicated in pathological activities including fibrosis, arthritis, inflammation and cancer (Amălinei, Căruntu, Giușcă, & Bălan, 2010). MMP activities are not only regulated at the transcriptional level but also at the posttranslational level by tissue inhibitor of metalloproteinases (TIMPs) (Peng et al., 2012).

The MMP family is made up of 28 members, subdivided into classes with numerical designation based on their structure, ECM substrate similarities and subcellular localization (Nagase & Woessner, 1999). These groups include collagenases, gelatinases, matrilysins, stromelysins and membrane-type matrix metalloproteinases (MT-MMP's) (**Fig 1.9**) (Chow, Cena, & Schulz, 2007).

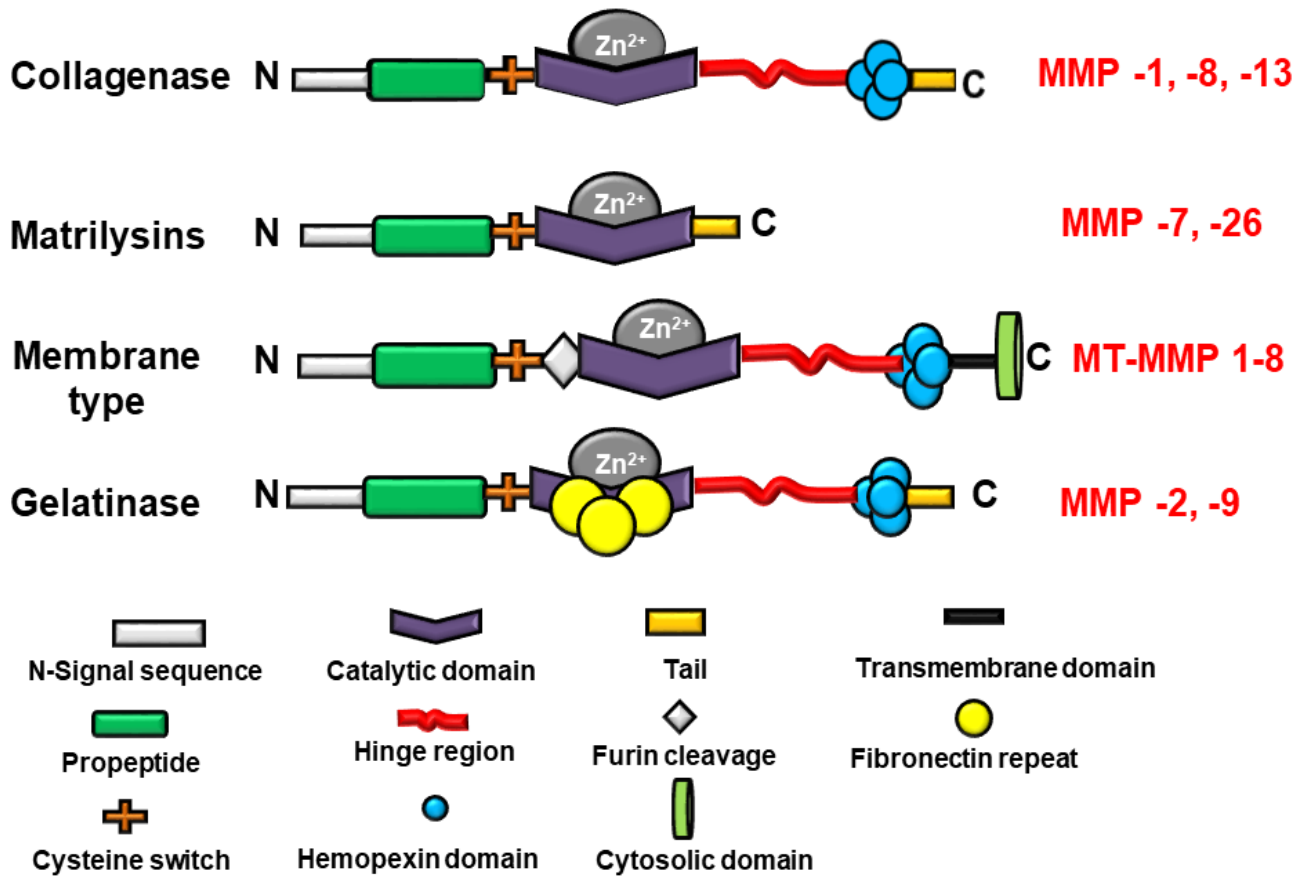


Fig 1. 9. Structure of matrix metalloproteinases and their various classes based on their structure and function. The various domains in MMP's include signal sequence, Pro-domain, a catalytic domain, Hemopexin domain, hinge region. Adapted and modified from (Chow et al., 2007)

Traditional classification of MMP	Numerical classification	MMP null Mutant Phenotype	Enzyme substrates
<i>Collagenases</i>			
Collagenase-1	MMP-1		Collagen (I, II, III, VII, VIII, X), casein, entactin, laminin, pro-MMP-1, -2, -9, and serpins
Collagenase-2	MMP-8	Causes skin tumors; resistance to tumor necrosis factor (TNF)-induced lethal hepatitis	Collagen (I–III, V, VII, VIII, X), gelatin, aggrecan, fibronectin
Collagenase-3	MMP-13	Bone remodeling defects; reduction in hepatic fibrosis; increased collagen deposition in atherosclerotic plaques	
<i>Gelatinases</i>			
Gelatinase A	MMP-2	Reduced body size; reduced neovascularization; decreased primary ductal invasion in the mammary gland; reduced lung saccular development	Gelatin, collagen (IV–VI, X), elastin, fibronectin
Gelatinase B	MMP-9	Bone-development defects; defective neuronal re-myelination after nerve injury; delayed healing of bone fractures; impaired vascular remodeling; impaired angiogenesis	Gelatin, collagens (IV, V, VII, X, XIV), elastin, fibrillin, osteonectin
<i>Stromelysins</i>			
Stromelysin-1	MMP-3	Altered structure of neuromuscular junctions; reduced purse stringing during wound healing; altered secondary branching morphogenesis in the mammary gland	Laminin, aggrecan, gelatin, fibronectin
Stromelysin-2	MMP-10	Increased inflammation and increased mortality in response to infection or injuries	Collagens (III–V), gelatin, casein, aggrecan, elastin, MMP-1,8
Stromelysin-3	MMP-11	Delayed mammary tumorigenesis	Fibronectin, laminin, aggrecan, gelatin

Matrilysin	MMP-7	Innate immunity defects; decreased re-epithelialization after lung injury	Collagen (IV–X), fibronectin, laminin, gelatin, aggrecan, pro- MMP-9
Metalloelastase	MMP-12	Diminished recovery from spinal cord crush; increased angiogenesis due to decreased angiostatin	Elastin, gelatin, collagen I, IV, fibronectin, laminin, vitronectin, proteoglycan
Matrilysin-2	MMP-26		Gelatin, collagen IV, pro-MMP-9
<i>Membrane-type MMPs (MT-MMP)</i>			
MT-MMP-1	MMP-14	Skeletal remodeling defects; angiogenesis defects; inhibition of tooth eruption and root elongation; defects in lung and submandibular gland and lethality	Collagen (I, II, III), gelatin, fibronectin, laminin aggrecan, tenascin
MT-MMP-2	MMP-15		Fibronectin, laminin, aggrecan, perlecan
MT-MMP-3	MMP-16		Collagen III, gelatin, casein
MT-MMP-4	MMP-17		Fibrinogen, TNF precursor
MT-MMP-5	MMP-24	Abnormal response to sciatic nerve injury	Proteoglycans

Table 1. 4- Classifications of MMPs, substrates and phenotypes from knock out animals. Table was adapted from (Jabłońska-Trypuć, Matejczyk, & Rosochacki, 2016; Page-McCaw et al., 2007).

1.7.1 Membrane Type-1 Matrix Metalloproteinase (MT1-MMP)

MT1-MMP, also commonly referred to as MMP-14 in the numerical classification of MMP's, was first discovered as a transmembrane metalloproteinase which was the first of its kind at the time. The protein showed a unique ability to activate progelatinase-A (proMMP2) and it was proposed to have a potential role in tumor invasion (Sato et al., 1994). The gene is found on chromosome 14 in both humans and mice, encoding a 582 amino acid protein of approximately 63kDa (Mignon,

Okada, Mattei, & Basset, 1995). The human *MMP14* gene consists of 10 exons and 9 introns (fig1.10).

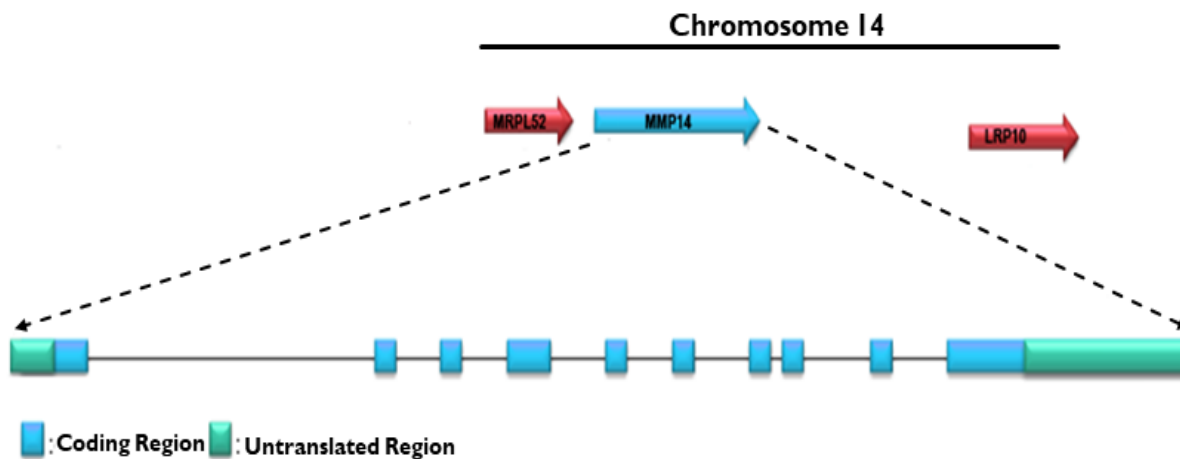


Fig 1. 10. *MT1-MMP* gene located on chromosome 14. Figure made by Adekunle Alabi, idea adapted and modified from (Cem Kuscu, Evensen, & Cao, 2010)

1.7.2 Structure and function of MT1-MMP

The protein is expressed at adequately regulated levels in most tissues including the liver, skin, kidney, placenta, lungs, ovary, spleen, fibroblasts, osteoblasts, adipocytes, epithelial cells (Yoshifumi Itoh, 2015); the levels are however upregulated during development, tissue injury and cancer invasion (Cem Kuscu et al., 2010). The protein contains seven domains in its latent form; the signal peptide guides the protein through the secretory pathway.

The pro-domain contains a cysteine switch which keeps the protein inactive, this region contains a conserved cysteine whose thiol group interacts with Zn^{2+} in the active site, thereby blocking and preventing access of substrates to the active site (Ra & Parks, 2007). The inactive protein only gains activity after the removal of its pro-domain. The thiol-zinc interaction needs to be broken;

this can be achieved by 1) Oxidation of the free cysteine thiol group by oxidants, 2) allosteric disruption of the thiol-zinc interaction, and 3) proteolytic cleavage. MT1-MMP contains a furin recognition site in the pro-domain RXKR, that is cleaved by furin during the secretion of the protein in the trans-Golgi (Thomas, 2002), and as such the protein is delivered to the cell surface in an active form.

The catalytic domain is the site of proteolytic activity, it has a conserved zinc-binding motif (HEXXHXXGXXH) with 3 histidine residues bound to Zn^{2+} . Once the pro-domain is excised, a water molecule associates with the catalytic zinc. The water molecule further forms a hydrogen bond with nearby glutamate residue (E240) (**fig 1.11**), thereby impacting on the water a nucleophilic property required for proteolytic cleavage of peptide bonds (Decaneto et al., 2017). The catalytic region is connected to a hinge region which is a flexible linker, this region helps maintain proper conformation of the protein and deletion of this region is known to reduce MT1-MMP capacity to activate pro-gelatinase A (Osenkowski, Meroueh, Pavel, Mobashery, & Fridman, 2005). The hemopexin-like domain bears similarity to the serum protein hemopexin, it is the largest region of MT1-MMP, providing a surface flat enough for protein-protein interactions. Mutation in this region that affects MT1-MMP protein dimerization compromises its ability to activate pro-gelatinase A and collagen degradation (Tochowicz et al., 2011). The transmembrane region localizes and anchors MT1-MMP to the plasma membrane, while the cytoplasmic domain is critical for endocytosis of the protein (Cem Kuscu et al., 2010).

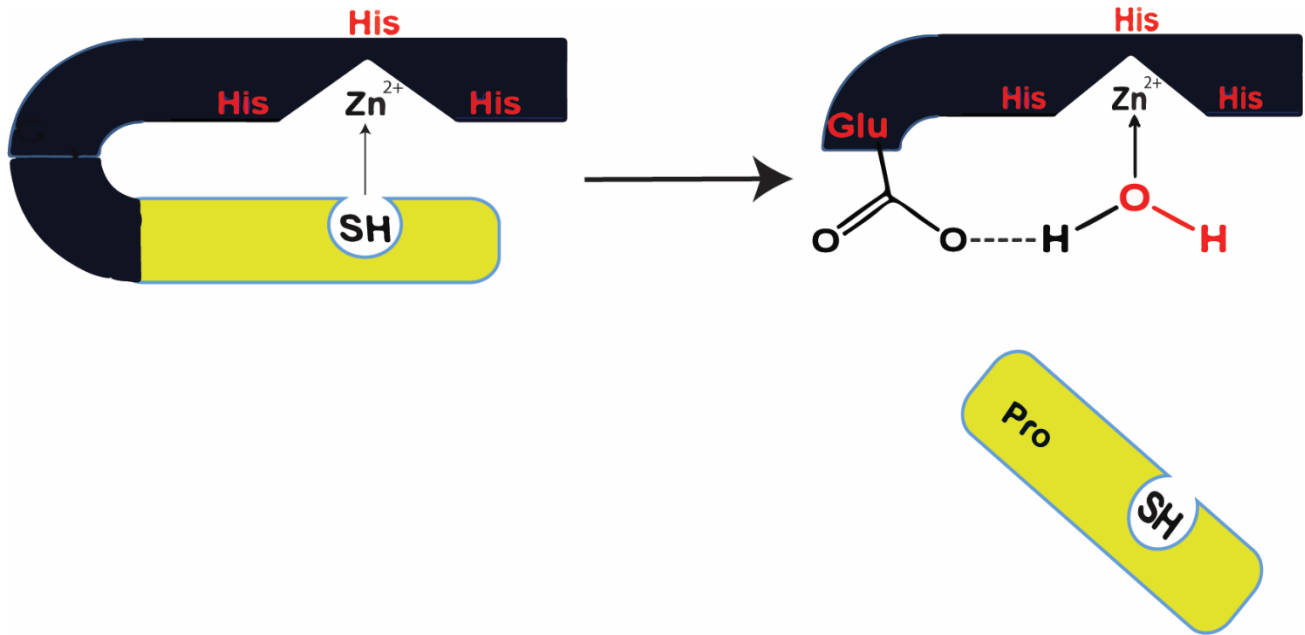


Fig 1. 11. Activation of MT1-MMP and interaction of water molecule with glutamate residue to attain nucleophilicity. Distortion of the association between the thiol group within the pro-domain and the catalytic Zn^{2+} exposes the enzyme active site and further binding of a water molecule to attained nucleophilicity. Figure made by Adekunle Alabi.

MT1-MMP is the most studied MMP with diverse substrates identified ranging from extracellular matrix materials, other MMP's, soluble proteins and cell surface receptors (Barbolina & Stack, 2008). Substrates that have been reported for MT1-MMP include collagen I, II and III, gelatin, fibronectin, laminin-1 (Ohuchi et al., 1997), α -integrins (Deryugina, Bourdon, Jungwirth, Smith, & Strongin, 2000), pro-gelatinase A (pro-MMP2) (Sato et al., 1994), proMMP13 (Knäuper et al.,

1996), ADAM9 (Wong et al., 2012), syndecan-1 (Endo et al., 2003), ApoE (Aoki et al., 2005), apoA1 (Stegemann et al., 2013), LYVE-1 (Wong et al., 2016) and LRP1 (Rozanov et al., 2004). While some of these substrates are confirmed physiological targets of MT1-MMP, some may not, given that most were identified by incubation of MT1-MMP with the proteins *in-vitro* or by proteomic approaches (Yoshifumi Itoh, 2015).

MT1-MMP is a double edge sword protein with functions critical to physiological processes and disease progression (Itoh & Seiki, 2004). MT1-MMP-mediated physiological processes include angiogenesis (Hiraoka, Allen, Apel, Gyetko, & Weiss, 1998), skeletal development (Holmbeck et al., 1999) and wound healing (Okada et al., 1997). MT1-MMP-mediated pathophysiological processes include cancer cell invasion (Sato et al., 1994), cancer metastasis (Tsunezuka et al., 1996), atherosclerosis (Rajavashisth et al., 1999a), inflammation (Sakamoto & Seiki, 2009) and rheumatoid arthritis (Miller et al., 2009). MT1-MMP knockout results in lethality few weeks after birth, which is the most drastic phenotype amongst MMP's, given that their structural and functional similarities make them compensate for each other (Itoh & Seiki, 2004). Knockout mice or mice carrying a mutation in the hemopexin domain (S466P) which generates a misfolded ER variant exhibit similar phenotypes such as arthritis, osteopenia, dwarfism, fibrosis, lack of collagen turnover and consequently die from tissue wasting (Holmbeck et al., 1999; Sakr et al., 2018).

1.7.3 Regulation of MT1-MMP

1.7.3.1 Transcriptional Regulation of MT1-MMP Gene Expression

Aside from the characteristic tissue expression pattern of MT1-MMP, the protein is highly expressed in cancer cells. However, the mechanism of activation is not clearly understood (Itoh,

2015). The promoter region of MT1-MMP has no TATA box and contains overlapping SP-1 and EGR-1 binding sites (Haas, Stitelman, Davis, Apte, & Madri, 1999). Collagen stimulated transcription of *MT1-MMP* is mediated by Egr-1. The clustering of integrins which results from the interaction between integrins and 3-dimensional collagen induces phosphorylation of Src kinase which causes the induction of the transcriptional factor Egr-1 and consequently activation of *MT1-MMP* transcription (Barbolina & Stack, 2008). Other transcriptional binding sites within the MT1-MMP promoter include NFkB, E-box, AP-4, CARG Box (Haas et al., 1999). Some growth factors and inflammatory cytokines such as TNF- α , TGF- β 1, and EGF have also been reported to induce the expression of *MT1-MMP* (Kuscu et al., 2010).

1.7.3.2 Post-transcriptional Regulation of MT1-MMP

Tissue inhibitors of metalloproteinase (TIMP's) are a major endogenous inhibitor of MT1-MMP, TIMPs 2,3 and 4 but not TIMP-1 are capable of inhibiting MT1-MMP at physiological levels (Brew & Nagase, 2010). TIMP-2 mediates pro-MMP2 activation by MT1-MMP; the protein forms a bridge between both MT1-MMP and pro-MMP2 (Yoshifumi Itoh, 2015). Reversion inducing cysteine-rich protein of kazal motifs (RECK) is also an endogenous inhibitor of MT1-MMP (Oh et al., 2001).

MT1-MMP undergoes dimerization either through its hemopexin domain (Itoh et al., 2001; Tochowicz et al., 2011) or the transmembrane domain (Itoh, Ito, Nagase, & Seiki, 2008). These interactions occur at the cell surface, while hemopexin interaction of monomeric units is required for collagen degradation, it is not required for proMMP2 activation. Interactions at the transmembrane domain are only required for proMMP2 activation but not for MT1-MMP collagenolytic properties (Itoh et al., 2008).

MT1-MMP undergoes regulatory proteolytic cleavage of itself at high levels of activity (Itoh, 2015), this removes the whole catalytic domain of the protein. The active protein is a 60kDa protein that undergoes autocatalytically cleaving Gly284-Gly285 and Ala255-Ile256 peptide bond in the hinge and catalytic region, generating a 44kDa specie (Pahwa, Stawikowski, & Fields, 2014). The released 18kDa protein and the 44kDa protein generated are both catalytically inactive and do not bind to TIMP-2 (Toth et al., 2002).

MT1-MMP undergoes endocytic internalization and recycling, which may be through clathrin pits or caveolae dependent mechanisms (Remacle, Murphy, & Roghi, 2003). Endocytosis dependent on clathrin is mediated by the association of LLY573 in the C-terminal with adapter protein 2, which is a component of clathrin-coated pits. The internalization of MT1-MMP has been reported to be critical for its function in cellular invasion (Uekita, Itoh, Yana, Ohno, & Seiki, 2001). Other posttranslational modifications that regulate MT1-MMP activities and affect its ability to promote cellular invasion include O-glycosylation in its linker region (Wu et al., 2004), palmitoylation at cysteine 574 downstream of LLY573 in the C-terminal that is important for endocytosis of the proteinase (Anilkumar et al., 2005) and phosphorylation (Lagoutte et al., 2016).

1.7.4 MT1-MMP and Atherosclerosis

Pro-inflammatory molecules play key roles in the development and progression of atherosclerosis; interleukins, tumor necrosis factor- α (TNF- α) and oxidized-LDL have all been identified as players that trigger smooth muscle cells and macrophages to upregulate MT1-MMP levels (Rajavashisth et al., 1999). Increased expression of MT1-MMP correlates to increased activation of pro-MMP2, both MT1-MMP and MMP2 contribute to extracellular matrix turnover that may play a key role

in plaque development, progression and rupture (Kuscu, Evensen, & Cao, 2011; Raggi et al., 2018).

75% of cardiovascular events are caused by atherosclerotic plaque rupture (Esper & Nordaby, 2019). Collagen is known to confer tensile strength on the fibrous cap of atherosclerotic plaques, and as well influences the stability of the plaques (Aikawa & Libby, 2004). MT1-MMP is a collagenase that has been implicated in the matrix remodeling of atherosclerotic plaque (Rajavashisth et al., 1999b), the protein is almost 26-fold upregulated in macrophage-derived from foam cells in rabbit plaques (Johnson, Sala-Newby, Ismail, Aguilera, & Newby, 2008). Given the key role of MT1-MMP in collagen hydrolysis and plaque localization, the metalloproteinase indispensably participates in collagen digestion in plaques and consequentially affects plaque disruption and stability. Mice engrafted with *MT1-MMP*^{-/-} bone marrow contained more collagen content in aortic arch compared with control mice engrafted with *MT1-MMP*^{+/+} bone marrow (Schneider et al., 2008). Schneider et al showed that macrophages lacking MT1-MMP may not influence the size of atherosclerotic lesion or composition but rather significantly increase the content of fibrillar collagen in plaque and as such reducing its instability. Similarly, foam cell macrophages with an increased level of MT1-MMP have been reported to be highly invasive with increased proliferation and apoptosis that elicit instability of atherosclerotic plaques (Johnson et al., 2008). However, opposing phenotypes have reported in smooth muscle cells, *MT1-MMP* deletion in smooth muscle cells significantly increased the severity of atherosclerotic plaque compared to controls (Barnes et al., 2017).

1.8 Rationale, Hypothesis and Aim of thesis

The LDLR pathway is the main route for clearing plasma LDL-C. Mutations in LDLR cause familial hypercholesterolemia, which is characterized by elevated circulating levels of cholesterol, specifically LDL-C (Goldstein & Brown, 2009b). Dyslipidemia resulting from the compromise of the structure and function of the LDLR is associated with high levels of circulating cholesterol which is pro-atherogenic and as such increases the risk of cardiovascular diseases (Shepherd & Packard, 1986). Statins, currently the most prescribed lipid-lowering therapy, decrease plasma LDL-C and reduce cardiovascular events by 20 to 40% (Brautbar & Ballantyne, 2011; Stancu & Sima, 2001). Monoclonal antibodies against PCSK9 significantly lower LDL-C when administered to humans (Lambert et al., 2014; Stein & Raal, 2014). However, intolerance to statin therapy as well as numerous side effects of statins have been reported (Ahmad, 2014; Thompson, Panza, Zaleski, & Taylor, 2016). On the other hand, PCSK9 monoclonal antibody therapy requires injections of large amounts of antibodies to achieve clinical efficacy, with extremely high production costs limiting the wide use of these drugs. Thus, the need for more effective and cost-efficient therapy to lower LDL-C cannot be overemphasized.

The ectodomain of LDLR can be cleaved by proteases, leading to the release of a soluble form (sLDLR) into cell culture media and human plasma (Begg et al., 2004; Fischer et al., 1993). Serum levels of sLDLR are positively correlated with plasma LDL-C levels (Shimohiro et al., 2015). However, the protease(s) responsible for LDLR cleavage are yet to be identified. Broad-spectrum inhibitors of metalloproteinase reduce LDLR cleavage and sLDLR production (Begg et al., 2004), therefore implicating a metalloproteinase as a key player in the process. We have identified for the first time, the extracellular matrix degrader, Membrane type-1 Matrix Metalloproteinase (MT1-

MMP) as a key player in the cleavage of the LDLR. Thus, we propose that MT1-MMP-induced LDLR cleavage decreases LDLR-mediated LDL uptake, leading to increased plasma LDL-C levels. Similarly, the increased circulating LDL-C associated with MT1-MMP cleavage of the LDLR may contribute to the development of atherosclerosis. We also propose that the cleaved sLDLR, which retains its ligand-binding repeats may bind to LDLR ligands in circulation and prevent ligand uptake by the membrane-tethered LDLR. Thus, we hypothesize that MT1-MMP regulates the homeostasis of plasma lipoprotein cholesterol. To test this hypothesis, we chose the following research aims.

- 1. Characterization and mechanistic study of MT1-MMP-mediated ectodomain cleavage of the LDLR.**
- 2. Determination of the role of hepatic MT1-MMP in the regulation of lipid metabolism and atherosclerosis.**
- 3. Determination of the fate of cleaved soluble LDLR in circulation.**

Chapter 2

Materials and Methods

2.1 Materials

Minimum Essential Medium α (MEM α) without nucleosides, RMPI 1640 medium, Opti-MEMTM, penicillin-streptomycin, trypsin-EDTA solution, Dil-labeled human LDL, unlabeled human LDL, Lipofectamine[®] 3000, Lipofectamine[®] RNAiMAX, High Capacity Complementary DNA (cDNA) Reverse Transcription Kit, SYBR[®]Select Master Mix, GeneJet and PureLinkTM HiPure plasmid miniprep kit, Bicinchoninic acid (BCA) protein assay kit and TRIzol[®] were obtained from ThermoFisher Scientific. High-density lipoprotein (HDL) and LDL/Very low-density lipoprotein (VLDL) Cholesterol Assay Kit was purchased from Cell Biolabs Inc. Total Cholesterol Assay Kit was from Wako Life Sciences. Human and mouse LDLR DuoSet[®] and human LDLR Quantikine[®] ELISA kits were from R&D Systems. Alanine transaminase colorimetric activity assay kit was obtained from Cayman Chemical. RNeasy[®] Mini kit was from Qiagen. Dulbecco's Modified Eagle's Medium (DMEM), fetal bovine serum (FBS), bovine serine albumin (BSA), CompleteTM EDTA-free protease inhibitors, and X-tremeGENETM HP DNA transfection reagent were purchased from Millipore Sigma. All other reagents were obtained from Fisher Scientific unless otherwise indicated.

Recombinant full-length human PCSK9 with a FLAG tag at the C-terminus was purified from culture medium of human embryonic kidney (HEK)-293S cells stably expressing PCSK9 using ANTI-FLAG[®] M2 affinity gel (Sigma) and FLAG peptide (Sigma) as described in our previous studies (H. M. Gu, Adijiang, Mah, & Zhang, 2013; D.-W. Zhang et al., 2007). The following antibodies were used: a rabbit anti-LDLR monoclonal antibody; HL-1, a mouse monoclonal anti-the linker sequence between ligand binding repeat (LR) 4 and LR5 of LDLR antibody; 3143, a rabbit anti-LDLR polyclonal anti-serum directed against the C-terminal 14 amino acid residues of

LDLR; 15A6, a mouse anti-PCSK9 monoclonal antibody; mouse anti-MT1-MMP monoclonal antibodies (Millipore, clone LEM-2/15.8 and clone 113-5B7); rabbit anti-MT1-MMP polyclonal antibodies (Millipore and ThermoFisher); a rabbit anti-MT1-MMP monoclonal antibody (Abcam); a rabbit anti-MT2-MMP polyclonal antibody (ThermoFisher); a rabbit anti-LRP1 polyclonal antibody (Novus Biologicals); a mouse anti-calnexin monoclonal antibody (BD Biosciences); a mouse anti-actin monoclonal antibody (BD Biosciences); mouse anti-transferrin receptor monoclonal antibodies (BD Biosciences and ThermoFisher); Dylight™ 800 and Dylight™ 680 conjugated rabbit anti-hemagglutinin epitope (HA) antibody (Rockland Immunochemicals, Limerick, PA); a mouse anti-Myc monoclonal antibody 9E10 that was purified from culture medium from hybridoma cells obtained from the American Type Culture Collection (CRL-1729) using Protein G Sepharose Fast Flow (GE Healthcare); and a custom-made rabbit anti-MT1-MMP antibody, 2247, that was produced by GenScript® using a recombinant mouse MT1-MMP (amino acid residues 24-400) as the antigen.

2.2 Animal

C57BL/6J, *ApoE*^{-/-} and *Pcsk9*^{-/-} mice were purchased from The Jackson Laboratory. The *Cre-lox* strategy was used to selectively inactivate *MT1-MMP* in mouse liver. The vector, in which exon 2 and exon 4 of mouse *MT1-MMP* gene were flanked by LoxP sites, was purchased from EUCOMM. *MT1-MMP*^{FRT-FLOX} mice were generated in the Clara Christie Centre for Mouse Genomics at the University of Calgary using embryonic stem cells that have a 50% C57 background. The homozygous *MT1-MMP*^{FRT-FLOX} was crossed to the FLPo mice (The Jackson Laboratory) to remove the FRT-flanked selection marker. The resulting *MT1-MMP*^{FLOX} mice were then backcrossed with C57BL/6J for 6 times and then crossed with transgenic mice expressing Cre recombinase under the control of the albumin promoter (The Jackson Laboratory) to produce mice

with no active MT1-MMP in hepatocytes (MT1-MMP^{LKO}). Genotyping was performed by PCR using AccuStartTM II mouse genotyping kit (Quanta Biosciences, Beverly, MA) and three primers that were designed with Primer3 and synthesized by Integrated DNA Technologies (IDT®, Coralville, CA).

Mice were housed 3 to 5 per cage with free access to water in a climate-controlled facility with a 12 h light/dark cycle. After weaning, mice were fed chow diet ad libitum containing 20% protein, 5% fat, and 48.7% carbohydrates (LabDiet, PICO Laboratory Rodent Diet 20, gross energy 4.11 kcal/gm). For the high fat/high cholesterol experiment, mice were fed Western-Type Diet containing 0.15% cholesterol (TestDiet, kcal from fat 40%, protein 16%, and carbohydrate 44%). All animal procedures were approved by the University of Alberta's Animal Care and Use Committee and were conducted in accordance with the guidelines of the Canadian Council on Animal Care.

2.3 Culture and treatment of cell lines

2.3.1 Cell Culture

All cells were cultured at 37 °C in a 5% CO₂ humidified incubator. Cell culture experiments were carried out under aseptic conditions in a class II laminar flow cabinet.

2.3.2 Thawing of frozen cells

Cells stored in liquid nitrogen or -80°C freezer in cryovials (corning) were rapidly transferred into a 37°C water bath to thaw for 30 sec. The content was then transferred into a 15 ml conical tube containing 10 ml appropriate culture media for the cell and centrifuged at 150 x g for 5 min. The supernatant was discarded, and the pellet was resuspended in 10 ml of culture media. Cells and media were then transferred into a 100 mm culture dish and placed in an incubator.

2.3.3 Cryopreservation of immortalized Cells

Culture media was removed from cells with 90-100% confluence in 100 mm plates and washed twice with 2 ml of PBS. The cells were treated with the addition of 1 ml of trypsin (Sigma) for 5 min and suspended in 8 ml of appropriate culture media and transferred into a 15 ml conical tube for centrifugation at 150 x g for 5 min. 1 ml of freezing solution (DMEM or MEM + 10% FBS + 10% DMSO) was added to resuspend the pellet. The cells were then transferred into cryovials. The vials were stored in a freezing container containing isopropanol (Nalgene®) to be frozen in a -80°C freezer overnight and subsequently stored in liquid nitrogen.

2.3.4 Immortalized cells

HEK293, HepG2, Huh7, and McA-RH7777 cells were maintained in DMEM (high glucose) containing 10% (v/v) FBS and seeded at a density of 2×10^5 cells per 1 ml. Hepa1c1c7 cells were maintained in MEM α (no nucleotides) containing 10% FBS.

2.3.5 Primary Hepatocytes

2.3.5.1 Primary Human Hepatocyte

Commercially available primary human hepatocytes (Triangle Research Labs) cells were thawed from liquid nitrogen stocks and seeded onto a 12-well collagen-coated plate at the density of 2×10^5 cells per well in 1 ml of RPMI containing 10% FBS. Cells were incubated at 37 °C and allowed to attach to the plate for 4 h before treatments and analysis.

2.3.5.2 Primary Mice Hepatocyte

Mice primary hepatocytes were isolated from anesthetized mice, subjected to abdominal surgery as described (Wei et al., 2010). The liver was perfused through the portal vein with HBSS buffer containing 0.5mM EGTA through a single ligature around the portal vein, after which the vena cava was quickly cut below the ligature. The liver lobes appeared clear after a short while and a ligature was then made around the upper vena cava. The lower vena cava was tied up and the heart was cut, letting the perfusate run out through the heart. The liver was then perfused with HBSS containing 1mg/ml collagenase for 6 to 10 min. When digestion was complete, the liver was dissected into a culture dish and transferred into a sterile 50 ml tube containing serum medium. The liver suspension was washed, centrifuged at 100 x g for 2 min and filtered twice with a coarse (80µm) and fine (20µm) filter. The cells were then resuspended in DMEM, counted and finally seeded in a 60 mm collagen-coated culture plate (Corning) with DMEM high glucose + 10% FBS for 5 h, after which the medium was changed to DMEM containing 0.5% FBS for treatments and analysis.

2.3.6 Transfection

Dicer-Substrate siRNA (DsiRNA) and plasmid DNA were introduced into cells using LipofectamineTM RNAiMAX and X-tremeGENETM HP (HEK293, Huh7, and Hepa1c1c7 cells) or LipofectamineTM 3000 (HepG2 cells), respectively, according to the manufacturer's instructions and briefly described below for 6 well culture plates. Scrambled and predesigned DsiRNAs against MT1-MMP were purchased from IDT[®] and listed in **Section 2.14**.

2.3.6.1 X-tremeGENE HP Transfection

2 µg DNA was added to 200 µl serum reduced Opti-MEM medium and vortexed briefly. Next, 2 µl of X-tremeGENE HP DNA transfection reagent was added and vortexed. The transfection mixture was then incubated for 30 min at room temperature before adding drop by drop to cells.

2.3.6.2 Lipofectamine 3000 Transfection

2 µg DNA and 5 µl P3000 reagent was added to 125 µl serum reduced Opti-MEM medium and vortexed (Transfection mixture A). 5 µl Lipofectamine 3000 reagent was then added to 125 µl Opti-MEM medium and vortexed (Transfection mixture B). Transfection mixture A and B were then combined and vortexed briefly, followed by a 5 min incubation at room temperature. The Mixture was then added drop by drop to cells.

2.3.6.3 RNAiMAX Transfection

2 µl of 20 µM siRNA solution was added to 100 µl Opti-MEM medium and vortexed (Solution A). 6 µl RNAiMAX reagent was then added to 100 µl Opti-MEM medium and vortexed (Solution B). Solution A and B were then combined, vortexed and incubated for 5 min at room temperature. The solution mixture was then added to cells drop by drop.

2.3.7 Drug and inhibitor treatment of cells

2.3.7.1 *Statin Treatment*

24 h prior to cell collection for lysis, culture medium was replaced with fresh media containing Lovastatin (J&K scientific) dissolved in Dimethylformamide (DMF) at a final concentration of 7.5 µg/ml and mevalonate (5 µg/ml). Same amount of DMF was added to the control group.

2.3.7.1 *Ilomastat GM6001*

Culture medium in Huh7 cells at 90% confluence in 6 well plates was removed and replaced with medium containing GM6001 (DMEM + 10% FBS medium at 30 and 100µM final concentration of GM6001). Cells were then incubated for 16 h prior to lysis for western blot analysis.

2.3.7.3 *DAPT (tert-butyl (2S)-2-[[[(2S)-2-[[2-(3,5-difluorophenyl) acetyl] amino] propanoyl] amino]-2-phenylacetate)*

Cells were treated directly with 10 µM DAPT (Tocris, Bioctechne) for 24 h prior to lysis. DAPT was solubilized in Dimethyl sulfoxide (DMSO); Same amount of DMSO was added to the control group.

2.3.8 Binding of PCSK9 to recombinant extracellular LDLR

2.3.8.1 *Incubation of PCSK9 and LDLR*

4 µg of PCSK9 (D374Y) was incubated with or without various concentrations of rLDLR (A22-R788) (0,1,2,4, and 8 µg) in the presence of 1% BSA to initiate binding of both proteins. The mixture was incubated at 37°C for 1 h in a thermal cycler (C1000, Biorad). The mixture was then added to 500 µl serum deficient DMEM.

2.3.8.2 Addition of LDLR and PCSK9 mixture to Huh7 cells

Huh7 cells were seeded at 2×10^5 cells/ml in 6 well plates in 2 ml of DMEM containing 10% FBS per well. 24 h after, the cells were washed twice with PBS and then incubated with 500 μ l of DMEM containing PCSK9 (D374Y) and rLDLR complex overnight at 37 °C in a 5% CO₂ humidified incubator.

2.3.9 PCSK9-promoted LDLR degradation

Huh7 cells seeded in a 12-well plate (1.5×10^5 cells/well) were transfected with scrambled or MT1-MMP siRNA. 48 h after, cells were washed twice with DMEM, followed by a 4 h-incubation with PCSK9 (2 μ g/ml) in 0.5 ml of DMEM containing 5% Newborn calf lipoprotein poor serum (NCLPPS). The cells were then collected for the preparation of whole cell lysate. Protein concentrations were determined using the BCA protein assay. Same amount of whole cell lysate was subjected to immunoblotting.

2.3.10 Measurement of Dil-LDL uptake in Huh7 cells

2.3.10.1 Dil-LDL incubation in cells with MT1-MMP Knockdown prior to LDL uptake assay

Huh7 cells were seeded at a density of 3×10^4 cells/well in a 96-well plate with 100 μ l of DMEM containing 10% FBS. 24 h later, the cells were transfected with scrambled or MT1-MMP siRNA using Lipofectamine RNAiMAX. 48 h after, the LDL binding assay was performed. Briefly, cells were washed with Opti-MEM once. Dil-labeled LDL (10 μ g/ml) was then added to cells in 100 μ l of DMEM containing 5% NCLPPS in the presence or absence of unlabeled human LDL (600 μ g/ml). The plate was incubated at 37 °C for 6 h.

2.3.10.2 Recombinant LDLR incubation with Dil-LDL prior to LDL uptake assay

5 µg of Dil-LDL was mixed with various concentrations of recombinant extracellular domain of rLDLR (0.5, 1, 2 and 4 µg) in 1% BSA. The mixture was incubated at 37°C for 1 h in a thermal cycler (C1000, Biorad) to initiate the binding of both proteins. After, the mixture was transferred into a 96 well plate seeded with Huh7 at the density of 3×10^4 cells/well and 90% confluent for 4 h. The Huh7 cells were incubated with DMEM without serum overnight to increase LDLR expression prior to the addition of Dil-LDL and rLDL mixture.

2.3.10.3 Fluorescent detection of LDL uptake

Cells were washed four times in a washing buffer (50 mM Tris-HCl, pH7.4, 150 mM NaCl, 2 mg/ml BSA) and then lysed in 100µl of RIPA buffer (50 mM Tris-HCl, pH7.4, 150 mM NaCl, 1% Triton X-100, 0.5% sodium deoxycholate, 0.1% SDS) containing 1× protease inhibitors. The lysate was then transferred to a 96-well black plate for the measurement of fluorescence using a SYNERGY plate reader (Excitation:520nm; Emission:580nm). The concentrations of total proteins in each well were measured using BCA protein assay. LDL uptake was calculated by normalization of the fluorescence units to the amount of total proteins in each well. The result obtained in the presence of excess unlabeled LDL revealed nonspecific binding of Dil-LDL. Specific binding was calculated by subtraction of nonspecific binding from the total counts measured in the absence of unlabeled LDL.

2.3.11 Biotinylation of cell surface proteins

Cell surface proteins were biotinylated from modified method as described (Huang, 2012). Huh7 cells were seeded in a 6-well plate in 2 ml of culture medium at the density of 2.5×10^5 cells/ml. 24 h later, cells were transfected with scrambled or MT1-MMP siRNA. 24 h after transfection,

cells were cultured in DMEM containing 5% NCLPPS for 16 h. Cell surface proteins were then biotinylated. Briefly, cells were incubated with 1 ml EZ-Link Sulfo-NHS-LC-Biotin (Pierce) in PBS (0.5mg/ml, pH 8.0) for 15 min at 4 °C with gentle rocking. The cells were then washed twice in cold quenching buffer (0.1mM CaCl₂ +1mM MgCl₂ + 100mM Glycine), followed by a 20 min incubation in 1 ml quenching buffer at 4°C with gentle shaking. The cells were then washed twice with cold PBS and transferred to a 1.5 ml microtube for centrifugation at 2000 x g for 5 min (Eppendorf Centrifuge, 5430R). The supernatant was discarded, and the pellet was lysed in 150 µl of lysis buffer A containing 1 X PMSF. A total of 50 µl of cell lysate was saved and approximately 100 µl of the lysate (same amount of total proteins between the control and MT1-MMP knockdown cells) was added to 60µl of 50% slurry of Neutravidin agarose (Pierce), in a 1.5ml microtube. The sample was then rotated at 4°C overnight to immunoprecipitate biotinylated cell surface proteins. The mixture was centrifuged at 5000 x g for 3 min. The supernatant was then discarded; the pellet was washed 3X in lysis buffer A followed by a 5000 x g centrifugation each time. After the final wash, the supernatant was discarded, and the beads were centrifuged again at 20,000 x g for 1 min to remove the remaining solution. Biotinylated proteins attached to the beads were then eluted by adding 1 × SDS loading buffer with a brief vortex, followed by heating at 85°C for 5 min. Eluted proteins were then analyzed by immunoblotting.

2.4 Quantification of mRNA Expression

2.4.1 RNA Isolation

Total RNAs were extracted from cultured cells and mouse tissue using Trizol (Life Technologies) according to the manufacturer's instructions. Briefly, 1ml of Trizol was added to an extraction tube containing 50 mg of animal tissue, followed by homogenization using a PowerGen 500

Homogenizer (Fischer Scientific). Extraction from cultured cells involved the removal of growth media and the addition of 0.4 ml Trizol per 1×10^5 - 10^7 cells directly in the culture plates. The content in each well of the culture plate was then pipetted up and down several times for homogenization. Lysate from animal tissue and cultured cell were then incubated for 5 min at room temperature. 0.2 ml of chloroform per 1 ml Trizol used for lysis was added and incubated for 3 min. The mixture was centrifuged at $12,000 \times g$ at $4^\circ C$ for 15 min to separate the aqueous phase and the phenol red-chloroform phase. The aqueous phase containing RNA was then transferred into a new tube; isopropanol was added (0.5 ml per 1ml of Trizol initially used for lysis) and incubated for 10 min at room temperature. After, the sample was centrifuged for 10 min at $12,000 \times g$ and $4^\circ C$. The supernatant was discarded, and the RNA pellet was washed with 1ml of 75% ethanol. The sample was vortexed for 5 sec and centrifuged at $7500 \times g$ for 5 min at $4^\circ C$. The supernatant was discarded. The pellet was air-dried for 5 min and then dissolved in 50 μ l of RNase Free water for further analysis. RNA was quantified using Nanodrop spectrophotometer (Nanoview Plus, GE)

2.4.2 cDNA synthesis

cDNA was synthesized using High Capacity cDNA Reverse Transcription Kit (Applied Biosystems). Samples were mixed with reagent as indicated in (Table 2.1) in PCR tubes in a thermal cycler (C1000, Biorad) under the following condition: $25^\circ C$ for 10 min, $37^\circ C$ for 120 min, $85^\circ C$ for 5 min and $4^\circ C$ as the holding temperature.

Component	Quantity
RNA	2 μ g
10X RT buffer	2 μ l

25X dNTP Mix	0.8µl
10X Random Primers	2µl
Reverse Transcriptase	1µl
Nuclease free water	Made up to 10µl
Total per reaction	10µl

Table 2. 1-Reverse Transcription Reaction mixture

2.4.3 Quantitative Real-Time PCR (qRT-PCR)

Relative quantification of mRNA was done using qRT-PCR measurement of cDNA carried out on a StepOnePlus™ using SYBR® Select Master Mix. Standards were generated from dilutions (4X, 16X, 64X and 156X) of a pool of control samples. Samples for analysis were diluted 15X. Each reaction was carried out in 20 µl of sample mixture as indicated in (**Table 2.2**) in a Microamp® 96 well reaction plate (Applied Biosystems) with a PCR program as indicated in (**Table 2.3**).

Reaction Reagent	Volume
Sample and standards	2µl
SYBR Green Master Mix	10µl
Forward and Reverse primers (10µM)	2 µl each
Nuclease free water	4µl

Table 2. 2-qRT-PCR reaction mixture

Stage	Time (seconds)	Temperature (° C)
Holding	120	95
Cycling (40X cycles)	15	95
	60	60
Melt Curve	15	95
	60	60
	15	95

Table 2. 3-qRT-PCR running parameters

Each sample was processed in triplicate, and the average cycle threshold was calculated. Relative gene expression was normalized to the glyceraldehyde-3-phosphate dehydrogenase gene (*GAPDH*) that had a similar amplification efficiency as that of the target genes. Primers for human and mouse *GAPDH*, *MT1-*, *MT2-*, *MT3-*, *MT4-*, *MT5-*, *MT6-MMP*, *HMGCR*, *LDLR*, *PCSK9*, *SREBP2*, and *IDOL* were designed by PrimerQuest Real-Time PCR Design Tool, synthesized by IDT, Inc., and listed in the **Section 2.14**.

2.5 Site-directed mutagenesis

Plasmid pCR3.1 containing cDNA of the full-length MT1-MMP with an HA-tag between Asp115 and Glu116 (pCR3.1-MT1-MMP, a gift from Dr. Weiss, University of Michigan) was used to generate the mutant form of MT1-MMP. Plasmid pBudCE4.1 containing full-length hLDLR with an N-terminal HA-tag was used to generate the mutant forms of LDLR. Mutagenesis was performed using QuickChange Lightning site-directed mutagenesis kit (Agilent Technologies). The reaction mixture was set up in a PCR tube as indicated in (**Table 2.4**), PCR analysis was

conducted in a thermal cycler (C1000, Biorad) with parameters as shown in (Table 2.5). After completion of the PCR run, 1 μ l of Dpn1 restriction enzyme was added to the reaction mixture and gently mixed by pipetting the solution up and down. The mixture was then incubated at 37 °C for 30 min, after which 2 μ l solution was used for transformation into 50 μ l of DH5 α competent cell in an eppendorf tube. The competent cells were then incubated on ice for 20 min, heat pulsed at 42 °C for 30 sec in a water bath, and then incubated on ice for 2 min. 500 μ l of prewarmed Lysogeny broth (LB) was added to the tube containing DH5 α and incubated at 37 °C for 1 h with shaking at 225–250 rpm in a MAXQ 4450 (Thermo Scientific) incubator. 50 μ l of LB broth was then spread on a LB-agar plate containing 50mg/ml zeocin for pBudCE4.1 plasmid or 100mg/ml ampicillin for pCR3.1 vector. The plates were incubated at 37°C overnight (16 h) to allow bacterium growth. A single colony was picked and transferred into a tube containing LB broth with appropriate antibiotics, the mixture was incubated at 37°C for 16 h with shaking at 225–250 rpm in a shaker (MAXQ 4450, Thermo Scientific). Plasmid DNA was isolated from cultured bacteria using high pure miniprep kit (Invitrogen).

Briefly, 2-3 ml of E. coli bacteria culture in LB medium was centrifugated at 4,500 x g for 5 min in an Eppendorf tube, the supernatant was discarded while the pellet was then resuspended in 0.4 ml resuspension buffer with RNase A. 0.4 ml lysis buffer was then added and the mixture was gently inverted to mix for 5 X without vortex, followed by a 5 min incubation at room temperature. Next, 0.4 ml precipitation buffer was added and mixed by inverting the tube until the mixture was homogenous. The mixture was then spun at 12,000 x g for 10 min at room temperature. The supernatant was loaded onto an equilibration column and allowed to drain by gravity flow. The column was washed twice with wash buffer and then placed on a microcentrifuge tube; DNA was eluted with 0.9 ml elution buffer. The DNA was then precipitated with 0.63 ml isopropanol and a

12,000 x g centrifugation for 10 min. The supernatant was discarded, and the pellet was washed with 1 ml 70% ethanol and a 12,000 x g centrifugation for 10 min. The supernatant was once more discarded and the DNA pellet was dissolved in 50 μ l TE buffer and measured using Nanodrop spectrophotometer (Nanoview Plus, GE).

Reagent	Amount
10X Reaction buffer	2.5 μ l
dsDNA	100ng
Primer 1 (10 μ M)	0.5 μ l
Primer 2 (10 μ M)	0.5 μ l
dNTP mix	0.5 μ l
Quick solution	0.75 μ l
QuickChange enzyme	0.5 μ l
Water	Made up to 25 μ l
Total	25 μ l

Table 2. 4-Mutagenesis PCR Reaction Mixture

Segment	Cycles	Temperature	Time
1	1	95°C	2mins
2	18	95°C	20sec
		60°C	10sec
		68°C	30sec/kb plasmid
3	1	68°C	5mins

Table 2. 5-Mutagenesis PCR parameters

The sequences of the oligonucleotides containing the residues to be mutated were synthesized by IDT[®] and listed in **Section 2.14**. The presence of the desired mutation and the integrity of each construct was verified by sanger sequencing in the Applied Genomics Core (TAGC) at the University of Alberta.

2.6 Western Blot and Protein Expression Analysis

2.6.1 Protein extraction from cultured cells

Protein extraction from cultured cells was mostly carried out 48 h after transfection. Culture medium was removed from plates and cells were washed with 1 ml of PBS. The cells were scraped, collected in 1 ml of PBS, and then centrifuged (1,500 x g, 4 °C for 5 min). The supernatant was discarded. Cells were lysed in lysis buffer A (1% Triton, 150 mM NaCl, 50 mM HEPES, pH 7.4) containing 1 × Complete EDTA-free protease inhibitors for 30 min on ice and vortexed intermittently every 10 min. Cell lysis was spun for 10 min at 20,000 × g at 4 °C, the supernatant

was collected as whole cell lysate. Protein concentrations were determined by the BCA protein assay.

2.6.2 Protein extraction from animal tissues

Snap frozen liver tissue samples stored at -80 °C were thawed and weighed into a 2 ml tube. Homogenization buffer (250mM Sucrose, 50mM Tris-HCl, pH7.4, 1mM EDTA, and 1X protease inhibitors) was added in a volume 4 X the tissue weight to obtain 20% homogenate as described (Bahitham, Watts, Nelson, Lian, & Lehner, 2016). Homogenization was carried out using a PowerGen 500 Homogenizer (Fischer Scientific). Homogenized tissue was then incubated on ice for 30 min with intermittent vortex every 10 min. The samples were then spun for 10 min at 20,000 × g at 4 °C. The supernatant was collected as tissue homogenate. Protein concentrations were determined by the BCA protein assay.

2.6.3 Protein Assay and quantification

Protein concentrations from tissue and cell lysate homogenate were determined using Bicinchoninic acid assay (BCA, Thermo Scientific), BCA protein assay reagent A and B were mixed 50:1 (BCA solution) to make the working BCA solution. Protein standards for the assay were made from bovine serum albumin (BSA) at concentrations ranging from 0,2,4,6,8 and 10 mg/ml. 4 µl of standards or samples of tissue and cell lysate was added to a 96 well plate, followed by the addition of 200 µl of the working BCA solution. The plate was then incubated at 37 °C for 30 min. Absorbance was read at 562nm using a SPECTRA MAX 250 microplate reader.

2.6.4 Immunoprecipitation

2.6.4.1 Immunoprecipitation of LDLR and MT1 from cell lysate

Briefly, cells were cultured in DMEM containing 5% NCLPPS for 16 h to increase the expression of LDLR and then lysed in lysis buffer A containing 1× Complete EDTA-free protease inhibitors. Same amount of total proteins was applied to a monoclonal anti-LDLR antibody (HL-1), a monoclonal anti-MT1-MMP antibody (Millipore, clone LEM-2/15.8), or a monoclonal anti-Myc antibody (9E10) and rotated for 2 h. After, 50 µl of protein-G beads (50 % slurry) was added and rotated overnight.

2.6.4.2 Immunoprecipitation of sLDLR From Plasma

500 µl of pooled plasma isolated from *Ldlr*^{-/-} or wild-type mice were applied to a rat anti-mouse LDLR antibody (4 µg/ml, R&D System) and rotated for 2 h. After, 50 µl of prewashed protein-G beads (50 % slurry) was added, followed by a rotation overnight at 4 °C.

2.6.4.3 Elution of immunoprecipitated Protein

Immunoprecipitated samples were washed 3 X in 1 ml of lysis buffer A and spun at 5,000 x g for 5 min, the supernatant was discarded. The immunoprecipitated proteins were then eluted from the beads by addition of 2 × SDS-PAGE sample buffer (100 mM Tris-HCl, pH 6.8, 4% SDS, 20% glycerol, 0.04% bromophenol) containing 5% β-mercaptoethanol with heating at 85°C for 5 min. The eluted samples and whole cell lysate or plasma input were then subjected to SDS-PAGE (8-20%) and immunoblotting.

2.6.5 Immunoblotting

Same amount of whole cell and tissue lysate was subjected to immunoblotting as described (AU - Gallagher & AU - Chakavarti, 2008). Protein content in the lysates was denatured and exposed to a reducing agent with the addition of 4X laemmli sample buffer (0.2M Tris pH 6.8, 8% SDS, 40% glycerol, 0.08% bromophenol blue and 5% β -mercaptoethanol), followed by heating at 65 °C for 10 min. Samples and a protein ladder (FroggaBio) were loaded into an 8% acrylamide gel (1.5 mm thick) except otherwise stated, in an electrophorator (Biorad) connected to a power supply. Samples were then separated on the gel based on their sizes by running at 80V for 10 min followed by 120V in running buffer (25 mM Tris, 192 mM glycine, 0.1% SDS) until the blue dye ran out of the gel. Separated proteins were then transferred from the gel to nitrocellulose membranes (10600004, GE Healthcare) in a transfer apparatus (Biorad) containing transfer buffer (25 mM Tris, 192 mM glycine, 10% methanol). Transfer was carried out at 400 mA constant current for 90 min with the Electro-transfer apparatus on ice. The membrane was then blocked in PBST containing 5% skimmed milk for 60 min, after which they were washed 3 X in PBST for 5 min. Primary antibodies were added in appropriate dilutions in PBST with 0.2% sodium azide as indicated in **Table 2.6**. The membrane was incubated overnight at 4°C on a shaker. After, the membrane was washed 3 X in PBST. Antibody binding was detected using IRDye[®]680 or IRDye[®]800-labeled goat anti-mouse or anti-rabbit IgG secondary antibodies. The signals were detected on a Licor Odyssey Infrared Imaging System (Li-Cor).

Antibody	Company	Catalogue No	Dilutions
Rabbit anti-LDLR (3143)	N/A	N/A	1:5000
Mouse anti- LDLR (HL-1)	N/A	N/A	1:2000
Mouse anti-PCSK9	Millipore	MAB3328	1:2000
Rabbit anti-MT1-MMP	abcam	ab51074	1:5000
Rabbit anti-LRP1	NOVUS	NBP1-40726	1:5000
Mouse anti-calnexin	BD Bioscience	610524	1:5000
Mouse anti-actin	BD Bioscience	612657	1:10000
Mouse anti-transferrin receptor	BD Bioscience	612125	1:3000
Rabbit anti-HA	Thermo Scientific	OPA1-10980	1:10000

Table 2. 6-Antibody dilution

2.6.6 TCA Precipitation

TCA precipitation was determined from modified method as described (Koontz, 2014). Cold 100% Trichloroacetic acid (TCA) was added to culture media samples to be precipitated in a 2 ml Eppendorf tube. The final concentration of TCA was 15% (v/v). The samples were vortexed immediately for 30 sec. The samples were then rotated overnight at 4 °C using a Rotator (Glas-Col), followed by centrifugation at 20,000 x g for 20 min at 4 °C. The supernatant was discarded,

and 2 ml of cold acetone (-20 °C) was added to pellet, followed by a 10 sec vortex and incubation on ice for 15 min. The sample was then spun at 20,000 x g for 20 min at 4°C. The supernatant was discarded, and the pellet was air-dried until the color was changed from white to transparent. The pellet was then dissolved in 60 µl of 9M urea with the addition of 20 µl of 4X SDS loading buffer prior to western blot analysis.

2.6.7 Gelatin Zymography

Culture medium was collected from cells 48 h after treatment, and protein concentrations were measured by the BCA assay. Same amount of culture medium (80 µg of total proteins) or 5 µl of plasma sample from mice were used for zymography analysis (Brooks, Schumacher, Toth, & Fridman, 2003). Briefly, samples were mixed with 4 × denaturing sample buffer (200 mM Tris-HCl, pH 6.8, 8% SDS, 40% glycerol, 0.08% bromophenol) and subjected to electrophoresis on an 8% SDS gel containing 2 mg/ml of gelatin. The gel was washed 3 X with 2.5% Triton X-100 in water and then incubated for 16 to 20 h in a renaturing buffer (50 mM Tris-HCl, pH7.5, 5 mM CaCl₂, 150 mM NaCl, and 0.05% NaN₃). Gels were stained with Coomassie Blue R250, de-stained in a solution containing 40% (v/v) methanol and 10% (v/v) acetic acid, and then scanned on a Licor Odyssey Imaging System. MMP2 was visualized as a clear band of degraded gelatin on the blue background of Coomassie Blue staining.

2.6.8 Immunofluorescence

Confocal microscopy was carried out as described in our previous study (H. Gu et al., 2016). Huh7 or HepG2 cells seeded onto coverslips (1.0×10^5 cells/ml) were transfected with or without MT1-MMP cDNA as indicated. 36 h later, cells were cultured in DMEM containing 5% NCLPPS for 16 h, fixed with 3% paraformaldehyde, and then permeabilized with cold methanol for 10 min at

-20 °C. The cells were then incubated with a mouse anti-LDLR monoclonal antibody and a rabbit anti-MT1-MMP (Abcam) (1:100) or anti-HA antibody. Antibody binding was detected using Alexa Fluor 488 goat anti-rabbit IgG and Alexa Fluor 568 goat anti-mouse IgG. Nuclei were stained with 4', 6-diamidino-2-phenylindole (DAPI, ThermoFisher). After washing, coverslips were mounted on the slides with ProLong Diamond Antifade Mountant (ThermoFisher). Localizations of LDLR and MT1-MMP were determined using a Leica SP5 laser scanning confocal microscope (filters: 461 nm for DAPI, 519 nm for Fluor 488, and 543 nm for Fluor 568).

2.6.9 Immunohistochemistry

All liver sectioning and staining were performed by the HistoCore facility in Alberta Diabetes Institute at the University of Alberta. Briefly, a portion of the liver was fixed in 10% formalin and embedded in paraffin, followed by sectioning at 5 µm thickness onto Histobond slides. The slides were then subjected to hematoxylin and eosin (H&E) or trichrome staining. Cryo-sectioned liver tissues were used for Oil Red O staining. The resulting slides were imaged using ZEISS Axio Observer A1. The relative stained area was then quantified with ImageJ software (National Institute of Health) using color segmentation and threshold analysis.

2.7 Agarose Gel Electrophoresis and MT1-MMP FLOX genotyping

2.7.1 DNA Extraction from tissue

DNA extraction from mouse tissue and PCR reaction was carried out using AccuStart™ II Mouse Genotyping Kit (Quanta, Bioscience). Briefly, 2 mm of mouse ear notch tissue was added into PCR tube containing 50 µl of extraction reagent. Samples were heated at 95 °C for 30 min and allowed to cool down to room temperature. An equal volume of stabilization buffer was then added

into each sample, after which 1µl of extract sample was used for PCR reaction conducted in a thermal cycler (C1000, Biorad), as indicated below in **Table 2.7 and 2.8.**

Reaction Component	Quantity(µl)
Tissue DNA extract	1
Water	1
10µM WT-F Primer	1
10µM WT-R Primer	1
10µM FLOX-F Primer	1
2X PCR SuperMix	10

Table 2. 7-Reaction Mixture for Genotyping

Segment	Cycles	Temperature	Time
1	1	94°C	3mins
2	35	94°C	15sec
3		63°C	15sec
4		72°C	30sec
5	1	12°C	∞

Table 2. 8-PCR parameters for Genotyping

2.7.2 Agarose gel

Agarose gels were prepared in TBE (Tris borate and EDTA) at 2% (w/v) concentration of agarose. The mixture was heated in a microwave for 1 min and allowed to cool down for 3 min, after which SYBR Safe DNA gel stain (Invitrogen) was added at 0.005% (v/v). The gel was then poured to a Gel setting device (Biorad) with 15 well comb and allowed to solidify for 1 h at room temperature.

2.7.3 Gel Electrophoresis

The gel was transferred into Sub-cell GT gel electrophoresis apparatus (Biorad) connected to a power source (VWR) and covered with 1 X TBE. 5 μ l of 100bp DNA ladder (FroggaBio) was used as the marker. 20 μ l of PCR product was added to each well. The electrophoretic apparatus was subjected to a constant voltage at 100V for 40 min, Gel was then imaged using G-Box (Syngene).

2.8 Extraction of lipids

Folch lipid extraction protocol was used to isolate lipids (Folch, Lees, & Sloane Stanley, 1957). Liver samples were lysed with a homogenization buffer (50 mM Tris-HCl, 250 mM sucrose and 1 mM EDTA, pH 7.4) using PowerGen 500 Homogenizer (Fischer Scientific). Lipids were extracted from 4 mg of liver homogenate transferred into a glass tube and made up to 1ml with PBS; 4 ml of chloroform-methanol mixture (2:1) was then added and vortexed for 1 min. The glass tube was then spun at 700 x g for 10 min in a centrifuge (Eppendorf, 5810R), the chloroform bottom phase was transferred to a new glass tube using a 9-inch glass Pasteur pipette (Fischer) and dried under nitrogen. Lipids were then dissolved in 1 ml chloroform with 2% Triton X-100 and dried under nitrogen again. The dried samples were then re-dissolved in 1 ml of distilled H₂O and incubated in a 37 °C water bath for 15min with intermittent vortex every 5 min. The levels of TG

and total cholesterol in 50 µl of samples were measured using commercial kits from Roche Diagnostics and Wako Diagnostics, respectively.

2.9 Plasma lipid and Alanine aminotransferase (ALT)

Blood samples were collected into heparin-coated tubes (BD Biosciences) from the tail or saphenous veins of mice (age of 8-12 weeks) on chow or the Western-type diet. The blood was centrifuged at 3,000 x g for 20 min to isolate plasma. Plasma from each mouse was subjected to ALT measurement using the ALT enzymatic activity assay kit (Cayman Chemical), plasma triglyceride was measured with Trig/GB kit (Roche Diagnostics) and total cholesterol measurement with Cholesterol E kit (Wako Diagnostics), respectively, according to the manufacturer's instructions.

2.9.1 ALT determination

ALT measurement was carried out using ALT enzymatic activity assay kit (Cayman Chemical). Briefly, 5 µl plasma and positive control samples were loaded into 96 well plates containing 50 µl ALT substrate and 5 µl enzyme cofactor. The plate was covered and incubated at 37 oC for 15 min. The plate was removed, and the enzymatic reaction was initiated by the addition of 5 µl ALT assay initiator as quickly as possible. Immediately absorbance was read at 340 nm once every minute for a period of 5 min. ALT activity was calculated from the equations below.

$$\Delta A_{340}/\text{min} = \frac{\Delta A_{340}(\text{Time 2}) - \Delta A_{340}(\text{Time 1})}{\text{Time 2 (min)} - \text{Time 1 (min)}}$$

$$\text{ALT activity (U/L)} = \left(\frac{\Delta A_{340}/\text{min} \times 0.065\text{ml}}{4.11\text{mM}^{-1} \times 0.065\text{ml}} \right) \times 1000$$

2.9.2 Cholesterol determination

Total cholesterol was measured using cholesterol E kit (Wako Diagnostics). Briefly, a working colour reagent solution was prepared by mixing colour reagent with buffer solution. 3 µl of sample and standard solution (0, 10, 20, 40, 60, 100 and 150 mg/dl) were added into 96 well plate. Next, 200 µl colour reagent solution was added, and the plate was incubated for 5 min at 37 °C followed by absorbance reading with a SPECTRA MAX 250 plate reader at 600 nm. A graph of absorbance vs standard concentration was plotted to generate a standard curve and plasma concentration was determined from extrapolation of measured absorbance.

Plasma HDL and non-HDL were separated using the HDL and LDL/VLDL Cholesterol Assay Kit (Cell Biolabs). Briefly, 5 µl of plasma was mixed with 5 µl of the Precipitation Reagent, centrifuged at 2,000 x g for 20 min. The supernatant (HDL fraction) was transferred to a new tube. The pellet was dissolved in 10 µl of PBS. Cholesterol content in each fraction was measured using the Cholesterol E kit (Wako Diagnostics).

Lipoprotein profiles were analyzed by the Lipidomic Core Facility at the University of Alberta. Briefly, 5µl of plasma from each mouse in the same experiment group was pooled and 30 µl was subjected to Fast Protein Liquid Chromatography (FPLC) with a Superose 6 column.

2.9.3 Triglycerides determination

Triglycerides were measured using Trig/GB kit (Roche Diagnostics). Briefly, 5 µl of plasma was added to 96 well plate followed by the addition of 100 µl colour reagent R1, the sample was mixed and incubated for 10 min at 37 °C. Blank absorbance was read at 540 nm, this was followed by the addition of 5 µl glycerol standards (0, 0.0087, 0.017, 0.035, 0.07, 0.14 and 0.28 mM). 100 µl colour

reagent R2 was added to the mixture and incubated for 1 h at 37 °C, absorbance was then read with a SPECTRA MAX 250 plate reader at 540 nm and plasma concentrations were extrapolated from standard curve.

2.10 ELISA Measurement of sLDLR and PCSK9

Plasma sLDLR and PCSK9 were both measured using their respective DUOSET ELISA kits (R&D Systems) according to the manufacturer's instructions.

2.10.1 Plate Preparation

Capture antibody was diluted to working concentration in PBS and immediately coated to a 96 well microplate at 100 µl per well. The plate was sealed and incubated overnight at room temperature; this was followed by a 3 X wash with 400 µl wash buffer. The plate was then blocked with 300 µl reagent diluent solution and incubated at room temperature for 1 h. Reagent diluent was discarded, and the plate was washed 3 X with 400 µl wash buffer.

2.10.2 Assay Procedure

100 µl of sample and standards in reagent diluent was added to the plate in triplicate and covered with an adhesive strip for an incubation period of 2 h at room temperature. This was followed by a 3 X wash with wash buffer and the addition of 100 µl per well detection antibody diluted in reagent diluent with a 2 h incubation at room temperature. After incubation, the plates were once again washed 3 X with wash buffer. 100 µl per well of working dilution streptavidin-HRP in reagent diluent was then added to the plate with a 20 min room temperature incubation, which was followed by a 3 X wash with wash buffer as stated earlier. 100 µl per well of working substrate solution made from 1:1 mixture of colour reagent A and B was added to the plate and incubated for 20 min while avoiding direct light contact. 50 µl per well stop solution was added to the plate

and tapped gently for thorough mixing. The optical density of each well in the microplate was measured with a SPECTRA MAX 250 plate reader at 540 nm; unknown sample concentrations were determined by extrapolations of optical density from standard curve.

Reagent/Sample	Mouse sLDLR	Human sLDLR	Mouse PCSK9	Human PCSK9
Capture Antibody	4 µg/ml	4 µg/ml	2 µg/ml	2 µg/ml
Detection Antibody	200 ng/ml	400 ng/ml	400 ng/ml	100 ng/ml
Streptavidin-HRP	200 X dilution	200 X dilution	200 X dilution	200 X dilution
Standard	125-4000 pg/ml	125-8000 pg/ml	31.2-2000 pg/ml	125-8000 pg/ml
Plasma	20 X dilution	20 X dilution	40 X dilution	40 X dilution
Cell culture media	-	5 X dilution	-	10 X dilution

Table 2. 9-Working Concentration of Reagents and Samples for ELISA measurement of sLDLR and PCSK9

2.11 Expression of MT1-MMP in mice using Adenovirus or Adeno-associated virus (AAV)

Recombinant adenoviral vectors containing cDNAs for the wild-type and mutant human MT1-MMP were generated using the AdEasy™ Adenoviral Vector System (Agilent Technologies) as described (D. W. Zhang, Graf, Gerard, Cohen, & Hobbs, 2006). Briefly, MT1-MMP cDNA was subcloned into the pShuttle-CMV vector between the restriction enzyme sites HindIII and EcoRV, followed by *in vitro* cre-lox recombination. Adenoviruses were packaged and amplified in QBI 293 cells and then purified using CsCl density-gradient ultracentrifugation. After desalting with the EconoPac 10DG column (Bio-Rad), adenoviral particles were injected into mice intravenously (1.0×10^{11} particles/mouse). 72 h later, tissues and blood were collected from euthanized mice. For cultured cells, cells were plated on a 12-well plate at the density of 1.5×10^5 cells/well in 1 ml of culture medium. 24 h later, cells were infected with adenovirus (4×10^9 particles/well). 48 h after infection, the cells were collected for analysis.

AAV carrying human MT1-MMP cDNA under the control of a hepatocyte-specific thyroxine-binding globulin (TBG) promoter was generated using the AAV-DJ/8 Helper Free Expression Complete System in accordance with the manufacturer's instruction (Cell Biolabs, Inc). Briefly, pAAVTBG.PI.EGFP.WPRE.bGH (Addgene) was cut with NotI and HindIII and a fragment of about 4.8 kb was isolated. Human MT1-MMP cDNA was amplified from plasmid pCR3.1-MT1-MMP with PCR using a forward primer with the Not I site at the beginning and a reverse primer containing the Hind III site at the end. The PCR fragment was digested with NotI and Hind III, purified, and then ligated to NotI-HindIII digested pAAVTBG.PI.EGFP.WPRE.bGH using the Quick ligation kit (NEB). The integrity of MT1-MMP cDNA was verified by DNA sequencing. The resulting vector together with pAAV-helper and pAAV-DJ/8 was transfected to QBI 293A

cells using polyethylenimine (DNA: PEI=1:4. PEI. Polysciences, Warrington, PA). 72 h post-transfection, AAV was purified from the cells using OptiPrep™ (Sigma) density-gradient ultracentrifugation as described (Zolotukhin et al., 1999). AAV particles were collected from the 40% density step, diluted in PBS, concentrated with Amicon Ultra-15 Centrifugal Filter Unit (Millipore, 100K NMWL), and tittered using qRT-PCR. Purified AAV particles were injected into mice retro-orbitally (1.0×10^{11} genomic copy (GC)/mouse). 30 days after injection, mice were euthanized, blood and tissues were collected for analysis.

2.12 Atherosclerosis Study

8-week-old male apoE^{-/-} mice were randomly divided into two groups (6 mice/group) and injected with AAV-Empty (Control group) or AAV-MT1-MMP (1.0×10^{10} GC/mouse) for MT1-MMP overexpression experiment. Similarly, 8-week-old male *MT1^{Flox}/apoE^{-/-}* mice (6 mice/group) were injected with either AAV-GFP (Control group) or AAV-TBG-cre (1.0×10^{10} GC/mouse) to knockdown hepatic MT1-MMP expression in the liver. The mice were then fed the Western-Type Diet containing 0.15% cholesterol (TestDiet, kcal from fat 40%, protein 16%, and carbohydrate 44%) for 8 weeks.

2.12.1 Histological Quantification of Plaques

Plaque quantification was carried out as described (Daugherty & Whitman, 2003). Briefly, the heart and aorta were perfused with heparin and 4% paraformaldehyde. After perfusion and fixation, the aortas and hearts were collected immediately from euthanized mice and fixed in 4% paraformaldehyde. Serial sections (8 μm thick) were taken throughout the three aortic valves of each mouse and six sections per mouse were collected for the analysis. Images were taken using

an OMAX M837ZL-C140U3 microscope (Magnification 100X). The atherosclerotic burden was quantified by measuring the surface area of Oil Red O positive lesions on the cross-sectional area of the aorta sinus. Lesion areas were quantified with OMAX ToupView.

2.12.2 Lipid Extraction and Cholesterol Ester Determination from the Aorta

Aortic lipid extraction was carried out as described (Denis et al., 2012). The aorta was cut into small pieces and homogenized in 250 μ L of 50 mM Tris-HCl (pH7.4), 250 mM sucrose, and 1 mM EDTA by a glass/Teflon homogenizer. Samples were sonicated 3 \times 10 sec on ice and the volume was completed to 1 ml with PBS. Homogenized samples were transferred into a glass tube with 4 mL of chloroform/ methanol (2:1) and incubated for 1 h with vigorous agitation. Samples were then centrifuged at 1000 g for 10 min, the bottom phase was transferred to a new glass tube and dried under nitrogen. 500 μ l of 2% Triton X-100 in chloroform was added before final evaporation under nitrogen. Lipid extracts were then dissolved in 250 μ l of distilled water. For the determination of total and free cholesterol, 30 μ l of lipid extract was loaded per well on a 96-well plate together with a set of known cholesterol standards using Cholesterol assay kit (Cell Biolabs). CE was determined by deducting the values of free cholesterol from Total cholesterol measurements.

2.13 Statistical analysis

All statistical analyses were carried out by GraphPad Prism version 8.0 (GraphPad Software). Student's *t*-test or one-way ANOVA with Tukey post-hoc test was carried out to determine the significant differences between groups. All data met normal distribution criteria and variance between groups that was analysed by F-test showed no significant difference ($P>0.05$). Values of all data unless otherwise indicated were mean \pm S.D. The significance was defined as * $p<0.05$, **

p<0.01, *** p<0.001. All experiments except for where indicated were repeated at least three times.

2.14 Primers

1) Genotyping

Primers for genotyping MT1-MMP^{Flox} mice

Forward1-CCTACCATGGGCATAACCTG;

Reverse-AGGGTGCAGACAGATGGAAG;

Forward 2-TCTGGATTCATCGACTGTGG.

Primers for detecting MT1-MMP^{LKO} mice

Forward1-CCTACCATGGGCATAACCTG;

Reverse-AGGGTGCAGACAGATGGAAG;

Forward 2-TCTGGATTCATCGACTGTGG.

2) Site-Directed Mutagenesis and PCR Primers

E240A MT1-MMP: Forward-5'-GGTGGCTGTGCACGCGCTGGGCCATGCCC-3';

Reverse-5'-GGGCATGGCCCAGCGCGTGCACAGCCACC-3'

A37P MT1-MMP: Forward-5'-AGCTTCAGCCCCGAACCCTGGCTACAGCAA-3';

Reverse-5'-TTGCTGTAGCCAGGGTTCGGGGCTGAAGCT-3'

A521V LDLR: Forward-5'-CTCCAAGCCAAGGGTCATCGTGGTGGAT-3';

Reverse-5'-ATCCACCACGATGACCCTTGGCTTGGAG -3'

A529V LDLR: Forward-5'-GTGGATCCTGTTCATGTCTTCATGTACTGG-3';

Reverse-5'-CCAGTACATGAAGACATGAACAGGATCCAC-3'

N645V LDLR: Forward-5'-AACTTGTTGGCTGAAGTCCTACTGTCCCCA-3';

Reverse-5'-TGGGGACAGTAGGACTTCAGCCAACAAGTT-3'

A789V LDLR: Forward-5'-CAGTAGCGTGAGGGTTCTGTCCATTGTC-3';

Reverse-5'-gACAATGGACAGAACCCTCACGCTACTG-3'

PCR: NotI-Forward-5'-

TCTAGAGCGGCCGCATGTCTCCCGCCCCAAGACCCCCCGTTGTC-3'); HindIII-

Reverse-5'- CCATGGAAGCTTTCAGACCTTGTCCAGCAGGGAACGCTGGCAG -3'

3) DsiRNA

Scrambled DsiRNA Forward-AUUAGUGUGCGAUGUACCCAGGAAC; Reverse-

GUUCCUGGGUACAUCGCACACUAAUUAU

MT1-MMP DsiRNA1 Forward-UCCGUGGAAACAAGUACUACCGUTT; Reverse-

AAACGGUAGUACUUGUUUCCACGGAAG

MT1-MMP DsiRNA2 Forward- CGCCGACUAAGCAGAAGAAAGAUCA; Reverse-

UGAUCUUUCUUCUGCUUAGUCGGCGAA

4) qRT-PCR Primers

Human

GAPDH Forward-GGTGTGAACCATGAGAAGTATGA; Reverse-

GAGTCCTTCCACGATACCAAAG

MT1-MMP Froward-TGCCTACCGACAAGATTGATG; Reverse-

ATCCCTTCCCAGACTTTGATG

MT2-MMP Froward-ACA ACTATCCCATGCCCATC; Reverse-

CTTCTCGAAAGAGCCAGTAGC

PCSK9 Forward-CACAGAGTGGGACATCACAG; Reverse-

TTTGGCAGAGAAGTGGATCAG

LDLR Forward-TTCACTCCATCTCAAGCATCG; Reverse-
ACTGAAAATGGCTTCGTTGATG

IDOL Forward-TGCTGTGTTATGTGACGAGG; Reverse-
CTTTGCTACCCGTAAACTGC

SREBP2 Forward-TTCCTGTGCCTCTCCTTTAAC; Reverse-
TCATCCAGTCAAACCAGCC

HMGCR Forward-ACAGATACTTGGGAATGCAGAG; Reverse-
CTGTCCGGCGAATAGATACACC

Mouse

GAPDH Forward-AACTTTGGCATTGTGGAAGG; Reverse-
GGATGCAGGGATGATGTTCT

MT1-MMP Forward-TCACCCCAGTCACTCTCAG; Reverse-
CTCAGTCCCAAACCTTATCCGG

MT2-MMP Forward-CGTTCTAGACAACCTACCCCATG; Reverse-
TTCTCGGAAAAGCCAGTAGC

MT3-MMP Forward-CGCTACGCATTAACCTGGACAG; Reverse-
AGGAGTTACATTCTGCCACAC

MT4-MMP Forward-GCTCAAATGCATCGCTTCTG; Reverse-
TGTCCTTAAACACCCAGTATCTG

MT5-MMP Forward-AGAAGTGGAGGCAGAAACAC; Reverse-
CTCTTCAAAGGTCAGTGGAGTC

MT6-MMP Forward-GTCCCAAATCCAAATGCCAG; Reverse-
AAAATTTCCCCTCGAATGTTGG

ADAM17 Forward-GGGTTTTGCGACATGAATGG; Reverse-
GAAAACCAGAACAGACCCAAC

LDLR Forward-ACCCGCCAAGATCAAGAAAG; Reverse-
GCTGGAGATAGAGTGGAGTTTG

HMGCR Forward-GCCCTCAGTTCAAATTCACAG; Reverse-
TTCCACAAGAGCGTCAAGAG

PCSK9 Forward-TTTTATGACCTCTTCCCTGGC; Reverse-
ATTCGCTCCAGGTTCCATG

SREBP2 Forward-CCCTATTCCATTGACTCTGAGC; Reverse
CACATAAGAGGATTCGAGAGCG

Chapter 3

Membrane type 1 matrix metalloproteinase promotes ectodomain shedding of low-density lipoprotein receptor and accelerates the development of atherosclerosis

All experiments were conducted and analyzed by Adekunle Alabi in Zhang's lab except

Fig 3.1a,3.1b, 3.1f, 3.2b,3.2e,3.3e (Faqi Wang and Ayinuer Adijiang- Zhang Lab)

Fig 3.3b and c (Hong-mei Gu-Zhang Lab)

Fig 3.1i (Shi-jun Deng and Adekunle Alabi-Zhang Lab)

Fig 3.10 (Data collection by Nana Yang, Yazhuo Xue, Li Chen and Shucun Qin- Institute of Atherosclerosis in Shandong First Medical University China. Data analysis by Dawei Zhang and Adekunle Alabi)

Fig 3.11c and 11g (Xiao-dan Xia and Adekunle Alabi-Zhang lab)

3.1 Introduction

Atherosclerotic cardiovascular disease is one of the main causes of morbidity and mortality in Western societies. Plasma levels of low-density lipoprotein cholesterol (LDL-C) are positively correlated with the risk of atherosclerosis (Goldstein & Brown, 2015). LDL receptor (LDLR) mediates LDL uptake and plays an essential role in removing plasma LDL-C. Upon LDL binding, LDLR is internalized via clathrin-coated pits and delivered to endosomes, where LDL is released from the receptor and delivered to the lysosome for degradation, LDLR is then recycled to the cell surface (Rudenko et al., 2002). Mutations in LDLR cause familial hypercholesterolemia and increase the risk of atherosclerosis and coronary heart disease (Goldstein & Brown, 2015).

LDLR is transcriptionally regulated by the sterol regulatory element-binding protein 2 (SREBP-2). Statins inhibit 3-Hydroxy-3-Methylglutaryl-CoA Reductase (HMGCR) and consequently activate the transcriptional activity of SREBP2, leading to increased LDLR expression (Goldstein & Brown, 2015). Posttranslationally, proprotein convertase subtilisin/kexin 9 (PCSK9) binds to LDLR and redirects the receptor for lysosomal degradation (Lagace, 2014; Rashid et al., 2005; Seidah, Awan, Chrétien, & Mbikay, 2014; Zhang et al., 2007), while the inducible degrader of LDLR (IDOL) reduces LDLR levels via the polyubiquitination and lysosomal degradation pathway (Zelcer, Hong, Boyadjian, & Tontonoz, 2009). In addition, the ectodomain of LDLR can be cleaved by proteases with the released extracellular domain detected in cell culture media and in human plasma as a soluble form (sLDLR) (Begg, Sturrock, & van der Westhuyzen, 2004; Fischer, Tal, Novick, Barak, & Rubinstein, 1993; Shimohiro, Taniguchi, Koda, Sakai, & Yamada, 2015). Serum levels of sLDLR are positively correlated with plasma LDL-C levels (Mayne et al., 2018; Shimohiro et al., 2015). It has been shown that the ectodomain cleavage of LDLR is inhibited by metalloproteinase inhibitors (Begg et al., 2004; Strøm, Tveten, Laerdahl, & Leren,

2014). Knockdown of a disintegrin and metalloproteinase 17 (ADAM17), a metalloproteinase responsible for the shedding of many transmembrane proteins, however, has only a marginal effect on ectodomain cleavage of LDLR in HepG2 cells (Strøm et al., 2014). Thus, the metalloproteinase(s) responsible for the bulk of LDLR shedding is unknown.

Membrane type-I matrix metalloproteinase (MT1-MMP/MMP14), a Zn^{2+} -dependent endopeptidase, belongs to a six-member family of membrane-type MMPs that includes four transmembrane type MMPs (MT1-, MT2-, MT3-, MT5-MMP), and two glycosyl phosphatidylinositol-anchored membrane-associated MMPs (MT4-, MT6-MMP) (Itoh, 2015). MT1-MMP is widely expressed in various tissues and cell types and plays key roles in both physiological processes and disease progression through the remodelling of extracellular matrix and pericellular proteolysis (Feinberg et al., 2018; Holmbeck et al., 1999; Zhou et al., 2000). MT1-MMP has been reported to cleave transmembrane proteins such as death receptor-6, neuropilin-1, and LDLR-related protein 1 (LRP-1) in breast cancer cells (Dmitri V Rozanov, Hahn-Dantona, Strickland, & Strongin, 2004; Tam, Morrison, Wu, Stack, & Overall, 2004). Cleavage of LDLR is enhanced by 4 β -phorbol 12-myristate 13-acetate that can induce the trafficking of MT1-MMP to the cell surface and enhance its cleavage function (Begg et al., 2004). The exact role of MT1-MMP in LDLR shedding, however, is unclear. Here, we found that reducing MT1-MMP expression increased LDLR levels in cultured cells. Furthermore, specific knockout of MT1-MMP in mouse hepatocytes increased hepatic LDLR levels and reduced plasma levels of lipoprotein cholesterol. An opposite phenotype was observed when the wild-type MT1-MMP, but not the enzymatically dead mutant E240A, was overexpressed in cultured cells and mice. Consequently, overexpression of MT1-MMP significantly increased atherosclerotic lesion area in the aortic sinus, while knockdown of MT1-MMP reduced cholesterol accumulation in the aortas in apolipoprotein E

knockout (apoE^{-/-}) mice. Mechanistically, we found that MT1-MMP directly associated with LDLR and promoted its ectodomain cleavage. Taken together, these findings **demonstrate that hepatic LDLR ectodomain is shed by MT1-MMP and that MT1-MMP regulates plasma LDL-C metabolism and the development of atherosclerosis.**

3.2 Results

3.2.1 MT1-MMP regulates LDLR expression

MT1-MMP activates pro-MMP2 (Butler et al., 1998; Zhou et al., 2000). We have previously reported that active MMP2 can cleave PCSK9 (Wang et al., 2015). Thus, we initially assumed that inhibition of MT1-MMP could reduce the amount of active MMP2 and suppress MMP2-induced cleavage of PCSK9, thereby enhancing PCSK9-promoted LDLR degradation and consequently decreasing LDLR levels. To test this hypothesis, we knocked down the expression of MT1-MMP in human hepatoma-derived Huh7 cells. The two MT1-MMP siRNAs that target different regions in the *MT1-MMP* mRNA efficiently reduced the levels of MT1-MMP but not MT2-MMP (the closest family member to MT1-MMP) (**Fig. 3.1a**). The addition of PCSK9 reduced cellular LDLR levels in scrambled siRNA-transfected cells, as well as in cells transfected with MT1-MMP siRNA (**Fig. 3.1b**). We then co-transfected Huh7 cells with MT1-siRNA and a plasmid containing PCSK9 cDNA and found that overexpression of PCSK9 efficiently stimulated LDLR degradation in cells transfected with either scrambled or MT1-MMP siRNA (**Fig. 3.1c**). Thus, knockdown of MT1-MMP did not affect PCSK9-promoted LDLR degradation. Surprisingly, we found that LDLR levels were markedly increased in MT1-MMP knockdown cells in the absence of PCSK9 (**Fig. 3.1b, lanes 3 and 5 vs 1**). We noticed that knockdown of MT1-MMP appeared not to markedly affect the levels of LDLR in the presence of exogenous PCSK9 (**Fig. 3.1b, lanes 4 and 6 vs 2**). It is of note that the experiment was performed in the presence of excess PCSK9 and under a non-physiological condition. First, Huh7 cells express endogenous PCSK9. Second, the cells were incubated in medium containing 5% NCLPPS that is known to increase endogenous PCSK9 expression and enhance PCSK9-promoted LDLR degradation. Third, the cells were supplied with an additional 2 $\mu\text{g/ml}$ of recombinant human PCSK9. Thus, it was likely that PCSK9-promoted

LDLR degradation became overwhelming under this condition. To further confirm the impact of MT1-MMP on LDLR expression, we knocked down MT1-MMP expression in another human hepatoma-derived cell line (HepG2) and found that LDLR levels were significantly increased in MT1-MMP siRNA-transfected cells, whereas the levels of MT2-MMP, LRP-1 and transferrin receptor were comparable in cells transfected with scrambled or MT1-MMP siRNA (**Fig. 3.1d, lanes 2 and 3 vs 1**). Similar results were observed in mouse hepatocytes, Hepa1C1C7 (**Fig. 3.1e**). Next, we overexpressed HA-tagged MT1-MMP in Huh7 cells and observed that MT1-MMP reduced cellular LDLR levels in a dose-dependent manner (**Fig. 3.1f**). Overexpression of MT1-MMP, however, had no significant effect on the levels of endogenous PCSK9 (**Fig. 3.1g, lanes 4-6 vs. 1-3**). LDLR resides on the plasma membrane, where it binds to and mediates LDL internalization. Thus, cell surface proteins in Huh7 cells were assessed using biotinylation. As shown in **Figure 3.1h**, expression of MT1-MMP in both whole cell lysate and the cell surface fraction was reduced by its siRNA. Conversely, expression of LDLR was increased in the whole-cell lysate (**lane 2 vs 1**) and the surface fraction (**lane 4 vs 3**) in MT1-MMP-knockdown cells. Calnexin (an ER protein) was undetectable in the surface fraction. Analysis of basal LDL uptake by these cells demonstrated a role for MT1-MMP in this process, with knockdown of MT1-MMP showing significantly increased cellular LDL uptake (**Fig. 3.1i**). Together, these findings demonstrate that MT1-MMP regulates LDLR expression and LDL uptake in cultured hepatocytes.

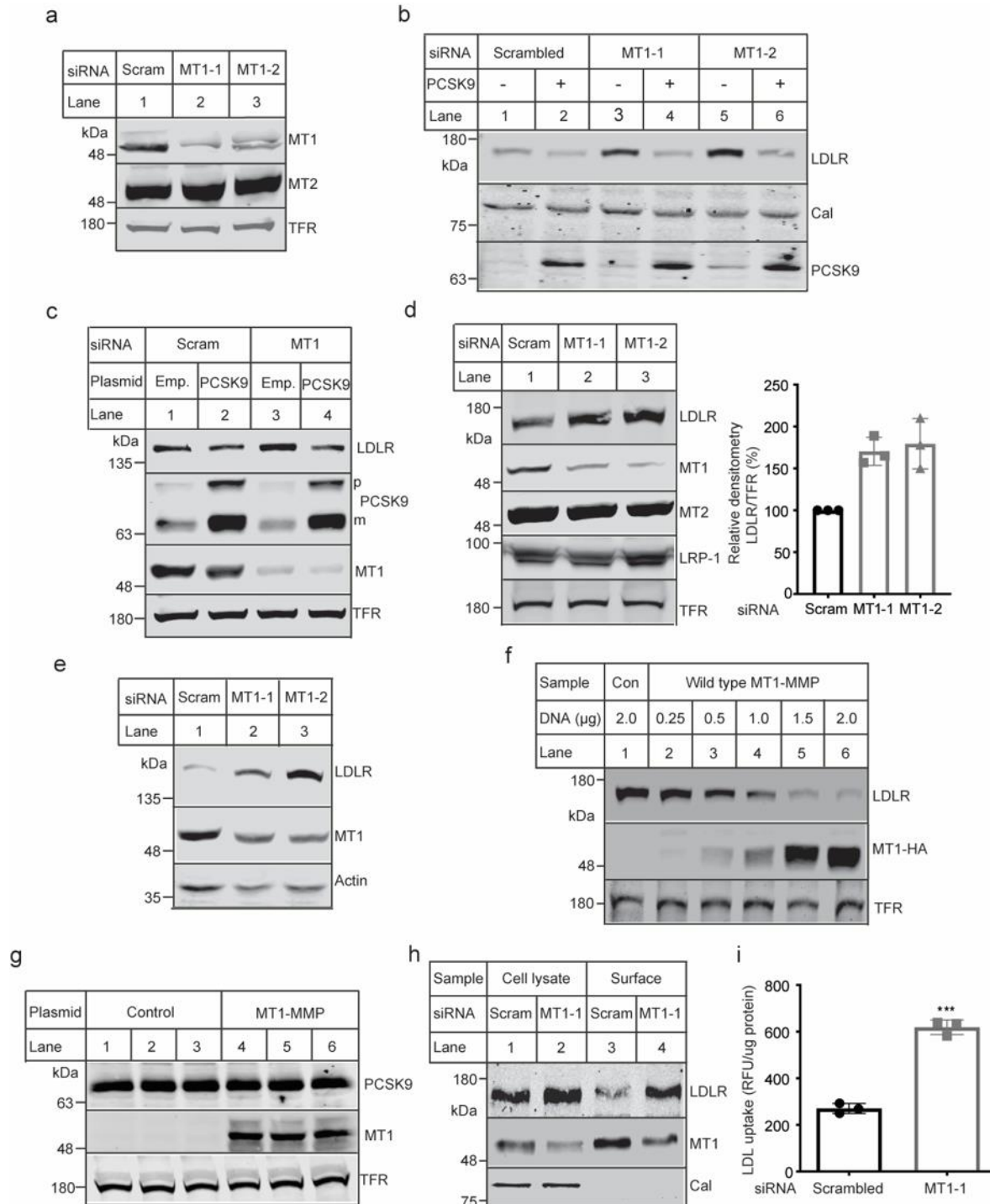


Fig 3. 1. MT1-MMP-mediated LDLR degradation. (a) Knockdown of MT1-MMP expression. Huh7 cells were transfected with scrambled (Scram) or one of the two different MT1-MMP siRNAs (MT1-1, MT1-2). 48 h later, cells were harvested for the preparation of whole cell lysate.

The same amount of total proteins in whole cell lysate was applied to Western blot. The membrane was cut into halves along the 100-kDa protein marker. The top was blotted with a mouse anti-transferrin receptor (TFR) monoclonal antibody and the bottom was blotted with a rabbit anti-human MT1-MMP monoclonal antibody (MT1) or a rabbit anti-MT2-MMP (MT2) polyclonal antibody. **(b) Effect of MT1-MMP knockdown on PCSK9-promoted LDLR degradation.** Huh7 cells transfected with scrambled or MT1-MMP siRNA for 48 h were incubated with DMEM containing 5% NCLPPS with or without PCSK9 (2 µg/ml) for 4 h. Same quantities of whole cell lysate were applied to Western blot. The membranes were cut into halves above the 75-kDa marker. The top parts were blotted with a monoclonal anti-human LDLR antibody or a mouse anti-calnexin (Cal) monoclonal antibody. The bottom part was blotted with a mouse anti-PCSK9 monoclonal antibody. **(c) Effect of MT1-MMP on PCSK9-promoted LDLR degradation.** Huh7 cells were transfected with scrambled (Scram) or MT1-MMP (MT1) siRNA together with either empty plasmid pCDNA3.1 (Emp) or pCDNA3.1 containing PCSK9 cDNA (PCSK9). 48 h later, cells were collected for the isolation of whole cell lysate. The same amount of total proteins in whole cell lysate was subjected to Western blot. The membranes were cut into halves along the 100-kDa protein standard. The top parts were blotted with a rabbit anti-LDLR polyclonal antibody (3143) and a mouse anti-Transferrin receptor (TFR) monoclonal antibody. The bottom parts were blotted with a mouse anti-PCSK9 monoclonal antibody (15A6) and a rabbit anti-MT1-MMP monoclonal antibody (abcam). **(d) Effect of MT1-MMP knockdown in HepG2 cells.** The cells were transfected with scrambled (Scram) or MT1-MMP siRNAs (MT1-1, MT1-2) for 48 h. The same amount of whole cell lysate was applied to immunoblotting as described above. The membranes were cut into halves along the 75-kDa marker. The top parts were blotted with a mouse anti-human LDLR monoclonal antibody, a mouse anti-transferrin receptor (TFR) monoclonal antibody, or a rabbit anti-LRP1 polyclonal antibody. The bottom part was blotted with a rabbit anti-MT1-MMP monoclonal or a rabbit anti-MT2-MMP polyclonal antibody. The images showed representative protein levels. The relative densitometry was the ratio of the densitometry of LDLR to that of TFR in the same condition. The percentage of relative densitometry was the ratio of the relative densitometry of LDLR at different treatments to that of LDLR at the control condition, which was defined as 100%. **(e) Effect of MT1-MMP knockdown on LDLR levels.** Hepa1c1c7 cells were transfected with scrambled (Scram) or MT1-MMP siRNA, followed by immunoblotting with antibodies indicated. **(f) Effect of MT1-MMP overexpression on LDLR.** Huh7 cells were transfected with empty plasmid (Con) or different amounts of plasmid carrying MT1-MMP cDNA for 48 h. The same amount of whole cell lysate was subjected to immunoblotting as described above. The top parts were blotted with a mouse anti-human LDLR or transferrin receptor (TFR) monoclonal antibody. The bottom part was blotted with a rabbit anti-HA polyclonal antibody to detect HA-tagged MT1-MMP. **(g) Effect of MT1-MMP on PCSK9 expression.** Huh7 cells were transfected with either empty plasmid pCDNA3.1 (Control) or pCDNA3.1 containing MT1-MMP cDNA (MT1-MMP). 48 h later, cells were collected for the isolation of whole cell lysate. The same amount of total proteins in whole cell lysate was subjected to Western blot. The membranes were cut into halves along the 100-kDa protein standard. The top parts were blotted with a mouse anti-Transferrin receptor (TFR) monoclonal antibody. The bottom parts were blotted with a mouse anti-PCSK9 monoclonal antibody (15A6) and a rabbit anti-HA antibody. **(h) Biotinylation of cell surface proteins.** Huh7 cells transfected with scrambled (Scram) or MT1-MMP siRNA (MT1-1) were biotinylated. The same amount of total proteins in whole cell lysate was applied to NeutrAvidin beads to pull down cell surface proteins, followed by immunoblotting. The membranes were cut into halves along the 75-kDa marker. The top halves were blotted with a

mouse anti-human LDLR or calnexin (Cal) monoclonal antibody. The bottom parts were blotted with a rabbit anti-MT1-MMP monoclonal antibody (Abcam). **(i) LDL uptake.** Huh7 cells transfected with scrambled or MT1-MMP siRNA (MT1-1) for 48 h were labeled with Dil-LDL in the absence and presence of unlabeled LDL. Fluorescence intensity (RFU) was measured. Specific binding was calculated by subtraction of binding in the presence of cold LDL from total binding without cold LDL and normalized to protein concentrations in the same well.

3.2.2 MT1-MMP promotes ectodomain cleavage of LDLR

We then examined what mechanisms mediated the effect of MT1-MMP on LDLR expression. Ilomastat (GM6001), a collagen-based peptidomimetic hydroxamate that can inhibit MT1-MMP activity (Nam, Rodriguez, Remacle, Strongin, & Ge, 2016), did not alter the expression of MT1-MMP but increased endogenous LDLR levels in Huh 7 cells (**Fig. 3.2a**). Leupeptin (an inhibitor of serine and cysteine proteases) and pepstatin (an inhibitor of aspartyl proteases), however, had no effect on LDLR levels (**Fig. 3.2b**). These findings were consistent with previous reports that LDLR cleavage depends on MMPs (Begg et al., 2004). Moreover, MT1-MMP could efficiently promote LDLR degradation in the absence and presence of MG132, a proteasome inhibitor, or chloroquine, a lysosome inhibitor (**Fig. 3.2c**), indicating a negligible role of the two pathways in MT1-MMP's action on the receptor. qRT-PCR data showed that both MT1-MMP siRNAs efficiently reduced mRNA levels of *MT1-MMP* but not that of *MT2-MMP*, *LDLR*, *SREBP-2*, *PCSK9*, or *IDOL* (**Fig. 3.2d**), indicating that MT1-MMP had no dramatic effect on transcription of *LDLR*. We then generated a catalytically inert mutant MT1-MMP by replacing Glu at position 240 (E240) with Ala (MT1-E240A) since E240 is critical for MT1-MMP proteolytic activity (Dmitry V. Rozanov et al., 2001). As shown in **Figure 3.2e**, overexpression of the wild-type MT1-MMP but not MT1-E240A markedly reduced LDLR levels in HepG2, Huh7, Hepa1C1C7 and rat hepatoma-derived McArdle cells, indicating the requirement of the proteolytic activity of MT1-MMP for its effect on LDLR expression. We then collected culture medium from Huh7 cells transfected with scrambled or MT1-MMP siRNA to measure cleaved ectodomain of LDLR. As shown in **Figure 3.2f**, knockdown of MT1-MMP significantly reduced the intensity of an LDLR band with a molecular weight of approximately 100-120 kDa in the culture medium. Concomitantly, LDLR abundance in whole cell lysate was increased in MT1-MMP knockdown

cells (**Fig. 3.2f, lane 2 vs 1**). On the other hand, co-expression of N-terminal Myc-tagged LDLR and HA-tagged MT1-MMP in HEK293 cells significantly reduced LDLR levels in whole-cell lysate but increased cleaved ectodomain of LDLR in culture medium that was detected by an anti-Myc antibody (**Fig. 3.2g, lane 2 vs 1**). The size of the cleaved extracellular domain of LDLR was consistent with the size of the soluble ectodomain of LDLR reported in previous studies (Begg et al., 2004; Guo et al., 2002). We also measured sLDLR levels in culture medium using ELISA and found that knockdown of MT1-MMP significantly reduced (**Fig. 3.2h**), while co-expression of MT1-MMP and LDLR significantly increased the levels of sLDLR in culture medium (**Fig. 3.2i**). Thus, MT1-MMP can proteolytically cleave LDLR.

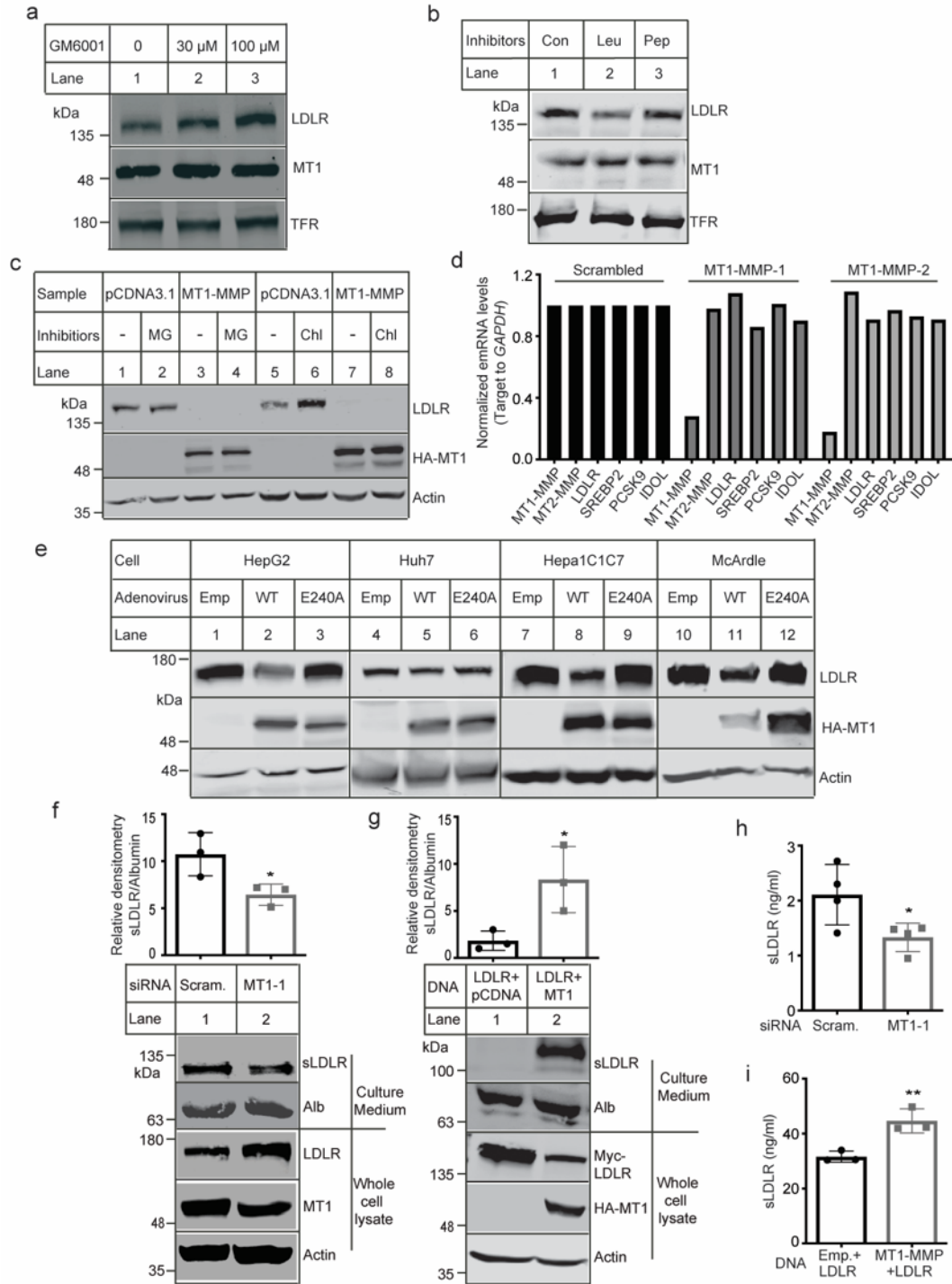


Fig 3. 2. MT1-MMP-mediated LDLR cleavage. (a) *Effect of GM6001 on LDLR expression.* Huh7 cells were incubated with GM6001 at concentrations indicated for 16 h. The same amount of whole cell lysate was applied to immunoblotting with a mouse anti-human LDLR monoclonal antibody, a mouse anti-transferrin receptor (TFR) monoclonal antibody, and a rabbit anti-MT1-MMP monoclonal antibody. (b) *Effect of broad-spectrum protease inhibitors on LDLR levels.* Immunoblotting of the same amount of whole cell lysate isolated from Huh7 cells treated with

Leupeptin (50 µg/ml) or Pepstatin (1 µg/ml) for 5 h. **(c) Inhibitors treatment.** Huh7 cells were transfected with empty pCDNA3.1 or HA-tagged MT1-MMP-pCDNA3.1. 48 h later, the cells were incubated with MG132 (10 µM, MG) or chloroquine (10 µM, Chloro) for 6 h. After, cells were harvested for the preparation of whole cell lysate. The same amount of total proteins in whole cell lysate was then subjected to immunoblotting. The top parts of the membranes were blotted with a mouse anti-LDLR monoclonal antibody. The bottom parts were blotted with a rabbit anti-HA polyclonal antibody and a mouse anti-actin monoclonal antibody. **(d) Effect of MT1-MMP knockdown on gene expression.** The same amount of total RNAs extracted from Huh7 cells transfected with scrambled or MT1-MMP siRNAs was used for cDNA synthesis and then qRT-PCR. The relative mRNA levels were the ratio of the mRNA levels of the target genes to that of *GAPDH* in the same condition. The fold-change of the relative mRNA levels of target gene expression in MT1-MMP siRNA treated groups was determined in comparison with that in the control group that was defined as 1. **(e) Effect of MT1-MMP overexpression in different cell types.** Cells as indicated were set up in a six-well plate and infected with either empty (**Emp**), the wild-type (**WT**), or mutant E240A (**E240A**) MT1-MMP adenoviruses. 48 h later, cells were collected for the preparation of whole cell lysate. The same amount of total proteins in whole cell lysate was subjected to immunoblotting. Antibodies used were a mouse anti-LDLR monoclonal antibody, a rabbit anti-HA tag polyclonal antibody, and a mouse anti-actin monoclonal antibody. **(f) LDLR cleavage.** Huh7 cells set up in a 6-well plate were transfected with scrambled (**Scram**) or MT1-MMP siRNA (**MT1-1**). 36 h later, cells were cultured in DMEM only medium for 16 h. Cells and culture medium were then collected separately. Culture media were concentrated using TCA precipitation. The same quantities of whole cell lysate (**bottom**) and concentrated media (**top**) were subjected to immunoblotting with a monoclonal anti-LDLR antibody, a rabbit anti-MT1-MMP (**MT1**) monoclonal antibody, a goat anti-albumin (**Alb**) polyclonal antibody or a mouse anti-transferrin receptor (**TFR**) monoclonal antibody. **(g) Ectodomain cleavage.** HEK293 cells were transfected with plasmid containing N-terminal Myc-tagged LDLR plus empty vector (1:1), or the same total amount of plasmid containing HA-tagged MT1-MMP plus plasmid containing Myc-tagged LDLR (1:1). After 36 h, culture medium was changed to DMEM containing 0.5% FBS overnight. Whole-cell lysate (**bottom**) and culture medium (**top**) were prepared as described above and subjected to immunoblotting with a rabbit anti-Myc polyclonal antibody to detect Myc-tagged LDLR, a goat anti-albumin (**Alb**) polyclonal antibody, a rabbit anti-HA polyclonal antibody to detect HA-tagged MT1-MMP and a mouse anti-actin monoclonal antibody. The bottom figures in panels *f* and *g* showed representative protein levels. The densitometry was determined using a Li-Cor Odyssey Infrared Imaging System. The relative densitometry was the ratio of the densitometry of sLDLR to that of albumin in culture medium in the same sample. **(h and i) Soluble LDLR.** Culture medium was collected from Huh7 cells that were transfected with scrambled (**Scram**) or MT1-MMP siRNA (**MT1-1**) for 48 h (**h**) or from HEK293 cells that were transfected with *LDLR* +empty vector or *LDLR*+*MT1-MMP* for 48 h (**i**). The levels of sLDLR in culture medium were then measured using a commercial ELISA kit (R&D system).

Our next experiments were to investigate the interaction between MT1-MMP and LDLR. As shown in **Figure 3.3a**, LDLR was immunoprecipitated from whole cell lysate isolated from HepG2 cells by its specific monoclonal antibody, but not a monoclonal anti-Myc antibody. MT1-MMP was present only in the LDLR-immunoprecipitated sample (**lane 1**). Transferrin receptor was not detectable in the immunoprecipitated pellets. A reciprocal immunoprecipitation using an anti-MT1-MMP antibody to pull down MT1-MMP revealed that LDLR co-immunoprecipitated with MT1-MMP but not the anti-Myc antibody (**Fig. 3.3b, lane 1 vs 2**). Similarly, immunoprecipitation of MT1-MMP from whole cell lysate of Huh7 cells pulled down LDLR (**Fig. 3.3c, lane 2 vs 1**) and vice versa (**Fig. 3.3d, lane 1 vs 2**). To further confirm these findings, we performed confocal microscopy and found that a majority of endogenous MT1-MMP (**green**) and LDLR (**red**) could be detected on the cell periphery and co-localized in Huh7 cells (**Fig. 3.3e, yellow** in Merged panel).

Next, we determined the effects of MT1-MMP on LDLR expression in human primary hepatocytes that are more representative of the functions of human liver than immortalized human hepatoma-derived cell lines, such as HepG2 and Huh7. As shown in **Figure 3.3f**, MT1-MMP siRNA reduced mRNA levels of MT1-MMP but not that of LDLR. Conversely, LDLR protein levels were markedly increased in MT1-MMP knockdown cells (**Fig. 3.3g**) but reduced in MT1-MMP-overexpressing cells (**Fig. 3.3h**). Consistently, sLDLR in the culture medium was reduced when the expression of MT1-MMP was silenced (**Fig. 3.3i**) but increased when MT1-MMP was overexpressed (**Fig. 3.3j**). Collectively, these findings demonstrate that MT1-MMP promotes ectodomain cleavage of LDLR.

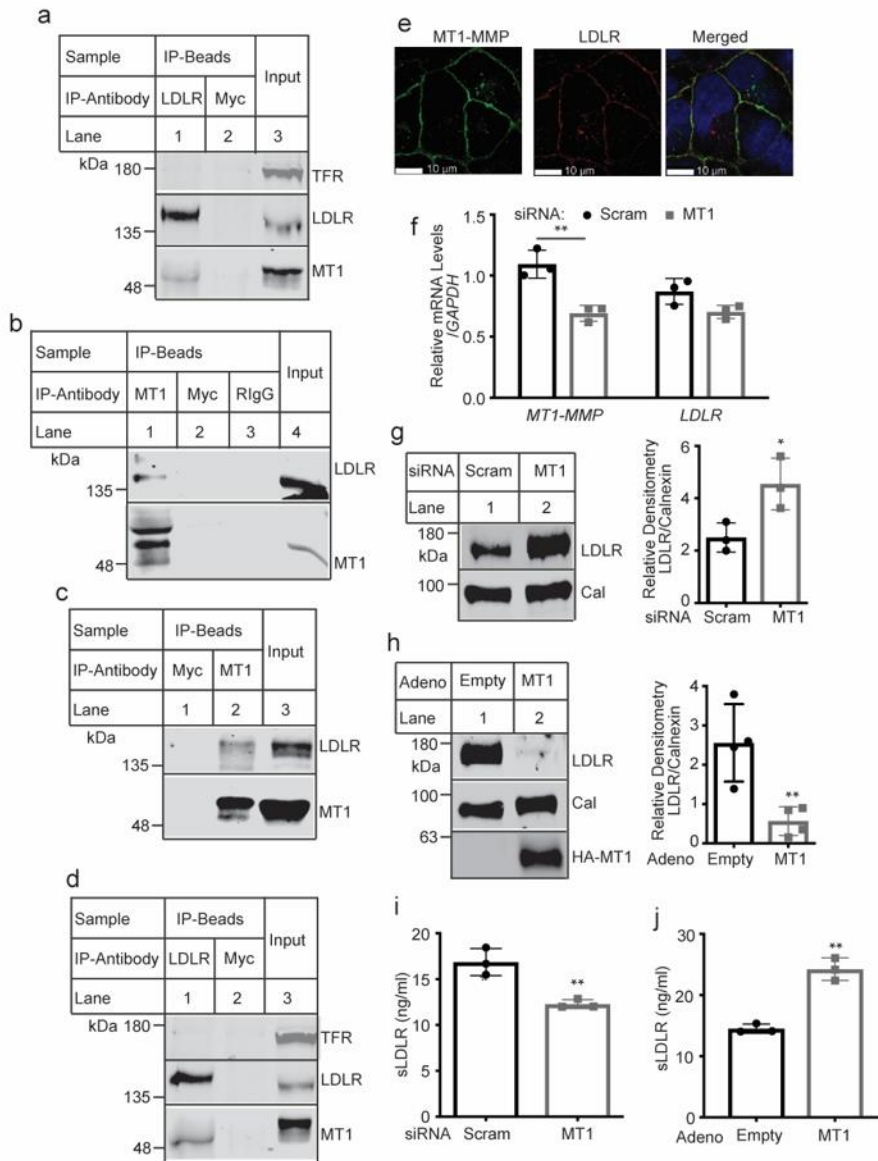


Fig 3. 3. Effects of MT1-MMP on LDLR. (a and b) Immunoprecipitation of LDLR (a) and MT1-MMP (b). Whole-cell lysate was isolated from HepG2 cells cultured in DMEM containing 5% NCLPPS for 16 h. The same amount of total proteins in whole cell lysate was subjected to immunoprecipitation using protein G beads and a mouse anti-LDLR (LDLR) or anti-Myc (Myc) antibody (a), or protein G beads and a mouse anti-MT1-MMP monoclonal antibody (Millipore), a mouse anti-Myc (Myc) antibody or rabbit IgG (RlgG). The immunoprecipitated proteins (**IP-Beads**) and whole cell lysate (**Input**) were subjected to Western blot. The membranes were cut into halves along the 100kDa protein standard. The top half was blotted with a rabbit anti-LDLR

polyclonal antibody (3143) and a monoclonal anti-TFR antibody. The bottom half was blotted with a rabbit anti-MT1-MMP monoclonal antibody (abcam). **(c and d) Immunoprecipitation of MT1-MMP (c) and LDLR (d).** The experiments were performed as described in panels 3a and b except that whole cell lysate was isolated from Huh7 cells. **(e) Confocal microscopy.** Huh7 cells were seeded on coverslips and cultured in DMEM containing 5% NCLPPS for 16 h. After fixing and permeabilization, the cells were incubated with a mouse anti-LDLR monoclonal and a rabbit anti-MT1-MMP monoclonal antibody. Antibody binding was detected using Alexa Fluor 488 goat anti-rabbit IgG (green) and Alexa Fluor 568 goat anti-mouse IgG (red). Nuclei were visualized with DAPI and shown as blue. An x-y optical section of the cells illustrates the cellular distribution of proteins (magnification: 100X). **(f and g) Knockdown of MT1-MMP in human primary hepatocytes.** Primary human hepatocytes cultured in a 12-well plate were transfected with scrambled (Scram) or MT1-MMP siRNA (MT1). Total RNAs were extracted and used for the synthesis of cDNA, followed by qRT-PCR. The relative mRNA levels were the ratio of the mRNA levels of the target genes to that of *GAPDH* at the same condition **(f)**. The same amount of total proteins in whole cell lysate derived from siRNA-transfected primary cells was subjected to immunoblotting. Antibodies used were a mouse anti-LDLR monoclonal antibody and a mouse anti-calnexin (Cal) monoclonal antibody. Relative densitometry was the ratio of the densitometry of LDLR to that of calnexin at the same condition **(g)**. **(h) Overexpression of MT1-MMP.** Primary human hepatocytes cultured in a 12-well plate were infected with empty or the wild-type MT1-MMP (MT1)-adenovirus (2.5×10^9 particles/well). 48 h later, whole-cell lysate was prepared. The same amount of total proteins in whole cell lysate was applied to immunoblotting. Antibodies used were a mouse anti-LDLR monoclonal antibody, a mouse anti-calnexin (Cal) monoclonal antibody, and a rabbit anti-HA tag polyclonal antibody. The relative densitometry was determined as described above. **(i and j) sLDLR in culture medium.** Primary human hepatocytes were treated with siRNA **(i)** or adenovirus **(j)** as indicated in panels 3g and h, respectively. 36 h after, the cells were incubated in serum-free DMEM medium overnight. The same amount of medium was used to measure sLDLR with a commercial ELISA kit (R&D system).

3.2.3 MT1-MMP promotes LDLR cleavage *in vivo*

We further sought to understand the regulatory role of MT1-MMP in LDLR expression *in vivo*. Considering that MT1-MMP null mice die at 3–4 weeks (Holmbeck et al., 1999; Zhou et al., 2000) and that the catabolism of plasma LDL-C is mainly mediated via hepatic LDLR, we generated MT1-MMP liver-specific knockout mice ($MT1^{LKO}$) through crossing $MT1^{FLOX}$ mice with Alb-Cre mice that express Cre recombinase under the control of a hepatocyte-specific albumin promoter (**Fig. 3.4a**). The $MT1^{FLOX}$ mice, in which exons 2 and 4 of the *MT1-MMP* gene (containing prodomain and catalytic domain) are flanked by LoxP sites, have been successfully used to generate knockout of MT1-MMP in monocytes/macrophages and epidermis (Klose, Zigrino, & Mauch, 2013; Zigrino et al., 2012). The expression of MT1-MMP in primary hepatocytes isolated from mouse livers was markedly reduced in $MT1^{LKO}$ mice (**Fig. 3.4b**). Genotyping results also revealed that the *MT1-MMP* gene was essentially undetectable in the liver of $MT1^{LKO}$ but not $MT1^{FLOX}$ mice (**Fig. 3.4c**) or other tissues isolated from $MT1^{LKO}$ mice (**Fig. 3.4d**). mRNA levels of *MT1-MMP* were also drastically reduced in the liver of $MT1^{LKO}$ mice (**Fig. 3.4e**). $MT1^{LKO}$ mice were active, fertile and indistinguishable from floxed littermates (**Fig. 3.4f**). Bodyweight and plasma ALT activities were also comparable in $MT1^{LKO}$ and $MT1^{FLOX}$ mice (**Figs. 3.4g and h**).

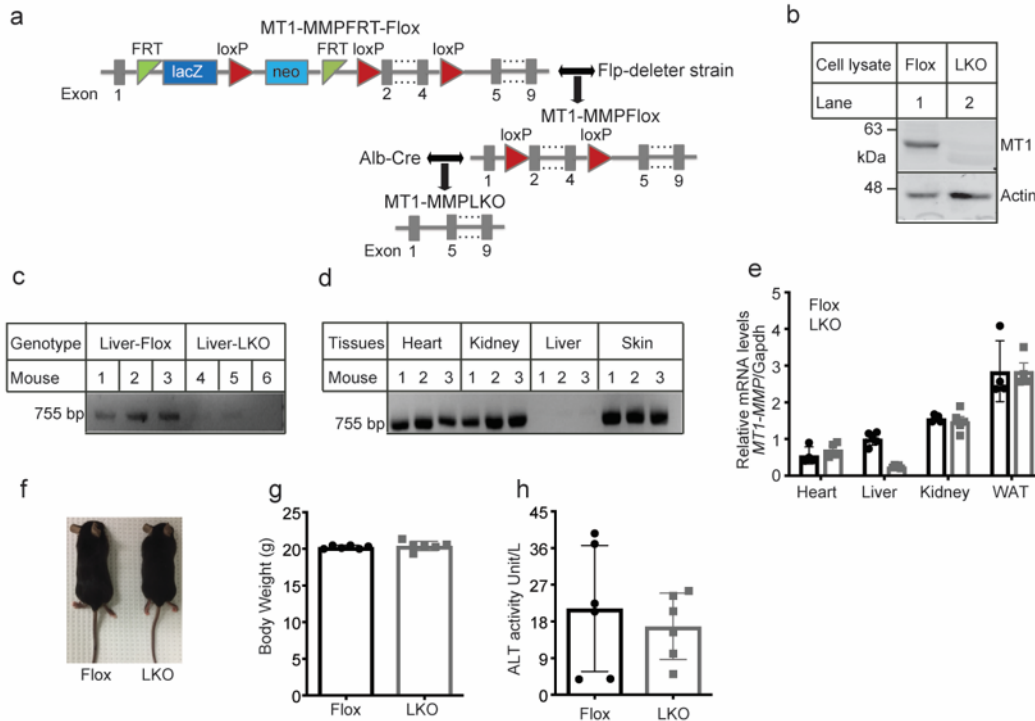


Fig 3. 4. Metabolic effects of $MT1^{LKO}$ mice. (a) A schematic of $MT1-MMP^{LKO}$ mice generation.

A vector containing the loxP sites that flanked exons 2 to 4 of the $MT1-MMP$ gene was used to generate $MT1-MMP^{FRTFLOX}$. $MT1-MMP^{FRTFLOX}$ heterozygotes were crossed to generate homozygotes. The resulting homozygotes were then mated to the Flp-deleter strain (the Jackson Laboratory) to obtain $MT1^{FLOX}$ mice without the FRT-flanked selection marker. $MT1^{FLOX}$ mice were then mated with Alb-Cre mice (the Jackson laboratory) to delete functional MT1-MMP in hepatocytes to generate $MT1^{LKO}$ mice. FRT= flippase recognition target. loxP=locus of X-ing of bacteriophage P. **(b) $MT1-MMP$ deletion in primary mouse hepatocytes.** Primary mouse hepatocytes were isolated from $MT1^{FLOX}$ and $MT1^{LKO}$ mice and cultured for 48 h. Cells were then collected to make whole cell lysate. The same amount of total proteins in whole cell lysate was subjected to immunoblotting. Antibodies used were a rabbit anti-MT1-MMP monoclonal antibody (MT1, abcam) and a mouse anti-actin monoclonal antibody. **(c and d) Genotyping.** DNA was extracted from the liver of $MT1^{FLOX}$ and $MT1^{LKO}$ mice **(c)** or different tissues of $MT1^{LKO}$ mice **(d)** for genotyping using PCR to detect the LoxP-flanked exons 2–4 of the $MT1-MMP$ gene with the AccuStartTM II Mouse Genotyping Kit (Quanta Biosciences). One of the two primers was located within of the LoxP sites. A PCR product was only amplified in $MT1^{FLOX}$ but not in $MT1^{LKO}$ mice after recombination leading to the deletion of the flanked exons. **(e) Relative expression of $MT1-MMP$.** Total RNAs was extracted from various tissues of $MT1^{FLOX}$ and $MT1^{LKO}$ mice with TRizol, followed with qRT-PCR measurement of mRNA levels of $MT1-MMP$ in different tissues (Heart, Liver, Kidney and White adipose tissue) **(f) Pictures showing phenotypical similarity in $MT1^{FLOX}$ and $MT1^{LKO}$ mice (8- week old).** **(g) Bodyweight of $MT1^{FLOX}$ and $MT1^{LKO}$ mice** (age of 8 weeks, n=3 males and 3 females). **(h) Plasma ALT activity measured by a commercial kit.** Plasma from each $MT1^{FLOX}$ or $MT1^{LKO}$ mouse was subjected to the measurement according to the manufacturer's instruction. Each sample was assayed in triplicate.

The expression of *MT3*, *MT4*, *MT5* and *MT6-mmp* was undetectable by qRT-PCR in the liver of both *MT1^{LKO}* and *MT1^{FLOX}* mice. We also did not observe a significant difference in mRNA levels of liver *MT2-mmp* and *Adam17* (**Fig. 3.5a**), indicating that the loss of hepatic MT1-MMP was not compensated by these metalloproteinases. *MT1^{LKO}* mice, however, did not display a significant collagen difference in Mason's trichrome staining of liver sections (**Fig. 3.5b**) and plasma active MMP2 (**Fig. 3.5c**). Thus, knockout of MT1-MMP in hepatocytes did not cause obvious liver damage.

Consistent with our findings in cultured cells, the protein levels of LDLR but not LRP1 in liver homogenate were significantly increased (**Fig. 3.5d**), while the levels of plasma sLDLR were significantly reduced in *MT1^{LKO}* mice (**Fig. 3.5e**). On the other hand, the levels of PCSK9 in the liver homogenate and plasma were comparable in *MT1^{LKO}* mice and *MT1^{Flox}* mice (**Figs. 3.5f** and **g**). It was previously reported that active MMP2 inhibited PCSK9-promoted LDLR degradation in hepatic cells (Wang et al., 2015). However, the levels of plasma pro- and active forms of MMP2 were not significantly altered in *MT1^{LKO}* mice (**Fig. 3.5c**), implying that MMP2 did not play an important role in the action of MT1-MMP on LDLR in mice.

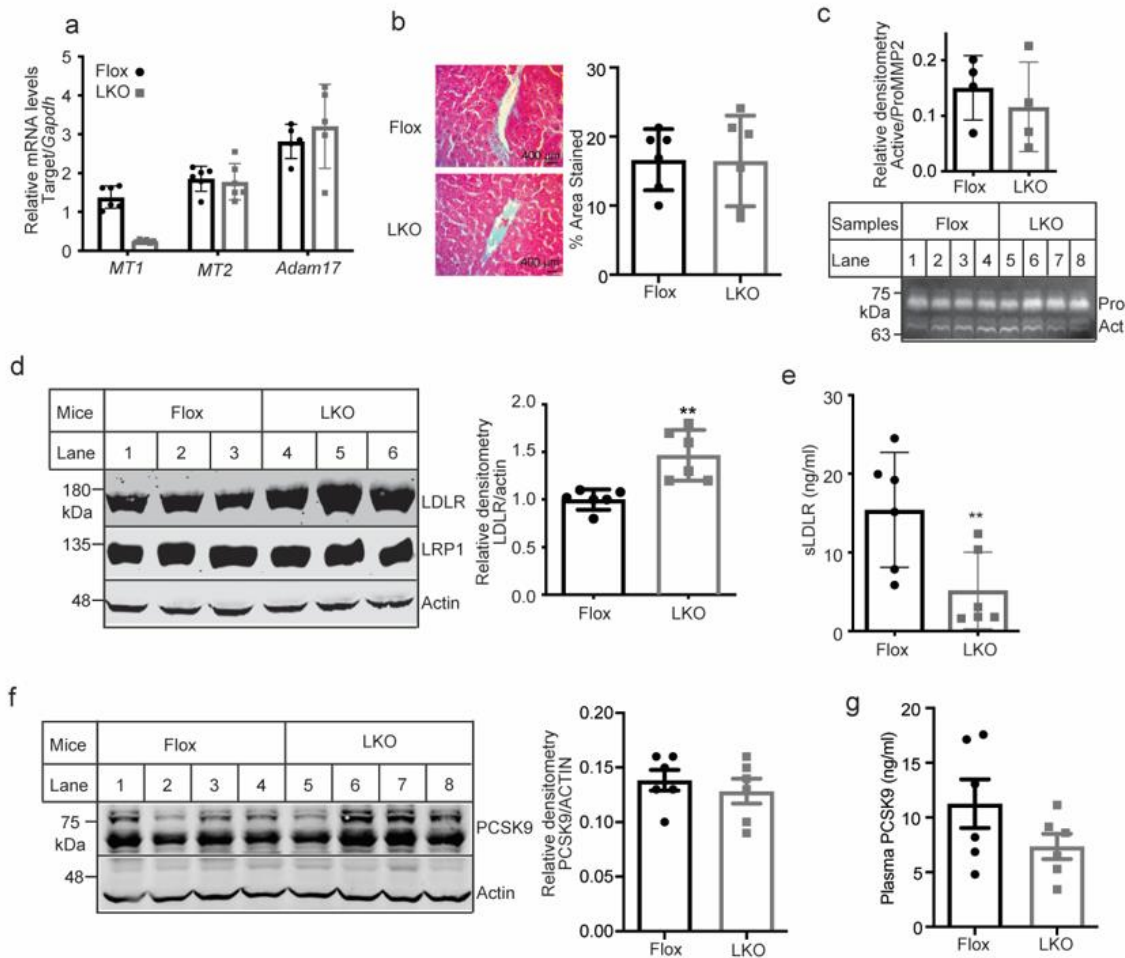


Fig 3. 5. Phenotype associated with MT1-MMP loss in $MT1^{LKO}$ mice I. (a) **Relative expression of target genes.** The relative mRNA levels were the ratio of the mRNA levels of the *target genes* (*MT1-MMP*, *MT2-MMP*, and *Adam17*) from the liver to that of *Gapdh*. (b) **Representative Masson's Trichrome staining of liver sections and its quantification** (n=6). Mice (age of 8-10 weeks) were fed a regular chow diet. (c) **Effect of hepatic knockout of MT1-MMP on MMP2 activation.** Active and pro-MMP2 of plasma samples of mice were detected by the gelatin zymography experiment using 5 μ l of plasma from each mouse. The gel was stained with Coomassie Blue R250. The densitometry of active (Act) and pro-MMP2 (Pro) was determined using a Licor Odyssey Infrared Imaging System. The relative densitometry was the ratio of the densitometry of the active form of MMP2 to that of the pro-MMP2 at the same condition. (d) **Liver LDLR levels.** The same amount of liver homogenate from each mouse (80 μ g/well) was subjected to immunoblotting. Antibodies used were a rabbit anti-LDLR polyclonal antibody (3143), a rabbit anti-LRP1 polyclonal antibody, and a mouse anti-actin monoclonal antibody. Relative densitometry was the ratio of the densitometry of LDLR of different mice to that of actin of the

same mouse. **(e) Plasma sLDLR.** The same amount of plasma from each mouse was subjected to ELISA determination of sLDLR levels using a commercial ELISA kit (R&D system) according to the manufacturer's instruction. Plasma sample from *Ldlr*^{-/-} mice was used as a negative control. Specific levels were calculated by subtraction of counts of plasma samples of *Ldlr*^{-/-} mice from that of *MT1*^{LKO} and *MT1*^{FLOX} mice. **(f) Expression of liver PCSK9.** The same amount of total proteins in liver homogenate isolated from *MT1*^{Flox} or *MT1*^{LKO} mice was subjected to Western Blot. Antibodies used were a rabbit anti-mouse PCSK9 antibody (abcam) and a mouse anti-actin monoclonal antibody. The relative densitometry was the ratio of the densitometry of PCSK9 to that of actin in the same mouse. **(g) Plasma levels of PCSK9.** PCSK9 in the same amount of plasma from each mouse was measured using the mouse PCSK9 DuoSet® ELISA kit accordingly to the manufacturer's instruction (R&D System).

Furthermore, mRNA levels of *Ldlr*, *Srebf2*, *Hmgcr* and *Pcsk9* in mouse liver were also not affected by hepatic deficiency of MT1-MMP (**Fig. 3.6a**). On the other hand, *MT1*^{LKO} mice displayed a mild but significant reduction in plasma levels of total cholesterol (**Fig. 3.6b**). FPLC data showed that cholesterol levels in both LDL and HDL fractions were mildly reduced (**Fig. 3.6c**). Conversely, plasma TG levels were comparable in *MT1*^{LKO} and *MT1*^{Flox} mice (**Fig. 3.6d**). Similarly, the lack of MT1-MMP in hepatocytes did not significantly affect the levels of liver TG or total cholesterol (**Figs. 3.6e and f**). To confirm the specific contribution of MT1-MMP on LDLR and plasma cholesterol levels, we introduced human MT1-MMP into hepatocytes of *MT1*^{LKO} via AAV under the control of a hepatocyte-specific TBG promoter. HA-tagged MT1-MMP was detected in the liver homogenate by a polyclonal anti-HA antibody (**Fig. 3.6g**). Reintroduction of MT1-MMP essentially eliminated the increase in liver LDLR (**Fig. 3.6g**) and the reduction in plasma levels of sLDLR (**Fig. 3.6h**) and total cholesterol (**Fig. 3.6i**) in *MT1*^{LKO} mice. These findings indicate the important role of MT1-MMP in the regulation of liver LDLR levels.

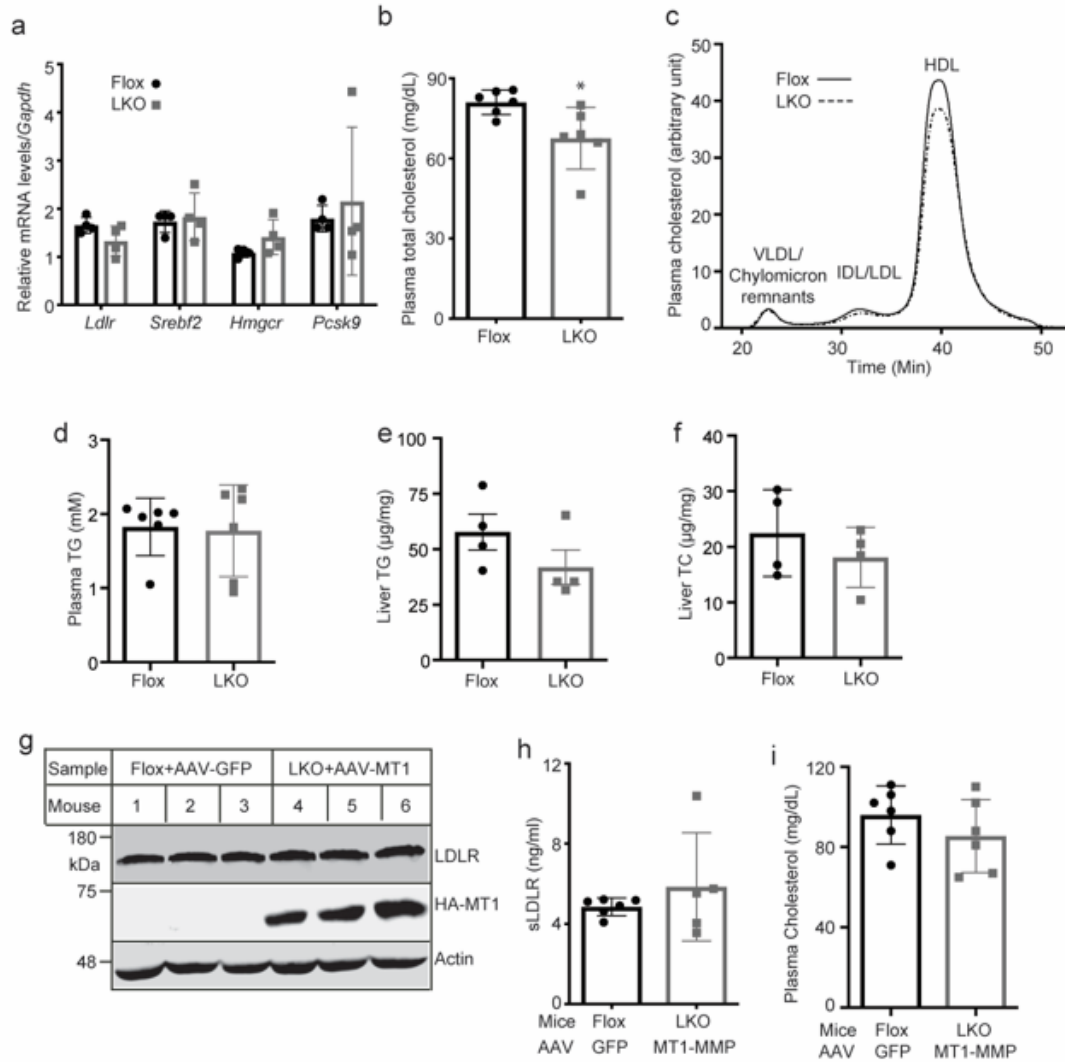


Fig 3. 6. Phenotype associated with MT1-MMP loss in $MT1^{LKO}$ mice II. (a) Relative mRNA levels of target genes. The relative mRNA levels were the ratio of the mRNA levels of the target genes (*Ldlr*, *Srebf2*, *Hmgcr* and *Pcsk9*) from the liver to that of *Gapdh*. **(b) Plasma levels of total cholesterol.** Plasma from each mouse were applied to the measurement using a commercial kit. **(c) Lipid profile.** The same amount of plasma from each mouse in the same group was pooled and applied to a FPLC analysis of plasma cholesterol. **(d) Plasma TG.** 5 ul of plasma from each mouse was used to determine plasma TG levels using a commercial kit (Roche Diagnostics) in accordance with the manufacturer’s instruction. **(e and f) Levels of triglycerides (TG, e) and total cholesterol (TC, f) in the liver.** Briefly, lipids were extracted from 4 mg of liver homogenate using the Folch method and then subjected to the determination of TG and TC levels using their specific commercial kits. **(g to i). Effects of expression of human MT1-MMP.** $MT1^{FLOX}$ and $MT1^{LKO}$ mice were injected with AAVs encoding GFP or human MT1-MMP, respectively. 30 days after injection, liver homogenate was prepared and applied to immunoblot with a rabbit anti-LDLR polyclonal antibody, a rabbit anti-HA polyclonal antibody, and a mouse anti-actin monoclonal

antibody (**g**). Plasma samples were used to measure sLDLR levels (**h**), and total cholesterol levels (**i**) using their specific kits as described above. The values of all data unless otherwise indicated were mean \pm S.D. of at least 6 mice in each group. *, $p < 0.05$. **, $p < 0.01$.

We then overexpressed human MT1-MMP in the wild-type C57BL/6J mice using adenovirus under the control of a CMV promoter. As shown in **Figure 3.7a**, overexpression of MT1-MMP significantly reduced LDLR levels in the liver. Consistently, plasma levels of HDL (**Fig. 3.7b**) and non-HDL cholesterol (**Fig. 3.7c**) were significantly increased. Mice on a chow diet normally have very low levels of plasma non-HDL-C. To further confirm our findings, we fed $MT1^{LKO}$ and $MT1^{FLOX}$ mice with the Western-Type diet for 8 weeks. The protein levels of LDLR but not LRP1 in liver homogenate were significantly increased in $MT1^{LKO}$ mice (**Fig. 3.7d**). Masson's Trichrome and Oil Red-O staining of liver sections, however, displayed no significant difference between $MT1^{LKO}$ and $MT1^{FLOX}$ mice (**Figs. 3.7e and f**). $MT1^{LKO}$ mice also did not display a significant difference in the levels of liver TG ($p=0.1$) and total cholesterol ($p=0.073$) compared to $MT1^{FLOX}$ mice (**Figs. 3.7g and h**). The mRNA levels of *Ldlr*, as well as other SREBP2 target genes (*Hmgcr* and *Pcsk9*), were also not altered by hepatic deficiency of MT1-MMP (**Fig. 3.7i**).

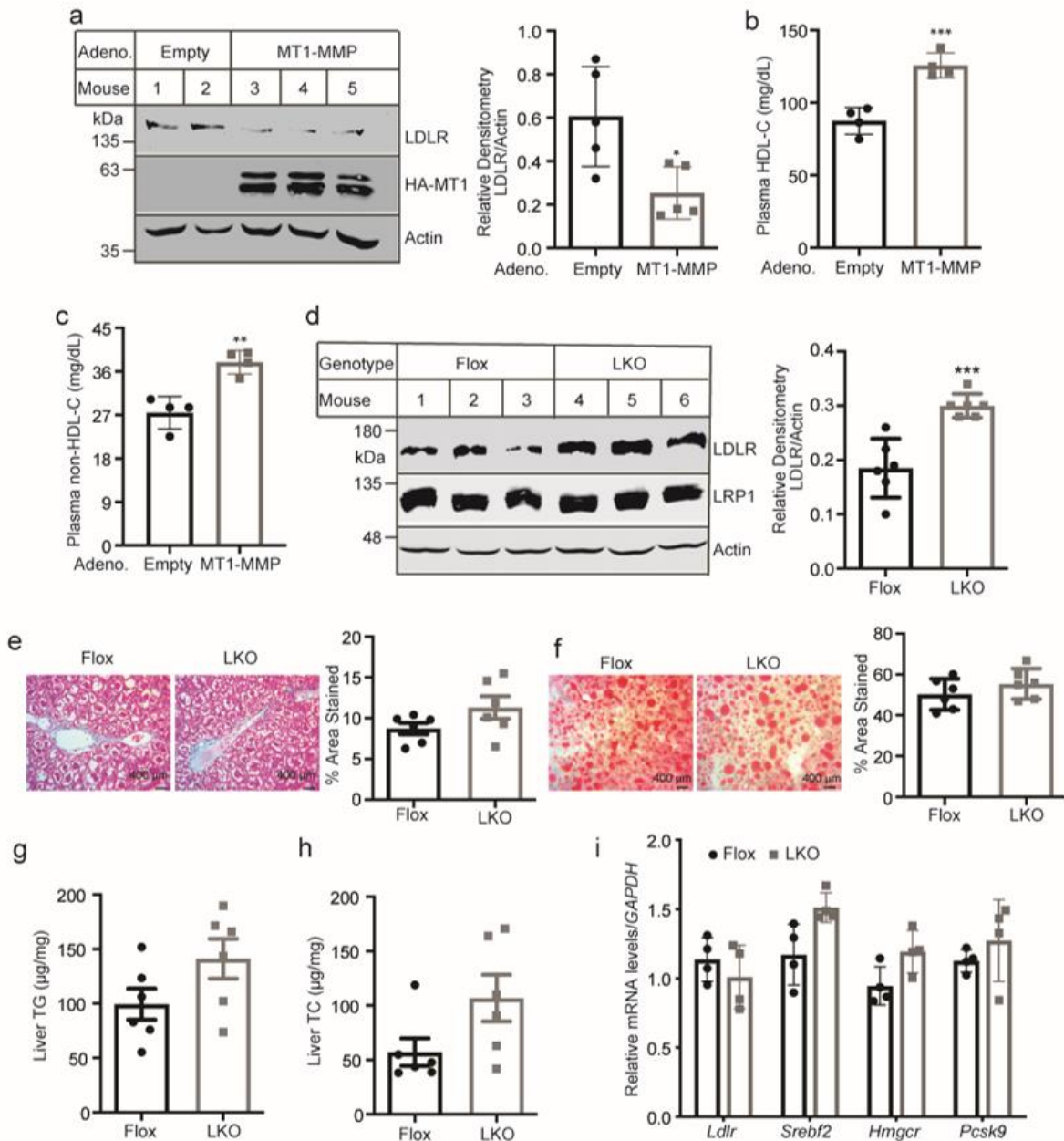


Fig 3. 7. MT1-MMP overexpression in C57BL/6J mice and effect of western-type diet feeding in $MT1^{LKO}$ mice. (a) *Overexpression of human MT1-MMP.* Male C57BL/6J mice were injected with empty or the wild-type MT1-MMP adenoviruses (1.0×10^{11} viral particles/mouse) and euthanized 72 h later. The same amount of liver homogenate was subject to immunoblotting, followed by quantification of LDLR levels relative to actin in the same mouse. (b and c) *Plasma cholesterol levels.* Plasma was subjected to the measurement of HDL (b) and non-HDL cholesterol

(c) using a commercial kit as described above. (d) **Effect of the Western-type diet.** Mice were fed the Western-type diet for 8 weeks. The same amount of whole liver homogenate was subjected to immunoblotting. Relative densitometry of LDLR was determined as described. Actin was used as a loading control. (e and f) **Liver section staining.** Representative figures of Masson's Trichrome (e) and oil Red-O staining (f) analysis in cross-sections of the liver and quantification data (n=6) (magnification: 400X). (g and h) **Levels of total triglycerides (TG, g) and total cholesterol (TC, h) in the liver.** Briefly, lipids were extracted from 4 mg of liver homogenate using the Folch method and then subjected to the determination of TG and TC levels using their specific commercial kits. (i) **Relative mRNA levels determined by qRT-PCR.** The relative mRNA levels were the ratio of the mRNA levels of the target genes to that of *Gapdh* in the same condition.

In addition, *MT1*^{LKO} mice showed similar body weight gain (Fig. 3.8a), H&E staining of liver sections (Fig. 3.8b), plasma ALT activities (Fig. 3.8c) and plasma levels of active MMP2 (Figs. 3.8d and e) as *MT1*^{FLOX} mice. Conversely, hepatic knockout of MT1-MMP significantly and markedly reduced plasma levels of non-HDL and HDL cholesterol (Figs. 3.8f and g). FPLC results revealed that cholesterol levels in all fractions including VLDL/chylomicron remnants, LDL and HDL were significantly reduced in *MT1*^{LKO} mice (Fig. 3.8h). Thus, MT1-MMP regulates hepatic LDLR and plasma cholesterol levels in mice.

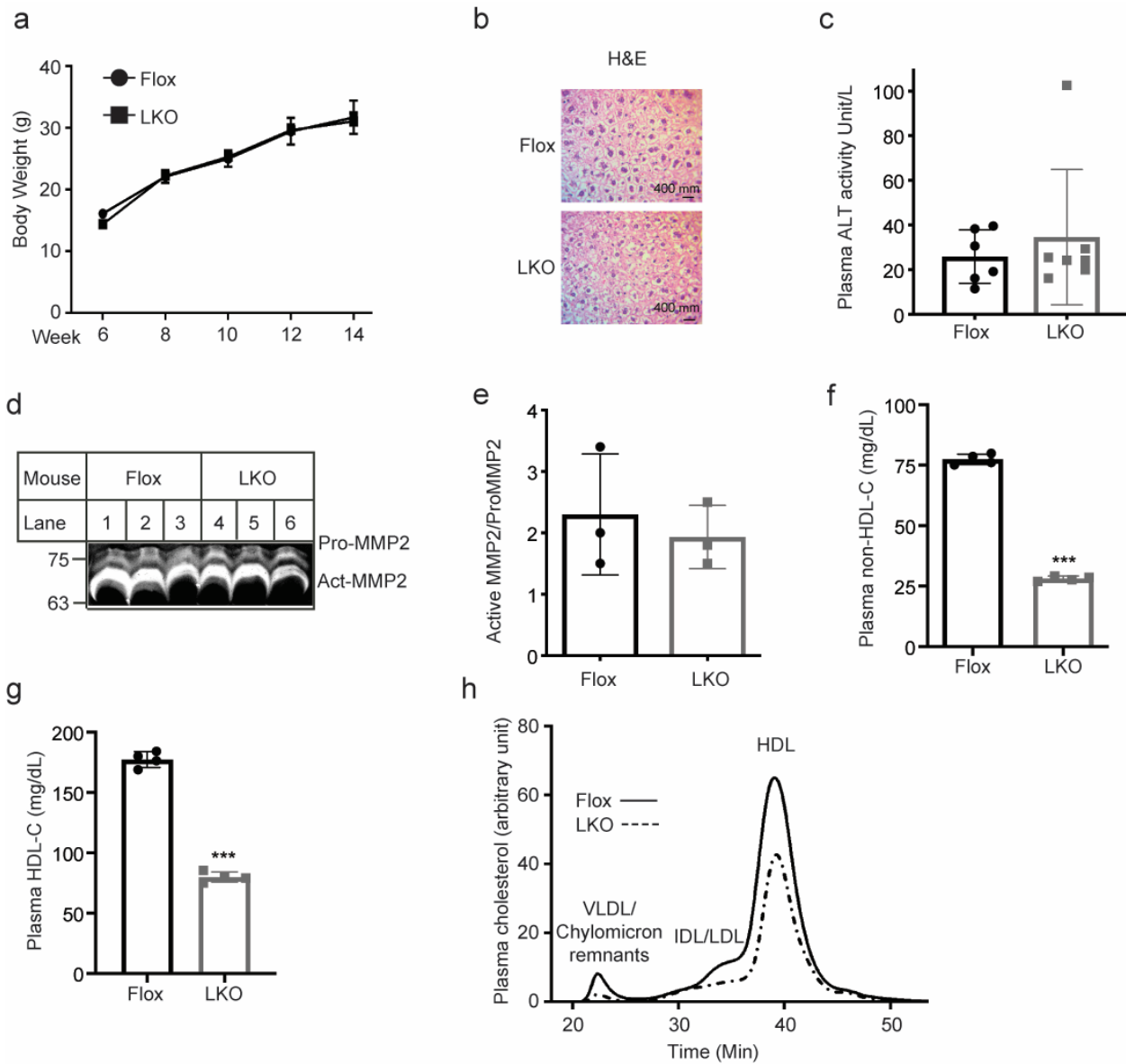


Fig 3. 8. Phenotypes associated with 8-weeks western-type diet feeding in $MT1^{LKO}$ mice. (a) Bodyweight of $MT1^{FLOX}$ and $MT1^{LKO}$ mice. 5 male mice per group. (b) Liver section staining. Representative figures of H&E staining of cross-sections of liver tissues. (c) Plasma ALT activity. Each sample was assayed in triplicate. (d and e) Gelatin zymography analysis of plasma MMP2. (f) and (g) Plasma levels of cholesterol. Plasma was isolated from mice. Cholesterol content in non-HDL (f) and HDL (g) was measured using a commercial kit in accordance with the manufacturer's instructions. (h) Lipid profile. The same amount of plasma from each mouse in the same group (same amount of mice) was pooled and applied to FPLC analysis of plasma cholesterol. The values of all data unless otherwise indicated were mean \pm S.D. of at least 6 mice in each group. *, $p < 0.05$. **, $p < 0.01$. *, $p < 0.001$.**

3.2.4 sLDLR and plasma lipoproteins

The molecular mass of the main form of sLDLR detected in our study was around 100 kDa that should consist of the entire ligand-binding domain of the receptor, indicating that sLDLR might retain the ability to bind LDLR ligands. Thus, we hypothesized that plasma sLDLR could bind to circulating apoB and apoE-containing lipoproteins. To test this possibility, we utilized gel filtration to determine the distribution of sLDLR in fasting mouse plasma. As shown in **Figure 3.9a**, sLDLR was eluted at fractions 8 to 17 with a wide peak at fractions 11 to 13 that were the fractions of LDL even though LDL only accounted for a very small portion of plasma cholesterol (**Fig. 3.9b**). There was a shoulder at fraction 15 that was partially overlapped with HDL. An additional small peak of sLDLR was present in the VLDL fractions 8 to 10. These could be caused by the binding of sLDLR to apoE in VLDL and HDL particles. We also immunoprecipitated sLDLR from mouse plasma. The antibody efficiently pulled down sLDLR from plasma of the wild-type mice but not the *Ldlr*^{-/-} mice (**Fig. 3.9c, lane 2 vs 1**), indicating the specificity of the antibody. Both apoB100 and apoB48, as well as apoE, were co-immunoprecipitated with sLDLR only from the wild-type mouse plasma (**Fig. 3.9c, lane 2**) even though the levels of apoB and apoE were much higher in *Ldlr*^{-/-} mouse plasma (**Fig. 3.9d, lane 1**). Next, we analyzed human plasma using gel filtration chromatography. As shown in **Figure 3.9e**, the majority of sLDLR were eluted at the fractions of the VLDL/chylomicron remnants and LDL even though VLDL/chylomicron remnants only accounted for a minor portion of plasma cholesterol (**Fig. 3.9f**). In addition, we noticed that, unlike mouse sLDLR, only a small peak of human sLDLR was eluted at the HDL fractions (**Figs. 3.9e and f**). We then measured sLDLR levels in purified human lipoproteins. As shown in **Figure 3.9g**,

VLDL exhibited the highest levels of sLDLR per μg proteins, followed by LDL and HDL. The levels of sLDLR in VLDL were approximately 35-fold more than that in LDL. The discrepancy between purified lipoproteins and plasma samples could be simply due to the relatively lower levels of VLDL present in human plasma. Taken together, these findings suggest that sLDLR associates with apoB and apoE-containing lipoproteins in plasma.

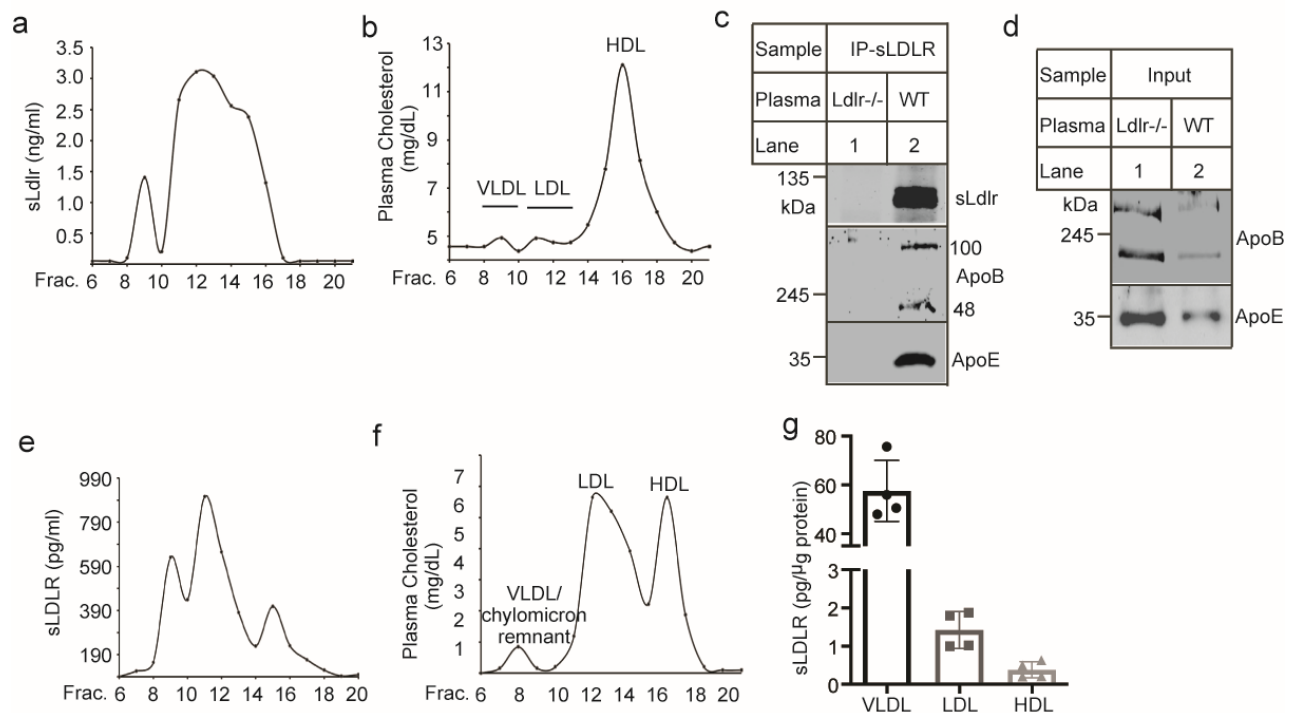


Fig 3. 9. Analysis of plasma sLDLR. (a and b) profiles of plasma sLDLR (a) and lipoprotein cholesterol (b). Fasting mouse plasma was applied to a size exclusion-FPLC column. The eluate was collected in 1 ml per fraction. sLDLR and total cholesterol in each fraction were measured using their specific commercial kits from R&D system and Wako Life Sciences, respectively. The levels of cholesterol and sLDLR in fractions 1 to 5 were negligible and were not shown in the figures. **(c) Immunoprecipitation of sLDLR.** 500 μl of pooled plasma isolated from *Ldlr^{-/-}* or the wild-type mice was applied to 7 μl of a rat anti-mouse LDLR antibody (R&D System) and 50 μl of protein-G beads (50 % slurry) and rotated overnight. The bound proteins were eluted and subjected to immunoblotting with a rabbit anti-LDLR polyclonal antibody, 772B, a goat anti-apoB polyclonal antibody, and a rabbit anti-apoE polyclonal antibody. **(d) Immunoblotting of mouse plasma.** 3 μl of pooled plasma isolated from *Ldlr^{-/-}* or the wild-type mice that were used in the immunoprecipitation experiment was applied to immunoblotting with a goat anti-apoB polyclonal

antibody and a rabbit anti-apoE polyclonal antibody. *(e and f) profiles of human plasma sLDLR (e) and lipoprotein cholesterol (f)*. The experiment was performed as described in panels 6a and b except that 500 μ l of fasting human plasma was used. *(g) The amount of sLDLR in lipoproteins*. sLDLR in purified human plasma VLDL, LDL and HDL were measured using the commercial ELISA kit and normalized to protein concentrations.

Next, we recruited 148 adult Chinese and measured their plasma levels of total cholesterol, LDL cholesterol, and sLDLR. There were 87 men (average age=52.6), 46 women (average age=53.7), and 15 individuals whose gender and age were undisclosed. The levels of sLDLR were comparable among the men, women, and undisclosed group (**Fig. 3.10a**). There was no significant correlation between plasma levels of sLDLR and ages (**Fig. 3.10b**, $r=0.047$, $p=0.5925$). On the other hand, the correlation between sLDLR and plasma total cholesterol levels was statistically significant (**Fig. 3.10c**, $r=0.41$, $p=0.00000028$). Plasma LDL-C levels were also significantly correlated to sLDLR levels (**Fig. 3.10d**, $r=0.198$, $p=0.0199$), but to a lesser extent than plasma total cholesterol levels. We also divided participants into three groups based on their plasma levels of total cholesterol or LDL cholesterol, group 1) the normal/desirable cholesterol levels (total cholesterol <5.2 mM and LDL cholesterol <3.4 mM, $N=87$), group 2) the medium/borderline high plasma cholesterol levels (5.2 mM \leq total cholesterol <6.1 mM or 3.4 mM \leq LDL cholesterol <4.1 mM, $N=40$), and group 3) the high plasma cholesterol levels (total cholesterol ≥ 6.1 mM or LDL cholesterol ≥ 4.1 mM, $N=21$). The levels of sLDLR in the medium and high groups were significantly higher than that in the normal group, while there was no significant difference between the medium and high groups (**Fig. 3.10e**). Given the critical role of PCSK9 in the regulation of plasma LDL cholesterol and hepatic LDLR levels, we also measured circulating PCSK9 in these subjects. As shown in **Figures 3.10f and g**, plasma levels of PCSK9 did not

significantly associate with plasma LDL cholesterol in the whole group or women but did exhibit a positive correlation with plasma LDL cholesterol levels in men ($r=0.2255$, $p=0.0303$; **Fig. 3.10h**). On the other hand, there was no significant association between plasma levels of PCSK9 and sLDLR in the whole group, women or men (**Figs. 3.10i to k**). Together, these findings indicate that plasma levels of cholesterol but not PCSK9 are positively correlated to sLDLR levels.

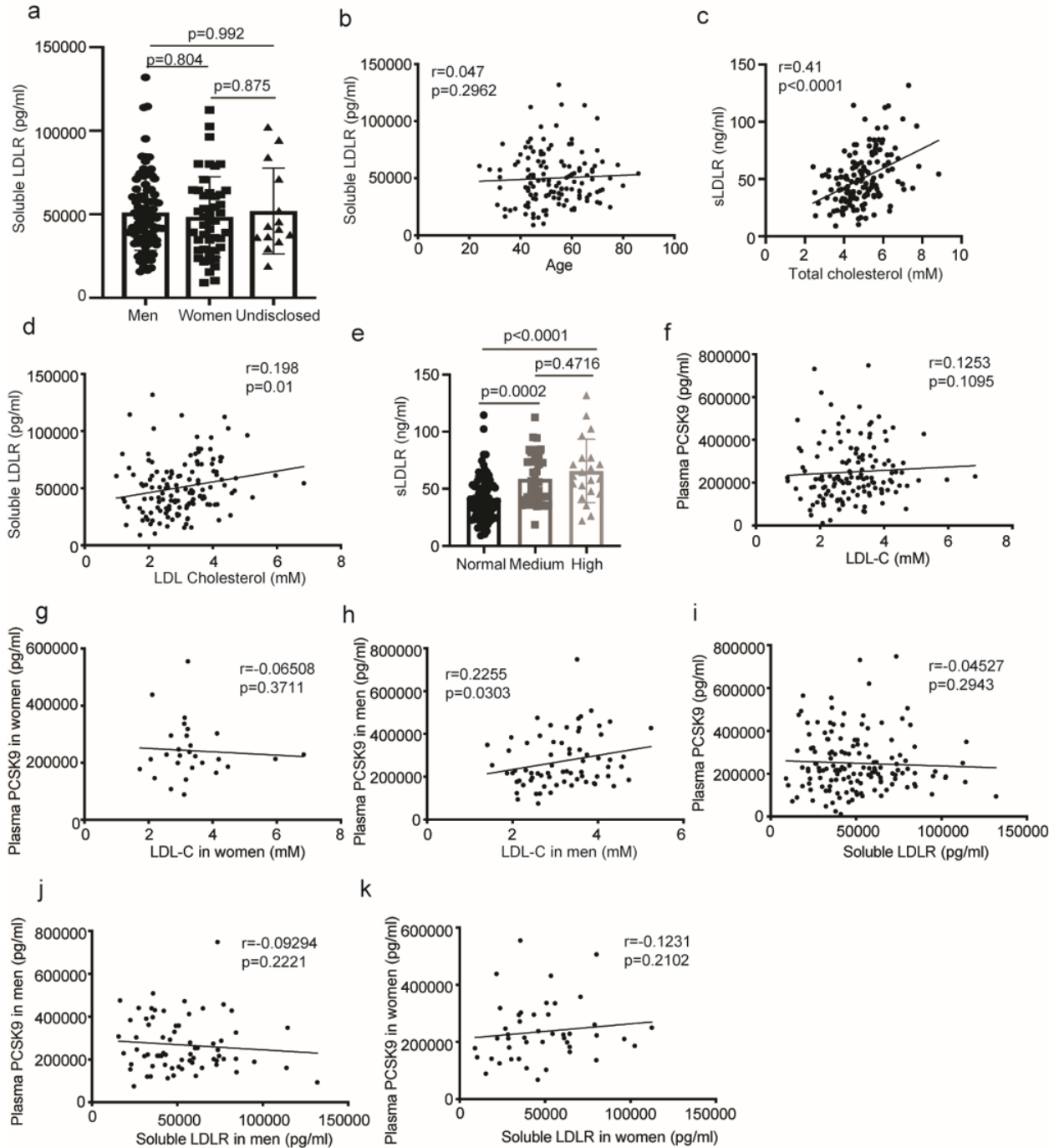


Fig 3. 10. Association between plasma sLDLR and LDL-C, Total cholesterol, PCSK9 in humans. (a to k) Plasma levels of sLDLR and PCSK9. Fasting plasma samples were collected from 148 subjects. sLDLR and PCSK9 were measured using their specific commercial kits (R&D System). (a) Quantification of sLDLR in men, women, and undisclosed gender. The data were analyzed with one-way ANOVA and Tukey post-hoc test using GraphPad Prism 8. (b) Correlation between plasma sLDLR levels and age of participants (c) Association between sLDLR and total cholesterol. sLDLR and total cholesterol in fasting human plasma samples were measured using

their commercial kits from R&D system and Nanjing Jiangcheng Bioengineering Institute, respectively. The association **(c)** was analyzed using the Pearson's correlation coefficient and statistical significance among different groups. **(d)** Correlation between sLDLR and LDL-C in all participants. **(e)** sLDLR content in participants with normal, medium, and high plasma cholesterol content. Statistical analysis was carried out with was with one-way ANOVA and Tukey post-hoc test using GraphPad Prism 8. Correlation between plasma PCSK9 and LDL-C **(f)**, PCSK9 and LDL-C in women **(g)**, PCSK9 and LDL-C in men **(h)**, PCSK9 and sLDLR **(i)**, PCSK9 and sLDLR in men **(j)**, PCSK9 and sLDLR in women **(k)**. **(f to k)** was analyzed with the Pearson's correlation coefficient and plotted using GraphPad Prism 8.

Next, we examined the effect of MT1-MMP on the development of atherosclerosis in mice. ApoE^{-/-} mice were injected with empty AAV or AAV containing human MT1-MMP cDNA and then fed the Western-type diet for 8 weeks. Overexpression of MT1-MMP reduced LDLR levels in the liver (**Fig. 3.11a**) and increased plasma levels of total cholesterol about 24% in mice (730 mg/dL in the control, 911 mg/dL in MT1-MMP overexpressing mice, p=0.0772; **Fig. 3.11b**). We found that lesion area in the aortic sinuses was significantly increased in MT1-MMP-overexpressing mice ($157.5 \pm 21.03 \mu\text{m}^2 \times 10^3$ in the control group and $238.0 \pm 21.23 \mu\text{m}^2 \times 10^3$ in MT1-MMP overexpressing mice, p=0.0228; **Fig. 3.11c**). Next, we generated *MTI*^{Flox}/apoE^{-/-} mice through crossing *MTI*^{Flox} mice with apoE^{-/-} mice. Cre recombinase was then introduced into the liver of *MTI*^{Flox}/apoE^{-/-} via AAV under the control of a hepatocyte-specific TBG promoter (AAV-TBG-cre) to knock down hepatic MT1-MMP expression. The mRNA levels of MT1-MMP were significantly reduced (**Fig. 3.11d**), while hepatic LDLR levels were significantly increased in mice injected with AAV-TBG-Cre when compared to the AAV-GFP injected mice (p=0.0385, **Fig. 3.11e**). However, knockdown of hepatic MT1-MMP did not significantly affect plasma cholesterol levels (p=0.2981, **Fig. 3.11f**). Similarly, it has been reported that knockout of PCSK9 in apoE^{-/-} mice does not significantly affect plasma cholesterol levels or atherosclerotic plaque sizes despite

increased hepatic LDLR levels (Denis et al., 2012). Consistently, we did not observe a significant difference in lesion sizes between the control and MT1-MMP knockdown mice (**Fig. 3.11g**, $p=0.7405$). Denis *et al.* reported that knockout of PCSK9 reduced cholesteryl ester accumulated in the aortas of apoE^{-/-} mice by approximately 39%, even though the sizes of the entire lesions were not significantly reduced (Denis et al., 2012). We employed the same approach in our study and found a similar phenotype, MT1-MMP knockdown caused a reduction of approximately 45% in cholesteryl ester accumulation in the aorta of *MT1^{Flox}/apoE^{-/-}* mice (mean value: 5.49 μg of cholesteryl ester per aorta in AAV-GFP injected mice *vs.* 3.04 μg of cholesteryl ester per aorta in MT1-MMP knockdown mice. **Fig. 3.11h**). Together, these findings indicate that MT1-MMP promotes ectodomain shedding of LDLR and accelerates the development of atherosclerosis.

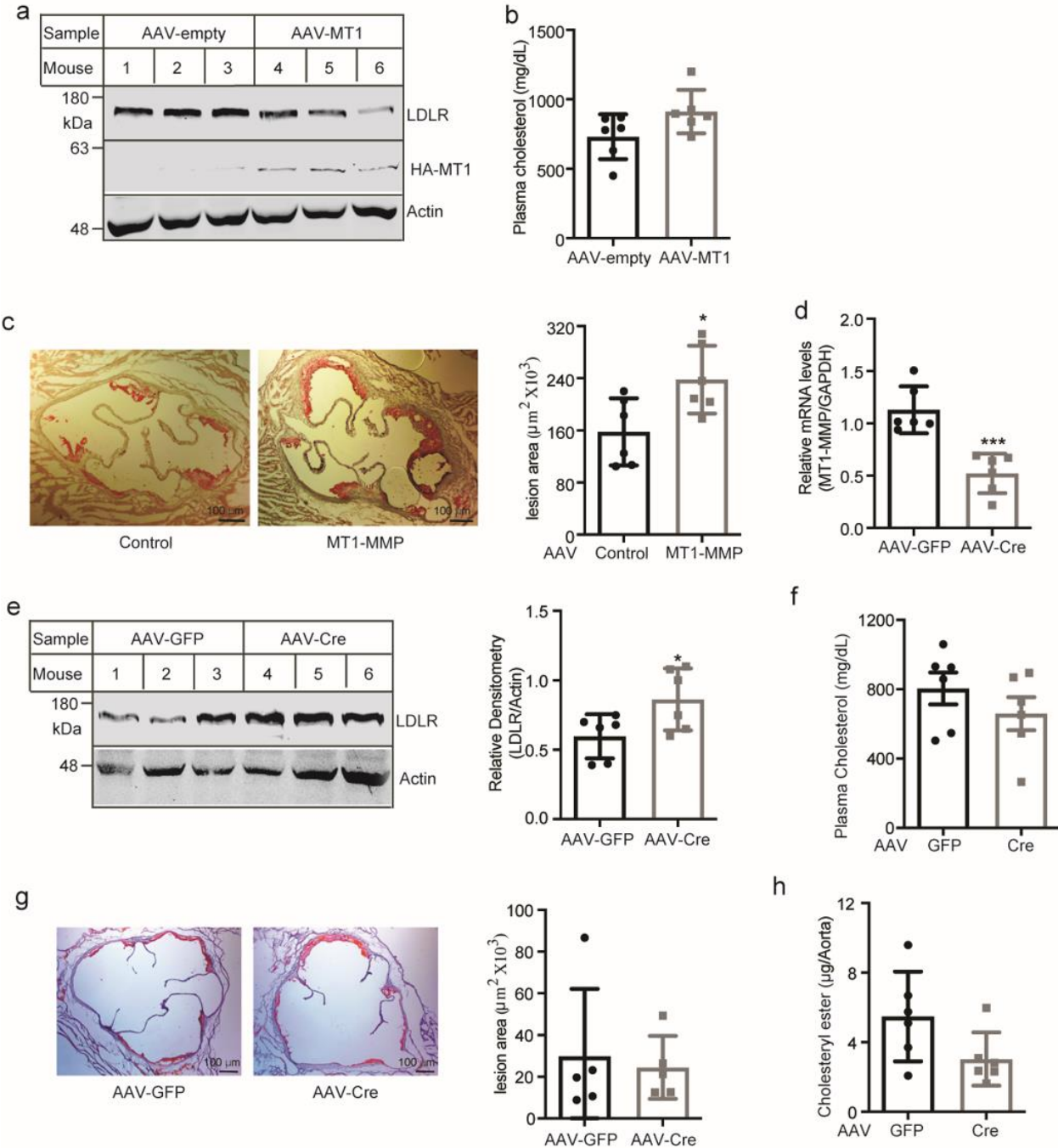


Fig 3. 11. Atherosclerosis study. (a and b) Overexpression of MT1-MMP. (a) 8-week-old male apoE^{-/-} mice were injected with empty AAV or AAV-MT1-MMP (AAV-MT1) and then fed Western-type diet for 8 weeks. After euthanasia, the liver was collected. The same amount of total proteins in liver homogenate was subjected to Western blot using a rabbit anti-LDLR polyclonal antibody (3143), a rabbit anti-MT1-MMP monoclonal antibody and a mouse anti-actin monoclonal antibody. (b) Plasma from each mouse were used to determine plasma total cholesterol levels using a commercial kit (Wako Life Sciences) in accordance with the manufacturer's instruction. (c) **Analysis of atherosclerosis.** 8-week-old male ApoE^{-/-} mice were injected with AAV-Empty (Control) or AAV-MT1-MMP (MT1-MMP) and then fed the Western-type diet for 8 weeks. After

euthanasia, the heart was collected and subjected to sectioning the aortic sinus. The slides were stained with Oil Red O and imaged on OMAX M837ZL-C140U3 microscope (Magnification 40X). Atherosclerotic lesions in the aortic sinus were quantified using OMAX ToupView. **(d and e) Knockdown of MT1-MMP.** 8-week male $MT1^{Fllox}/ApoE^{-/-}$ mice were injected with AAV-GFP or AAV-TBG-Cre (AAV-Cre) and then fed the Western-type diet for 8 weeks. After euthanasia, the liver was collected. Total RNAs were extracted for qRT-PCR **(d)**. The same amount of total proteins in liver homogenate was subjected to Western blot using a rabbit anti-LDLR polyclonal antibody (3143) and a mouse anti-actin monoclonal antibody. The relative densitometry was the ratio of the densitometry of LDLR to that of actin in the same mouse **(e)**. **(f)** Plasma levels of total cholesterol were measured using a commercial kit from Cell Biolabs. **(g)** After euthanasia, the heart was collected and subjected to sectioning the aortic sinus. The slides were stained with Oil Red O and imaged on OMAX M837ZL-C140U3 microscope (Magnification 40X). Atherosclerotic lesions in the aortic sinus were quantified using OMAX ToupView. * $p < 0.05$, ** $p < 0.01$, *** $p < 0.001$. The aorta was collected and then subjected to lipid extraction for the measurement of cholesteryl ester **(h)**.

3.3 Discussion

LDLR and its family members such as VLDLR, apoER and LRP1 undergo ectodomain shedding to release their soluble forms into the extracellular milieu such as cerebrospinal fluid and blood (Chen, Takahashi, Oka, & Ma, 2016; Rebeck, LaDu, Estus, Bu, & Weeber, 2006). Recently, Girona et al reported that plasma levels of sLDLR were positively associated with non-HDL-C and small LDL numbers in FH children (Girona et al., 2017). Consistently, two independent studies revealed a mild but significant correlation between serum concentrations of sLDLR and LDL-C in healthy adult Japanese and Canadian white population (Mayne et al., 2018; Shimohiro et al., 2015). Here, we also found that sLDLR levels were positively correlated to plasma levels of total cholesterol and LDL cholesterol and significantly increased in subjects with high plasma levels of total or LDL cholesterol in adult Chinese. In addition, we observed a weak positive association between plasma levels of PCSK9 and LDL cholesterol in men but not in the whole group or women, consistent with a previous report (Mayne et al., 2007). Conversely, PCSK9 did not significantly correlate to sLDLR in men, women or the whole group. Circulating PCSK9 is mainly secreted from the liver but the underlying mechanism is unclear (Zaid et al., 2008). Loss-of-function PCSK9 mutations increase hepatic LDLR levels, which should render more receptors for MT1-MMP-mediated shedding and increase plasma sLDLR levels. Conversely, gain-of-function PCSK9 mutations reduce the amount of hepatic LDLR susceptible to shedding, which should reduce sLDLR in plasma. However, both loss-of-function PCSK9 mutations and gain-of-function PCSK9 mutations can impair PCSK9 secretion and reduce plasma levels of PCSK9 (Cameron et al., 2006; Chorba, Galvan, & Shokat, 2018; Seidah, 2016). Thus, a detailed analysis of genotype-phenotype association might be needed to explore the correlation between circulating

PCSK9 and sLDLR. Nevertheless, these findings indicate that LDLR shedding plays an important role in lipid metabolism.

The proteinase responsible for LDLR ectodomain shedding, however, remains unknown. In the present study, we found that 1) MT1-MMP interacted with LDLR and knockdown of MT1-MMP expression in different cell types including human primary hepatocytes increased cellular LDLR levels but decreased sLDLR levels in culture medium, 2) knockout of hepatic MT1-MMP in mice increased LDLR in the liver and reduced plasma levels of sLDLR, 3) overexpression of MT1-MMP reduced LDLR in cultured cells and mouse liver and increased sLDLR in culture medium and mouse plasma but had no effect on PCSK9 expression, 4) knockdown of MT1-MMP had no effect on the mRNA levels of LDLR and other SREBP2 target genes including *PCSK9*, *SREBP2* and *HMGCR*, and 5) lysosomal inhibition with chloroquine that suppresses PCSK9- and IDOL-promoted LDLR degradation had no effect on MT1-MMP-induced reduction in LDLR. MT1-MMP knockdown also had no effects on the mRNA levels of *PCSK9* and *IDOL*. Taken together, our findings show for the first time that MT1-MMP regulates LDLR levels via promoting ectodomain cleavage of the receptor. We noticed that knockout of hepatic MT1-MMP in mice markedly reduced the levels of plasma sLDLR by approximately 67% and significantly increased liver LDLR levels (**Figs. 3.5d and e**). This indicates that, at least in the liver, MT1-MMP is the proteinase mainly responsible for the ectodomain shedding of LDLR. Given the ubiquitous expression of LDLR, LDLR shedding in other tissues may contribute to plasma sLDLR detected in *MT1*^{LKO} mice. However, we cannot rule out the possibility that other hepatic proteinases might also mediate LDLR shedding in the liver. For example, it has been reported that ADAM17 can promote LDLR shedding in HepG2 cells to a small extent (Strøm et al., 2014). More experiments are needed to define these possibilities.

Hepatic LDLR is critical for the clearance of circulating apoB-100 and apoE containing lipoproteins. Knockdown of MT1-MMP in cultured cells indeed enhanced cellular LDL uptake. Furthermore, *MT1*^{LKO} mice, especially on the Western-type diet exhibited an increase in liver LDLR levels and a significant reduction in plasma levels of total cholesterol, HDL and non-HDL cholesterol. This reduction is likely caused by enhanced LDLR-mediated clearance of LDL, chylomicron remnants, as well as apoE containing HDL particles as reported in PCSK9 knockout mice (Choi et al., 2013; Rashid et al., 2005; Zaid et al., 2008). On the other hand, overexpression or knockdown of MT1-MMP in apoE^{-/-} mice did not significantly affect plasma cholesterol levels. Although we could not exclude the possibility that the insignificance might be caused by the relatively small sample size used in the study (six mice per group), it is of note that majority of plasma cholesterol in apoE^{-/-} mice is remnant cholesterol. apoE^{-/-} mice do not express apoE, the ligand of LDLR. Thus, chylomicron and VLDL remnants cannot be cleared by LDLR. This may explain why overexpression of MT1-MMP significantly increased and knockdown of MT1-MMP significantly reduced plasma cholesterol levels in mice with the wild-type background (**Figs. 3.6b, 3.7b, and 3.7c**) but not in apoE^{-/-} mice (**Fig. 3.11f and 3.11b**). Similarly, overexpression or knockout of PCSK9 does not significantly affect plasma cholesterol levels in apoE^{-/-} mice. Conversely, overexpression of PCSK9 enhances the development of atherosclerosis and knockout of PCSK9 reduces the levels of aortic cholesterol in apoE^{-/-} mice (Denis et al., 2012). Consistently, we found that the atherosclerotic lesion area in the aortic sinuses was significantly increased in apoE^{-/-} mice overexpressed MT1-MMP, while MT1-MMP knockdown reduced cholesteryl ester accumulated in the aorta of apoE^{-/-} mice. Thus, MT1-MMP stimulates the development of atherosclerosis most likely through promoting hepatic LDLR shedding.

The shed ectodomains of VLDLR and apoER contain the ligand-binding domain and can bind to their ligand, Reelin, functioning as a competitive negative regulator to block binding of Reelin to the cell surface receptors (Chen et al., 2016; Koch et al., 2002; Rebeck et al., 2006). Here, we also found that mouse plasma sLDLR co-eluted with VLDL, LDL and part of HDL on the size-exclusion chromatograph and co-immunoprecipitated with apoB and apoE. Similarly, the majority of human sLDLR was present in the fractions of VLDL and LDL. A small amount of human sLDLR was also present in the HDL fractions of human plasma, but to a much lesser extent as compared to mouse sLDLR. This might be caused by the fact that mouse HDL is more enriched in apoE compared to human HDL (Shapiro, Tavori, & Fazio, 2018). For example, knockout of PCSK9 in mice dramatically reduces plasma levels of LDL and HDL due to enhanced LDLR-mediated clearance of LDL and apoE-HDL (Choi et al., 2013; Rashid et al., 2005). On the other hand, inhibition of PCSK9 in human markedly reduces plasma levels of LDL but not HDL cholesterol (Sabatine, 2019). It will be of interest to examine if sLDLR-bound LDL can be taken up by cell-surface LDLR as efficiently as sLDLR-free LDL.

MT1-MMP plays an essential role in tissue remodelling by cleaving extracellular matrix components and many non-extracellular matrix substrates (Itoh, 2015; Dmitri V Rozanov et al., 2004; Tam et al., 2004). However, compared to its roles in collagenolysis (Amar, Smith, & Fields, 2017), our understanding of the non-extracellular matrix targets of MT1-MMP and their related physiological roles is poor. Recently, MT1-MMP has been shown to shed LRP1 in breast carcinoma MCF7 cells as well as in vascular smooth muscle cells and in cartilage (Kishimoto, Iga, Yamamoto, Takamune, & Misumi, 2017; Lehti, Rose, Valavaara, Weiss, & Keski-Oja, 2009; Dmitri V Rozanov et al., 2004). However, we found that MT1-MMP had no detectable effect on LRP1 expression in cultured hepatocytes and mouse liver. It has been reported that MT1-MMP

efficiently mediates LRP1 shedding in fibroblastoid type but not the epithelioid variant of HT1080 cells (Dmitri V Rozanov et al., 2004). Thus, MT1-MMP appears to cleave LRP-1 in a cell-type dependent manner.

Taken together, our findings uncover the fact that hepatic LDLR is cleaved by MT1-MMP. It is well documented that MT1-MMP is highly expressed in various types of cancer cells and promotes cancer metastasis and angiogenesis (Naseh, Mohammadifard, & Mohammadifard, 2016; Pekkonen et al., 2018; Swayampakula et al., 2017). In addition, MT1-MMP is expressed in human atherosclerotic plaques and promotes plaque rupture by enhancing the degradation of collagens (Johnson, Sala-Newby, Ismail, Aguilera, & Newby, 2008). We further demonstrated that overexpression of MT1-MMP increased the development of atherosclerosis while knockdown of MT1-MMP reduced aortic cholesteryl ester accumulation in apoE^{-/-} mice. Collectively, these findings indicate that MT1-MMP may act as a shared risk factor for both cardiovascular disease and cancers, the two leading causes of morbidity and mortality globally. Thus, inhibition of MT1-MMP may become a very promising and valuable therapeutic target since it has the potential to increase hepatic LDLR levels, lower circulating LDL-C levels, increase atherosclerotic plaque stability and reduce the risk of cancer metastasis and invasion.

Chapter 4

Tandem inhibition of MT1-MMP and other LDLR regulating pathways increase availability of LDLR and cholesterol clearance

All experiments were conducted and analyzed by Adekunle Alabi in Zhang's lab except Fig 4.4 and 4.5 (Faqi Wang designed experiments and Adekunle Alabi conducted and analyzed experimental data- Zhang Lab)

4.1 Introduction

The low-density lipoprotein receptor (LDLR) plays a very critical role in regulating low-density lipoprotein (LDL); LDLR binds LDL on the cell surface and mediates its endocytosis for lysosomal degradation (Davis, Driel, Russell, Brown, & Goldstein, 1987). Structurally, LDLR consists of seven ligand-binding repeats (LRs) at its N terminus, followed by the epidermal growth factor (EGF) precursor homology domain. Next in the LDLR amino acid sequence is the clustered O-linked sugar domain, followed by the transmembrane domain and a cytoplasmic tail. Upon ligand binding to the LRs, LDLR is internalized via clathrin-coated pits and delivered to endosomes (Brown & Goldstein, 1986). In the low pH environment of the endosome, LDLR undergoes a conformational change so that LR4 and LR5 form a physical interaction with the YWTD repeats, promoting the release of the bound LDL for delivery to lysosomes for degradation. LDLR is then recycled to the cell surface (Rudenko et al., 2002).

Mutations in LDLR that disrupt its structure and function cause familial hypercholesterolemia, which is characterized by elevated levels of circulating LDL cholesterol and causes tendon and skin xanthomas as well as cardiovascular deposit, leading to a high risk of cardiovascular diseases and mortality (Goldstein & Brown, 2009). Given its key role in regulating cholesterol homeostasis, LDLR is regulated by multiple mechanisms at both the transcriptional and post-translational levels. LDLR is transcriptionally regulated by SREBP-2 and post-translationally regulated by PCSK9, inducible degrader of the LDLR (IDOL) and γ -secretase. PCSK9 binds to LDLR and promotes lysosomal degradation of the receptor (Lagace et al., 2006), while IDOL down-regulates LDLR via the polyubiquitination and lysosomal degradation pathway (Zelcer, Hong, Boyadjian, & Tontonoz, 2009). γ -secretase cleaves LDLR cytoplasmic region, leading to the lysosomal degradation of the protein (Kim et al., 2018). Inhibition of the posttranslational regulators of LDLR

such as PCSK9 and Υ -secretase has been shown to increase LDL cholesterol clearance. Similarly, statins are the most widely used cholesterol-lowering therapy, they inhibit HMG-CoA reductase, the rate-limiting enzyme in cholesterol biosynthesis pathway, upregulating the transcriptional activity of SREBP-2 (Stancu & Sima, 2001) and consequently increasing expression of LDLR and the clearance of circulating LDL.

The ectodomain of LDLR can be cleaved by proteases, with the released soluble LDLR ectodomain (sLDLR) detected in cell culture media and in human plasma (Begg, Sturrock, & van der Westhuyzen, 2004; Fischer, Tal, Novick, Barak, & Rubinstein, 1993). Serum levels of sLDLR are positively correlated with plasma LDL-C levels (Shimohiro, Taniguchi, Koda, Sakai, & Yamada, 2015). We recently reported that membrane-type matrix metalloproteinase-1 (MT1-MMP) plays a key role in the cleavage of LDLR and the release of sLDLR into circulation, functioning as an important regulator of LDLR and cholesterol homeostasis. The aim of our current research was to determine the potential beneficial effect on lipid-lowering through a combination of MT1-MMP inhibition with other strategies that can increase LDLR levels. In addition, sLDLR contains binding sites for LDL and PCSK9, hence we studied the possibility of the binding of sLDLR to circulating LDL and PCSK9 and its functional impacts.

4.2 Results

4.2.1 Combined treatment of MT1-MMP knockdown and other LDLR regulating mechanisms

4.2.1.1 *Gamma-secretase inhibition*

Gamma-secretase has been implicated in the cleavage of the cytoplasmic C-terminal region of LDLR (Kim et al., 2018) and its inhibition by the chemical compound DAPT slightly increases LDLR on the cell surface (Strøm, Tveten, Laerdahl, & Leren, 2014). We knocked down MT1-MMP expression in HepG2 cells and then treated cells with DAPT to inhibit γ -secretase; combined inhibition of both proteinases showed a significant increase in the levels of LDLR compared to the inhibition of individual protein. Similarly, treatment of DAPT led to an increase in the 17kDa cytoplasmic fragment of the protein (**fig 4.1a&b**). This suggests that the ectodomain cleavage of LDLR on the cell surface, mediated by MT1-MMP results in a C-terminal portion of the protein that may be degraded by γ -secretase.

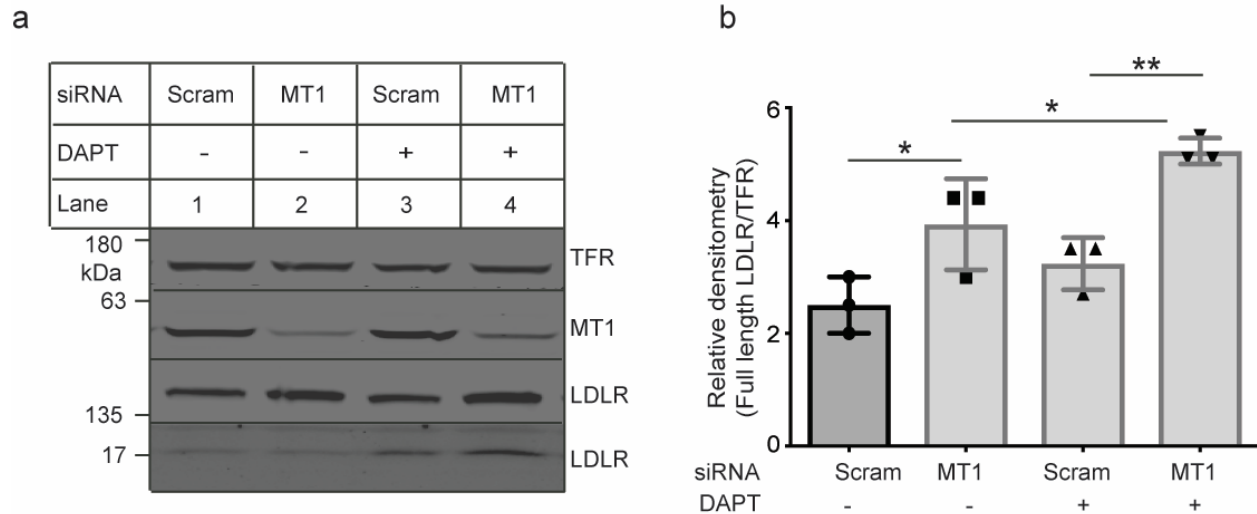


Fig 4. 1. Combined knockdown of MT1-MMP and inhibition of other LDLR regulating pathways invitro. (a) Inhibition of γ -secretase and MT1-MMP Knockdown. HepG2 cells were transfected with either scrambled or *MT1-MMP* siRNA. 24 h after transfection, cells were treated accordingly with 10 μ M DAPT solubilized in DMSO to inhibit γ -secretase for 16 h. Cells were collected for lysis and the whole-cell lysates were applied to SDS-PAGE, followed by immunoblotting with a polyclonal anti-human LDLR c-terminal, 3143, a polyclonal anti-transferrin receptor (TFR), and polyclonal anti-MT1-MMP (MT1) antibodies. **(b) Quantification of LDLR immunoblot in HepG2 cells.** Values are mean \pm SD of independent triplicate experiments. * $P < 0.05$, ** $P < 0.01$ control vs test variants.

4.2.1.2 PCSK9 inhibition

PCSK9 reroutes LDLR for lysosomal degradation (Lambert, Charlton, Rye, & Piper, 2009). Numerous clinical studies using monoclonal antibodies against PCSK9 have shown a significant reduction in LDL-C levels when used either alone or in combination with statin therapy (Auer & Berent, 2018). Hence, to further understand the role of MT1-MMP in the cleavage of LDLR, we investigated if LDLR increase associated with inhibition of PCSK9 is prone to proteolytic MT1-MMP cleavage. A combined knockdown of *PCSK9* and *MT1-MMP* gene in Huh7 cell showed that both siRNA treatments had an additive effect on the increase of cellular levels of LDLR (**fig 4.2a&b**), indicating that a combined therapy inhibiting both proteins could be beneficial. We then

knocked down expression of *MT1-MMP* gene in *Pcsk9* Knockout mice, an established mouse model with significantly increased hepatic LDLR and reduced LDL-cholesterol compared to wild type C57BL/6 mice (Rashid et al., 2005). *Pcsk9*^{-/-} mice were completely devoid of the protein in plasma compared to the wild type mice (**fig 4.2c**). AAV-shRNA-mediated *MT1-MMP* knockdown in *Pcsk9*^{-/-} mice showed a significant reduction in mRNA levels of *MT1-MMP* in the liver as indicated by qRT-PCR (**fig 4.2d**). The knockdown of *MT1-MMP* also caused a significant increase in hepatic levels of LDLR (**fig 4.2e**) and a corresponding reduction in the levels of total cholesterol (**fig 4.2f**) when compared to *Pcsk9*^{-/-} mice injected with AAV-scrambled shRNA. Collectively, these findings demonstrate that combined *MT1-MMP* and *PCSK9* inhibition has an additive beneficial effect on LDLR and cholesterol clearance.

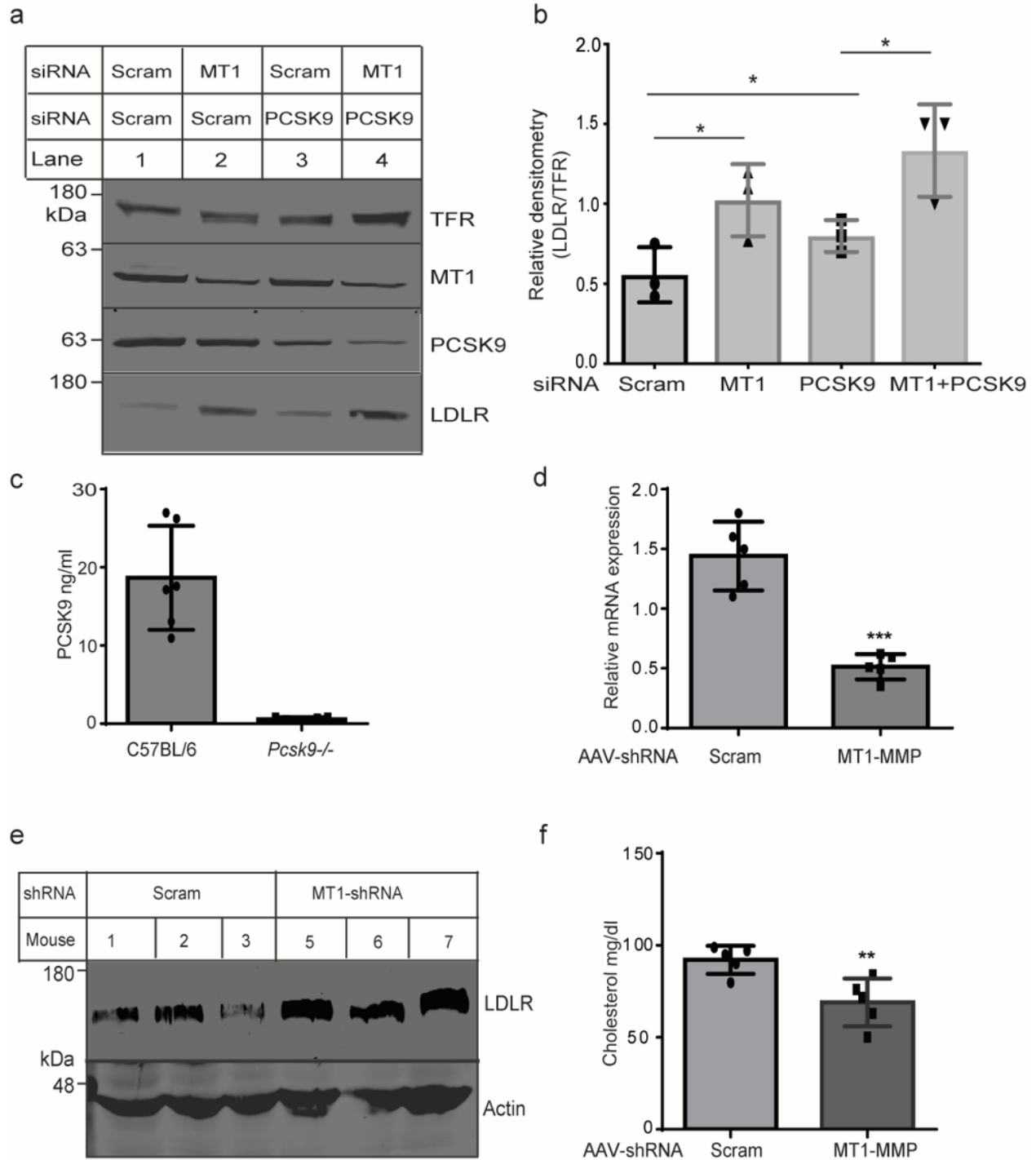


Fig 4. 2. Combined gene knockdown of *MT1-MMP* and *PCSK9*. (a) Knockdown of *MT1-MMP* and *PCSK9* in Huh7 cells. Huh7 cells were co-transfected with either scrambled and *MT1-MMP* siRNA, scrambled and *PCSK9* siRNA or *MT1-MMP* and *PCSK9* siRNA. 48 h after transfection, whole cell lysate was collected and applied to SDS-PAGE. This was followed by immunoblotting with a polyclonal anti-human LDLR c-terminal, 3143, a polyclonal anti-transferrin receptor (TFR), and monoclonal anti-PCSK9 (PCSK9) antibodies. (b) Quantification of LDLR immunoblot

from Huh7 cells. Values are mean \pm SD of independent triplicate experiments. * $P < 0.05$, ** $P < 0.01$ control vs test variants. **(c) Plasma PCSK9 levels**, as determined by R&D system ELISA kit from C57BL/6 and *Pcsk9*^{-/-} mice after an overnight fast. **Figure d to f**, *Pcsk9*^{-/-} mice were injected with 1×10^{10} genomic copies of Adeno-associated virus carrying scrambled shRNA or shRNA targeting *MT1-MMP* gene. The mice were fed ad libitum a chow diet for 2 weeks, followed by an additional 2 weeks of western diet feeding. Mice were sacrificed after an overnight fast one month from shRNA injection. **(d) Gene expression levels of liver *MT1-MMP***, as determined by qRT-PCR. **(e) Liver immunoblot**, with a polyclonal anti-LDLR c-terminal, 3143, a polyclonal anti-actin (Actin), and polyclonal anti-MT1-MMP (MT1) antibodies. **(f) Plasma total cholesterol.** Values of data are mean \pm S.D. of 6 mice in each group. *, $p < 0.05$. **, $p < 0.01$. ***, $p < 0.001$.

4.2.1.3 Statin treatment

Statins inhibit HMG-COA reductase and subsequently activate the transcriptional activity of SREBP2. This leads to enhanced expression of LDLR with a corresponding reduction in plasma LDL-C. Thus, we hypothesized that the statin-induced increase of LDLR could be subjected to MT1-MMP-mediated cleavage, reducing the lipid-lowering efficacy of statins. To test this, we knocked down *MT1-MMP* expression in Huh7 cells and then treated cells with Lovastatin. As shown in **(fig 4.3a&b)**, lovastatin combined with *MT1-MMP* knockdown enhanced the increase in LDLR levels in Huh7 cells compared to either treatment alone.

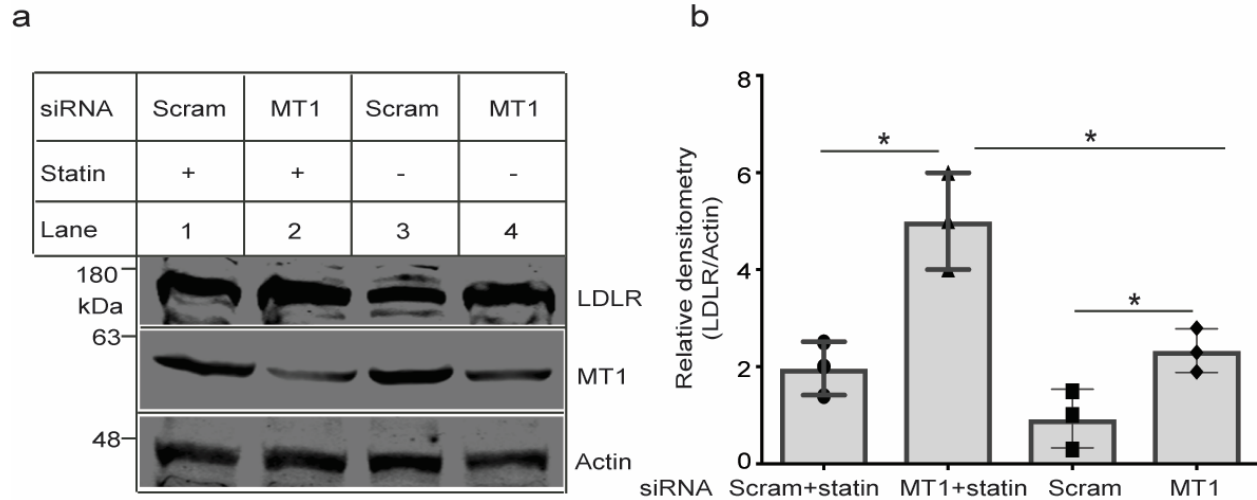


Fig 4. 3. *MT1-MMP* knockdown and statin treatment in Huh7 cells. Huh7 cells were transfected with either scrambled or *MT1-MMP* siRNA. After 24 h culture media was removed and replaced with 7.5 $\mu\text{g/ml}$ lovastatin supplemented with 5 $\mu\text{g/ml}$ mevalonate in DMEM+10% FBS. Cells were incubated with statin for 16hrs before lysis and western blot analysis. **(a) Immunoblot of Huh7 cell treated with statin.** Immunoblotting was carried out with a polyclonal anti-human LDLR c-terminal, 3143, a polyclonal anti-actin (Actin), and polyclonal anti-*MT1-MMP* (MT1) antibodies. **(b) Quantification of LDLR immunoblot of Huh7 cells treated with statin.** Values are mean \pm SD of independent triplicate experiments. * $P < 0.05$, ** $P < 0.01$ control vs test variants.

We further tested the effect of *MT1-MMP* knockdown in tandem with statin treatment in mice. Male mice (10-12 weeks old) on chow diet were injected with either AAV-DJ/8 scrambled or *MT1-MMP* shRNA and then supplied with or without statin. *MT1-MMP* shRNA targeted knockdown showed a significant reduction in *MT1-MMP* protein levels in the liver of both non-statin and statin fed mice (**fig 4.4a&d**). Similarly, reduction in liver *MT1-MMP* caused a significant increase in LDLR levels in both statin and non-statin fed mice (**fig 4.4a to d**). Statins elicit their action by upregulating LDLR transcription, which was confirmed by qRT-PCR. The mRNA and protein levels of *Ldlr* were significantly increased in statin fed mice compared to the non-statin fed group (**fig 4.4e&f**).

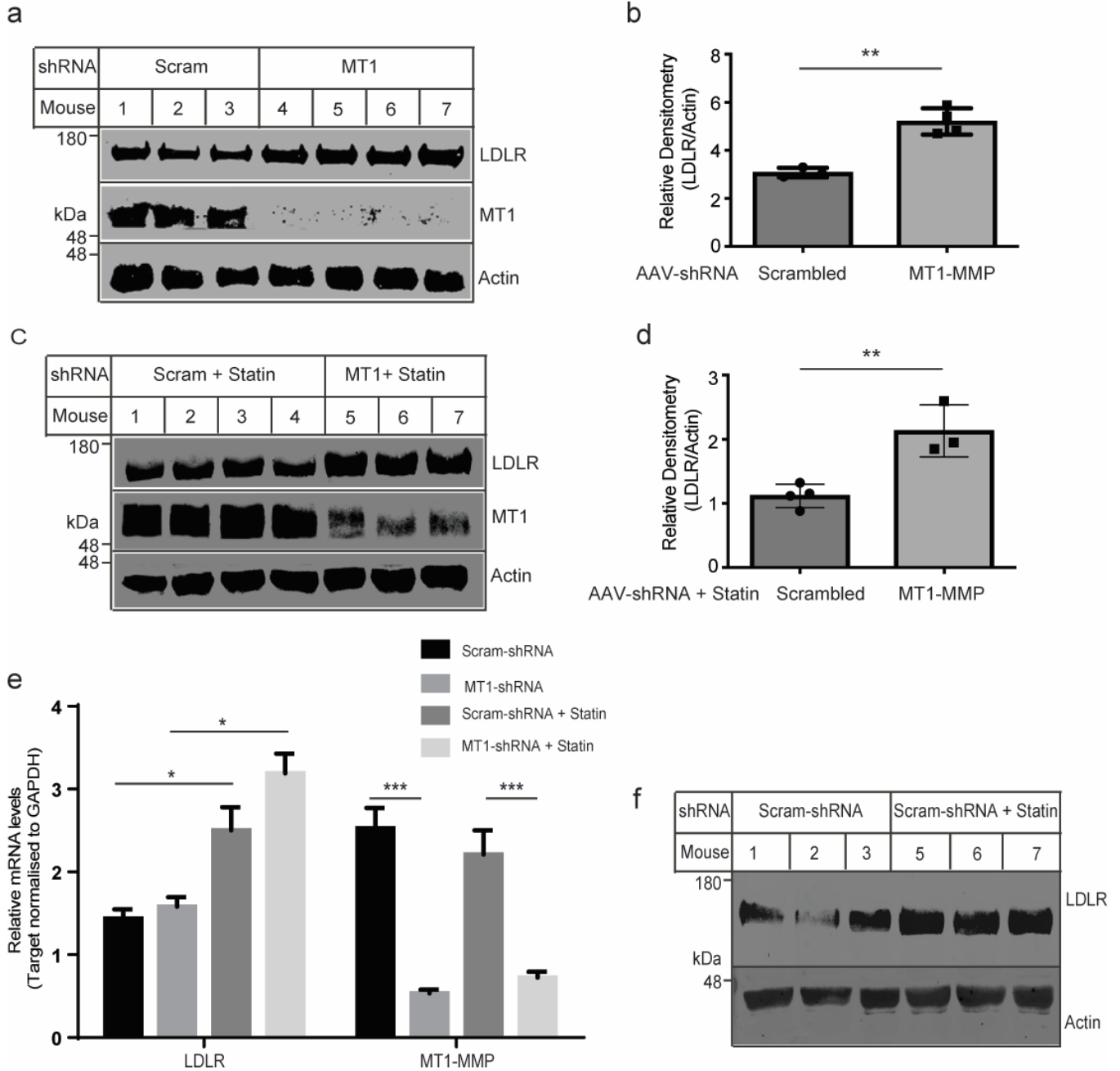


Fig 4. 4. MT1-MMP knockdown and statin treatment. Mice were injected with 1×10^{10} genomic copies of Adeno-associated virus carrying scrambled shRNA or shRNA targeting *MT1-MMP* gene. Statin fed group of Mice were fed ad libitum a chow diet for 20 days, after which their diet was supplemented with 0.2% statin (wt/wt) for 10 days and fasted 8hrs before euthanasia. Non-statin fed group of mice were fed chow diet for 30 days without statin supplementation. Both groups of mice were sacrificed 30 days after shRNA injection followed by blood and tissue collection. **(a) Liver homogenate immunoblot and (b) LDLR quantification**, of mice without statin supplementation. **(c) Liver homogenate immunoblot and (d) LDLR quantification**, of

mice with statin supplementation. Immunoblotting was carried out with polyclonal anti- LDLR c-terminal, 3143, a polyclonal anti-actin (Actin), and polyclonal anti-MT1-MMP (MT1) antibodies. **(e) Gene expression levels of liver *Ldlr* and *MT1-MMP***, as determined by qRT-PCR. **(f) Effect statin supplementation on LDLR protein levels in the liver.** Immunoblot compares liver LDLR between scrambled shRNA injected mice of non-statin and statin fed mice. Immunoblotting was carried out with a polyclonal anti-human LDLR c-terminal, 3143, a polyclonal anti-actin (Actin) antibody. Values of data are mean \pm S.D. of 4-6 mice in each group. *, $p < 0.05$. **, $p < 0.01$. ***, $p < 0.001$.

MT1-MMP knockdown also reduced plasma levels of HDL and non-HDL-C in non-statin fed (**fig 4.5a**) and in statin fed group (**fig 4.5b**) because the increased LDLR levels can enhance clearance of apoB-100 or apoE containing non-HDL lipoproteins and apoE containing HDL. Similarly, FPLC analysis showed a reduction in both non-HDL and HDL cholesterol in MT1-MMP knockdown mice (**fig 4.5c&d**). MT1-MMP knockdown appeared to reduce plasma levels of apoB100 and apoB48 in the presence or absence of statin treatment, however, the reduction was more drastic in the statin fed group. Silencing MT1-MMP expression did not affect plasma levels of apoE in mice without statin treatment, however, combination of statin and MT1-MMP knockdown reduced apoE levels (**fig 4.5e&f**). Together, our findings suggest LDLR upregulation associated with statin treatment, is subject to MT1-MMP cleavage and as such a combined treatment of statin therapy and MT1-MMP inhibition may be of additive benefit.

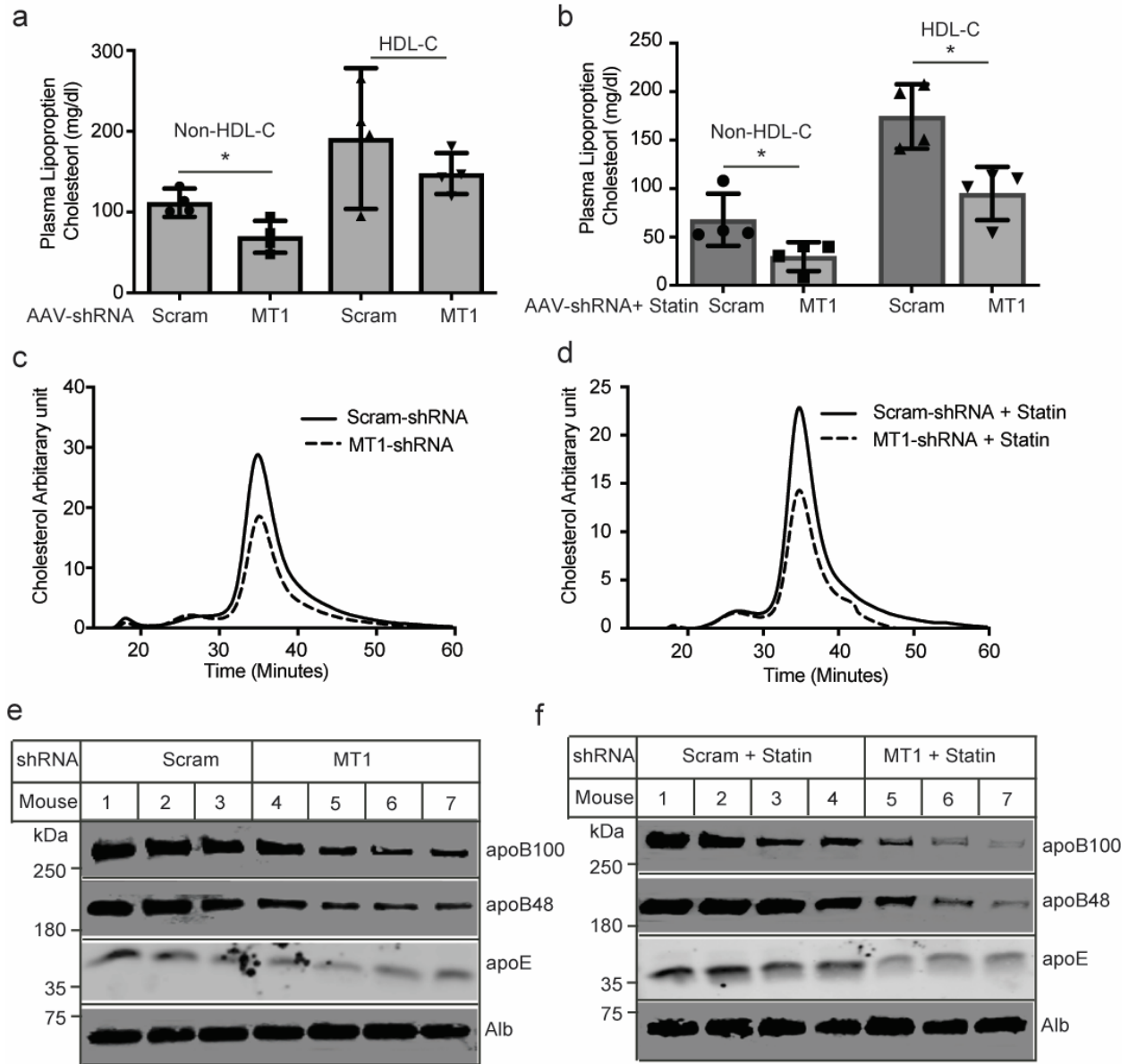


Fig 4. 5. Effect of MT1-MMP knockdown and statin treatment on apolipoproteins and lipoprotein cholesterol levels. (a) Plasma HDL and Non-HDL cholesterol measurements in Non-statin fed mice (b) Plasma HDL and Non-HDL cholesterol measurements in statin fed mice. 5 μ l plasma sample from individual mouse was added to 5 μ l LDL precipitating reagent to separate HDL from Non-HDL cholesterol. HDL portion was transferred into a new tube, while the precipitated Non-HDL cholesterol was resuspended and dissolved in 10 μ l PBS. Both forms of cholesterol were measured using a commercial kit from Cell Biolabs. **(c&d) Plasma FPLC cholesterol profile for Non-statin and statin fed mice.** Plasma was pooled from 5 mice, for both control and MT1-MMP knockdown mice and applied to FPLC column for lipoprotein separation. **(e&f) Immunoblot of plasma apolipoproteins for Non-statin and statin fed mice.** Plasma samples were diluted 10 X with distilled water, 10 μ l of diluted samples were added to 10 μ l sample loading buffer and applied to SDS-PAGE. Immunoblotting was carried out with a

polyclonal anti-apoB (apoB48 & 100), a polyclonal anti-apoE (apoE), and polyclonal anti-albumin (Alb) antibodies.

4.2.2 LDLR Extracellular Domain binds LDL and prevents its Endocytosis

We then investigated the effect of sLDLR on LDL and its subsequent receptor-mediated endocytosis. Based on the molecular mass of sLDLR, it contains most of its extracellular domain including its ligand-binding repeats, and as such, it may retain its ability to bind LDL. To test this hypothesis, we purified recombinant extracellular domain of LDLR with a Flag tag at the C-terminus (A22- R788). Our recombinant LDLR (rLDLR) mimics the sLDLR with a very similar molecular weight. Hence, we incubated fluorescent Dil-labelled LDL in 1% BSA in the presence or absence of rLDLR at 37°C for 1 hour. The mixture was then added to Huh7 cells that were incubated in NCLPPS medium to increase expression of endogenous LDLR, after which, the cells were washed to remove unbound LDL. LDL uptake was then measured as residual fluorescence signal. As shown in Figure 4.6a, Huh7 cells effectively took up fluorescent-labeled LDL, however, preincubation with rLDLR virtually abrogated uptake of Dil-LDL (**fig 4.6a**). This suggests that rLDLR bound to LDL and then blocked its uptake by native membrane tethered LDLR in Huh7 cells. To further understand the process, we examined the dose-dependent effect of sLDLR on Dil-LDL uptake. We incubated 5µg Dil-LDL with various concentrations of rLDLR ranging from 0.5,1,2 and 4µg and then administered the mixture to Huh7 cells. Analysis of fluorescent signals revealed that rLDLR inhibited the uptake of Dil- LDL in a dose-dependent manner (**fig 4.6b**). This experiment suggests that sLDLR-mediated inhibition of LDL uptake depends on the amount of sLDLR available for binding to LDL.

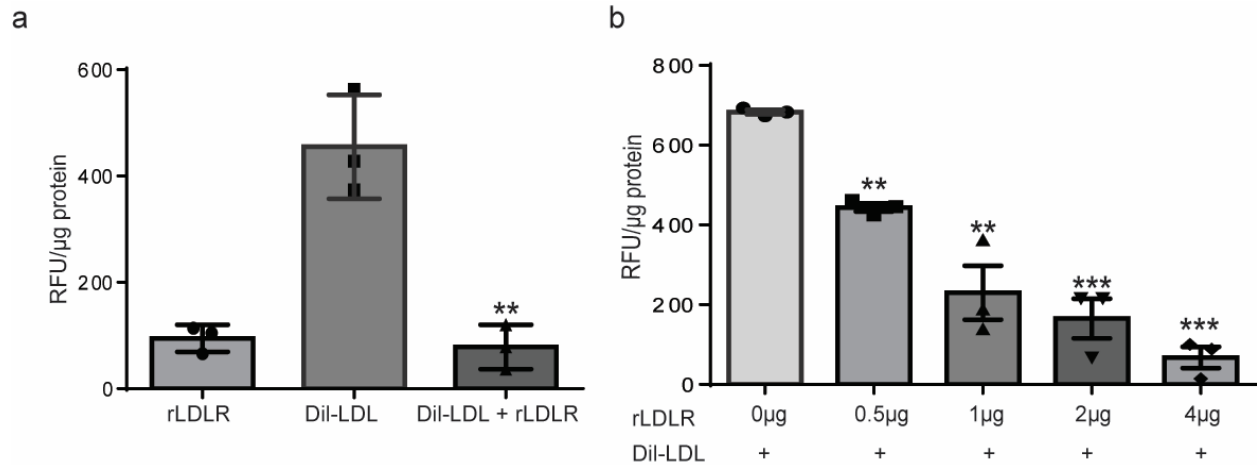


Fig 4. 6. Recombinant LDLR binds LDL and prevents its endocytosis. a) Quantification of LDL uptake in Huh7 cells. 4 µg Dil-LDL was incubated with or without 4 µg rLDLR in 1% BSA for 1 h, the mixture was then transferred to Huh7 cell in 96 well plate. **(b) Quantification of rLDLR Dose-dependent LDL uptake.** 5 µg Dil-LDL was incubated with varying concentrations of rLDLR (0.5,1,2 and 4 µg) in 1% BSA for 1 h. The mixture was then transferred to Huh7 cell in 96 well plate, after which media was removed and cells washed for fluorescent measurement at Excitation: 520 nm; Emission:580 nm. Values are mean ± SD of independent triplicate experiments. * P< 0.05, ** P<0.01, *** P<0.001 control vs test variants.

4.2.3 LDLR Extracellular Domain binds PCSK9 and inhibits its ability to mediate LDLR

Degradation

Next, we determined if rLDLR could bind to PCSK9. In order to test this possibility, we incubated various concentrations of rLDLR with recombinant gain of function mutant PCSK9 (D374Y) that has a much higher binding affinity to LDLR than the wild-type PCSK9. The mixture was then added to Huh7 cells for overnight incubation at 37 °C. Same amount of whole cell lysate was applied to western blotting. We found that rLDLR dose-dependently suppressed PCSK9-promoted LDLR degradation (**fig 4.7a&b**). This finding suggests that sLDLR that retains the PCSK9 binding site may bind to PCSK9 in circulation and competitively prevent the protein binding to cell surface LDLR.

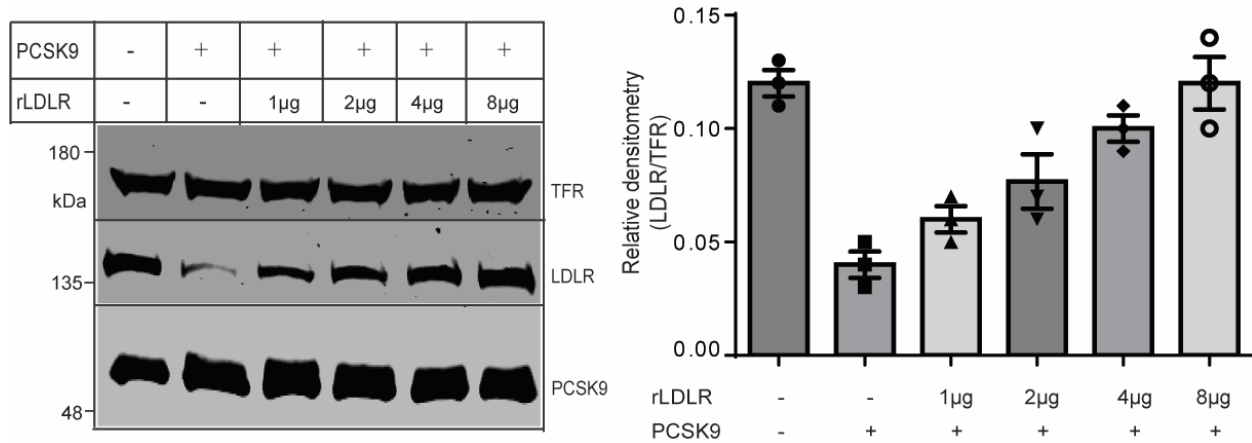


Fig 4. 7. Recombinant LDLR binds PCSK9 and inhibits LDLR degradation. (a&b) Immunoblot and quantification of lysate from Huh7 cells treated with PCSK9 incubated with rLDLR. 4 µg PCSK9 (D374Y) was incubated with or without varying concentration of rLDLR (0,1,2,4, and 8 µg) in 1% BSA at 37 for 1 h, the mixture was then added to Huh7 cells in 6 well plate. Cells were lysed and lysates were applied to SDS-PAGE, followed by immunoblotting with a polyclonal anti-human LDLR c-terminal, 3143, a polyclonal anti-transferrin receptor (TFR), and monoclonal anti-PCSK9 (PCSK9) antibodies. Values are mean \pm SD of independent triplicate experiments. * $P < 0.05$, ** $P < 0.01$, *** $P < 0.001$ control vs test variants.

4.2.4 Soluble LDLR is not a mediator of PCSK9 binding to LDL in Circulation.

It has been reported that LDL binds PCSK9 in human plasma and then inhibits the ability of PCSK9 to degrade LDLR (Kosenko, Golder, Leblond, Weng, & Lagace, 2013). We have shown that rLDLR binds to both LDL and PCSK9 independently. Hence, we hypothesize that sLDLR might mediate the binding of PCSK9 to LDL. To test this hypothesis, we tested PCSK9 in the LDL fractions of wild type C57BL/6 mice and *Ldlr* knockout mice. If sLDLR was required for the

binding of PCSK9 and LDL, PCSK9 would be absent or reduced in the LDL fractions of *Ldlr* knockout mice. The absence of sLDLR was confirmed in *Ldlr* knockout mice (**fig 4.8a**). Analysis of FPLC cholesterol showed elevated LDL content in *Ldlr* knockout mice as compared to the wild type mice (**fig 4.8b**). We then measured PCSK9 in the LDL fraction collected from FPLC of the wild type and *Ldlr* knockout mice plasma using ELISA. As shown in Figure 4.8c, PCSK9 was detectable in the LDL fractions of both the wild type and *Ldlr* knockout mice. PCSK9 was significantly higher in the LDL fraction of *Ldlr* knockout mice probably due to higher levels of plasma LDL. This result indicates that sLDLR plays a negligible role in the binding of PCSK9 to LDL.

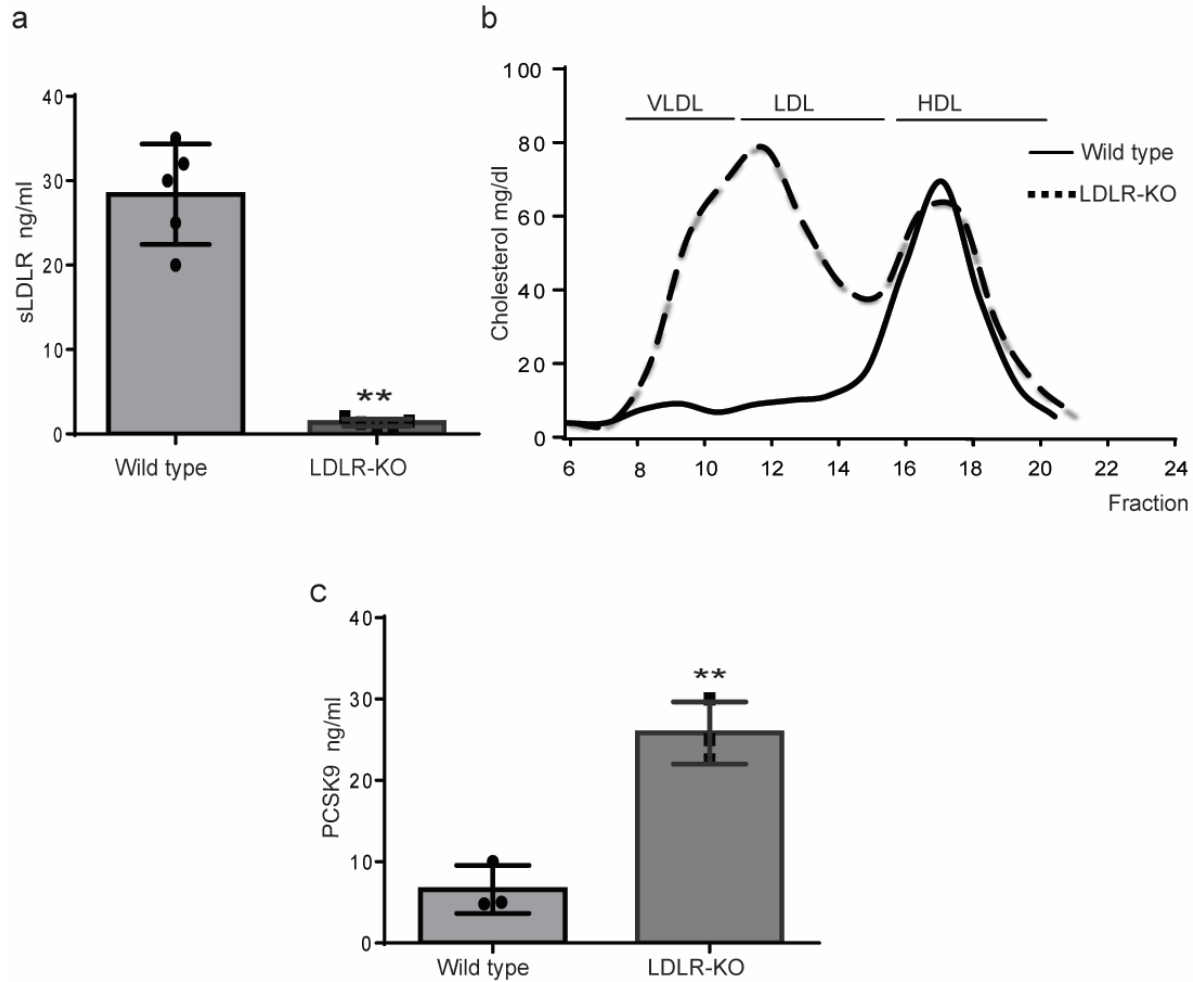


Fig 4. 8. Soluble LDLR does not mediate PCSK9 binding to LDL (a) Plasma soluble LDLR quantification. Male wild type and *Ldlr*^{-/-} mice were fasted overnight prior to blood sample collection and plasma isolation. Blood plasma was then subjected to ELISA sLDLR measurement. **(b) FPLC cholesterol profile of wild type and *Ldlr*^{-/-} mice plasma.** Fasting mice from each group of wild type and *Ldlr*^{-/-} were pooled. 500 μ l of pooled plasma was applied to a size-exclusion FPLC column and the eluate was collected in 1 ml per fraction. Total cholesterol in each fraction was measured using Wako Life Sciences kit and a cholesterol profile graph was plotted accordingly **(c) Quantification of PCSK9 content in LDL fraction from wild type and *Ldlr*^{-/-} mice.** PCSK9 was measured by commercial ELISA kit from R&D system, on pooled eluate corresponding to LDL fractions between 10-14. Values of data are mean \pm S.D. of 5-6 mice in each group. *, $p < 0.05$. **, $p < 0.01$. ***, $p < 0.001$.

4.3 Discussion

LDLR is regulated at both transcriptional and post-translational levels. We have recently identified MT1-MMP as a posttranslational regulator of LDLR, cleaving the ectodomain of the protein and releasing sLDLR into the extracellular milieu. The findings from this study suggest that MT1-MMP inhibition in tandem with inhibition of other LDLR regulating pathways such as γ secretase and PCSK9 may be beneficial. It may be possible that MT1-MMP and γ -secretase work in tandem since MT1-MMP cleaves the extracellular domain of the LDLR, leaving the cytoplasmic region of the protein to be quickly degraded by γ -secretase. Similarly, combined therapy of MT1-MMP knockdown and statin treatment showed an additive effect on the increase in LDLR, leading to a significant effect on LDL cholesterol clearance. The combined therapy of PCSK9 monoclonal antibody inhibitors with statin treatment has shown more beneficial effects on lipid-lowering than statin alone, effectively reducing atherosclerotic cardiovascular diseases (Dixon et al., 2019). Given the successful combination of PCSK9 and statin in the treatment of cardiovascular diseases, the positive results from our experiments suggest that a combined therapy of MT1-MMP inhibition and other treatments may be worthwhile. The increase in LDLR associated with inhibition of gamma secretase and PCSK9, as well as statin treatment can be subjected to MT1-MMP-mediated cleavage, therefore, the additive effect of the combined treatment on the increase in LDLR is most likely a result of reduced shedding of the LDLR.

sLDLR in circulation retains its ligand-binding repeats. Thus, it retains the ability to bind LDL. The binding of rLDLR (sLDLR mimic) to LDL inhibits the uptake of the LDL in a dose-dependent manner; this may explain why previous studies showed a significant correlation between circulating lipoproteins and sLDLR (Mayne et al., 2018; Shimohiro et al., 2015). Each LDL particle has one apoB100 with one LDLR binding site (Hevonoja, Pentikäinen, Hyvönen,

Kovanen, & Ala-Korpela, 2000). The binding of sLDLR to the sole LDLR binding site on the LDL may prevent the binding of the lipoprotein particle to native LDLR, blocking the cellular uptake of LDL for lysosomal degradation. This explains the reduced uptake of LDL by cells with an increasing amount of rLDLR from our incubation experiment. Another ligand of the LDLR that may serve as a potential binding partner for sLDLR is PCSK9; our experiment suggests that rLDLR binds to PCSK9 and prevent its LDLR degradation effect. This effect of rLDLR mimics inhibitory peptides of PCSK9 that are structurally similar to the EGFA region of LDLR, which is the binding site of PCSK9 on the receptor. (Zhang et al., 2014). Thus, our findings suggest that sLDLR could inhibit PCSK9-mediated degradation of the LDLR by attaching to its binding site on PCSK9 and protecting the native LDLR.

Previous study showed that LDL inhibits PCSK9 mediated LDLR degradation in HEK293 cells (Fisher et al., 2007). The authors suggested that this might be caused by reduced accessibility of PCSK9 to LDLR due to the competitive advantage of LDLR for LDL over PCSK9. However, kosenko et al. (2013) found that LDL directly or indirectly binds to PCSK9, inhibiting LDLR degradation. X-ray crystallography modeling shows that the binding site of the LDL and PCSK9 on the LDLR is not in close proximity (Kwon, Lagace, McNutt, Horton, & Deisenhofer, 2008), indicating that the possibility of a steric or allosteric hindrance of concurrent binding of both proteins is low. We proposed that sLDLR that retains the EGFA domain (the binding site of PCSK9) and ligand binding repeats (the binding site of LDL) may act as a linker for the binding of PCSK9 to LDL. We observed that LDL fraction collected from *Ldlr* knockout mice plasma that did not contain sLDLR showed more associated PCSK9 than LDL fraction from plasma of the wild type mice. Thus, sLDLR is not required for the binding of PCSK9 to LDL. This indicates that an alternative mechanism is responsible for the process. Further investigation is required to

understand the underlying mechanism because it could shed light on PCSK9 as a key regulator of plasma LDL-cholesterol and cardiovascular diseases.

Chapter 5

Mechanistic Study of MT1-MMP cleavage of the Low-Density Lipoprotein Receptor and its related Proteins

All experiments were conducted and analyzed by Adekunle Alabi in Zhang's lab

5.1 Introduction

The Low-density lipoprotein receptor (LDLR) plays a critical role in the receptor-mediated clearance of plasma LDL cholesterol (LDL-C) and as such regulates cholesterol homeostasis in the body (Brown & Goldstein, 1986). Mutations in LDLR cause familial hypercholesterolemia (FH), which is characterized by elevated circulating levels of cholesterol, specifically LDL-C (Brown & Goldstein, 2006). LDLR deficient mice are hypercholesterolaemic which is reversible with adenovirus-mediated delivery of *LDLR* (Ishibashi et al., 1993), highlighting its importance in cholesterol homeostasis. High levels of circulating cholesterol are pro-atherogenic and increase the risk of coronary heart disease risk (Shepherd & Packard, 1986).

Structurally, LDLR consists of seven ligand-binding repeats (LRs) at its N terminus, followed by the so-called epidermal growth factor (EGF) precursor homology domain. Next in the LDLR amino acid sequence is the clustered O-linked sugar domain, followed by the transmembrane domain and a cytoplasmic tail. Upon ligand binding to the LRs, LDLR is internalized via clathrin-coated pits and delivered to endosomes (Brown & Goldstein, 1986).

The ectodomain of LDLR can be cleaved by proteases, with the released soluble ectodomain LDLR (sLDLR) detected in cell culture media and in human plasma (Begg, Sturrock, & van der Westhuyzen, 2004; Fischer, Tal, Novick, Barak, & Rubinstein, 1993). Serum levels of sLDLR are positively correlated with plasma LDL-cholesterol (LDL-C) levels (Shimohiro, Taniguchi, Koda, Sakai, & Yamada, 2015). Membrane type 1 matrix metalloproteinase (MT1-MMP) has been identified as one of the proteases responsible for LDLR cleavage. MT1-MMP is a membrane-bound proteinase with multiple physiological and pathological functions elicited through pericellular proteolysis and extracellular matrix remodeling (Wong et al., 2016). MT1-MMP

consists of a signal sequence followed by a pro-domain that keeps the enzyme in an inactive form, a catalytic domain that has a conserved zinc-binding motif, a flexible hinge region, a hemopexin-like domain that may mediate protein-protein interaction, a transmembrane domain, and a C-terminal cytoplasmic tail that is required for MT1-MMP recycling (Fernandez-Garcia et al., 2014; Remacle, Murphy, & Roghi, 2003). These regions within the protein may or may not play a critical role in MT1-MMP targeting and proteolysis of its multiple substrates (Cerofolini et al., 2016). Mutations in various domains of MT1-MMP are known to lead to a complete or partial loss of its activity (Dmitry V. Rozanov et al., 2001; Sakr et al., 2018), which may cause deleterious or favorable phenotypes. MT1-MMP has also been reported to cleave LDLR related family proteins, such as LRP1, releasing their ectodomain into the culture medium (Dmitri V Rozanov, Hahn-Dantona, Strickland, & Strongin, 2004; Selvais et al., 2011). Similarly, metalloproteinases have been reported to cause the release of soluble forms of LDLR structurally related proteins such as VLDLR and ApoER2 (Hoe & Rebeck, 2005), however, the exact metalloproteinase eliciting this activity is yet to be determined.

The aim of this study was to understand the cleavage pattern of MT1-MMP on LDLR and to determine substrate specificity for both MT1-MMP and LDLR as compared to other closely related members within each protein family. We also studied the effect of a naturally occurring mutation in MT1-MMP pro-domain on its ability to cleave the LDLR.

5.2 Results

5.2.1 MT1-MMP-Mediated LDLR Cleavage occurs at Multiple Sites on the LDLR

The LDLR has five distinct regions that play critical roles in the functionality of the protein and may be required for MT1-MMP-mediated cleavage of the protein or maybe the site of cleavage. Hence, we sort to determine if any region of the protein was critical for its MT1-MMP mediated cleavage. In order to test this possibility, we made cDNA with deletions in the regions coding for different parts of the LDLR protein, ligand binding repeat deletion (Δ R1-R7), EGF-like domain deletion (Δ EGF), O-Linker sugar domain (Δ O-Linker) and C-terminal domain (Δ 812). Each deletion mutant was co-expressed with MT1-MMP in HEK293 cells. We found out that MT1-MMP cleaved all LDLR mutants tested in a similar manner to the wild type (**fig 5.1a, lane 1-12**), indicating that the regions in LDLR we tested are not required for MT1-MMP's cleavage of the LDLR or MT1-MMP has multiple cleavage sites on the protein. Similarly, to explore the possibility of LDLR cleavage occurring at the cell surface or after endocytosis, we investigated if the loss of recycling property of LDLR affected its cleavage by MT1-MMP. Using cDNA derived from site-directed mutagenesis of WT-LDLR cDNA to JD mutant, a naturally occurring mutation that changes the tyrosine of the NPVY motif to cysteine (Y807C) and as such prevents endocytosis of the protein (Davis, Driel, Russell, Brown, & Goldstein, 1987). Co-expression of the JD-mutant with MT1-MMP did not prevent MT1-MMP cleavage of the protein (**fig 5.1a, lane 13&14**), indicating that the endocytosis pathway of the protein does not play an important role in the cleavage of the protein by MT1-MMP.

To further understand the cleavage pattern of LDLR by MT1-MMP, and if indeed it cleaves LDLR at multiple sites, we used purified recombinant proteins of c-terminal His tagged MT1-MMP with

its pro-domain A21-S538 (Pro-MT1) and c-terminal Flag-tagged LDLR A22- R788 (rLDLR) in an invitro cleavage experiment. The pro-domain of Pro-MT1 was cleaved to generate the active rMT1, which was then incubated with rLDLR; western blot analysis of the incubated mixture showed that full-length extracellular rLDLR was cleaved to multiple bands in the presence of rMT1 (**fig 5.1b**). This further reiterated the possibility of multiple cleavage sites on the LDLR. We then used a software CleavePredict to predict the cleavage sites of MT1-MMP on LDLR. CleavePredict is a validated free access web server for substrate cleavage pattern prediction by matrix metalloproteinase, the prediction employs matrix metalloproteinase specific position weight matrices which is derived from statistical analysis of high-throughput phage display experimental cleavage results of metalloproteinases (Kumar, Ratnikov, Kazanov, Smith, & Cieplak, 2015). The putative MT1-MMP cleavage sites of LDLR as predicted by the software are shown in **Table 5.1**. The software predicted 22 possible cleavage sites on the LDLR protein, with a spread across all its extracellular domain; to test our hypothesis, we selected 4 locations based on the position weight matrix score and proximity to the transmembrane domain which has been suggested to be the cleavage region of MT1-MMP on LRP1 (Dmitri V Rozanov et al., 2004). The positions we picked were A521, G529, N645 in the YWTD region of the EGF-Like domain and A789 within the transmembrane domain of the protein. We generated cDNA with a mutation to valine for each (A521V, G529V, N645V, A789V). Valine was chosen as a substitute amino acid because it was the most structurally related amino acid to wild type residues that caused a bypass of cleavage site identified by the Cleavepredict software. We then co-expressed each of these mutants with MT1-MMP in HEK293 cells. Like the wild type protein, all mutants were cleaved by MT1-MMP (**fig 5.1c**). The outcome of this experiment suggests that each of these predicted

cleavage sites is not required for MT1-MMP-mediated cleavage of LDLR. In summary, our data suggest that MT1-MMP may cleave LDLR at more than one site within the entire protein.

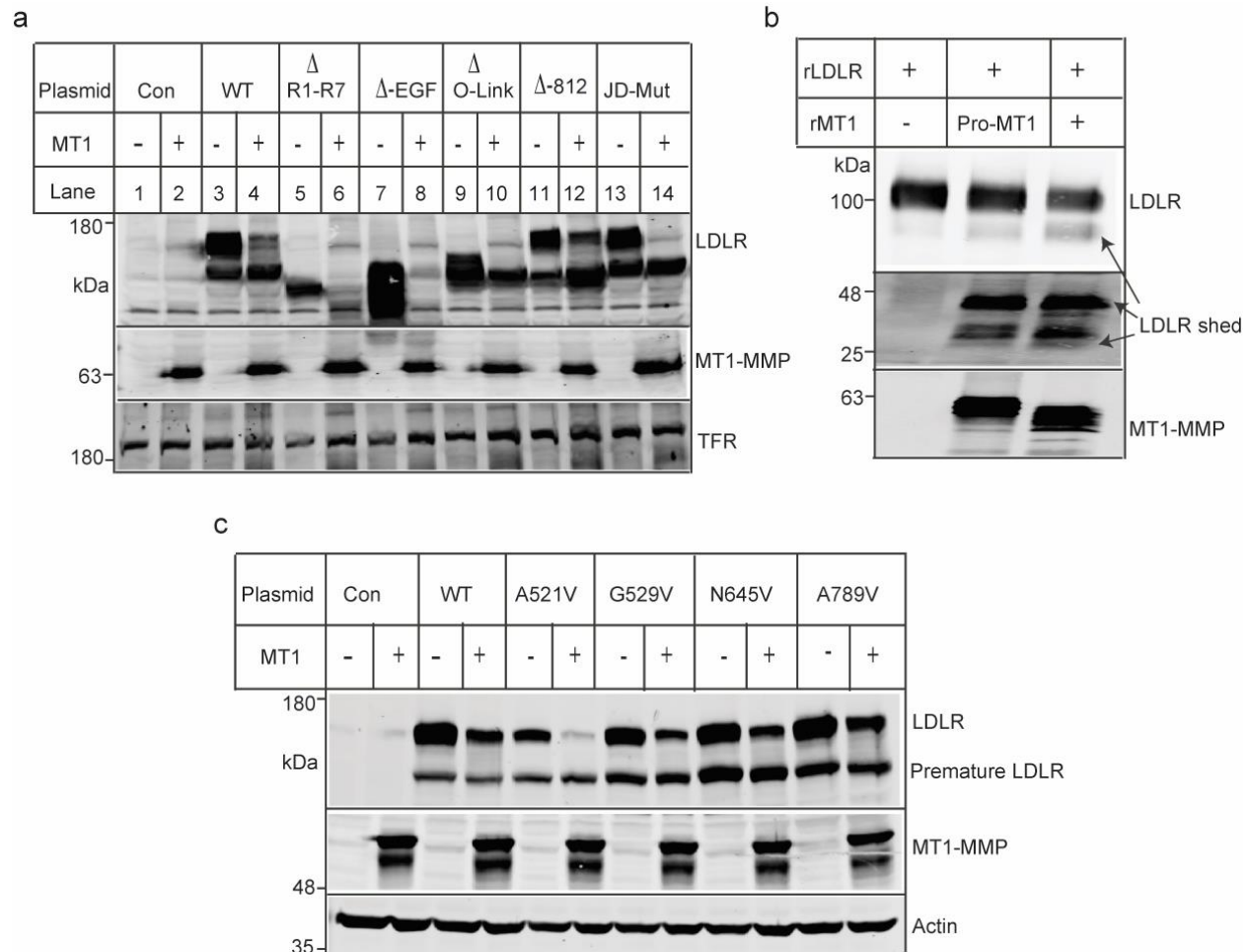


Fig 5. 1. MT1-MMP Cleavage of the LDLR is not restricted to a single region within the protein. (a) Co-expression of MT1-MMP and LDLR deletion mutants. HEK293 cells were co-transfected with either wild type LDLR or deletion mutants of LDLR with MT1-MMP cDNA. After 48 h, cells were collected. Whole-cell lysates were applied to SDS-PAGE, followed by immunoblotting with a polyclonal anti-human LDLR c-terminal, 3143, a polyclonal anti-transferrin receptor (TFR), and polyclonal anti-MT1-MMP (MT1) antibody. **(b) Invitro cleavage assay of rLDLR and rMT1.** Purified MT1-MMP with its pro-domain (Pro-MT1) was preincubated with trypsin in assay buffer for 1h at 37 °C to initiate cleavage of the pro-domain and generate active MT1-MMP (rMT1), the reaction was stopped with AEBSF. rLDLR was then incubated for 1h with or without Pro-MT1/rMT1 at 37 °C in assay buffer. Whole incubation content was subjected to SDS-PAGE and immunoblotting. rLDLR and its cleaved fragments were detected using a monoclonal anti-FLAG antibody, while rMT1 was detected with a polyclonal anti-MT1-MMP (MT1) antibody. **(c) Co-expression of MT1-MMP and LDLR mutants.** HEK293 cells were co-transfected with either the wild-type or mutant LDLR with the wild-type

MT1-MMP. After 48 h, cells were collected. Whole-cell lysates were applied to SDS-PAGE, followed by immunoblotting with a polyclonal anti-human LDLR c-terminal, 3143, a polyclonal anti-actin (Actin), and polyclonal anti-MT1-MMP (MT1) antibody.

Table 5. 1-LDLR Cleavage site prediction by CleavePredict. Indicating cleavage position, residues and position weight matrix score associated with each point of cleavage. Selected Positions highlighted in Red.

P1 cleavage positions	Residues	PWM ^ Score
14	WTV A L-LLAAA	0.54
86	CIPQF-WRCDG	1.94
152	CGPAS-FQCNS	5.51
186	QR C RG-LYVFQ	2.87
397	KAVGS-IAYLF	1.14
400	GSIA Y -LFFTN	3.05
421	SEYTS-LIPNL	2.97
425	SLIPN-LRNVV	2.30
521	SKPRA-IVVDP	4.90
529	DPVHG-FMYWT	5.37
541	GTPAK-IKKGG	1.95
554	VDIYS-LVTEN	1.17
565	QWPNG-ITL D L	5.36
584	SKLHS-ISSID	3.26
608	RLAHP-FSLAV	2.38
610	AHPFS-LAVFE	1.45
645	LLAEN-LLSPE	5.96
657	VLFHN-LTQPR	4.07
685	CLPAP-QINPH	2.54
701	ACPDG-MLLAR	0.81

707	LLARD-MRSCL	1.93
789	SSVRA-LSIVL	7.55

5.2.2 The Catalytic Domain of MT1-MMP is critical for LDLR Shedding

Given the unique functions of the various regions of MT1-MMP, contributing to the overall proteolytic activity of the metalloproteinase, we sort to determine if any region was critical for MT1-MMP-mediated cleavage of LDLR. Hence, deletion of specific regions of MT1-MMP with an HA tag in the hemopexin-like domain of the protein was co-expressed with wild type LDLR in HEK293 cells. The cleavage property was lost with the catalytic region deletion (**fig 5.2**), reinforcing the importance of the catalytic property of the proteinase for LDLR cleavage as earlier revealed from our previous experiment with the catalytically dead E240A mutant of MT1-MMP. In addition, deletions of amino acid residues 163-170 (MT-loop) of the MT1-MMP protein led to a loss of the cleavage property of MT1-MMP even though the protein still retained its catalytic property as indicated by its autocatalysis to generate a 44 KDa fragment of the protein. All other deletion within the MT1-MMP protein did not affect its ability to cleave LDLR. Thus, the catalytic activity and the MT-loop are required for MT1-MMP cleavage of LDLR.

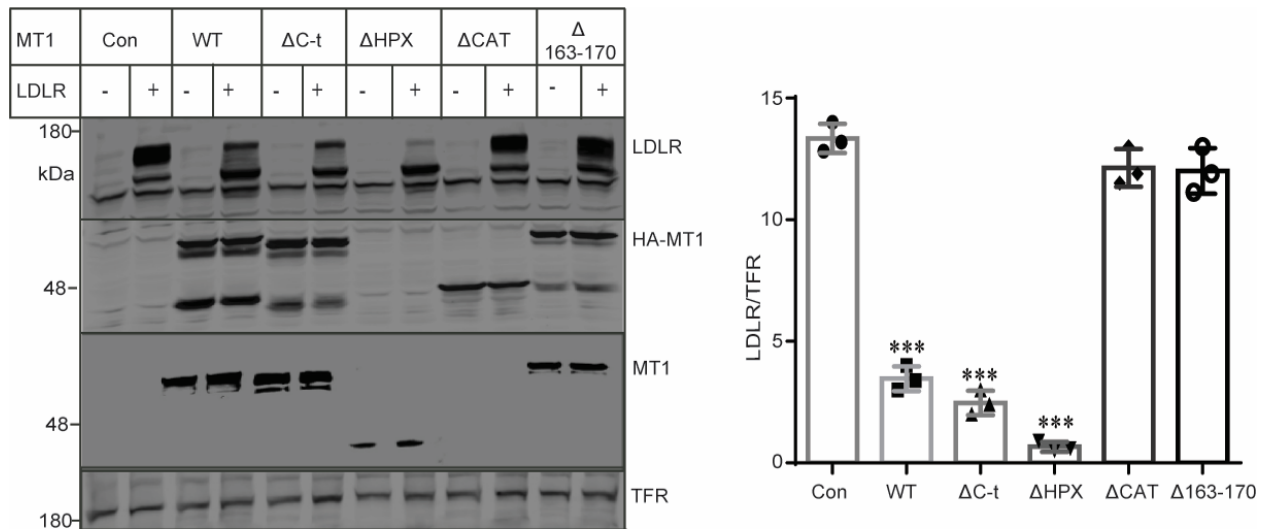


Fig 5. 2. MT1-MMP catalytic region plays a critical role in the cleavage of the LDLR. HEK293 cells were co-transfected with either wild type MT1-MMP or deletion mutants of MT1-MMP with LDLR cDNA. After 48 h, cells were collected. Whole-cell lysates were applied to SDS-PAGE, followed by immunoblotting with a monoclonal anti-human LDLR, HL-1, a polyclonal anti-transferrin receptor (TFR), a monoclonal anti HA (MT1-MMP Hemopexin region) and a monoclonal anti-MT1-MMP (MT1-catalytic region) antibody. Densities were determined using a Licor Odyssey Infrared Imaging System. The relative density is the ratio of the LDLR density to that of the transferrin receptor (TFR) under the same conditions. Values are mean \pm SEM independent triplicate experiments. *** $P < 0.001$ control vs MT1-MMP variants.

5.2.3 MT1-MMP Cleaves Members of the LDLR related Protein Family

Proteins within the LDLR related family share a similar structure, however, the most closely related to the LDLR are VLDLR and APOER2 (LRP8) (He, Semenov, Tamai, & Zeng, 2004). Sequence alignment shows that LDLR shares 59% and 46% homology with VLDLR and ApoER2 respectively (Poirier et al., 2008). Metalloproteinases have been implicated in the shedding of VLDLR to release soluble VLDLR (sVLDLR) into the culture medium from retina cells (Chen, Takahashi, Oka, & Ma, 2016) and in HeLa cells (Marlovits, Abrahamsberg, & Blaas, 1998). Similarly, soluble ApoER2 (sApoER2) from metalloproteinase shedding has been reported (Hoe & Rebeck, 2005). Hence, we investigated if MT1-MMP cleaved VLDLR and APOER2 protein in

a similar mechanism as the LDLR, given their structural similarity. We co-expressed LDLR, VLDLR and APOER2 with MT1-MMP in HEK293 cells. Our result showed that VLDLR and APOER2 were cleaved by MT1-MMP in a dose-dependent manner (**fig 5.3a**), but to a lesser extent compared to LDLR, suggesting that MT1-MMP preferably cleaved LDLR. (**fig 5.3b**).

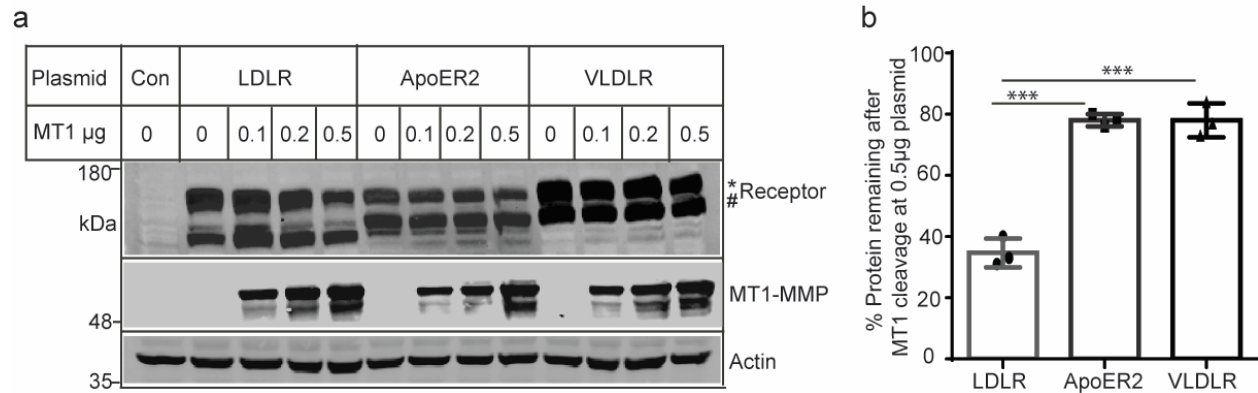


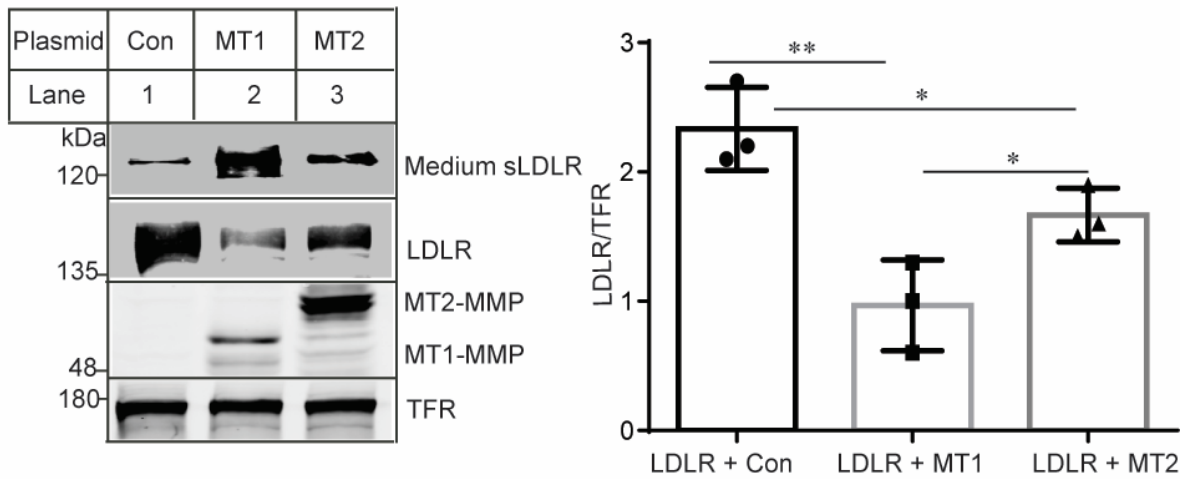
Fig 5. 3. MT1-MMP sheds closely related family members within the LDLR family (a) MT1-MMP cleaves LDLR, ApoER2 and VLDLR. HEK293 cells were co-transfected with either wild type LDLR family protein 0.5 μ g cDNA (LDLR, flag tagged ApoER2 and HA-tagged VLDLR) with varying amounts of MT1-MMP cDNA 0.1, 0.2 and 0.3 μ g in a 12-well plate. After 48 h, cells were collected. Whole-cell lysates were applied to SDS-PAGE, followed by immunoblotting with a polyclonal anti-human LDLR antibody, 3143, polyclonal anti-flag antibody (ApoER2), polyclonal anti-HA antibody (VLDLR), monoclonal anti-MT1-MMP antibody and a polyclonal anti-actin (Actin) antibody. (*) signifies the matured receptor protein of LDLR, ApoER2 and VLDLR after glycosylation of the premature protein (#). **(b) Quantification of the percentage of receptor protein remaining after cleavage**, from the co-transfection experiment of LDLR, ApoER2, VLDLR (0.5 μ g cDNA) and MT1-MMP (0.5 μ g cDNA) in 12 well plate. Values are mean \pm SEM of independent triplicate experiments. ***, $p < 0.001$ LDLR vs ApoER2 and VLDLR

5.2.4 Effect of MT1-MMP related Metalloproteinase on LDLR Cleavage

MT1-MMP is the most studied of the membrane-type matrix metalloproteinase family which consists of MT1, MT2, MT3, MT4, MT5, and MT6- MMP. They share similar structures and

substrates and sometimes can compensate for the loss of each other. This makes it very challenging to develop specific metalloproteinase inhibitors (Fields, 2015). MT2-MMP is the most similar to MT1-MMP with 53% sequence homology, and is appreciably expressed in the liver and hepatoma cells at a level comparable to MT1-MMP; while other MT-MMP's are almost undetectable in the liver (Duarte, Baber, Fujii, & Coito, 2015). To this effect, we investigated the possibility of LDLR shedding by MT2-MMP relative to MT1-MMP shedding of the LDLR protein. We co-expressed LDLR and MT1 or MT2-MMP in Huh7, both metalloproteinases cleaved the LDLR, however, coexpression of MT1-MMP with LDLR showed less cellular receptor than MT2-MMP (**fig 5.4a**). To further confirm this finding, we co-transfected LDLR with different amounts of MT1-MMP or MT2-MMP in HEK293 cells. As shown in Figure 5.4b, both MT1-MMP and MT2-MMP shed LDLR in a dose-dependent manner, however, the shedding effect of MT2-MMP was less than that of MT1-MMP (**fig 5.4b**). Taken together, these data suggest that both MT1 and MT2-MMP can cleave LDLR, however, MT1-MMP has a much higher cleavage efficiency.

a



b

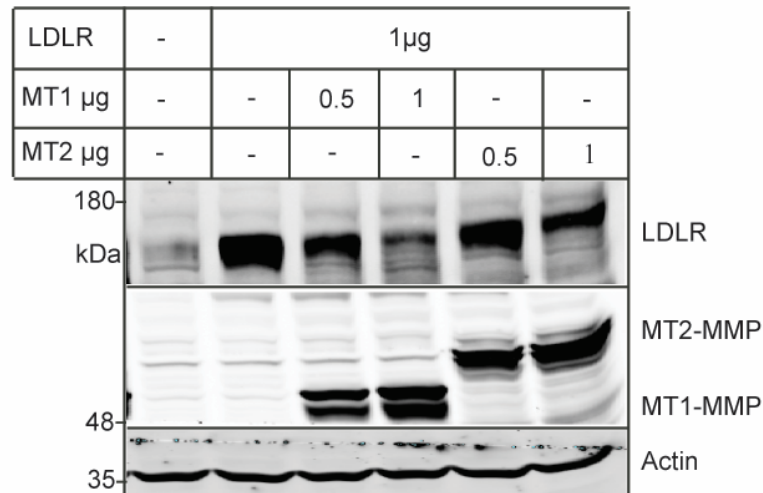


Fig 5. 4. MT2-MMP cleaves the LDLR in a similar fashion as MT1-MMP but to a lower extent. (a) Co-expression of LDLR with MT1 or MT2-MMP. Huh7 cells in 6 well plates, were co-transfected with 1 μ g LDLR and 1 μ g HA-tagged MT1-MMP or HA-tagged MT2-MMP cDNA. After 24 h, the medium was changed to DMEM without FBS for 16 h, after which cells and medium were collected. Whole-cell lysates and medium were applied to SDS-PAGE, followed by immunoblotting with a monoclonal anti-human LDLR, HL-1, polyclonal anti HA antibody (MT1 and MT2) and polyclonal anti-transferrin receptor (TFR). Quantification of the relative densitometry of data includes values of 3 independent experiment mean \pm S.D. *, $p < 0.05$. **, $p < 0.01$. **(b) Dose-dependent cleavage of LDLR by MT1 and MT2-MMP.** HEK293 cells were co-transfected with wild type LDLR and varying amounts of MT1-MMP cDNA 0.5 and 1 μ g in a 6-well plate. Whole-cell lysates were applied to SDS-PAGE, followed by immunoblotting with a monoclonal anti-human LDLR, HL-1, a monoclonal anti-MT1-MMP (MT1) antibody and polyclonal anti-actin (Actin) antibody for loading control. experiments.

5.2.5 A37P mutation in the Pro-domain of MT1-MMP Reduces its ability to cleave LDLR

We identified a variant of MT1-MMP (rs139288377) in the Dallas Heart Study that is significantly associated with plasma LDL-C levels. The average LDL-C levels of 36 people with the variant were about 87 mg/dl, compared with 110 mg/dl in the controls. This variant mutates alanine at position 37 to proline in the pro-domain of MT1-MMP (MT1-A37P). Ala37 is completely conserved in MT1-MMP among different species (Fig. 5.5).

```

Human.          m-spaprppr-clllplltlgtalasalgsaqsssfspeawalqqygylppgdlrrhtqrsp
Chimpanzee.    m-spaprpsr-clllplltlgtalasalgsaqsssfspeawalqqygylppgdlrrhtqrsp
Monkey.        m-spaprpsr-clllplltlgtalasalgstqsstfspeawalqqygylppgdlrrhtqrsp
Gelada.         m-spaprpsr-clllplltlgtalasalgstqsstfspeawalqqygylppgdlrrhtqrsp
Cow.           m-spaprpac-slllpvltlasalasalssaqss-fspeawalqqhgylppgdlrrhtqrsp
Buffalo.       m-spaprpac-slllpvltlasalasalssaqss-fspeawalqqygylppgdlrrhtqrsp
Sheep.         m-spaprpac-slllpvltlasalasalssaqss-fspeawalqqygylppgdlrrhtqrsp
Goat.          m-spaprpac-slllpvltlasalasalssaqss-fspeawalqqygylppgdlrrhtqrsp
Deer.          m-spaprpac-slllpvltlasalasalssaqss-fspeawalqqygylppgdlrrhtqrsp
Fox.           m-spaprpac-slllpvltlasalasalssaqss-fspeawalqqygylppgdlrrhtqrsp
Dog.           m-spaprpac-slllpvltlasalasalssaqss-fspeawalqqygylppgdlrrhtqrsp
Cat.           m-spaprpac-slllpvltlasalasalssaqss-fspeawalqqygylppgdlrrhtqrsp
Horse.         m-spaprpac-slllpvltlasalasalssaqss-fspeawalqqygylppgdlrrhtqrsp
Wild.          m-spaprpac-slllpvltlasalasalssaqss-fspeawalqqygylppgdlrrhtqrsp
Porpoise.      m-slaprpar-slllpvltlasalasalssaqss-fspeawalqqygylppgdlrrhtqrsp
Whale.         m-slaprpar-slllpvltlasalasalssaqss-fspeawalqqygylppgdlrrhtqrsp
Elephant.     m-spaprpar-rlllpvltlasalasalssaqss-fspeawalqqygylppgdlrrhtqrsp
Mouse.         m-spaprpsr-slllpvltlgtalasalgsaqssnfspeawalqqygylppgdlrrhtqrsp
Rat.           m-spaprpsr-slllpvltlgtalasalgsaqssnfspeawalqqygylppgdlrrhtqrsp
Beaver.        m-spsprtsr-slllpvltlgtalasalgsaqssnfspeawalqqygylppgdlrrhtqrsp
Hamster.       m-spaprpsc-flllpvltlgtalasalgsaqssnfspeawalqqygylppgdlrrhtqrsp
Squirrel.     m-spaprpsc-slllpvltlgtalasalgsaqssnfspeawalqqygylppgdlrrhtqrsp
Guinea        m-srgrpr---slllpvltlgtalasalgltqssnfspeawalqqygylppgdlrrhtqrsp
Armadillo.    m-sraprppr-nlllpvltlgtalasalgsaqssnfspeawalqqygylppgdlrrhtqrsp
Rabbit.       m-spaprpsr-rlllpvltlgtalasalgsaqssnfspeawalqqygylppgdlrrhtqrsp
Puma.         m-qehcstsr-----agpratfslslqawalqqygylppgdlrrhtqrsp
Alligator.    m-gps-----llsaglvlgsl--qlgvgdpgfspeawalqqygylppgdlrrhtqrsp
Turtle.       m-spspslap-sllsatlvliall--rgaagdpnfspeawalqqygylppgdlrrhtqrsp
Lizard.       mvgpaargapffrllpllalalsallhptfstsgvspeawalqqygylppgdlrrhtqrsp
Frog.         m-----epltraawicflcscvcssnpskfspeawalqqygylppgdlrrhtlrsp
Cynoglossus. m-----llqlftlasalccftsvsanvlkaqawalqtygylplgdgraqairs
Zebrafish.    m-iwsgftr---llllifvca----hrssskqdmkpeawalqqygylppgdlrrhtarsp
*
.. :**** :**** ** *::: ***

```

Fig 5. 5. Sequence alignment, showing residues 1-58 of MT1-MMP and conservation of alanine (a) at position 37 across a variety of species. * indicate conserved residue within the aligned sequence.

To dissect the potential underlying mechanism, we examined the impact of the mutation on the ability of MT1-MMP to activate pro-MMP2 and cleave LDLR. LDLR and wild type or mutant

MT1-MMP were co-expressed in HEK293 cells. We observed that LDLR abundance in whole cell lysate was reduced and sLDLR levels in culture medium were increased in cells expressing either wild type or mutant MT1-MMP (**fig. 5.6a, lanes 2 and 3 vs 1; fig. 5.6b**). MT1-A37P also retained the ability to activate pro-MMP2 (**fig. 5.6c**). However, MT1-A37P displayed a significantly reduced ability to cleave LDLR and activate pro-MMP2 when compared to wild type MT1-MMP (**fig. 5.6a to 5.6c**). Thus, mutation MT1-A37P that reduces plasma levels of LDL-C in humans significantly decreases the ability of MT1-MMP to cleave LDLR.

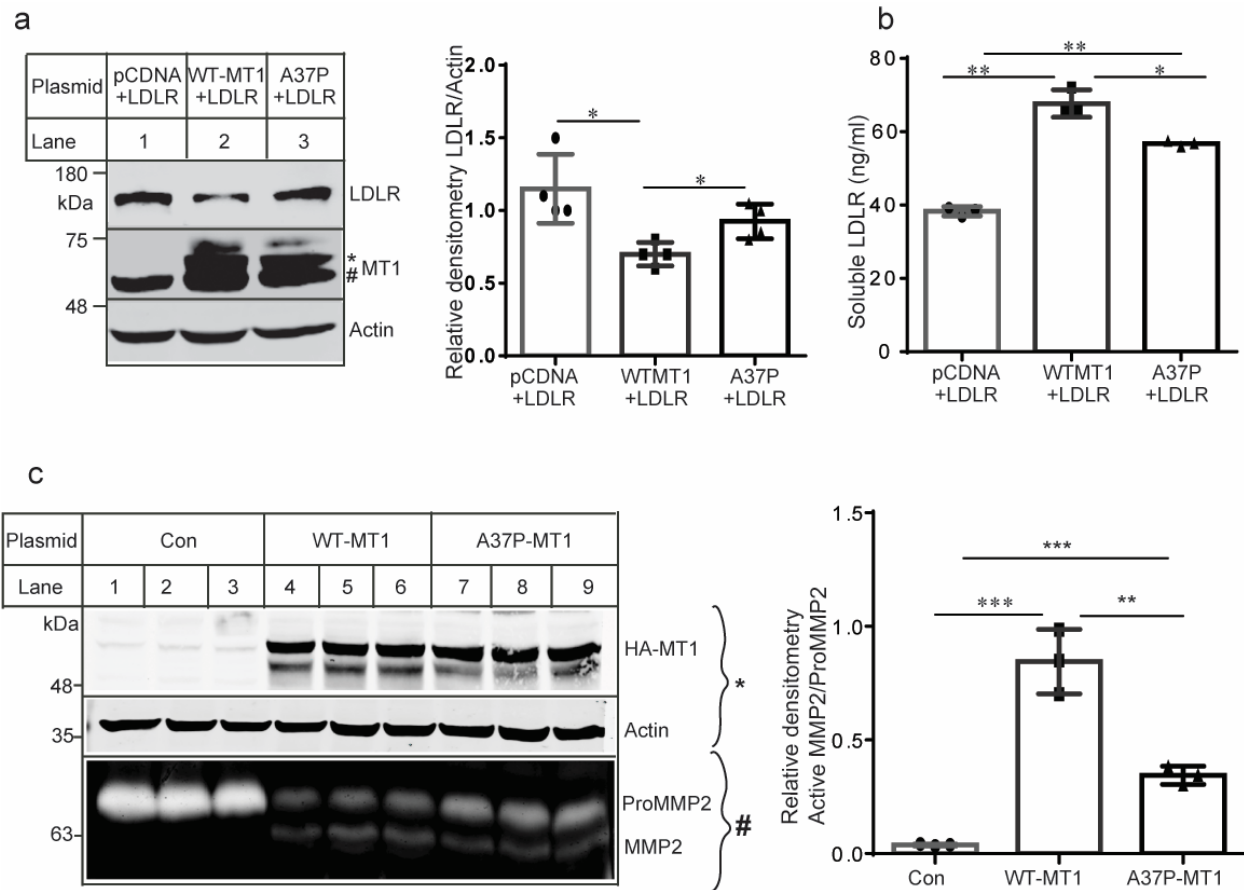


Fig 5. 6. Effect of A37P mutation on MT1-MMP's ability to cleave the LDLR. (a) Co-expression of wild type and A37P LDLR with MT1-MMP. HEK293 cells were co-transfected with a plasmid containing LDLR cDNA and empty pCDNA3.1, plasmid containing wild type (WT) MT1-MMP, or plasmid containing MT1-MMP A37P mutation using Lipofectamine 3000 (1 μ g of total DNA/well of a 12-well plate). 48 h after, whole-cell lysates were prepared and subjected to Western blot. Immunoblotting was done with a monoclonal anti-human LDLR, HL-1, a polyclonal anti-actin (Actin), and a monoclonal anti-MT1-MMP (MT1) antibody. Endogenous (#) and Overexpressed (*) MT1-MMP **(b) Soluble LDLR content.** HEK293 cells were transfected as described in panel a. 24 h after transfection, cells were cultured in serum-free medium overnight. The same amount of culture medium was subjected to sLDLR measurement using the commercial ELISA kit according to the manufacturer's instruction. **(c) Gelatin zymography.** HEK293 cells were transfected with empty, wild type, or mutant A37P MT1-MMP containing plasmid for 36 h. The medium was then changed to serum-free media, and conditioned media was collected over the subsequent 16 h. The same amount of total proteins in medium (80 μ g) was applied to gelatin supplemented SDS-PAGE for later zymography analysis (#), cell lysate was also subjected to immunoblot (*). Quantification of the relative densitometry of data includes values of 3 independent experiment mean \pm S.D. *, p<0.05. **, p<0.01. ***, p<0.001.

5.3 Discussion

MT1-MMP has been known to shed cell surface receptors at multiple sites within their extracellular domain, such as LYVE-1 (Wong et al., 2016) and Syndecan 1&4 (Manon-Jensen, Multhaupt, & Couchman, 2013). Herein, we also found that no particular region abrogated the MT1-MMP-mediated cleavage of the protein, suggesting that the proteolytic effect of MT1-MMP on LDLR is not solely restricted to a particular region of the LDLR. In order to confirm the possibility of multiple cleavage sites on the LDLR, we incubated purified recombinant proteins of MT1-MMP and LDLR *in vitro*. The outcome of the experiment showed that MT1-MMP caused multiple shed bands of LDLR, suggesting multiple cleavage sites on the protein. Consistently, cleavage site prediction by the software CleavePredict identified 22 possible sites in LDLR that are prone to be cleaved by MT1-MMP. Together, these findings suggest the possibility of a multiple site cleavage of the LDLR by MT1-MMP.

The deletion of the regions of MT1-MMP showed that only the catalytic domain of the protein was required for its cleavage of the LDLR. The catalytic region also harbors the MT-loop from amino acid residues 163-170. It has been reported that the loop within the catalytic region interacts with cell surface substrates, its deletion usually leads to MT1-MMP mislocalization relative to β 1-integrins adhesion complexes at the cell surface (Woskowicz, Weaver, Shitomi, Ito, & Itoh, 2013). The deletion of the MT-loop of MT1-MMP led to the loss of its ability to cleave LDLR, even though the protein still retained its catalytic property. This may suggest a role for β 1-integrin adhesion complexes in the MT1-MMP-mediated cleavage of LDLR.

MT1-MMP is an established promiscuous protease with a variety of substrates. Hence, we determined the specificity of MT1-MMP for the LDLR compared to other structurally similar

proteins. Structural close relatives of LDLR within the LDLR-related protein family are ApoER2 and VLDLR. Co-expression of these proteins with MT1-MMP revealed that MT1-MMP cleaved all three receptors, with a more efficient LDLR cleavage compared to others. However, it is yet to be determined if ApoER2 and VLDLR are natural substrates for MT1-MMP because our experiment only considered the overexpression of MT1-MMP, which may cause non-specific cleavage of the proteins. Similarly, MT1-MMP closely related metalloproteinase family member MT2-MMP has been known to share common substrates (proMMP-2, Laminin-1, collagen I and fibrin) with MT1-MMP (Itoh, 2015). Our experiments showed that MT2-MMP had similar cleavage property as MT1-MMP on the LDLR, however, its cleavage of LDLR was to a lesser extent as compared to MT1-MMP. We have also previously reported that MT2-MMP did not compensate for MT1-MMP LDLR cleavage, in our *MT1-MMP* liver-specific knockout mice model. Taken together, this suggests that MT1-MMP targets LDLR with higher specificity and efficiency over MT2-MMP.

Mutation of Ala 37 in the pro-domain of MT1-MMP to Pro (A37P) evidently reduced the ability of the proteinase to cleave LDLR and activate ProMMP2. The primary role of the MT1-MMP pro-domain is to maintain the protein in a latent state. It also functions as an intramolecular chaperone, playing a critical role in the folding and trafficking of the protein (Cao et al., 2000). MT1-MMP protein with a deleted pro-domain or deleted sequence between S34 to T51 within the pro-domain is poorly delivered to the cell surface. The proteinase without a pro-domain arrives at the cell surface as a catalytically inactive form and is unable to bind to TIMP2 (Cao et al., 1998; Pavlaki et al., 2002). Other mutations within the pro-domain and signal peptide such as T17R(Evans et al., 2012) and R111H (Vos et al., 2018) have been reported to reduce the activity of the metalloproteinase. This may explain why a mutation in the pro-domain such as A37P can affect

the overall function of the protein and reduce the ability of MT1-MMP to cleave LDLR. The reduced plasma circulating LDL-C in individuals with A37P mutation may be as a result of an increase in the availability of LDLR due to a partial loss of MT1- MMP's ability to cleave the receptor.

In conclusion, our study has shown that MT1-MMP targets LDLR and cleaves it at multiple sites. This cleavage is mediated by activities within the catalytic domain of the protein. Thus, inhibition of MT1-MMP may serve as a therapeutic target for the treatment of cardiovascular diseases associated with elevated levels of circulating LDL cholesterol.

Chapter 6

Conclusion and Future Directions

6.1 Conclusion

Metalloproteinases have long been implicated in the shedding and release of LDLR ectodomain; broad-spectrum metalloproteinase inhibitors were reported to have increased cell surface LDLR and reduced the availability of sLDLR in culture medium (Begg, Sturrock, & van der Westhuyzen, 2004). Similarly, the FH mutation G805R led to an increase in the amount of sLDLR in HepG2 cells caused by shedding of the protein, facilitated by matrix metalloproteinases (Strøm, Tveten, Laerdahl, & Leren, 2014). Even though metalloproteinases have been implicated in LDLR shedding, the exact protease(s) involved were unknown until recently Bone Morphogenetic Protein-1 (BMP-1) was identified as a metalloproteinase that cleaves Gly171-Asp172 within the linker sequence connecting ligand-binding repeat 4 and 5 of LDLR (Banerjee et al., 2019). Cleavage within this region generates a 120KDa C-terminal fragment protein attached to the membrane with lower LDLR uptake capacity and a 36KDa N-terminal fragment in culture media. The soluble 36KDa LDLR fragment is different from the cleaved extracellular domain reported in cell culture media and plasma (Begg et al., 2004; Mayne et al., 2018). Hence, there must be alternate proteases that mediate this process.

The experiments outlined within this thesis identified MT1-MMP as a key player in the cleavage of the LDLR to release soluble forms into culture media in vitro and plasma in vivo. Our study found that MT1-MMP interacts with the LDLR and cleaves the protein at multiple sites, however, the major cleavage site led to the release of an approximately 120KDa extracellular soluble fragment. Although MT1-MMP mediates its cellular activities either by catalytic or non-catalytic mechanisms (Pahwa, Stawikowski, & Fields, 2014), the shedding of LDLR by MT1-MMP requires its catalytic property. This was underscored by the inability of the catalytically inactive

mutant MT1-MMP E240A to initiate LDLR cleavage and the loss of the cleavage property of the mutant MT1-MMP, in which the catalytic region was deleted.

LDLR plays a critical role in the receptor-mediated clearance of plasma LDL-C, thus functioning as a key player in cholesterol homeostasis (Brown & Goldstein, 1986). LDLR deficiency leads to elevated plasma cholesterol levels (Ishibashi et al., 1993). High levels of circulating cholesterol are pro-atherogenic and increase the risk of atherosclerosis and coronary heart disease (Shepherd & Packard, 1986). Our data showed that MT1-MMP knockdown increased cell surface levels of LDLR with a corresponding increment in LDL uptake capacity in cultured cells. In order to evaluate the therapeutic potential of MT1-MMP in lowering plasma LDL-C, it is critical to understand the pathophysiological role of MT1-MMP in lipid metabolism. *MT1-MMP* null mice could not be used to study the effect of long-term MT1-MMP deficiency on lipid metabolism since they die between 3–4 weeks (Holmbeck et al., 1999). We developed *MT1-MMP* liver-specific knockout mice (*MT1^{LKO}*) to study MT1-MMP's role in lipid metabolism since no liver damage has been reported in *MT1-MMP* null mice and the clearance of circulating LDL-C is mainly mediated through hepatic LDLR (Vance & Vance, 1990). As expected, the deletion of *MT1-MMP* in mice liver led to a significant increase in hepatic LDLR and a significant reduction in levels of plasma sLDLR and LDL-C. Liver-specific overexpression of *MT1-MMP* in *ApoE^{-/-}* mice significantly increased atherosclerotic plaque deposition in the aorta. However, *MT1-MMP* knockdown did not alter plaque area in *ApoE^{-/-}* mice. It is noteworthy that histological quantification of plaque is an assessment limited to the aortic valves and root which does not allow detection of lipid levels in the remainder of the aorta. Cholesterol ester determination in the whole aorta has been shown to be a more reliable assessment criterion in the investigation of atherosclerosis progression in

ApoE^{-/-} mice with *Pcsk9* knockout (Denis et al., 2012). Indeed, the determination of aortic cholesterol ester levels in *ApoE*^{-/-} mice with *MT1-MMP* knockdown showed reduced accumulation of cholesterol ester in the aorta. Thus, MT1-MMP promotes the development of atherosclerosis by cleaving the LDLR.

Current therapies to increase LDLR levels and reduce LDL-C involve statins inhibiting HMG-CoA reductase and inhibition of the LDLR degrader PCSK9. Results from this thesis showed that a combined treatment of *MT1-MMP* knockdown and statin treatment or *Pcsk9* deletion had a combined beneficial lipid-lowering effect in mice. These treatments combined with *MT1-MMP* knockdown led to an additive increase in LDLR and reduction in the levels of total cholesterol in circulation, suggesting that LDLR increment caused by treatment with statin and PCSK9 inhibition is prone to cleavage by MT1-MMP. Thus, combined therapy may be of useful effect given the success accomplished with the combination of statin treatment and PCSK9 monoclonal antibody therapies (Auer & Berent, 2018). Taken together, our findings uncover the fact that MT1-MMP cleaves hepatic LDLR and regulates cholesterol metabolism, thus MT1-MMP could be a target to reduce hypercholesterolemia and the incidence of atherosclerosis.

The emerging sLDLR in circulation resulting from cleavage by proteinases or alternate inefficient splicing of LDLR contains the extracellular ligand-binding repeats of the protein (Begg et al., 2004; Rebeck, LaDu, Estus, Bu, & Weeber, 2006). One of the most profound implications of soluble receptor production is the possibility of a dominant-negative effect, which may compete with the native membrane-tethered receptor for its ligands (Rebeck et al., 2006). Studies have shown a positive correlation between sLDLR and some of its ligands such as LDL and VLDL (Girona et al., 2017; Mayne et al., 2018), which may be as a result of direct binding of the soluble receptor to these ligands, preventing their clearance or reduction of ligand uptake as a result of

Chapter 6: Conclusion and Future Directions

receptor shedding. However, within the context of this thesis, we have been able to ascertain that sLDLR is associated with its ligands in circulation, mostly LDL and VLDL, as well as PCSK9. The association of the soluble receptor to its ligands is able to impair ligand uptake by the native cell surface receptor. This suggests a deleterious phenomenon which may prevent the effective clearance of lipoproteins, especially LDL. It is worth noting, however, that the concentration of sLDLR in humans is in the range of 10-100 ng/ml, which is completely outnumbered by LDL with an average normal concentration of 100-110 mg/dl. This means the binding of sLDLR to LDL will only contribute minimally to the overall clearance efficiency and atherogenicity of LDL.

In summary, this thesis has been able to determine a novel metalloproteinase that cleaves the LDLR and reduces its capacity to take up its ligands, especially LDL, thus highlighting a new role for the metalloproteinase in cholesterol metabolism in addition to its well research function in cancer metastasis.

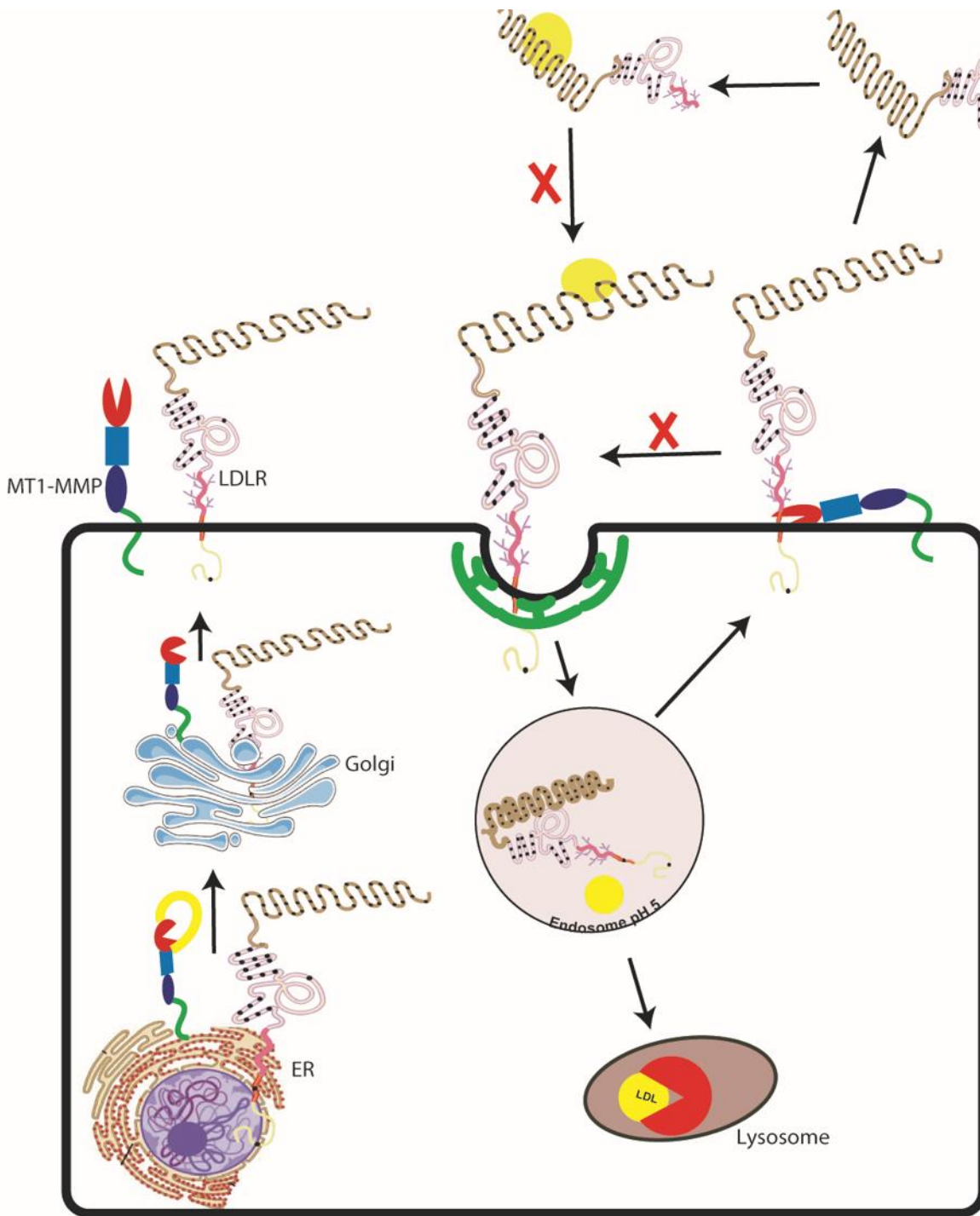


Fig 6. 1. Final Model of proposed MT1-MMP cleavage of the LDLR and fate of sLDLR. MT1-MMP cleavage of the LDLR prevents its uptake of LDL for lysosomal degradation. Cleaved sLDLR binds to LDL and reduces the accessibility of LDL to the cell surface LDLR for clearance. Both pathways ultimately leading to an increased level of circulating lipoproteins.

6.2 Future work

The results generated from experiments within this thesis enhanced our understanding of the shedding of the LDLR, how LDLR shedding regulates cholesterol metabolism and the fate of sLDLR. However, there is cause for further investigation into a few other points:

- **Determination of MT1-MMP cleavage site on the LDLR**

To develop inhibitors that will prevent or reduce MT1-MMP binding to the LDLR, it is essential to identify the cleavage sites of the proteinase on LDLR. Global inhibition of the proteinase is not feasible given other important physiological roles of MT1-MMP; hence only targeted inhibition would be effective. Results from chapter 5 of this thesis suggest multiple cleavage sites on LDLR; our effort to identify the cleavage sites with cleavepredict software was not successful. Similarly, our effort to determine the cleavage site using protein sequence mapping with mass spectrometry was limited by broad peaks developed because of the LDLR heterogenous glycoprotein structure (fig 6.2).

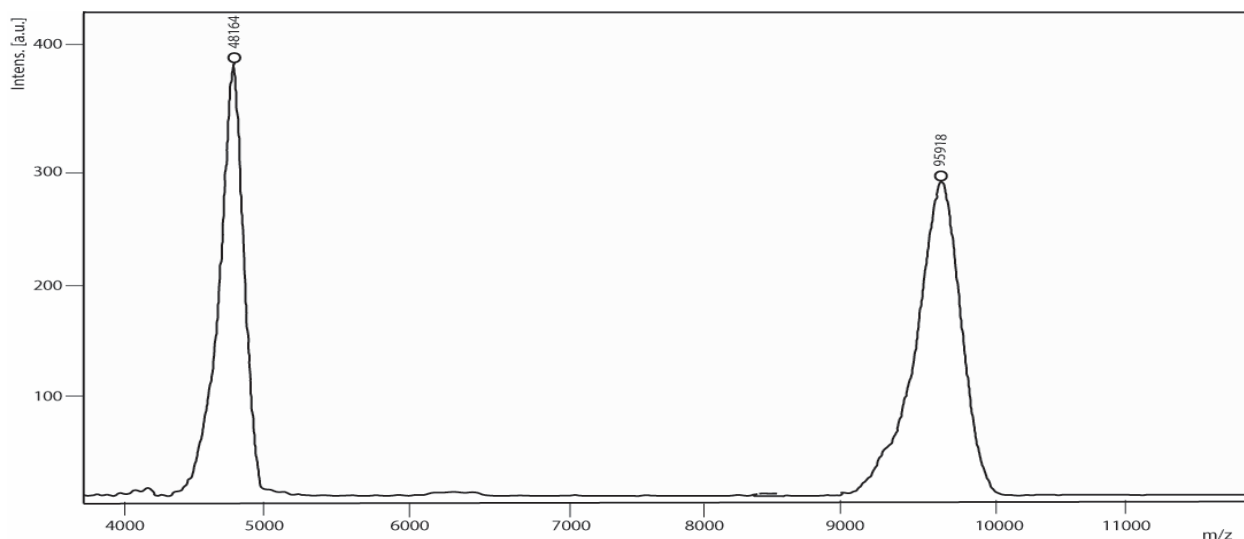


Fig 6. 2. Chromatogram of rLDLR ionization by MALDI-MS. Ionic variants of rLDLR indicated as m/z 48164 (+2) and 95918 (+).

- **Regulation of MT1-MMP cleavage of the LDLR**

Our results show that MT1-MMP cleaves the LDLR. However, further details are required on the regulation of MT1-MMP cleavage of LDLR; if at all it is dependent on the amount of cellular cholesterol available to the cell or other yet to be determined factors. LRP1 a closely related protein to the LDLR is cleaved by MT1-MMP in a process regulated by cellular availability of cholesterol (Dekky et al., 2016). Similarly, cellular cholesterol levels have been reported to regulate the shedding of membrane proteins such as interleukin-6 receptor and CD-30 (Matthews et al., 2003; von Tresckow et al., 2004). In all cases, depletion of cellular cholesterol was shown to increase the shedding of receptor proteins.

- **Clearance of sLDLR from circulation**

Our results show that sLDLR in circulation binds to its ligands in circulation, thus preventing ligand uptake by the membrane-tethered receptor. It is imperative that we understand how the sLDLR-LDL complex is finally cleared from circulation or their proatherogenic effects in the absence of a clearance mechanism by the body.

Bibliography

Ahmad, Z. (2014). Statin intolerance. *American Journal of Cardiology*. Elsevier Inc.

<https://doi.org/10.1016/j.amjcard.2014.02.033>

Aikawa, M., & Libby, P. (2004). The vulnerable atherosclerotic plaque: Pathogenesis and therapeutic approach. *Cardiovascular Pathology*, 13(3), 125–138.

[https://doi.org/10.1016/S1054-8807\(04\)00004-3](https://doi.org/10.1016/S1054-8807(04)00004-3)

Al-Allaf, F. A., Coutelle, C., Waddington, S. N., David, A. L., Harbottle, R., & Themis, M. (2010). LDLR-Gene therapy for familial hypercholesterolaemia: problems, progress, and perspectives. *International Archives of Medicine*, 3, 36. <https://doi.org/10.1186/1755-7682-3-36>

Amălinei, C., Căruntu, I. D., Giușcă, S. E., & Bălan, R. A. (2010). Matrix metalloproteinases involvement in pathologic conditions. *Romanian Journal of Morphology and Embryology = Revue Roumaine de Morphologie et Embryologie*, 51(2), 215–228. Retrieved from <http://www.ncbi.nlm.nih.gov/pubmed/20495735>

Amar, S., Smith, L., & Fields, G. B. (2017, November 1). Matrix metalloproteinase collagenolysis in health and disease. *Biochimica et Biophysica Acta - Molecular Cell Research*. Elsevier B.V. <https://doi.org/10.1016/j.bbamcr.2017.04.015>

Anilkumar, N., Uekita, T., Couchman, J. R., Nagase, H., Seiki, M., & Itoh, Y. (2005). Palmitoylation at Cys574 is essential for MT1-MMP to promote cell migration. *The FASEB Journal*, 19(10), 1326–1328. <https://doi.org/10.1096/fj.04-3651fje>

Anitschkow N, C. S. (1913). Ueber experimentelle Cholester-insteatose und ihre Bedeutung fuer

die Entstehung einiger pathologischer Prozesse. *Zentrbl Allg Pathol Pathol Anat*, 24, 1–9.

Aoki, T., Sato, D., Li, Y., Takino, T., Miyamori, H., & Sato, H. (2005). Cleavage of Apolipoprotein E by Membrane-Type Matrix Metalloproteinase-1 Abrogates Suppression of Cell Proliferation. *Journal of Biochemistry*, 137(1), 95–99.

<https://doi.org/10.1093/jb/mvi009>

Atherosclerosis. Fibrous Plaque Formation In The Artery. Artery.. Royalty Free Cliparts, Vectors, And Stock Illustration. Image 38814972. (n.d.). Retrieved December 20, 2019, from https://www.123rf.com/photo_38814972_stock-vector-atherosclerosis-fibrous-plaque-formation-in-the-artery-artery-wall-thickens-lipid-plaques-forms-with.html?fromid=czNDT1ByU1ITS0VKVmNMcdEamxDdz09

AU - Gallagher, S., & AU - Chakavarti, D. (2008). Immunoblot Analysis. *JoVE*, (16), e759. <https://doi.org/doi:10.3791/759>

Auer, J., & Berent, R. (2018, July 24). Alirocumab as add-on therapy to statins: current evidence and clinical potential. *Therapeutic Advances in Cardiovascular Disease*. SAGE PublicationsSage UK: London, England. <https://doi.org/10.1177/1753944718775352>

Bahitham, W., Watts, R., Nelson, R., Lian, J., & Lehner, R. (2016). Liver-specific expression of carboxylesterase 1g/esterase-x reduces hepatic steatosis, counteracts dyslipidemia and improves insulin signaling. *Biochimica et Biophysica Acta - Molecular and Cell Biology of Lipids*, 1861(5), 482–490. <https://doi.org/10.1016/j.bbalip.2016.03.009>

Banach, M., Rizzo, M., Toth, P. P., Farnier, M., Davidson, M. H., Al-Rasadi, K., ... Mikhailidis, D. P. (2015). Statin intolerance - an attempt at a unified definition. Position paper from an

- International Lipid Expert Panel. *Archives of Medical Science : AMS*, 11(1), 1–23.
<https://doi.org/10.5114/aoms.2015.49807>
- Banerjee, S., Andrew, R. J., Duff, C. J., Fisher, K., Jackson, C. D., Lawrence, C. B., ... Hooper, N. M. (2019). Proteolysis of the low density lipoprotein receptor by bone morphogenetic protein-1 regulates cellular cholesterol uptake. *Scientific Reports*, 9(1).
<https://doi.org/10.1038/s41598-019-47814-0>
- Barbolina, M. V., & Stack, M. S. (2008). Membrane type 1-matrix metalloproteinase: Substrate diversity in pericellular proteolysis. *Seminars in Cell & Developmental Biology*, 19(1), 24–33. <https://doi.org/10.1016/J.SEMCDB.2007.06.008>
- Barnes, R. H., Akama, T., Öhman, M. K., Woo, M.-S., Bahr, J., Weiss, S. J., ... Chun, T. (2017). Membrane-Tethered Metalloproteinase Expressed by Vascular Smooth Muscle Cells Limits the Progression of Proliferative Atherosclerotic Lesions. *Journal of the American Heart Association*, 6(7). <https://doi.org/10.1161/JAHA.116.003693>
- Begg, M. J., Sturrock, E. D., & van der Westhuyzen, D. R. (2004). Soluble LDL-R are formed by cell surface cleavage in response to phorbol esters. *European Journal of Biochemistry / FEBS*, 271(3), 524–533. Retrieved from <http://www.ncbi.nlm.nih.gov/pubmed/14728679>
- Beglova, N., & Blacklow, S. C. (2005). The LDL receptor: how acid pulls the trigger. *Trends in Biochemical Sciences*, 30(6), 309–317. <https://doi.org/10.1016/j.tibs.2005.03.007>
- Benjamin, E. J., Blaha, M. J., Chiuve, S. E., Cushman, M., Das, S. R., Deo, R., ... American Heart Association Statistics Committee and Stroke Statistics Subcommittee, P. (2017). Heart Disease and Stroke Statistics-2017 Update: A Report From the American Heart

- Association. *Circulation*, 135(10), e146–e603.
<https://doi.org/10.1161/CIR.0000000000000485>
- Betters, J. L., & Yu, L. (2010). NPC1L1 and cholesterol transport. *FEBS Letters*, 584(13), 2740–2747. <https://doi.org/10.1016/j.febslet.2010.03.030>
- Biglu, M.-H., Ghavami, M., & Biglu, S. (2016). Cardiovascular diseases in the mirror of science. *Journal of Cardiovascular and Thoracic Research*, 8(4), 158–163.
<https://doi.org/10.15171/jcvtr.2016.32>
- Black, R. A., Rauch, C. T., Kozlosky, C. J., Peschon, J. J., Slack, J. L., Wolfson, M. F., ... Cerretti, D. P. (1997). A metalloproteinase disintegrin that releases tumour-necrosis factor- α from cells. *Nature*, 385(6618), 729–733. <https://doi.org/10.1038/385729a0>
- Boren, J., Lee, I., Zhu, W., Arnold, K., Taylor, S., & Innerarity, T. L. (1998). Identification of the low density lipoprotein receptor-binding site in apolipoprotein B100 and the modulation of its binding activity by the carboxyl terminus in familial defective apo-B100. *The Journal of Clinical Investigation*, 101(5), 1084–1093. <https://doi.org/10.1172/JCI1847>
- Bradfute, D. L., & Simoni, R. D. (1994). Non-sterol compounds that regulate cholesterologenesis. Analogues of farnesyl pyrophosphate reduce 3-hydroxy-3-methylglutaryl-coenzyme A reductase levels. *The Journal of Biological Chemistry*, 269(9), 6645–6650. Retrieved from <http://www.ncbi.nlm.nih.gov/pubmed/8120018>
- Brautbar, A., & Ballantyne, C. M. (2011). Pharmacological strategies for lowering LDL cholesterol: statins and beyond. *Nature Reviews Cardiology*, 8(5), 253–265.
<https://doi.org/10.1038/nrcardio.2011.2>

- Brew, K., & Nagase, H. (2010). The tissue inhibitors of metalloproteinases (TIMPs): An ancient family with structural and functional diversity. *Biochimica et Biophysica Acta (BBA) - Molecular Cell Research*, *1803*(1), 55–71. <https://doi.org/10.1016/j.bbamcr.2010.01.003>
- Brooks, S. A., Schumacher, U., Toth, M., & Fridman, R. (2003). Assessment of Gelatinases (MMP-2 and MMP-9) by Gelatin Zymography. In *Metastasis Research Protocols* (Vol. 57, pp. 163–174). Humana Press. <https://doi.org/10.1385/1-59259-136-1:163>
- Brown, M S, & Goldstein, J. L. (1983). Lipoprotein receptors in the liver. Control signals for plasma cholesterol traffic. *The Journal of Clinical Investigation*, *72*(3), 743–747. <https://doi.org/10.1172/JCI111044>
- Brown, M S, & Goldstein, J. L. (1986). A receptor-mediated pathway for cholesterol homeostasis. *Science*, *232*(4746), 34–47. <https://doi.org/10.1126/science.3513311>
- Brown, M S, & Goldstein, J. L. (2006). Lowering LDL—Not Only How Low, but how long? *Science*, *311*(5768), 1721–1723. <https://doi.org/10.1126/science.1125884>
- Brown, Michael S., & Goldstein, J. L. (2009). Cholesterol feedback: from Schoenheimer’s bottle to Scap’s MELADL. *Journal of Lipid Research*, *50*(Supplement), S15–S27. <https://doi.org/10.1194/jlr.R800054-JLR200>
- Brown, Michael S., Herz, J., & Goldstein, J. L. (1997). Calcium cages, acid baths and recycling receptors. *Nature*, *388*(6643), 629–630. <https://doi.org/10.1038/41672>
- Butler, G. S., Butler, M. J., Atkinson, S. J., Will, H., Tamura, T., Van Westrum, S. S., ... Murphy, G. (1998). The TIMP2 membrane type 1 metalloproteinase “receptor” regulates the concentration and efficient activation of progelatinase A. A kinetic study. *Journal of*

- Biological Chemistry*, 273(2), 871–880. <https://doi.org/10.1074/jbc.273.2.871>
- Cameron, J., Holla, Ø. L., Ranheim, T., Kulseth, M. A., Berge, K. E., & Leren, T. P. (2006). Effect of mutations in the PCSK9 gene on the cell surface LDL receptors. *Human Molecular Genetics*, 15(9), 1551–1558. <https://doi.org/10.1093/hmg/ddl077>
- Cao, J., Drews, M., Lee, H. M., Conner, C., Bahou, W. F., Zucker, S., & Mt-mmp, M. U. (1998). The Propeptide Domain of Membrane Type 1 Matrix Metalloproteinase Is Required for Binding of Tissue Inhibitor of Metalloproteinases and for Activation of Pro-gelatinase A *. *The Journal of Biological Chemistry*, 273(52), 34745–34752.
- Cao, J., Hymowitz, M., Conner, C., Bahou, W. F., Zucker, S., Cao, C.-, & Chem, S. J. B. (2000). The Propeptide Domain of Membrane Type 1-Matrix Metalloproteinase Acts as an Intramolecular Chaperone when Expressed in trans with the Mature Sequence in COS-1 Cells * function of the membrane-bound enzyme in transfected. *The Journal of Biological Chemistry*, 275(38), 29648–29653. <https://doi.org/10.1074/jbc.M001920200>
- Cerofolini, L., Amar, S., Lauer, J. L., Martelli, T., Fragai, M., Luchinat, C., & Fields, G. B. (2016). Bilayer Membrane Modulation of Membrane Type 1 Matrix Metalloproteinase (MT1-MMP) Structure and Proteolytic Activity. *Scientific Reports*, 6(1), 29511. <https://doi.org/10.1038/srep29511>
- Chen, Q., Takahashi, Y., Oka, K., & Ma, J.-X. (2016a). Functional Differences of Very-Low-Density Lipoprotein Receptor Splice Variants in Regulating Wnt Signaling. *Molecular and Cellular Biology*, 36(20), 2645–2654. <https://doi.org/10.1128/mcb.00235-16>
- Chen, Q., Takahashi, Y., Oka, K., & Ma, J. (2016b). Functional Differences of Very-Low-

- Density Lipoprotein Receptor Splice Variants in Regulating Wnt Signaling. *Molecular and Cellular Biology*, 36(20), 2645–2654. <https://doi.org/10.1128/mcb.00235-16>
- Choi, S., Aljakna, A., Srivastava, U., Peterson, B. R., Deng, B., Prat, A., & Korstanje, R. (2013). Decreased APOE-containing HDL subfractions and cholesterol efflux capacity of serum in mice lacking Pcsk9. *Lipids in Health and Disease*, 12(1), 112. <https://doi.org/10.1186/1476-511X-12-112>
- Chorba, J. S., Galvan, A. M., & Shokat, K. M. (2018). Stepwise processing analyses of the single-turnover PCSK9 protease reveal its substrate sequence specificity and link clinical genotype to lipid phenotype. *Journal of Biological Chemistry*, 293(6), 1875–1886. <https://doi.org/10.1074/jbc.RA117.000754>
- Chow, A. K., Cena, J., & Schulz, R. (2007). Acute actions and novel targets of matrix metalloproteinases in the heart and vasculature. *British Journal of Pharmacology*, 152(2), 189–205. <https://doi.org/10.1038/sj.bjp.0707344>
- Cooper, A. D. (1997). Hepatic uptake of chylomicron remnants. *Journal of Lipid Research*, 38(11), 2173–2192. Retrieved from <http://www.ncbi.nlm.nih.gov/pubmed/9392416>
- Daugherty, A., & Whitman, S. C. (2003). Quantification of atherosclerosis in mice. *Methods in Molecular Biology*, 209, 293–309. <https://doi.org/10.1385/1-59259-340-2:293>
- Davis, C. Geoffrey, Goldstein, J. L., Südhof, T. C., Anderson, R. G. W., Russell, D. W., & Brown, M. S. (1987). Acid-dependent ligand dissociation and recycling of LDL receptor mediated by growth factor homology region. *Nature*, 326(6115), 760–765. <https://doi.org/10.1038/326760a0>

- Davis, C. Geoffrey, Lehrman, M. A., Russell, D. W., Anderson, R. G. W., Brown, M. S., & Goldstein, J. L. (1986). The J. D. mutation in familial hypercholesterolemia: Amino acid substitution in cytoplasmic domain impedes internalization of LDL receptors. *Cell*, *45*(1), 15–24. [https://doi.org/10.1016/0092-8674\(86\)90533-7](https://doi.org/10.1016/0092-8674(86)90533-7)
- Davis, C G, Elhammer, A., Russell, D. W., Schneider, W. J., Kornfeld, S., Brown, M. S., & Goldstein, J. L. (1986). Deletion of clustered O-linked carbohydrates does not impair function of low density lipoprotein receptor in transfected fibroblasts. *The Journal of Biological Chemistry*, *261*(6), 2828–2838. Retrieved from <http://www.ncbi.nlm.nih.gov/pubmed/3005267>
- Davis, G., Driel, V. I., Russell, D., Brown, M., & Goldstein, J. (1987). The low density lipoprotein receptor. Identification of amino acids in cytoplasmic domain required for rapid endocytosis. *Journal of Biological Chemistry*, *262*(9), 4075–4082. Retrieved from <http://www.jbc.org/content/262/9/4075.full.pdf>
- Decaneto, E., Vasilevskaya, T., Kutin, Y., Ogata, H., Grossman, M., Sagi, I., ... Cox, N. (2017). Solvent water interactions within the active site of the membrane type I matrix metalloproteinase. *Physical Chemistry Chemical Physics*, *19*(45), 30316–30331. <https://doi.org/10.1039/C7CP05572B>
- Dekky, B., Wahart, A., Sartelet, H., Féré, M., Angiboust, J.-F., Dedieu, S., ... Emonard, H. (2016). Cellular Cholesterol Distribution Influences Proteolytic Release of the LRP-1 Ectodomain. *Frontiers in Pharmacology*, *7*(FEB), 25. <https://doi.org/10.3389/fphar.2016.00025>
- Denis, M., Marcinkiewicz, J., Zaid, A., Gauthier, D., Poirier, S., Lazure, C., ... Prat, A. (2012).

Gene inactivation of proprotein convertase subtilisin/kexin type 9 reduces atherosclerosis in mice. *Circulation*, 125(7), 894–901.

<https://doi.org/10.1161/CIRCULATIONAHA.111.057406>

Deryugina, E. I., Bourdon, M. A., Jungwirth, K., Smith, J. W., & Strongin, A. Y. (2000).

Functional activation of integrin alpha V beta 3 in tumor cells expressing membrane-type 1 matrix metalloproteinase. *International Journal of Cancer*, 86(1), 15–23.

[https://doi.org/10.1002/\(sici\)1097-0215\(20000401\)86:1<15::aid-ijc3>3.0.co;2-b](https://doi.org/10.1002/(sici)1097-0215(20000401)86:1<15::aid-ijc3>3.0.co;2-b)

Dixon, D. L., Pamulapati, L. G., Bucheit, J. D., Sisson, E. M., Smith, S. R., Kim, C. J., ... Pozen, J. (2019). Recent Updates on the Use of PCSK9 Inhibitors in Patients with Atherosclerotic

Cardiovascular Disease. *Current Atherosclerosis Reports*, 21(5), 16.

<https://doi.org/10.1007/s11883-019-0778-6>

Duarte, S., Baber, J., Fujii, T., & Coito, A. J. (2015). Matrix metalloproteinases in liver injury, repair and fibrosis. *Matrix Biology*. NIH Public Access.

<https://doi.org/10.1016/j.matbio.2015.01.004>

Eberlé, D., Hegarty, B., Bossard, P., Ferré, P., & Foufelle, F. (2004). SREBP transcription factors: master regulators of lipid homeostasis. *Biochimie*, 86(11), 839–848.

<https://doi.org/10.1016/J.BIOCHI.2004.09.018>

Endo, K., Takino, T., Miyamori, H., Kinsen, H., Yoshizaki, T., Furukawa, M., & Sato, H.

(2003). Cleavage of Syndecan-1 by Membrane Type Matrix Metalloproteinase-1 Stimulates Cell Migration. *Journal of Biological Chemistry*, 278(42), 40764–40770.

<https://doi.org/10.1074/jbc.M306736200>

- Esper, R. J., & Nordaby, R. A. (2019). Cardiovascular events, diabetes and guidelines: the virtue of simplicity. *Cardiovascular Diabetology*, *18*(1), 42. <https://doi.org/10.1186/s12933-019-0844-y>
- Evans, B. R., Mosig, R. A., Lobl, M., Martignetti, C. R., Camacho, C., Grum-tokars, V., ... Martignetti, J. A. (2012). Mutation of Membrane Type-1 Metalloproteinase , MT1-MMP , Causes the Multicentric Osteolysis and Arthritis Disease Winchester Syndrome. *The American Journal of Human Genetics*, *91*(3), 572–576. <https://doi.org/10.1016/j.ajhg.2012.07.022>
- Fairoozy, R. H. (2018). *Genetic functional studies of low density lipoprotein-cholesterol (LDL-C) associated variants and the genetic spectrum of familial hypercholesterolemia in different ethnic groups*. UCL (University College London). Retrieved from <https://ethos.bl.uk/OrderDetails.do?did=1&uin=uk.bl.ethos.747249>
- Feinberg, T. Y., Zheng, H., Liu, R., Wicha, M. S., Yu, S. M., & Weiss, S. J. (2018). Divergent Matrix-Remodeling Strategies Distinguish Developmental from Neoplastic Mammary Epithelial Cell Invasion Programs. *Developmental Cell*, *47*(2), 145-160.e6. <https://doi.org/10.1016/j.devcel.2018.08.025>
- Feingold, K. R., & Grunfeld, C. (2000). *Introduction to Lipids and Lipoproteins*. Endotext. MDText.com, Inc. Retrieved from <http://www.ncbi.nlm.nih.gov/pubmed/26247089>
- Fernandez-Garcia, B., Eiró, N., Marín, L., González-Reyes, S., González, L. O., Lamelas, M. L., & Vizoso, F. J. (2014). Expression and prognostic significance of fibronectin and matrix metalloproteases in breast cancer metastasis. *Histopathology*, *64*(4), 512–522. <https://doi.org/10.1111/his.12300>

- Fielding, C. J., & Fielding, P. E. (1995). Molecular physiology of reverse cholesterol transport. *Journal of Lipid Research*, *36*(2), 211–228. Retrieved from <http://www.ncbi.nlm.nih.gov/pubmed/7751809>
- Fielding, C. J., Shore, V. G., & Fielding, P. E. (1972). A protein cofactor of lecithin:Cholesterol acyltransferase. *Biochemical and Biophysical Research Communications*, *46*(4), 1493–1498. [https://doi.org/10.1016/0006-291X\(72\)90776-0](https://doi.org/10.1016/0006-291X(72)90776-0)
- Fields, G. B. (2015). New strategies for targeting matrix metalloproteinases. *Matrix Biology*, *44–46*, 239–246. <https://doi.org/10.1016/j.matbio.2015.01.002>
- Fischer, D. G., Tal, N., Novick, D., Barak, S., & Rubinstein, M. (1993). An antiviral soluble form of the LDL receptor induced by interferon. *Science*, *262*(5131), 250–253. <https://doi.org/10.1126/science.8211145>
- Fisher, C., Abdul-Aziz, D., & Blacklow, S. C. (2004). A Two-Module Region of the Low-Density Lipoprotein Receptor Sufficient for Formation of Complexes with Apolipoprotein E Ligands. *Biochemistry*, *43*(4), 1037–1044. <https://doi.org/10.1021/bi035529y>
- Fisher, T. S., Lo Surdo, P., Pandit, S., Mattu, M., Santoro, J. C., Wisniewski, D., ... Sitlani, A. (2007). Effects of pH and low density lipoprotein (LDL) on PCSK9-dependent LDL receptor regulation. *The Journal of Biological Chemistry*, *282*(28), 20502–20512. <https://doi.org/10.1074/jbc.M701634200>
- Folch, J., Lees, M., & Sloane Stanley, G. H. (1957). A simple method for the isolation and purification of total lipides from animal tissues. *The Journal of Biological Chemistry*, *226*(1), 497–509. <https://doi.org/10.3989/scimar.2005.69n187>

- Garcia-Touchard, A., Henry, T. D., Sangiorgi, G., Spagnoli, L. G., Mauriello, A., Conover, C., & Schwartz, R. S. (2005). Extracellular Proteases in Atherosclerosis and Restenosis. *Arteriosclerosis, Thrombosis, and Vascular Biology*, 25(6), 1119–1127. <https://doi.org/10.1161/01.ATV.0000164311.48592.da>
- Gent, J., & Braakman, I. (2004). Low-density lipoprotein receptor structure and folding. *Cellular and Molecular Life Sciences*, 61(19–20), 2461–2470. <https://doi.org/10.1007/s00018-004-4090-3>
- Girona, J., Rodríguez-Borjabad, C., Ibarretxe, D., Heras, M., Amigo, N., Feliu, A., ... Zabala, E. (2017). Plasma inducible degrader of the LDLR, soluble low-density lipoprotein receptor, and proprotein convertase subtilisin/kexin type 9 levels as potential biomarkers of familial hypercholesterolemia in children. *Journal of Clinical Lipidology*. <https://doi.org/10.1016/j.jacl.2017.10.003>
- Go, G.-W., & Mani, A. (2012). Low-density lipoprotein receptor (LDLR) family orchestrates cholesterol homeostasis. *The Yale Journal of Biology and Medicine*, 85(1), 19–28. Retrieved from <http://www.ncbi.nlm.nih.gov/pubmed/22461740>
- Goldstein, J L, & Brown, M. S. (1974). Binding and degradation of low density lipoproteins by cultured human fibroblasts. Comparison of cells from a normal subject and from a patient with homozygous familial hypercholesterolemia. *The Journal of Biological Chemistry*, 249(16), 5153–5162. Retrieved from <http://www.ncbi.nlm.nih.gov/pubmed/4368448>
- Goldstein, Joseph L., & Brown, M. S. (2009). The LDL receptor. *Arteriosclerosis, Thrombosis, and Vascular Biology*, 29(4), 431–438. <https://doi.org/10.1161/ATVBAHA.108.179564>

- Goldstein, Joseph L., & Brown, M. S. (2015, March 26). A century of cholesterol and coronaries: From plaques to genes to statins. *Cell*. Cell Press.
<https://doi.org/10.1016/j.cell.2015.01.036>
- Goldstein, Joseph L., Brown, M. S., Anderson, R. G. W., Russell, D. W., & Schneider, W. J. (1985). Receptor-Mediated Endocytosis: Concepts Emerging from the LDL Receptor System. *Annual Review of Cell Biology*, 1(1), 1–39.
<https://doi.org/10.1146/annurev.cb.01.110185.000245>
- Goldstein, Joseph L., & Brown, M. S. (2009). The LDL receptor. *Arteriosclerosis, Thrombosis, and Vascular Biology*, 29(4), 431–438. <https://doi.org/10.1161/ATVBAHA.108.179564>
- Gross, J., & Lapiere, C. M. (1962). Collagenolytic activity in amphibian tissues: a tissue culture assay. *Proceedings of the National Academy of Sciences of the United States of America*, 48(6), 1014–1022. <https://doi.org/10.1073/pnas.48.6.1014>
- Gross, J., & Nagai, Y. (1965). Specific degradation of the collagen molecule by tadpole collagenolytic enzyme. *Proceedings of the National Academy of Sciences*, 54(4), 1197–1204. <https://doi.org/10.1073/pnas.54.4.1197>
- Gu, H. M., Adijiang, A., Mah, M., & Zhang, D. W. (2013). Characterization of the role of EGF-A of low density lipoprotein receptor in PCSK9 binding. *Journal of Lipid Research*, 54(12), 3345–3357. <https://doi.org/10.1194/jlr.M041129>
- Gu, H., Wang, F., Alabi, A., Deng, S., Qin, S., & Zhang, D. (2016). Identification of an Amino Acid Residue Critical for Plasma Membrane Localization of ATP-Binding Cassette Transporter G1--Brief Report. *Arteriosclerosis, Thrombosis, and Vascular Biology*, 36(2),

253–255. <https://doi.org/10.1161/ATVBAHA.115.306592>

Guo, L., Eisenman, J. R., Mahimkar, R. M., Peschon, J. J., Paxton, R. J., Black, R. A., & Johnson, R. S. (2002). A proteomic approach for the identification of cell-surface proteins shed by metalloproteases. *Molecular & Cellular Proteomics : MCP*, *1*(1), 30–36.

<https://doi.org/10.1074/mcp.M100020-MCP200>

Haas, T. L., Stitelman, D., Davis, S. J., Apte, S. S., & Madri, J. A. (1999). Egr-1 mediates extracellular matrix-driven transcription of membrane type 1 matrix metalloproteinase in endothelium. *The Journal of Biological Chemistry*, *274*(32), 22679–22685.

<https://doi.org/10.1074/jbc.274.32.22679>

He, X., Semenov, M., Tamai, K., & Zeng, X. (2004). LDL receptor-related proteins 5 and 6 in Wnt/beta-catenin signaling: arrows point the way. *Development (Cambridge, England)*, *131*(8), 1663–1677. <https://doi.org/10.1242/dev.01117>

Hevonoja, T., Pentikäinen, M. O., Hyvönen, M. T., Kovanen, P. T., & Ala-Korpela, M. (2000). Structure of low density lipoprotein (LDL) particles: Basis for understanding molecular changes in modified LDL. *Biochimica et Biophysica Acta (BBA) - Molecular and Cell Biology of Lipids*, *1488*(3), 189–210. [https://doi.org/10.1016/S1388-1981\(00\)00123-2](https://doi.org/10.1016/S1388-1981(00)00123-2)

Hiraoka, N., Allen, E., Apel, I. J., Gyetko, M. R., & Weiss, S. J. (1998). Matrix metalloproteinases regulate neovascularization by acting as pericellular fibrinolysins. *Cell*, *95*(3), 365–377. [https://doi.org/10.1016/s0092-8674\(00\)81768-7](https://doi.org/10.1016/s0092-8674(00)81768-7)

Hobbs, H. H., Russell, D. W., Brown, M. S., & Goldstein, J. L. (1990). The LDL Receptor Locus in Familial Hypercholesterolemia: Mutational Analysis of a Membrane Protein. *Annual*

Review of Genetics, 24(1), 133–170. <https://doi.org/10.1146/annurev.ge.24.120190.001025>

Hoe, H.-S., & Rebeck, G. W. (2005). Regulation of ApoE receptor proteolysis by ligand binding.

Molecular Brain Research, 137(1–2), 31–39.

<https://doi.org/10.1016/J.MOLBRAINRES.2005.02.013>

Holmbeck, K., Bianco, P., Caterina, J., Yamada, S., Kromer, M., Kuznetsov, S. A., ... Birkedal-

Hansen, H. (1999). MT1-MMP-deficient mice develop dwarfism, osteopenia, arthritis, and connective tissue disease due to inadequate collagen turnover. *Cell*, 99(1), 81–92.

[https://doi.org/10.1016/s0092-8674\(00\)80064-1](https://doi.org/10.1016/s0092-8674(00)80064-1)

Holmbeck, Kenn, Bianco, P., Caterina, J., Yamada, S., Kromer, M., Kuznetsov, S. A., ...

Birkedal-Hansen, H. (1999). MT1-MMP-deficient mice develop dwarfism, osteopenia, arthritis, and connective tissue disease due to inadequate collagen turnover. *Cell*, 99(1), 81–

92. [https://doi.org/10.1016/S0092-8674\(00\)80064-1](https://doi.org/10.1016/S0092-8674(00)80064-1)

Horton, J. D., Shah, N. A., Warrington, J. A., Anderson, N. N., Park, S. W., Brown, M. S., &

Goldstein, J. L. (2003). Combined analysis of oligonucleotide microarray data from transgenic and knockout mice identifies direct SREBP target genes. *Proceedings of the National Academy of Sciences*, 100(21), 12027–12032.

<https://doi.org/10.1073/pnas.1534923100>

Huang, G. (2012). Biotinylation of Cell Surface Proteins. *BIO-PROTOCOL*, 2(9).

<https://doi.org/10.21769/bioprotoc.170>

Hypercholesterolemia - Wikipedia. (n.d.). Retrieved December 20, 2019, from

<https://en.wikipedia.org/wiki/Hypercholesterolemia>

- Innerarity, T. L. (2002). LDL Receptor's β -Propeller Displaces LDL. *Science*, 298(5602), 2337–2339. <https://doi.org/10.1126/science.1080669>
- Ishibashi, S, Brown, M. S., Goldstein, J. L., Gerard, R. D., Hammer, R. E., & Herz, J. (1993). Hypercholesterolemia in low density lipoprotein receptor knockout mice and its reversal by adenovirus-mediated gene delivery. *The Journal of Clinical Investigation*, 92(2), 883–893. <https://doi.org/10.1172/JCI116663>
- Ishibashi, Shun, Schwarz, M., Philip, F., Joachim, H., & David, R. (1996). Disruption of cholesterol 7 α -hydroxylase gene in mice. *Journal of Biological Chemistry*, 271(30), 18017–18023. Retrieved from <http://www.jbc.org/content/271/30/18024.short%5Cnpapers://a66046c0-dbb4-40a6-bbd3-742e9e241be6/Paper/p9336>
- Itoh, Y., Takamura, A., Ito, N., Maru, Y., Sato, H., Suenaga, N., ... Seiki, M. (2001). Homophilic complex formation of MT1-MMP facilitates proMMP-2 activation on the cell surface and promotes tumor cell invasion. *The EMBO Journal*, 20(17), 4782–4793. <https://doi.org/10.1093/emboj/20.17.4782>
- Itoh, Y, & Seiki, M. (2004). MT1-MMP: an enzyme with multidimensional regulation. *Trends in Biochemical Sciences*, 29(6), 285–289. <https://doi.org/10.1016/j.tibs.2004.04.001>
- Itoh, Yoshifumi. (2015). Membrane-type matrix metalloproteinases: Their functions and regulations. *Matrix Biology*, 44–46, 207–223. <https://doi.org/10.1016/j.matbio.2015.03.004>
- Itoh, Yoshifumi, Ito, N., Nagase, H., & Seiki, M. (2008). The second dimer interface of MT1-MMP, the transmembrane domain, is essential for ProMMP-2 activation on the cell surface.

The Journal of Biological Chemistry, 283(19), 13053–13062.

<https://doi.org/10.1074/jbc.M709327200>

Jabłońska-Trypuć, A., Matejczyk, M., & Rosochacki, S. (2016). Matrix metalloproteinases (MMPs), the main extracellular matrix (ECM) enzymes in collagen degradation, as a target for anticancer drugs. *Journal of Enzyme Inhibition and Medicinal Chemistry*, 31(sup1), 177–183. <https://doi.org/10.3109/14756366.2016.1161620>

Janowski, B. A., Grogan, M. J., Jones, S. A., Wisely, G. B., Kliewer, S. A., Corey, E. J., & Mangelsdorf, D. J. (1999). Structural requirements of ligands for the oxysterol liver X receptors LXR and LXR. *Proceedings of the National Academy of Sciences*, 96(1), 266–271. <https://doi.org/10.1073/pnas.96.1.266>

Jia, L., Betters, J. L., & Yu, L. (2011). Niemann-Pick C1-Like 1 (NPC1L1) Protein in Intestinal and Hepatic Cholesterol Transport. *Annual Review of Physiology*, 73(1), 239–259. <https://doi.org/10.1146/annurev-physiol-012110-142233>

Johnson, J. L., Sala-Newby, G. B., Ismail, Y., Aguilera, C. M., & Newby, A. C. (2008). Low Tissue Inhibitor of Metalloproteinases 3 and High Matrix Metalloproteinase 14 Levels Defines a Subpopulation of Highly Invasive Foam-Cell Macrophages. *Arteriosclerosis, Thrombosis, and Vascular Biology*, 28(9), 1647–1653. <https://doi.org/10.1161/ATVBAHA.108.170548>

Jonas, A. (1991). Lecithin-cholesterol acyltransferase in the metabolism of high-density lipoproteins. *Biochimica et Biophysica Acta (BBA) - Lipids and Lipid Metabolism*, 1084(3), 205–220. [https://doi.org/10.1016/0005-2760\(91\)90062-M](https://doi.org/10.1016/0005-2760(91)90062-M)

- Kerr, A. (2016). *Novel molecular therapies for the treatment of familial hypercholesterolaemia*. University of Oxford. Retrieved from <https://ethos.bl.uk/OrderDetails.do?did=1&uin=uk.bl.ethos.730178>
- Keyel, P. A., Mishra, S. K., Roth, R., Heuser, J. E., Watkins, S. C., & Traub, L. M. (2006). A single common portal for clathrin-mediated endocytosis of distinct cargo governed by cargo-selective adaptors. *Molecular Biology of the Cell*, 17(10), 4300–4317. <https://doi.org/10.1091/mbc.e06-05-0421>
- Khalil, M. F., Wagner, W. D., & Goldberg, I. J. (2004). Molecular interactions leading to lipoprotein retention and the initiation of atherosclerosis. *Arteriosclerosis, Thrombosis, and Vascular Biology*, 24(12), 2211–2218. <https://doi.org/10.1161/01.ATV.0000147163.54024.70>
- Kim, K., Goldberg, I. J., Graham, M. J., Sundaram, M., Bertaggia, E., Lee, S. X., ... Pajvani, U. B. (2018). γ -Secretase Inhibition Lowers Plasma Triglyceride-Rich Lipoproteins by Stabilizing the LDL Receptor. *Cell Metabolism*, 27(4), 816-827.e4. <https://doi.org/10.1016/J.CMET.2018.02.010>
- Kishimoto, N., Iga, N., Yamamoto, K., Takamune, N., & Misumi, S. (2017). Virion-incorporated alpha-enolase suppresses the early stage of HIV-1 reverse transcription. *Biochemical and Biophysical Research Communications*, 484(2), 278–284. <https://doi.org/10.1016/j.bbrc.2017.01.096>
- Klose, A., Zigrino, P., & Mauch, C. (2013). Monocyte/macrophage MMP-14 modulates cell infiltration and T-cell attraction in contact dermatitis but not in murine wound healing. *American Journal of Pathology*, 182(3), 755–764.

<https://doi.org/10.1016/j.ajpath.2012.11.028>

- Knäuper, V., Will, H., López-Otin, C., Smith, B., Atkinson, S. J., Stanton, H., ... Murphy, G. (1996). Cellular Mechanisms for Human Procollagenase-3 (MMP-13) Activation. *Journal of Biological Chemistry*, 271(29), 17124–17131. <https://doi.org/10.1074/jbc.271.29.17124>
- Koch, S., Strasser, V., Hauser, C., Fasching, D., Brandes, C., Bajari, T. M., ... Nimpf, J. (2002). A secreted soluble form of ApoE receptor 2 acts as a dominant-negative receptor and inhibits Reelin signaling. *EMBO Journal*, 21(22), 5996–6004. <https://doi.org/10.1093/emboj/cdf599>
- Koontz, L. (2014). TCA precipitation. In *Methods in Enzymology* (Vol. 541, pp. 3–10). Academic Press Inc. <https://doi.org/10.1016/B978-0-12-420119-4.00001-X>
- Kosenko, T., Golder, M., Leblond, G., Weng, W., & Lagace, T. A. (2013). Low density lipoprotein binds to proprotein convertase subtilisin/kexin type-9 (PCSK9) in human plasma and inhibits PCSK9-mediated low density lipoprotein receptor degradation. *The Journal of Biological Chemistry*, 288(12), 8279–8288. <https://doi.org/10.1074/jbc.M112.421370>
- Kozarsky, K., Kingsley, D., & Krieger, M. (1988). Use of a mutant cell line to study the kinetics and function of O-linked glycosylation of low density lipoprotein receptors. *Proceedings of the National Academy of Sciences*, 85(12), 4335–4339. <https://doi.org/10.1073/pnas.85.12.4335>
- Kumar, S., Ratnikov, B. I., Kazanov, M. D., Smith, J. W., & Cieplak, P. C. (2015). CleavPredict: A platform for reasoning about matrix metalloproteinases proteolytic events. *PLoS ONE*, 10(5), e0127877. <https://doi.org/10.1371/journal.pone.0127877>

- Kuscu, C, Evensen, N., & Cao, J. (2011). MMP14 (matrix metalloproteinase 14 (membrane-inserted)). *Atlas of Genetics and Cytogenetics in Oncology and Haematology*, 15(6), 502–506. <https://doi.org/10.4267/2042/45036>
- Kuscu, Cem, Evensen, N., & Cao, J. (2010). MMP14 (matrix metalloproteinase 14 (membrane-inserted)). Retrieved September 27, 2019, from http://atlasgeneticsoncology.org/Genes/GC_MMP14.html
- Kwon, H. J., Lagace, T. A., McNutt, M. C., Horton, J. D., & Deisenhofer, J. (2008). Molecular basis for LDL receptor recognition by PCSK9. *Proceedings of the National Academy of Sciences*, 105(6), 1820–1825. <https://doi.org/10.1073/PNAS.0712064105>
- Lagace, T. A. (2014). PCSK9 and LDLR degradation. *Current Opinion in Lipidology*, 25(5), 387–393. <https://doi.org/10.1097/MOL.0000000000000114>
- Lagace, T. A., Curtis, D. E., Garuti, R., McNutt, M. C., Park, S. W., Prather, H. B., ... Horton, J. D. (2006). Secreted PCSK9 decreases the number of LDL receptors in hepatocytes and in livers of parabiotic mice. *The Journal of Clinical Investigation*, 116(11), 2995–3005. <https://doi.org/10.1172/JCI29383>
- Lagoutte, E., Villeneuve, C., Lafanechère, L., Wells, C. M., Jones, G. E., Chavrier, P., & Rossé, C. (2016). LIMK Regulates Tumor-Cell Invasion and Matrix Degradation Through Tyrosine Phosphorylation of MT1-MMP. *Scientific Reports*, 6(1), 24925. <https://doi.org/10.1038/srep24925>
- Lambert, G., Charlton, F., Rye, K. A., & Piper, D. E. (2009, March 1). Molecular basis of PCSK9 function. *Atherosclerosis*. Elsevier.

<https://doi.org/10.1016/j.atherosclerosis.2008.06.010>

Lambert, G., Chatelais, M., Petrides, F., Passard, M., Thedrez, A., Rye, K. A., ... Marais, A. D. (2014, December 2). Normalization of low-density lipoprotein receptor expression in receptor defective homozygous familial hypercholesterolemia by inhibition of PCSK9 with alirocumab. *Journal of the American College of Cardiology*. Elsevier USA.

<https://doi.org/10.1016/j.jacc.2014.07.995>

Lehti, K., Rose, N. F., Valavaara, S., Weiss, S. J., & Keski-Oja, J. (2009). MT1-MMP promotes vascular smooth muscle dedifferentiation through LRP1 processing. *Journal of Cell Science*, 122(1), 126–135. <https://doi.org/10.1242/jcs.035279>

Libby, P., Ridker, P. M., & Hansson, G. K. (2011). Progress and challenges in translating the biology of atherosclerosis. *Nature*, 473(7347), 317–325.

<https://doi.org/10.1038/nature10146>

Lichtenthaler, S. F., Lemberg, M. K., & Fluhrer, R. (2018). Proteolytic ectodomain shedding of membrane proteins in mammals—hardware, concepts, and recent developments. *The EMBO Journal*, 37(15), 1–24. <https://doi.org/10.15252/embj.201899456>

Lindgren, V., Luskey, K. L., Russell, D. W., & Francke, U. (1985). Human genes involved in cholesterol metabolism: chromosomal mapping of the loci for the low density lipoprotein receptor and 3-hydroxy-3-methylglutaryl-coenzyme A reductase with cDNA probes. *Proceedings of the National Academy of Sciences of the United States of America*, 82(24), 8567–8571. <https://doi.org/10.1073/pnas.82.24.8567>

Mabuchi, H., Nohara, A., & Inazu, A. (2014). Cholesteryl Ester Transfer Protein (CETP)

- Deficiency and CETP Inhibitors. *Molecules and Cells*, 37(11), 777–784.
<https://doi.org/10.14348/molcells.2014.0265>
- Manon-Jensen, T., Multhaupt, H. A. B., & Couchman, J. R. (2013). Mapping of matrix metalloproteinase cleavage sites on syndecan-1 and syndecan-4 ectodomains. *FEBS Journal*, 280(10), 2320–2331. <https://doi.org/10.1111/febs.12174>
- Marlovits, T. C., Abrahamsberg, C., & Blaas, D. (1998). Very-low-density lipoprotein receptor fragment shed from HeLa cells inhibits human rhinovirus infection. *Journal of Virology*, 72(12), 10246–10250. Retrieved from <https://www.ncbi.nlm.nih.gov/pmc/articles/PMC110607/pdf/jv010246.pdf>
- Matthews, V., Schuster, B., Schütze, S., Bussmeyer, I., Ludwig, A., Hundhausen, C., ... Rose-John, S. (2003). Cellular cholesterol depletion triggers shedding of the human interleukin-6 receptor by ADAM10 and ADAM17 (TACE). *Journal of Biological Chemistry*, 278(40), 38829–38839. <https://doi.org/10.1074/jbc.M210584200>
- Maxfield, F., & Wüstner, D. (2002). Intracellular cholesterol transport. *Journal of Clinical Investigation*, 110(7), 891–898. https://doi.org/10.1007/978-3-642-00300-4_6
- Mayne, J., Ooi, T. C., Tepliakova, L., Seebun, D., Walker, K., Mohottalage, D., ... Figeys, D. (2018). Associations Between Soluble LDLR and Lipoproteins in a White Cohort and the Effect of PCSK9 Loss-of-Function. *The Journal of Clinical Endocrinology & Metabolism*, 103(9), 3486–3495. <https://doi.org/10.1210/jc.2018-00777>
- Mayne, J., Raymond, A., Chaplin, A., Cousins, M., Kaefer, N., Gyamera-Acheampong, C., ... Ooi, T. C. (2007). Plasma PCSK9 levels correlate with cholesterol in men but not in

- women. *Biochemical and Biophysical Research Communications*, 361(2), 451–456.
<https://doi.org/10.1016/j.bbrc.2007.07.029>
- Merriam-Webster. (n.d.). Cholesterol | Definition of Cholesterol by Merriam-Webster. Retrieved September 17, 2019, from <https://www.merriam-webster.com/dictionary/cholesterol>
- Mignon, C., Okada, A., Mattei, M. G., & Basset, P. (1995). Assignment of the Human Membrane-Type Matrix Metalloproteinase (MMP14) Gene to 14q11-q12 by in Situ Hybridization. *Genomics*, 28(2), 360–361. <https://doi.org/10.1006/GENO.1995.1159>
- Miller, M.-C., Manning, H. B., Jain, A., Troeberg, L., Dudhia, J., Essex, D., ... Itoh, Y. (2009). Membrane type 1 matrix metalloproteinase is a crucial promoter of synovial invasion in human rheumatoid arthritis. *Arthritis & Rheumatism*, 60(3), 686–697.
<https://doi.org/10.1002/art.24331>
- Nagase, H., & Woessner, J. F. (1999). Matrix metalloproteinases. *The Journal of Biological Chemistry*, 274(31), 21491–21494. <https://doi.org/10.1074/jbc.274.31.21491>
- Nam, D. H., Rodriguez, C., Remacle, A. G., Strongin, A. Y., & Ge, X. (2016). Active-site MMP-selective antibody inhibitors discovered from convex paratope synthetic libraries. *Proceedings of the National Academy of Sciences of the United States of America*, 113(52), 14970–14975. <https://doi.org/10.1073/pnas.1609375114>
- Naseh, G., Mohammadifard, M., & Mohammadifard, M. (2016). Upregulation of cyclin-dependent kinase 7 and matrix metalloproteinase-14 expression contribute to metastatic properties of gastric cancer. *IUBMB Life*, 68(10), 799–805. <https://doi.org/10.1002/iub.1543>
- Oh, J., Takahashi, R., Kondo, S., Mizoguchi, A., Adachi, E., Sasahara, R. M., ... Noda, M.

- (2001). The membrane-anchored MMP inhibitor RECK is a key regulator of extracellular matrix integrity and angiogenesis. *Cell*, *107*(6), 789–800. [https://doi.org/10.1016/s0092-8674\(01\)00597-9](https://doi.org/10.1016/s0092-8674(01)00597-9)
- Ohuchi, E., Imai, K., Fujii, Y., Sato, H., Seiki, M., & Okada, Y. (1997). Membrane Type 1 Matrix Metalloproteinase Digests Interstitial Collagens and Other Extracellular Matrix Macromolecules. *Journal of Biological Chemistry*, *272*(4), 2446–2451. <https://doi.org/10.1074/jbc.272.4.2446>
- Okada, A., Tomasetto, C., Lutz, Y., Bellocq, J. P., Rio, M. C., & Basset, P. (1997). Expression of matrix metalloproteinases during rat skin wound healing: evidence that membrane type-1 matrix metalloproteinase is a stromal activator of pro-gelatinase A. *The Journal of Cell Biology*, *137*(1), 67–77. <https://doi.org/10.1083/jcb.137.1.67>
- Osenkowski, P., Meroueh, S. O., Pavel, D., Mobashery, S., & Fridman, R. (2005). Mutational and structural analyses of the hinge region of membrane type 1-matrix metalloproteinase and enzyme processing. *The Journal of Biological Chemistry*, *280*(28), 26160–26168. <https://doi.org/10.1074/jbc.M414379200>
- Page-McCaw, A., Ewald, A. J., & Werb, Z. (2007). Matrix metalloproteinases and the regulation of tissue remodelling. *Nature Reviews Molecular Cell Biology*, *8*(3), 221–233. <https://doi.org/10.1038/nrm2125>
- Pahwa, S., Stawikowski, M. J., & Fields, G. B. (2014). Monitoring and inhibiting MT1-MMP during cancer initiation and progression. *Cancers*, *6*(1), 416–435. <https://doi.org/10.3390/cancers6010416>

- Pavlaki, M., Cao, J., Hymowitz, M., Chen, W.-T., Bahou, W., & Zucker, S. (2002). A conserved sequence within the propeptide domain of membrane type 1 matrix metalloproteinase is critical for function as an intramolecular chaperone. *The Journal of Biological Chemistry*, 277(4), 2740–2749. <https://doi.org/10.1074/jbc.M108987200>
- Pekkonen, P., Alve, S., Balistreri, G., Gramolelli, S., Tatti-Bugaeva, O., Paatero, I., ... Ojala, P. M. (2018). Lymphatic endothelium stimulates melanoma metastasis and invasion via MMP14-dependent Notch3 and β 1-integrin activation. *ELife*, 7. <https://doi.org/10.7554/eLife.32490>
- Peng, W., Yan, J., Wan, Y., Wang, B., Tao, J., Yang, G., ... Wang, J. (2012). Matrix Metalloproteinases: A Review of Their Structure and Role in Systemic Sclerosis. *Journal of Clinical Immunology*, 32(6), 1409–1414. <https://doi.org/10.1007/s10875-012-9735-7>
- Peschon, J. J., Slack, J. L., Reddy, P., Stocking, K. L., Sunnarborg, S. W., Lee, D. C., ... Black, R. A. (1998). An Essential Role for Ectodomain Shedding in Mammalian Development. *Science*, 282(5392), 1281–1284. <https://doi.org/10.1126/science.282.5392.1281>
- Poirier, S., Mayer, G., Benjannet, S., Bergeron, E., Marcinkiewicz, J., Nassoury, N., ... Seidah, N. G. (2008). The proprotein convertase PCSK9 induces the degradation of low density lipoprotein receptor (LDLR) and its closest family members VLDLR and ApoER2. *The Journal of Biological Chemistry*, 283(4), 2363–2372. <https://doi.org/10.1074/jbc.M708098200>
- Ra, H.-J., & Parks, W. C. (2007). Control of matrix metalloproteinase catalytic activity. *Matrix Biology : Journal of the International Society for Matrix Biology*, 26(8), 587–596. <https://doi.org/10.1016/j.matbio.2007.07.001>

- Rader, D. J., & Hobbs, H. H. (2014). Disorders of Lipoprotein Metabolism. In D. Kasper, A. Fauci, S. Hauser, D. Longo, J. L. Jameson, & J. Loscalzo (Eds.), *Harrison's Principles of Internal Medicine, 19e*. New York, NY: McGraw-Hill Education. Retrieved from <http://accessmedicine.mhmedical.com/content.aspx?aid=1120816563>
- Radhakrishnan, A., Goldstein, J. L., McDonald, J. G., & Brown, M. S. (2008). Switch-like Control of SREBP-2 Transport Triggered by Small Changes in ER Cholesterol: A Delicate Balance. *Cell Metabolism*, 8(6), 512–521. <https://doi.org/10.1016/j.cmet.2008.10.008>
- Raggi, P., Genest, J., Giles, J. T., Rayner, K. J., Dwivedi, G., Beanlands, R. S., & Gupta, M. (2018). Role of inflammation in the pathogenesis of atherosclerosis and therapeutic interventions. *Atherosclerosis*, 276, 98–108. <https://doi.org/10.1016/J.ATHEROSCLEROSIS.2018.07.014>
- Rajavashisth, T B, Xu, X. P., Jovinge, S., Meisel, S., Xu, X. O., Chai, N. N., ... Shah, P. K. (1999a). Membrane type 1 matrix metalloproteinase expression in human atherosclerotic plaques: evidence for activation by proinflammatory mediators. *Circulation*, 99(24), 3103–3109. <https://doi.org/10.1161/01.cir.99.24.3103>
- Rajavashisth, T B, Xu, X. P., Jovinge, S., Meisel, S., Xu, X. O., Chai, N. N., ... Shah, P. K. (1999b). Membrane type 1 matrix metalloproteinase expression in human atherosclerotic plaques: evidence for activation by proinflammatory mediators. *Circulation*, 99(24), 3103–3109. Retrieved from <http://www.ncbi.nlm.nih.gov/pubmed/10377072>
- Rajavashisth, Tripathi B., Liao, J. K., Galis, Z. S., Tripathi, S., Laufs, U., Tripathi, J., ... Libby, P. (1999). Inflammatory Cytokines and Oxidized Low Density Lipoproteins Increase Endothelial Cell Expression of Membrane Type 1-Matrix Metalloproteinase. *Journal of*

Biological Chemistry, 274(17), 11924–11929. <https://doi.org/10.1074/jbc.274.17.11924>

Ramasamy, I. (2014). Recent advances in physiological lipoprotein metabolism. *Clinical Chemistry and Laboratory Medicine (CCLM)*, 52(12), 1695–1727.
<https://doi.org/10.1515/cclm-2013-0358>

Rashid, S., Curtis, D. E., Garuti, R., Anderson, N. H., Bashmakov, Y., Ho, Y. K., ... Horton, J. D. (2005). Decreased plasma cholesterol and hypersensitivity to statins in mice lacking Pcsk9. *Proceedings of the National Academy of Sciences of the United States of America*, 102(15), 5374–5379. <https://doi.org/10.1073/pnas.0501652102>

Rebeck, G. W., LaDu, M. J., Estus, S., Bu, G., & Weeber, E. J. (2006). The generation and function of soluble apoE receptors in the CNS. *Molecular Neurodegeneration*, 1, 15.
<https://doi.org/10.1186/1750-1326-1-15>

Remacle, A., Murphy, G., & Roghi, C. (2003). Membrane type I-matrix metalloproteinase (MT1-MMP) is internalised by two different pathways and is recycled to the cell surface. *Journal of Cell Science*, 116(19), 3905–3916. <https://doi.org/10.1242/jcs.00710>

Remacle, Albert, Murphy, G., & Roghi, C. (2003). Membrane type I-matrix metalloproteinase (MT1-MMP) is internalised by two different pathways and is recycled to the cell surface. *Journal of Cell Science*, 116(Pt 19), 3905–3916. <https://doi.org/10.1242/jcs.00710>

Rosenson, R. S., Brewer, H. B., Davidson, W. S., Fayad, Z. A., Fuster, V., Goldstein, J., ... Yvan-Charvet, L. (2012). Cholesterol efflux and atheroprotection: advancing the concept of reverse cholesterol transport. *Circulation*, 125(15), 1905–1919.
<https://doi.org/10.1161/CIRCULATIONAHA.111.066589>

- Ross, R. (1999). Atherosclerosis — An Inflammatory Disease. *New England Journal of Medicine*, 340(2), 115–126. <https://doi.org/10.1056/NEJM199901143400207>
- Rozanov, Dmitry V., Deryugina, E. I., Ratnikov, B. I., Monosov, E. Z., Marchenko, G. N., Quigley, J. P., & Strongin, A. Y. (2001). Mutation analysis of membrane type-1 matrix metalloproteinase (MT1-MMP): The role of the cytoplasmic tail Cys574, the active site Glu 240, and furin cleavage motifs in oligomerization, processing, and self-proteolysis of MT1-MMP expressed in breast carcin. *Journal of Biological Chemistry*, 276(28), 25705–25714. <https://doi.org/10.1074/jbc.M007921200>
- Rozanov, Dmitri V, Hahn-Dantona, E., Strickland, D. K., & Strongin, A. Y. (2004). The low density lipoprotein receptor-related protein LRP is regulated by membrane type-1 matrix metalloproteinase (MT1-MMP) proteolysis in malignant cells. *The Journal of Biological Chemistry*, 279(6), 4260–4268. <https://doi.org/10.1074/jbc.M311569200>
- Rozario, T., & DeSimone, D. W. (2010). The extracellular matrix in development and morphogenesis: A dynamic view. *Developmental Biology*, 341(1), 126–140. <https://doi.org/10.1016/J.YDBIO.2009.10.026>
- Rudenko, G., Henry, L., Henderson, K., Ichtchenko, K., Brown, M. S., Goldstein, J. L., & Deisenhofer, J. (2002). Structure of the LDL Receptor Extracellular Domain at Endosomal pH. *Science*, 298(5602), 2353–2358. <https://doi.org/10.1126/science.1078124>
- Rudenko, Gabby, Henry, L., Henderson, K., Ichtchenko, K., Brown, M. S., Goldstein, J. L., & Deisenhofer, J. (2002). Structure of the LDL receptor extracellular domain at endosomal pH. *Science (New York, N.Y.)*, 298(5602), 2353–2358. <https://doi.org/10.1126/science.1078124>

- Sabatine, M. S. (2019, March 1). PCSK9 inhibitors: clinical evidence and implementation. *Nature Reviews Cardiology*. Nature Publishing Group. <https://doi.org/10.1038/s41569-018-0107-8>
- Sakamoto, T., & Seiki, M. (2009). Cytoplasmic tail of MT1-MMP regulates macrophage motility independently from its protease activity. *Genes to Cells*, *14*(5), 617–626. <https://doi.org/10.1111/j.1365-2443.2009.01293.x>
- Sakr, M., Li, X.-Y., Sabeh, F., Feinberg, T. Y., Tesmer, J. J. G., Tang, Y., & Weiss, S. J. (2018). Tracking the Cartoon mouse phenotype: Hemopexin domain-dependent regulation of MT1-MMP pericellular collagenolytic activity. *The Journal of Biological Chemistry*, *293*(21), 8113–8127. <https://doi.org/10.1074/jbc.RA117.001503>
- Sato, H., Takino, T., Okada, Y., Cao, J., Shinagawa, A., Yamamoto, E., & Seiki, M. (1994). A matrix metalloproteinase expressed on the surface of invasive tumour cells. *Nature*, *370*(6484), 61–65. <https://doi.org/10.1038/370061a0>
- Schneider, F., Sukhova, G. K., Aikawa, M., Canner, J., Gerdes, N., Tang, S.-M. T., ... Libby, P. (2008). Matrix Metalloproteinase-14 Deficiency in Bone Marrow-Derived Cells Promotes Collagen Accumulation in Mouse Atherosclerotic Plaques. *Circulation*, *117*(7), 931–939. <https://doi.org/10.1161/CIRCULATIONAHA.107.707448>
- Sehayek, E., Lewin-Velvert, U., Chajek-Shaul, T., & Eisenberg, S. (1991). Lipolysis exposes unreactive endogenous apolipoprotein E-3 in human and rat plasma very low density lipoprotein. *The Journal of Clinical Investigation*, *88*(2), 553–560. <https://doi.org/10.1172/JCI115339>

- Seidah, N. G. (2016, June 1). New developments in proprotein convertase subtilisin-kexin 9's biology and clinical implications. *Current Opinion in Lipidology*. Lippincott Williams and Wilkins. <https://doi.org/10.1097/MOL.0000000000000295>
- Seidah, N. G., Awan, Z., Chrétien, M., & Mbikay, M. (2014, March 14). PCSK9: A key modulator of cardiovascular health. *Circulation Research*.
<https://doi.org/10.1161/CIRCRESAHA.114.301621>
- Selvais, C., D'Auria, L., Tyteca, D., Perrot, G., Lemoine, P., Troeberg, L., ... Emonard, H. (2011). Cell cholesterol modulates metalloproteinase-dependent shedding of low-density lipoprotein receptor-related protein-1 (LRP-1) and clearance function. *FASEB Journal : Official Publication of the Federation of American Societies for Experimental Biology*, 25(8), 2770–2781. <https://doi.org/10.1096/fj.10-169508>
- Shapiro, M. D., Tavori, H., & Fazio, S. (2018a). PCSK9. *Circulation Research*, 122(10), 1420–1438. <https://doi.org/10.1161/CIRCRESAHA.118.311227>
- Shapiro, M. D., Tavori, H., & Fazio, S. (2018b, May 1). PCSK9 from basic science discoveries to clinical trials. *Circulation Research*. Lippincott Williams and Wilkins.
<https://doi.org/10.1161/CIRCRESAHA.118.311227>
- Shepherd, J., Cobbe, S. M., Ford, I., Isles, C. G., Lorimer, A. R., Macfarlane, P. W., ... Packard, C. J. (1995). Prevention of Coronary Heart Disease with Pravastatin in Men with Hypercholesterolemia. *New England Journal of Medicine*, 333(20), 1301–1308.
<https://doi.org/10.1056/NEJM199511163332001>
- Shepherd, J., & Packard, C. J. (1986). Lipoprotein receptors and atherosclerosis. *Clinical*

Science, 70(1), 1–6. Retrieved from <http://www.clinsci.org/content/70/1/1.abstract>

Shimohiro, H., Taniguchi, S.-I., Koda, M., Sakai, C., & Yamada, S. (2015). Association between serum soluble low-density lipoprotein receptor levels and metabolic factors in healthy Japanese individuals. *Journal of Clinical Laboratory Analysis*, 29(1), 52–56.
<https://doi.org/10.1002/jcla.21727>

Sorrentino, V., & Zelcer, N. (2012). Post-transcriptional regulation of lipoprotein receptors by the E3-ubiquitin ligase inducible degrader of the low-density lipoprotein receptor. *Current Opinion in Lipidology*, 23(3), 213–219. <https://doi.org/10.1097/MOL.0b013e3283532947>

Stancu, C., & Sima, A. (2001). Statins: mechanism of action and effects. *Journal of Cellular and Molecular Medicine*, 5(4), 378–387. Retrieved from
<http://www.ncbi.nlm.nih.gov/pubmed/12067471>

Stegemann, C., Didangelos, A., Barallobre-Barreiro, J., Langley, S. R., Mandal, K., Jahangiri, M., & Mayr, M. (2013). Proteomic Identification of Matrix Metalloproteinase Substrates in the Human Vasculature. *Circulation: Cardiovascular Genetics*, 6(1), 106–117.
<https://doi.org/10.1161/CIRCGENETICS.112.964452>

Stein, E. A., & Raal, F. (2014). Reduction of Low-Density Lipoprotein Cholesterol by Monoclonal Antibody Inhibition of PCSK9. *Annual Review of Medicine*, 65(1), 417–431.
<https://doi.org/10.1146/annurev-med-022613-090402>

Steinberg, D., & Witztum, J. L. (2010). Oxidized low-density lipoprotein and atherosclerosis. *Arteriosclerosis, Thrombosis, and Vascular Biology*, 30(12), 2311–2316.
<https://doi.org/10.1161/ATVBAHA.108.179697>

- Storey, B. C., Staplin, N., Haynes, R., Reith, C., Emberson, J., Herrington, W. G., ... SHARP Collaborative Group, T. S. C. (2018). Lowering LDL cholesterol reduces cardiovascular risk independently of presence of inflammation. *Kidney International*, *93*(4), 1000–1007. <https://doi.org/10.1016/j.kint.2017.09.011>
- Strøm, T. B., Laerdahl, J. K., & Leren, T. P. (2015). Mutation p.L799R in the LDLR, which affects the transmembrane domain of the LDLR, prevents membrane insertion and causes secretion of the mutant LDLR. *Human Molecular Genetics*, *24*(20), 5836–5844. <https://doi.org/10.1093/hmg/ddv304>
- Strom, T. B., Tveten, K., Laerdahl, J. K., & Leren, T. P. (2014). Mutation G805R in the transmembrane domain of the LDL receptor gene causes familial hypercholesterolemia by inducing ectodomain cleavage of the LDL receptor in the endoplasmic reticulum. *FEBS Open Bio*, *4*(1), 321–327. <https://doi.org/10.1016/j.fob.2014.03.007>
- Strøm, T. B., Tveten, K., Laerdahl, J. K., & Leren, T. P. (2014). Mutation G805R in the transmembrane domain of the LDL receptor gene causes familial hypercholesterolemia by inducing ectodomain cleavage of the LDL receptor in the endoplasmic reticulum. *FEBS Open Bio*, *4*, 321–327. <https://doi.org/10.1016/j.fob.2014.03.007>
- Südhof, T. C., Russell, D. W., Brown, M. S., & Goldstein, J. L. (1987). 42 bp element from LDL receptor gene confers end-product repression by sterols when inserted into viral TK promoter. *Cell*, *48*(6), 1061–1069. [https://doi.org/10.1016/0092-8674\(87\)90713-6](https://doi.org/10.1016/0092-8674(87)90713-6)
- Sudhof, T., Goldstein, J., Brown, M., & Russell, D. (1985). The LDL receptor gene: a mosaic of exons shared with different proteins. *Science*, *228*(4701), 815–822. <https://doi.org/10.1126/science.2988123>

- Swayampakula, M., McDonald, P. C., Vallejo, M., Coyaud, E., Chafe, S. C., Westerback, A., ... Dedhar, S. (2017). The interactome of metabolic enzyme carbonic anhydrase IX reveals novel roles in tumor cell migration and invadopodia/MMP14-mediated invasion. *Oncogene*, *36*(45), 6244–6261. <https://doi.org/10.1038/onc.2017.219>
- Tam, E. M., Morrison, C. J., Wu, Y. I., Stack, M. S., & Overall, C. M. (2004). Membrane protease proteomics: Isotope-coded affinity tag MS identification of undescribed MT1-matrix metalloproteinase substrates. *Proceedings of the National Academy of Sciences of the United States of America*, *101*(18), 6917–6922. <https://doi.org/10.1073/pnas.0305862101>
- Thomas, G. (2002). Furin at the cutting edge: from protein traffic to embryogenesis and disease. *Nature Reviews. Molecular Cell Biology*, *3*(10), 753–766. <https://doi.org/10.1038/nrm934>
- Thompson, P. D., Panza, G., Zaleski, A., & Taylor, B. (2016). Statin-Associated Side Effects. *Journal of the American College of Cardiology*, *67*(20), 2395 LP – 2410. <https://doi.org/10.1016/j.jacc.2016.02.071>
- Tibolla, G., Norata, G. D., Artali, R., Meneghetti, F., & Catapano, A. L. (2011). Proprotein convertase subtilisin/kexin type 9 (PCSK9): From structure–function relation to therapeutic inhibition. *Nutrition, Metabolism and Cardiovascular Diseases*, *21*(11), 835–843. <https://doi.org/10.1016/J.NUMECD.2011.06.002>
- Tochowicz, A., Goettig, P., Evans, R., Visse, R., Shitomi, Y., Palmisano, R., ... Itoh, Y. (2011). The dimer interface of the membrane type 1 matrix metalloproteinase hemopexin domain: crystal structure and biological functions. *The Journal of Biological Chemistry*, *286*(9), 7587–7600. <https://doi.org/10.1074/jbc.M110.178434>

- Toth, M., Hernandez-Barrantes, S., Osenkowski, P., Bernardo, M. M., Gervasi, D. C., Shimura, Y., ... Fridman, R. (2002). Complex Pattern of Membrane Type 1 Matrix Metalloproteinase Shedding. *Journal of Biological Chemistry*, 277(29), 26340–26350.
<https://doi.org/10.1074/jbc.M200655200>
- Tsunezuka, Y., Kinoh, H., Takino, T., Watanabe, Y., Okada, Y., Shinagawa, A., ... Seiki, M. (1996). Expression of membrane-type matrix metalloproteinase 1 (MT1-MMP) in tumor cells enhances pulmonary metastasis in an experimental metastasis assay. *Cancer Research*, 56(24), 5678–5683. Retrieved from <http://www.ncbi.nlm.nih.gov/pubmed/8971175>
- Uekita, T., Itoh, Y., Yana, I., Ohno, H., & Seiki, M. (2001). Cytoplasmic tail-dependent internalization of membrane-type 1 matrix metalloproteinase is important for its invasion-promoting activity. *The Journal of Cell Biology*, 155(7), 1345–1356.
<https://doi.org/10.1083/jcb.200108112>
- Understanding Your Cholesterol Numbers | Cleveland Clinic. (n.d.). Retrieved December 20, 2019, from <https://my.clevelandclinic.org/health/articles/11920-cholesterol-numbers-what-do-they-mean>
- Van Lint, P., & Libert, C. (2007). Chemokine and cytokine processing by matrix metalloproteinases and its effect on leukocyte migration and inflammation. *Journal of Leukocyte Biology*, 82(6), 1375–1381. <https://doi.org/10.1189/jlb.0607338>
- Vance, J. E., & Vance, D. E. (1990). Lipoprotein assembly and secretion by hepatocytes. *Annual Review of Nutrition*, 10, 337–356. <https://doi.org/10.1146/annurev.nu.10.070190.002005>
- Voet, D., & Voet, J. G. (2011). *Biochemistry* (4th ed.). New Jersey: John Wiley & Sons.

- Von Tresckow, B., Kallen, K.-J., von Strandmann, E. P., Borchmann, P., Lange, H., Engert, A., & Hansen, H. P. (2004). Depletion of Cellular Cholesterol and Lipid Rafts Increases Shedding of CD30. *The Journal of Immunology*, *172*(7), 4324–4331. <https://doi.org/10.4049/jimmunol.172.7.4324>
- Vos, I. J. H. M. De, Tao, E. Y., Li, S., Ong, M., Goggi, J. L., Scerri, T., ... Steensel, M. A. M. Van. (2018). Functional analysis of a hypomorphic allele shows that MMP14 catalytic activity is the prime determinant of the Winchester syndrome phenotype. *Human Molecular Genetics*, *27*(16), 2775–2788. <https://doi.org/10.1093/hmg/ddy168>
- Wang, X., Berry, E., Hernandez-Anzaldo, S., Sun, D., Adijiang, A., Li, L., ... Fernandez-Patron, C. (2015). MMP-2 inhibits PCSK9-induced degradation of the LDL receptor in Hepal-c1c7 cells. *FEBS Letters*, *589*(4), 490–496. <https://doi.org/10.1016/j.febslet.2015.01.007>
- Wang, Y., Dubland, J. A., Allahverdian, S., Asonye, E., Sahin, B., Jaw, J. E., ... Francis, G. A. (2019). Smooth Muscle Cells Contribute the Majority of Foam Cells in ApoE (Apolipoprotein E)-Deficient Mouse Atherosclerosis. *Arteriosclerosis, Thrombosis, and Vascular Biology*, *39*(5), 876–887. <https://doi.org/10.1161/ATVBAHA.119.312434>
- Wei, E., Ben Ali, Y., Lyon, J., Wang, H., Nelson, R., Dolinsky, V. W., ... Lehner, R. (2010). Loss of TGH/Ces3 in Mice Decreases Blood Lipids, Improves Glucose Tolerance, and Increases Energy Expenditure. *Cell Metabolism*, *11*(3), 183–193. <https://doi.org/10.1016/j.cmet.2010.02.005>
- WHO. (2017). Cardiovascular diseases (CVDs). Retrieved September 17, 2019, from [https://www.who.int/news-room/fact-sheets/detail/cardiovascular-diseases-\(cvds\)](https://www.who.int/news-room/fact-sheets/detail/cardiovascular-diseases-(cvds))

- Willnow, T. E., Nykjaer, A., & Herz, J. (1999). Lipoprotein receptors: new roles for ancient proteins. *Nature Cell Biology*, *1*(6), E157–E162. <https://doi.org/10.1038/14109>
- Wilson, C., Wardell, M., Weisgraber, K., Mahley, R., & Agard, D. (1991). Three-dimensional structure of the LDL receptor-binding domain of human apolipoprotein E. *Science*, *252*(5014), 1817–1822. <https://doi.org/10.1126/science.2063194>
- Wong, H. L. X., Cao, R., Jin, G., Ming Chan, K., Cao, Y., & Zhou, Zhongjun. (2012). When MT1-MMP meets ADAMs. *Cell Cycle*, *11*(15), 2793–2798. <https://doi.org/10.4161/cc.20949>
- Wong, H. L. X., Jin, G., Cao, R., Zhang, S., Cao, Y., & Zhou, Z. (2016). MT1-MMP sheds LYVE-1 on lymphatic endothelial cells and suppresses VEGF-C production to inhibit lymphangiogenesis. *Nature Communications*, *7*, 10824. <https://doi.org/10.1038/ncomms10824>
- Woskowicz, A. M., Weaver, S. A., Shitomi, Y., Ito, N., & Itoh, Y. (2013). MT-LOOP-dependent localization of membrane type I matrix metalloproteinase (MT1-MMP) to the cell adhesion complexes promotes cancer cell invasion. *The Journal of Biological Chemistry*, *288*(49), 35126–35137. <https://doi.org/10.1074/jbc.M113.496067>
- Wu, Y. I., Munshi, H. G., Sen, R., Snipas, S. J., Salvesen, G. S., Fridman, R., & Stack, M. S. (2004). Glycosylation Broadens the Substrate Profile of Membrane Type 1 Matrix Metalloproteinase. *Journal of Biological Chemistry*, *279*(9), 8278–8289. <https://doi.org/10.1074/jbc.M311870200>
- Xing, Y., Xu, Q., & Lee, C. (2003). Widespread production of novel soluble protein isoforms by

- alternative splicing removal of transmembrane anchoring domains. *FEBS Letters*, 555(3), 572–578. [https://doi.org/10.1016/S0014-5793\(03\)01354-1](https://doi.org/10.1016/S0014-5793(03)01354-1)
- Yamamoto, T., Lu, C., & Ryan, R. O. (2011). A Two-step Binding Model of PCSK9 Interaction with the Low Density Lipoprotein Receptor. *Journal of Biological Chemistry*, 286(7), 5464–5470. <https://doi.org/10.1074/jbc.M110.199042>
- Yu, X.-H., Zhang, D.-W., Zheng, X.-L., & Tang, C.-K. (2019). Cholesterol transport system: An integrated cholesterol transport model involved in atherosclerosis. *Progress in Lipid Research*, 73, 65–91. <https://doi.org/10.1016/J.PLIPRES.2018.12.002>
- Zaid, A., Roubtsova, A., Essalmani, R., Marcinkiewicz, J., Chamberland, A., Hamelin, J., ... Prat, A. (2008). Proprotein convertase subtilisin/kexin type 9 (PCSK9): Hepatocyte-specific low-density lipoprotein receptor degradation and critical role in mouse liver regeneration. *Hepatology*, 48(2), 646–654. <https://doi.org/10.1002/hep.22354>
- Zelcer, N., Hong, C., Boyadjian, R., & Tontonoz, P. (2009a). LXR regulates cholesterol uptake through Idol-dependent ubiquitination of the LDL receptor. *Science (New York, N.Y.)*, 325(5936), 100–104. <https://doi.org/10.1126/science.1168974>
- Zelcer, N., Hong, C., Boyadjian, R., & Tontonoz, P. (2009b). LXR Regulates Cholesterol Uptake Through Idol-Dependent Ubiquitination of the LDL Receptor. *Science*, 325(5936), 100–104. <https://doi.org/10.1126/science.1168974>
- Zhang, D.-W., Lagace, T. A., Garuti, R., Zhao, Z., McDonald, M., Horton, J. D., ... Hobbs, H. H. (2007). Binding of Proprotein Convertase Subtilisin/Kexin Type 9 to Epidermal Growth Factor-like Repeat A of Low Density Lipoprotein Receptor Decreases Receptor Recycling

- and Increases Degradation. *Journal of Biological Chemistry*, 282(25), 18602–18612.
<https://doi.org/10.1074/jbc.M702027200>
- Zhang, D. W., Graf, G. A., Gerard, R. D., Cohen, J. C., & Hobbs, H. H. (2006). Functional asymmetry of nucleotide-binding domains in ABCG5 and ABCG8. *Journal of Biological Chemistry*, 281(7), 4507–4516. <https://doi.org/10.1074/jbc.M512277200>
- Zhang, L., Reue, K., Fong, L. G., Young, S. G., & Tontonoz, P. (2012). Feedback regulation of cholesterol uptake by the LXR-IDOL-LDLR axis. *Arteriosclerosis, Thrombosis, and Vascular Biology*, 32(11), 2541–2546. <https://doi.org/10.1161/ATVBAHA.112.250571>
- Zhang, Y., Eigenbrot, C., Zhou, L., Shia, S., Li, W., Quan, C., ... Kirchhofer, D. (2014). Identification of a small peptide that inhibits PCSK9 protein binding to the low density lipoprotein receptor. *The Journal of Biological Chemistry*, 289(2), 942–955.
<https://doi.org/10.1074/jbc.M113.514067>
- Zhou, Z., Apte, S. S., Soininen, R., Cao, R., Baaklini, G. Y., Rauser, R. W., ... Tryggvason, K. (2000). Impaired endochondral ossification and angiogenesis in mice deficient in membrane-type matrix metalloproteinase I. *Proceedings of the National Academy of Sciences of the United States of America*, 97(8), 4052–4057.
<https://doi.org/10.1073/pnas.060037197>
- Zigrino, P., Ayachi, O., Schild, A., Kaltenberg, J., Zamek, J., Nischt, R., ... Mauch, C. (2012). Loss of epidermal MMP-14 expression interferes with angiogenesis but not with re-epithelialization. *European Journal of Cell Biology*, 91(10), 748–756.
<https://doi.org/10.1016/j.ejcb.2012.05.003>

Zolotukhin, S., Byrne, B. J., Mason, E., Zolotukhin, I., Potter, M., Chesnut, K., ... Muzyczka, N. (1999). Recombinant adeno-associated virus purification using novel methods improves infectious titer and yield. *Gene Therapy*, 6(6), 973–985.
<https://doi.org/10.1038/sj.gt.3300938>